DECEMBER 2017

PhD in Physics Engineering

ÜNAL YILDIRIR

GAZİANTEP UNIVERSITY
GRADUATE SCHOOL OF
NATURAL & APPLIED SCIENCES

THE INVESTIGATION OF SUCCESS OF COMPUTER GLOW CURVE DECONVOLUTION (CGCD) BY MAKING NUMERICAL SOLUTIONS OF OTOR AND IMTS MODELS

Ph.D THESIS
in
PHYSICS ENGINEERING

ÜNAL YILDIRIR
DECEMBER 2017

The Investigation of Success of Computer Glow Curve Deconvolution (CGCD) by Making Numerical Solutions of OTOR and IMTS Models

PhD Thesis
in
Physics Engineering
University of Gaziantep

Supervisor
Prof. Dr. A. Necmeddin YAZICI

Co-Supervisor
Assoc. Prof. Dr. R.Güler YILDIRIM

By
Ünal YILDIRIR
December 2017

GAZİANTEP UNIVERSITY
GRADUATE SCHOOL OF
NATURAL & APPLIED SCIENCES
Department of Engineering Physics

Name of the thesis: The investigation of success of computer glow curve deconvolution (CGCD) by making numerical solutions of OTOR and IMTS models

Name of the student: Ünal YILDIRIR

Exam date: 25. 12. 2017

Approval of the Graduate School of Natural and Applied Sciences

Prof. Dr. A.Necmeddin YAZICI

Director

I certify that this thesis satisfies all the requirements as a thesis for the degree of Master of Science/Doctor of Philosophy.

Prof. Dr. Ramazan KOÇ
Head of Department

This is to certify that we have read this thesis and that in our opinion it is fully adequate, in scope and quality, as a thesis for the degree of Master of Science/Doctor of Philosophy.

Assoc. Prof. Dr. R. Güler YILDIRIM
Co- Supervisor

Prof. Dr. A. Necmeddin YAZICI
Supervisor

Examining Committee Members	Signature
Prof. Dr. A. Necmeddin YAZICI	.....
Prof. Dr. Mustafa TOPAKSU	.....
Prof. Dr. Eser OLĞAR	.....
Prof. Dr. Mustafa ÖZTAŞ	.....
Assoc. Prof. Dr. Vural E. KAFADAR	.....

I hereby declare that all information in this document has been obtained and presented in accordance with academic rules and ethical conduct. I also declare that, as required by these and conduct, I have fully cited and referenced all materials and results that are not original to this work.

Ünal YILDIRIR

ABSTRACT

THE INVESTIGATION OF SUCCESS OF COMPUTER GLOW CURVE DECONVOLUTION (CGCD) BY MAKING NUMERICAL SOLUTIONS OF OTOR AND IMTS MODELS

YILDIRIR, Ünal
PhD in Physics Engineering
Supervisor: Prof. Dr. A. Necmeddin YAZICI
Co-Supervisor: Assoc. Prof. Dr. R. Güler YILDIRIM
December 2017
133 pages

In the study, OTOR (One-Trap One Recombination Center) and IMTS (Interactive Multiple Trap System) thermoluminescence (TL) rate equations, first, second and general-order TL kinetic equations were solved numerically with aid of Mathematica program and TL glow curves were obtained. In numerical solutions, one kinetic parameter is kept constant at each time, and by changing the others, a large number of TL glow curves composed of different combinations glow peaks were obtained. All of the numerically obtained glow curves were analyzed using the computerized glow curve deconvolution (CGCD) method. Two CGCD programs (GLOCANIN and Microsoft Excel) were used in the analyzing and the results of the CGCD programs were compared with the kinetic parameters entered in the numerical solutions and the success of the CGCD methods was investigated. It was also determined which program gave more successful results than the other. When the results were compared, it was seen that the success of the CGCD method depends on the electron transfer coefficients (A_n/A_h) and trap occupancy rates (n_0/N_t) in the numerical solutions of TL-models. It has been observed in the researches that the CGCD program written in Microsoft Excel gives better results than the GLOCANIN program in the analysis of the luminescence curves including the multi-luminescence peak obtained as a result of numerical solutions of OTOR and IMTS models. As a result of the studies carried out, it has been understood that the trap occupancy rate (n_0/N_t) must be low in order to make the kinetic parameters more reliable by the CGCD method after experimental studies. For this reason, with the results of low-dose applications, it has been concluded that the TL-luminescence curves must be analyzed by the CGCD method.

Key words: Thermoluminescence, computer glow curve deconvolution method, trap parameters, numerical analysis, OTOR, IMTS**.**

ÖZET

BİLGİSAYAR İLE IŞILDAMA EĞRİSİ AYRIŞIM (CGCD) YÖNTEMİNİN BAŞARISININ OTOR VE IMTS MODELLERİNİN NÜMERİK ÇÖZÜMLERİNİN YAPILARAK ARAŞTIRILMASI

YILDIRIR, Ünal
Doktora Tezi, Fizik Mühendisliği Bölümü
Tez Yöneticisi: Prof. Dr. A. Necmeddin YAZICI
Tez Yöneticisi Yardımcısı: Doç. Dr. R. Güler YILDIRIM
Aralık 2017
133 sayfa

Yapılan çalışmada birinci, ikinci ve genel-dereceden TL kinetik denklemleri ile OTOR (Bir-Tuzak Bir-Birleşme Merkezi) ve IMTS (Etkileşimli Çoklu Tuzak Sistemi) TL-Modelleri Matematika programı ile nümerik olarak çözülmüş ve yapay TL ışıldama eğrileri elde edilmiştir. Nümerik çözümlemelerde her seferinde bir kinetik parametre sabit tutulmuş, diğerleri değiştirilerek farklı kombinasyonlardan oluşan çok sayıda ışıldama eğrileri elde edilmiştir. Elde edilen tüm ışıldama eğrileri, bilgisayar ile ışıldama eğrisi (CGCD) yöntemi kullanılarak analiz edilmiştir. Analizlerde iki adet CGCD programı (GLOCANIN ve Microsoft Excel) kullanılmış ve analizler sonucunda CGCD programlarının sonuçları nümerik çözümlerde girilen kinetik parametreler ile karşılaştırılmış ve CGCD yönteminin başarısı araştırılmıştır. Ayrıca hangi programın diğerinden daha başarılı sonuçlar verdiği belirlenmiştir. Sonuçlar karşılaştırıldığında CGCD yönteminin başarısının TL-modellerinin nümerik çözümlemelerinde elektron geçiş katsayılarına (A_n/A_h) ve tuzak doluluk oranlarına (n_0/N_t) bağlı olduğu görülmüştür. Yapılan araştırmalarda OTOR ve IMTS modellerinin nümerik çözümlemeleri sonucu elde edilmiş çoklu ışıldama tepesi içeren ışıldama eğrilerinin analizlerinin Microsoft Excel'de yazılmış CGCD programının GLOCANIN programından daha iyi sonuçlar verdiği gözlemlenmiştir. Yapılan çalışmalar sonucunda deneysel çalışmalar sonunda CGCD yöntemi ile kinetik parametrelerin daha güvenilir bulunabilmesi için tuzak doluluk oranının (n_0/N_t) düşük olması gerektiği anlaşılmıştır. Bunun içinde düşük doz uygulamaları sonucunda TL-ışıldama eğrilerinin CGCD yöntemi ile analizi gerektiği sonucuna varılmıştır.

Anahtar Kelimeler: Termolüminesans, bilgisayarla analiz yöntemi, tuzak parametreleri, nümerik çözümleme, OTOR, IMTS.

ACKNOWLEDGEMENTS

During the writing of this thesis, the author received many helps from people to whom he would like to thank. First of all I would like to thank my supervisor who authority in the field of the world Prof. Dr. A. Necmeddin YAZICI for his help and advices during the preparation of this thesis. Secondly, I have benefited from the aid and advices of Prof. Dr. Metin BEDİR, Assoc. Prof. Dr. Vural Emir KAFADAR, Assoc. Prof. Dr. Hüseyin TOKTAMIŞ, Assoc. Prof. Dr. R. Güler YILDIRIM during the writing and preparation of this thesis.

TABLE OF CONTENTS

LIST OF FIGURES

LIST OF TABLES

LIST OF SYMBOLS

A_h: recombination transition coefficient for electrons in the conduction band

A_n: transition coefficient for electrons in the conduction band

A_m: transition coefficient for electrons in the conduction band to the deep traps

b: order of kinetic

β: heating rate

E: activation energy

E_a: activation energy

I: thermoluminescence intensity

k: Boltzman's Constant

n: concentration of electrons in the electron traps

n_c: concentration of electrons in the conduction band

n_h: concentration of holes in the recombination centers

n_v: concentration of holes in the valance band

n_0: initial concentration of trapped electrons

N: concentration of available electron traps

N_h: concentration of available hole centers

m: concentration of electrons in the deep traps

M: concentration of available deep traps

p: probability per unit time of the release of an electron from the trap

s: frequency factor or pre-exponential factor

T: temperature

T_m: peak temperature

CHAPTER 1

INTRODUCTION

There have been a number of definitions related to the thermoluminescence (TL) for years but in simplest form is that the thermally stimulated luminescence or simply thermoluminescence is the emission of light from solids such as semiconductors or insulators when they are heated after the application of ionizing radiations such as X, gamma and beta [1]. According to this definition, there are three rules to obtain thermoluminescence phenomena from solids. Firstly, the material must have forbidden band gap. Therefore the materials must be insulators or semiconductors. Because, it is well known that only these materials have band gap. On the other hand, the metals do not have band gap thereupon, they do not exhibit thermoluminescent properties. The second necessity is that the material must be absorbed the energy of ionizing radiation before the heating process. Thirdly, the materials must be emitted light when they are heating process. During the heating process, the emitted light intensity plotted versus temperature is called as TL glow curve. The forms and peak temperatures (T_m) of the measured TL glow peaks are generally used to extract information on absorbed doses by the materials and also the various trapping parameters of the defects within the solid, such as frequency factor (s), trap depth (E_a) (also called the activation energy), trapping and re-trapping rates, the kinetic-order b of the TL glow peaks and etc. [2]. Since the early 1950s, the TL has been one of the important techniques for the measuring nuclear radiation doses [3]. Not only to measure radiation dose, but also the TL materials were applied in the archaeological and geological dating [4-7].

The TL rate equations are used to describe the TL phenomena. The simplest model to describe the physical processes of TL is a single type of trap and recombination center model. This model is called as one trap one recombination center (OTOR) model. The rate equations (analytic equations) are firstly obtained by using this model and then they can be solved under various assumptions to obtain TL

glow curve equations. In general, the experimentally obtained TL glow curves from the TL materials are analyzed by computerized fitting program which is called as computer glow curve deconvolution (CGCD) program to obtain kinetic (trapping) parameters and absorbed doses [8-11]. The application of this method to analyze and deconvolution of TL glow-curve into its individual glow-peaks have been widely applied since 1980 [8]. The CGCD method is a very famous method to obtain kinetic (trapping) parameters since 1990 and this method has great advantages over the other experimental methods (such as initial rise, peak shape, heating rate etc.) to obtain kinetic parameters. Because, this method simultaneous determine the trapping parameters of all TL glow peaks without additional heat treatments and experimental repetitions [12]. If there are more than one glow peak within the TL glow curve, it becomes very difficult to obtain trapping parameters. Because, some interactions and electron transfers are occurred between the traps during the heating process. These processes affect the TL kinetic parameters of glow peaks within the glow curve.

If there are more than one TL glow peaks in the glow curves and the electrons were released from one type of electrons trap may be trapped on other types of electron traps, simply when charge transfers occur among different types of traps, this model is described as the interactive multi traps system or model (IMTS). This situation does not imply that the simple TL model is invalid. Conversely, the IMTS model can assist to interpret the many properties of the one trap one recombination center model [9]. The interactive multitrap system (IMTS) model was generally employed to explain the dose dependence (linear or supralinear) of TL phenomena [10- 14]. In the interactive multi traps system model, it is not necessary to all the electron traps should be active in the temperature range in which the material is heated. Unlike in the one trap one recombination center model, in the interactive multi traps system model not all the electrons in the conduction band excited by the radiation dose are captured by the active electron traps. Another deep trap which is called as thermally disconnected deep trap can be filled with electrons during the irradiation process. These deep traps which also known as competitor captures some of free electrons in the CB during the irradiation stage. On the other hand, when the deep traps (competitors) approach saturation, the interaction between the active electron trap and competitor disappears and there upon, the interactive multi traps system model turns into the non-interactive multitrap system (NMTS) model [9].

In this thesis, we have investigated how well the fitting process (computer glow curve deconvolution) works in providing reliable values for the kinetic parameters of the traps with OTOR and IMTS (interactive multi trap system) methods by resorting mathematica program. Firstly, the relevant rate equations describing the transfer of electrons between traps and the luminescence center were used without approximation to numerically generate and obtain simulated TL glow curves after a wide range of trapping parameters. And then, the numerically simulated TL glow curves were analyzed by the general fitting method using analytical expressions. The obtained kinetic parameter values by fitting procedure were then compared with the input values used in generating the TL glow curves. In this study, one of the fitting program is GLOCANIN. It was written by A.J.J. Bos at the Reactor Institute at Delft, The Netherlands [15]. This program has been successfully used in TL&OSL laboratory in our department and in many laboratories over a number of years. On the other hand, it is well known that the CGCD method cannot yield the correct trapping parameters in cases where two or more peaks are highly overlapped [16]. Another fitting method in this study is the Microsoft Excel Spreadsheet program with the powerful solver utility [17]. It was developed by the G.Kitis in 2011 [17]. The computerized curve deconvolution (CCD) analysis of the TL glow curves into their individual glow peaks and optically stimulated luminescence (OSL) decay curves into their components have been recognized over the last 30 year to be of major importance [8, 18-20]. As a result, the obtained numerically generated glow curves with OTOR and IMTS models by Mathematica program were fitted each GLOCANIN and Excel Spreadsheet programs, and both analysis results were compared with each other and input values and all of them are reviewed.

The thesis consists of five chapters. Chapter 2 explains the thermoluminescence phenomena, its mathematical expressions and some important models for thermoluminescence and also the methods to evaluate the kinetic parameters responsible for the TL emission. Some Mathematica program examples were given for analyzing of some used situations in Chapter 3.

All the CGCD results after fitting with GLOCANIN and Excel Spreadsheet programs were given in chapter 4 with their inter comparisons. Finally, in Chapter 5 all the results of analysis were concluded and discussed with support of the literature.

CHAPTER 2

THEORY OF THERMOLUMINESCENCE

2.1 What is Luminescence?

When electromagnetic light is incident on a material, some of its energy may be absorbed by the material and then re-emit as light at a longer wavelength (Stoke's Law). This process is called as luminescence. The wavelength of the emitted light is only characteristic of the material and not dependent upon the incident radiation. Usually, the most studies of luminescence phenomena are concerned with the emission of visible light due to human eye response. On the other hand, other wavelengths such as ultraviolet or infrared can also be emitted during this process. There are various types of luminescence phenomena. They are given names which reflect the type of radiation used to excite the emission [2]. The some types of them are:

Photoluminescence: The source of energy is photon. There are two types of photoluminescence. They are: Fluoresans: Rapid (nanoseconds) emission of photons as electrons jump from excited state to ground level.

Phosphorescence: Delayed (milliseconds to hours) emission of photons that have been trapped in a 'forbidden' state.

Chemiluminescence: The source of energy is chemical reaction. Bioluminescence: Biochemical reactions in living organisms (like fireflies). Electrochemiluminescence: Resulting from electrochemical reactions.

Electroluminescence: The source of energy is electric current passing through a substance. It includes; cathodoluminescence which is resulting from electrons striking a luminescent material.

Mechanoluminescence: The source of energy is mechanical action on a solid. For example, it includes triboluminescence. It is generated when bonds in a material are broken when that material is scratched, crushed or rubbed. Fractoluminescence is generated when bonds in certain crystals are broken by

fractures. Piezoluminescence is produced by the action of pressure on certain solids. Sonoluminescence is generated by imploding bubbles in a liquid when excited by sound.

Radioluminescence: The source of energy is ionizing radiation. When the material is bombardment by ionizing radiation, it emits light.

Thermoluminescence: The source of energy is heat. When the substance is heated it reemits previously absorbed energy by the ionizing radiation.

When we characterize atoms of a crystal by three-dimensional periodicity it is observed that there are some point defects within the crystal. Point defects within a crystal are characterized as:

1. Intrinsic defects: Missing of atoms in its original location which is called as vacancy. The other forms are; interstitials, aggregate forms of defects.
2. Color centers: These types of point defects are induced by ionizing radiations. Some of them are F centers, V centers, V_k centers, etc.
3. Extrinsic (or impurity) defects: They are substitutional of impurities or interstitial impurities.

The property of storing energy is due to the presence of crystal defects such as vacancies and impurities. The luminescence phenomena can be observed due to all defects can be potentially acted as traps or recombination center for charge carriers created by suitable excitation. The defects are able to capture the electrons and holes generated in the irradiation process. A crystal defect is classified as a trap center if the defect is able to capture a charge carrier and reemit it back to the band it come from. A crystal defect where carriers of opposite sign can be captured, resulting in an electron-hole recombination, is classified as a recombination center. Efficient thermoluminescent materials have a high concentration of traps and recombination centers, provided by structural defects and impurities [21]. Thus, an electron-hole pair is assumed initially to consist of a conduction electron and a valence hole. Exchange of charge carriers between the crystal defects are assumed to take place through the conduction and valence band [22-23].

Figure 2.1 is a demonstration of an energy level diagram of crystalline materials that is commonly used to represent the trapping mechanism involved in luminescence. Electron traps are represented by T. Its trap depth is indicated by '*E*' as shown in Fig.2.1 (b). The trap depth is an indication of the efficacy of a given trap.

The lattice vibration is another important term that perturbs the stable traps that could dislodge the electrons from their traps. The stimulation of the crystal lattice structure by heating up to an appropriate temperature or by optical means using a suitable wavelength, these methods will excite the electrons out of the traps. Once electrons are expelled from their respective traps, they diffuse through the crystal lattice until they come across another site that is attractive to electrons and these are referred to as recombination centers[24].

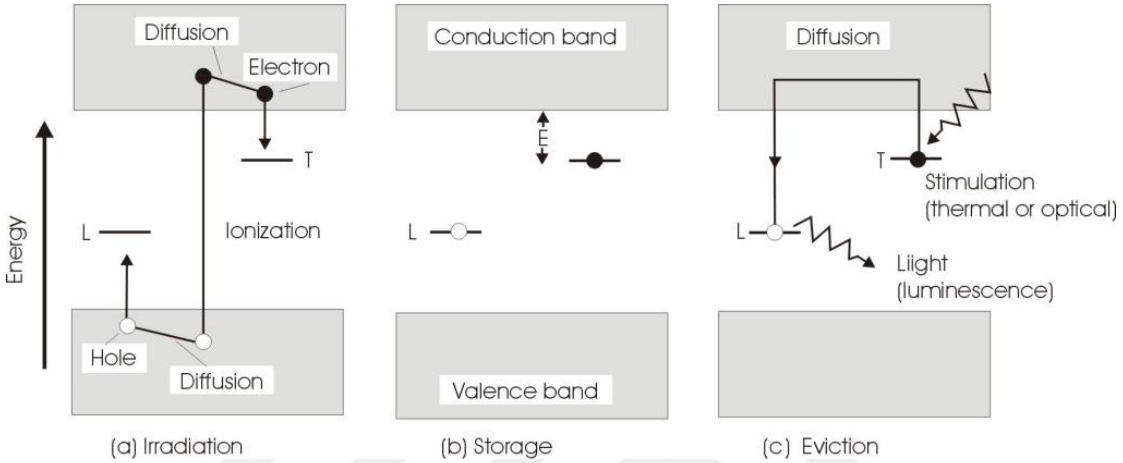

Figure2.1: The energy band diagram of crystals (redrawn by Ken Munyikwa from [17]). It illustrates the creation of trapping and luminescence centers in crystal lattices due to exposure to ionizing radiation. (a) Ionizing radiation leads to electrons in valance band (VB) being expelled from their original site to the conduction band (CB) and diffuse of electron within the lattice. (b) Electrons are trapped by electron traps while holes are localized at particular (luminescent) centers. (c) Stimulation of electrons from electron traps by heat or light results in electrons being evicted from the traps and diffusing until they meet are combination (luminescent) center. Light is emitted when luminescence centers are encountered by the electrons to give TL or OSL.

When the crystal is heated, the trapped (captured) electrons by electron traps and holes by the hole traps can be freed thermally into the CB or VB, respectively, and then make a transition to the radiative recombination center R. This process is termed thermally stimulated luminescence or simply thermoluminescence (TL). Alternatively, external light exposure of the crystal can release captured electrons from a trap center to the conduction band from where they can recombine into the recombination center R. This phenomenon is termed optically stimulated luminescence (OSL).

The optically or thermally freed charge carriers in the conduction/valance band can be measured as electrical current when a voltage source is applied across the crystal. These measurements are termed thermally and optically stimulated conductivity (TSC, OSC), respectively.

2.2 Thermally Stimulated Luminescence or Thermoluminescence (TL)

The thermally stimulated luminescence or usually termed as thermoluminescence (TL) is a physical phenomenon that thermoluminescence dosimetry (TLD) has been used extensively to measure nuclear radiation doses since the early 1950s [3] after availability of sufficiently sensitive and reliable photomultiplier (PM) tubes in TLD readers. On the other hand, the TL was subsequently applied to archaeological dating in the early 1960s [4-6] and to geological dating in the beginning of the 1980s [7]. TL phenomena and dating methods are reviewed by Aitken [5]. The TL is usually observed by heating a sample at a constant heating rate to the finite desired temperature (e.g. 500 ^{o}C) and recording emitted light from the sample by means of TLD reader as function of temperature. The observed TL signal is called as "glow curve", with distinct TL peaks occurring at different temperatures. The peak temperature is related with depth of electron traps present within the sample. The point defects in the lattice structure are generally responsible from these traps.

A typical defect may be created by the dislocation of a negative ion within the lattice it provides a negative ion vacancy that behaves as an electron trap. Once electrons are trapped, they will eventually be evicted by thermal vibrations of the lattice due to heating of samples. As the temperature of sample is raised, it causes an increase in the lattice vibrations of crystal, and the probability of eviction of electrons from the electron traps increases so rapidly that within a narrow temperature range, the trapped electrons are quickly liberated from electron traps. Some of the free electrons then give rise to radiative recombinations with trapped "holes" within the recombination (luminescent) centers, resulting in emission of light. This process is simply known as thermoluminescence (TL).

2.3 Models for Thermoluminescence

The main goal of a mathematical analysis related with the thermoluminescence emission of light is to obtain a satisfactory knowledge of the phenomena related to the TL. The TL is directly related with the energy band

structure of TL materials from a theoretical perspective. The band structure is especially affected with impurities and lattice irregularities which they are descried as defect centers. They can be occurred when ions of either sings (positive or negative)move away from their original points. Therefore, the leaving vacancy states are able to interact with free charges due to irradiation of materials and trap them. Alternatively, the ions can be diffused within the lattice and they can be settling down in interstitial positions. The sizes of these ions are different from their neighbors. Because of their size differences, they break locally the ideal lattice geometry and thereupon the impurity ions can disturb the lattice array of the crystal structure. Moreover, these defects can be interacted with each other, and then they can be form more complex defects. From an atomic concept, these defects can be explained by means of their sign and number of charge carriers that may interact with them. A characteristic energy for each center correspond the eventual existence of excited states within the band gap of material. To such a description, this may be defined as the amount of energy able to set the trapped free charges. Then the centers destroy and forma situation of local order. It is well known that the energy band structure is described in terms of VB and CBs which separated from each other by an energy forbidden gap. These defects are represented as localized sites at various depths within the band gap where free charges of either sign may be trapped. Therefore, the energy band structure reveals quite a complex configuration. The experimental TL studies can be providing a satisfactory tool to get detailed information on TL kinetic parameters. The most important of them are trap depth (E) of trap, a frequency factor (*s*) connected to the transition frequency, and a kinetic order (*b*) synthesizing the quality of the involved phenomena.

The kinetic order is generally obtained between 1 and 2. When the value of b=1, it corresponds to a situation where electrons are supplied energy to raise in the CB and, consequently, they fall to a luminescent center where it undergoes recombination with holes. If b=2; the free electrons in the CB has the same probability of retrapping and recombination. If b is between 1 and 2, it is likely to occur that retrapping and recombination probabilities are different from each other. The mathematical models based on these definitions are related with different equations. Each of them yields the evolution of charged carrier populations. The analytical forms of each of them are to be checked by means of suitable experimental data. Therefore, it is evident that how the involved parameters are to be conveniently

adjusted until a fair agreement between theory and practice is attained. The most important tool is firstly observation and recording of TL emission intensity as a function of temperature or time when the TL sample is heated after several experimental conditions. For a constant heating rate, the observations as a function of temperature or time are equivalent. The shape of glow curves depends on the physical and chemical properties of the material and on the kind of the preirradiation heat treatment before reading. A single- or multi-peak glow structure can be obtained. As may be expected from the TL equations, a correspondence can be pointed out between a peak and an electron trap level. At a certain temperature, the amount of thermal energy supplied reaches for a given electron trap level. It is the threshold energy which is necessary to raise the trapped charges in the trap to the conduction band from where they can give rise to radiative recombination events. For this purpose, recombination centers should be opposite sites to the electrons and they are involved as positive traps for charge carriers. They are likely to be connected to the quality of the emitted light. The analytical form for a single peak can fully described by means of some geometrical parameters such as the peak position, the overall peak width and the height. This last one is dependent on the heating rate and absorbed doses. It increases with the increasing of absorbed doses and at the same time heating rate for given experimental conditions. The geometrical parameters can be shown to correspond to the main physical ones: the mathematical expressions can be evaluated by a convenient analytical manipulation of the involved equations. It is also to be remarked that the experimental uncertainties, obtained by means of the glow-curve plot, allow for an estimate of the physical errors related to them, and their evaluations can point out a well-defined method as the fittest one.

2.3.1 Randall-Wilkins model (First-order kinetics)

Randall and Wilkins [25] were developed a mathematical equation for each TL peak in a glow curve, starting from studies based on the phosphorescence. Their mathematical equation was based on the energy band diagram. Nowadays, the developed equation is well-known as first-order TL expression. The Fig. 2.1 shows the simple band model used for theoretical treatment of TL model. As seen, there are two localized levels (metastable states) between the delocalized bands (CB and VB), one acting as a trap, T, and the other acting as a recombination center, R. The energy difference (distance) between the trap T and the bottom of the CB is

called as activation energy or simply the trap depth E. The activation energy is the required energy to liberate a charge trapped by the trap, i.e., an electron, which is trapped in T [25-27].

The absorption of light energy when its energy hν>E_g, it results in ionization of valence electrons from the VB to the CB. It produces energetic electrons in the CB and holes in the VB. Then, after excitation, free electrons pass to the CB(transition 1)and free holes in the VB. The free charge carriers recombine with each other or become trapped by their respective traps. When the free electrons are directly recombine with holes in the VB, an amount of energy which is equal to band gap energy (E_g) will be released. This energy may excite a luminescent center which relaxes (returns to the ground state) under the emission of light. However, in semiconductors and insulators, a certain percentage of the charge carriers was trapped at T and R (transition 2).

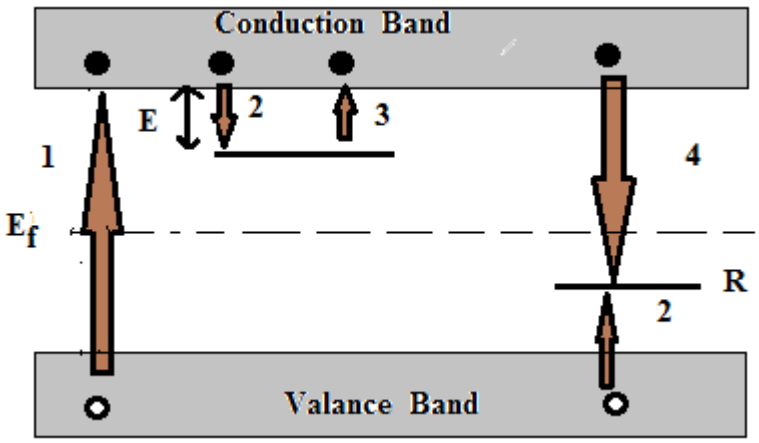

Figure 2.2. The energy band model showing the transitions of charges in a TL material according to a simple one trap one recombination center (OTOR) model (1) generation of electrons and holes; (2) trapping of electron and hole by the respective traps; (3) electron release due to thermal stimulation; (4) recombination. (•) shows electrons, (◦) shows holes. Level T is an electron trap, level R is a recombination center, E_f is Fermi level.

The Arrhenius equation gives the probability p, per unit of time, that a trapped electron will escape from the trap, or the probability rate of escape per second. According to this equation, the electrons in the trap have a Maxwellian distribution of thermal energies and it has a probability (p) to escape from the trap

$$p = s \exp\left\{-\frac{E}{kT}\right\} \tag{2.1}$$

where E is the trap depth (eV), k the Boltzmann's constant (8.85×10^{-23} J/K), T the absolute temperature (K), s the frequency factor ($\sec^{-1}$).The frequency factor is the number of hits of an electron to the potential well in the trap. The lifetime, τ, of the charge carrier in a trap (metastable state) at temperature T, is given by

$$\tau = p^{-1} \tag{2.2}$$

If n is the number of trapped electrons in the electron tarp$T$ and if the temperature is kept constant, then n decreases with time t according to the following expression:

$$\frac{dn}{dt} = -np \tag{2.3}$$

integrating this equation

$$\int_{n_o}^{n} \frac{dn}{n} = -\int_{t_o}^{t} p.dt \tag{2.4}$$

one obtains

$$n = n_o . \exp\left[- s \exp\left\{ - \frac{E}{kT} \right\} .t \right] \tag{2.5}$$

where n_o is the number of trapped electrons in the electron traps at the initial time $t_0 = 0$. After the following assumptions:

- During the irradiation process of the thermoluminescent material at a low enough temperature so that no electrons are released from the trap,
- the life time of the electrons in the CB is short,
- all the released charges, i.e. electrons, from trap recombine in luminescent center with opposite sign charges,
- the efficiency of luminescence of the recombination centers (RC) is independent of temperature,
- the concentrations of traps and RCs are temperature independent,
- no electrons released from the trap is re-trapped

The TL intensity (I (t)) (photons per second) at any time t during the heating process is proportional to the rate of recombination of electrons and holes at the recombination centers. If m (m^{-3}) is the concentration of holes trapped at RC, then the TL intensity I (t) can be written as

$$I(t) = -\frac{dh}{dt} \tag{2.6}$$

In here, it was assumed that each recombination process produces a photon and then all produced photons after recombination are detected by the TL reader. The rate of recombination probability will be proportional to the concentration of free electrons (n_c) in the CB and the concentration of holes h in the RC

$$I(t) = -\frac{dh}{dt} = n_c hA \tag{2.7a}$$

where A is a constant which is called recombination probability expressed in units of volume per unit time and it is assumed that A is independent to the temperature.

The rate of change in the concentration of trapped electrons n is equal to the rate of thermal release of electrons from the traps and minus the rate of re-trapping of electrons by the traps,

$$-\frac{dn}{dt} = np - n_c(N-n)A_r \tag{2.7b}$$

In here, N is the concentration of electron traps, N-n the empty traps and A_r the probability of retrapping (m^3/s). Along the same lines, the rate of concentration of free electrons in the CB is equal to the rate of thermal release from the electron traps minus the rate of retrapping by the traps and the rate of recombination by the RC,

$$\frac{dn_c}{dt} = np - n_c(N-n)A_r - n_c hA \tag{2.7c}$$

Equations (2.7a)-(2.7c) described the charge carrier traffic in the case of release of a trapped electron from an electron trap and recombination in a recombination center. Correlatively the rate equations for the release of holes from the hole traps are similar to equations (2.7a-c). These rate equations are the basis of many analyses of TL phenomena. On the other hand, there is no general analytical solution of these rate equations. Some simplifying assumptions must be made to develop an analytical expression. An important assumption is at any time

$$\left|\frac{dn_c}{dt}\right| << \left|\frac{dn}{dt}\right|, \qquad \left|\frac{dn_c}{dt}\right| << \left|\frac{dh}{dt}\right| \tag{2.8}$$

These assumptions were firstly made by Chen and McKeever [12]. They are called as the quasi-equilibrium assumption since it requires that the free electron concentration in the CB is quasi-stationary. The trapped electrons and holes are produced in pairs during the irradiation. Moreover, the charge neutrality dictates that

$$n_c + n = h \tag{2.9}$$

here $n \approx h$ when $n_c \approx 0$

$$I(t) = -\frac{dh}{dt} \approx -\frac{dn}{dt} \tag{2.10}$$

Since $dn_c/dt \approx 0$ one gets from (2.7a) and (2.7b):

$$I(t) = \frac{hAns \exp\left\{-\frac{E}{kT}\right\}}{(N-n)A_r + hA} \tag{2.11}$$

Equation (2.11) cannot be solved analytically without additional simplifying assumptions. Therefore, Randall and Wilkins [15-17, 21-22] assumed another approximation ($hA >> (N-n)A_r$) which is negligible retrapping during the heating stage. After this additional assumption, the above equation (2.11) can be rewritten as

$$I(t) = -\frac{dn}{dt} = n.p = sn \exp\left\{-\frac{E}{kT}\right\} \tag{2.12}$$

Equation (2.12) represents an exponential decay of phosphorescence. Substituting eqn. (2.5) in eqn. (2.12), we obtains:

$$I(t) = n_o.s.\exp\left(-\frac{E}{kT}\right)\exp\left[-s.t.\exp\left\{-\frac{E}{kT}\right\}\right] \tag{2.13}$$

The temperature is usually raised as a linear function of time according to

$$T(t) = T_o + \beta t \tag{2.14}$$

with β the constant heating rate and T_0 the temperature at t=0. With using eq.(2.14), heating rate can be rewritten as β=dT/dt and introducing it into equation (2.4)

$$\int_{n_o}^{n} \frac{dn}{n} = -\left(\frac{s}{\beta}\right)\int_{T_o}^{T} \exp\left(-\frac{E}{k.T'}\right)dT' \tag{2.15}$$

and the number of trapped electrons (n) in term of β

$$n = n_o.\exp\left[-\left(\frac{s}{\beta}\right)\int_{T_o}^{T} \exp\left(-\frac{E}{k.T'}\right)dT'\right] \tag{2.16}$$

Then, using eqn. (2.12), the TL intensity equation becomes as function of temperature

$$I(T) = -\frac{1}{\beta}\frac{dn}{dt} = n_o \frac{s}{\beta}\exp\left\{-\frac{E}{kT}\right\}\exp\left\{-\frac{s}{\beta}\int_{T_o}^{T}\exp\left\{-\frac{E}{kT'}\right\}dT'\right\} \tag{2.17}$$

As a result, the equation 2.17 is the well-known Randall–Wilkins first-order TL expression of a single glow peak. The first-order TL peak has a characteristic

asymmetric geometric shape. It is wider on the low temperature side than on the high temperature side. On the low temperature side of glow peak, i.e. in the initial rise of peak, the TL intensity is dominated by the first exponential (exp (-*E*/*kT*)). Thus, if the TL intensity (*I*) is plotted as function of 1/*T*, a straight line with the slope of -*E*/*k* is obtained in the initial rise temperature range from which the activation energy *E* is readily found.

Some of the properties of Randall–Wilkins equation are illustrated in Fig. 2.3. For example, figure 2.3 (a) shows how $I(T)$ varies as a function of n_0 while the other kinetic parameters are kept constant. It is seen that the peak temperature, T_m, stays fixed while increasing of n_o. This is a characteristic property of all first-order TL glow peaks. For first-order kinetic, when the derivative of peak maximum intensity is setting to zero $dI/dt=0$ (or, somewhat easier from $d\ln I(T)/dt=0$), one gets another equation (2.18) which frequency factor is easily obtained.

$$\frac{\beta E}{kT_m^2} = s\exp\left\{-\frac{E}{kT_m}\right\} \tag{2.18}$$

As seen, in this equation, n_0 does not appear. Therefore, it shows that T_m does not depend on n_0. It can be further seen from figure 2.3a that not only the peak height I_m at the maximum but also each point of the curve is proportional to n_0.

In the radiation dosimetry applications, n_0 is a most important parameter. Because, this parameter is proportional with the absorbed dose by the dosimetry. The area under the first order TL glow peak is equal to n_0 since n_∞ is zero for $t\to\infty$.

$$\int_0^\infty I(t)dt = -\int_0^\infty \frac{dn}{dt}dt = -\int_{n_0}^{n_\infty} dn = n_0 - n_\infty \tag{2.19}$$

Figure 2.3(b) shows the first-order TL glow peaks as a function of the activation energy *E* which has been varied from 0.8 to 1.2 eV. As seen, if *E* increases, the peak temperature shifts to higher temperature sides with a decreasing of TL intensity and an increase in the width keeping the area (i.e. n_0) constant.

On the other hand, when the frequency factor changes and it is increased (see Fig. 2.3(c)), now an opposite behavior is obtained. As seen, as *s* increases the peak temperature shifts to lower temperature sides with an increase of the height of peak intensity and a decrease in peak width.

Figure 2.3(d) shows the glow curves as a function of the heating rates. As seen, when β increases, the peak temperature shifts to higher temperature sides while the peak height decreases and the peak width increases just as in the case of decreasing *s*.

It is necessary to note that two parameters, namely the activation energy *E* and the frequency factor *s* are especially the main physical parameters. They are generally called as the trapping parameters or kinetic parameters. They depend upon the properties of the trapping center. On the other hand, the other important parameter is the kinetic-order (*b*) that can be obtained by the experimenter after choosing a certain dose (n_0) and read-out of the TL intensity at a certain heating rate β. Therefore, the investigations of trap depth and frequency factor of a new TL material will mostly start after studying the glow peak behavior under variation of the absorbed dose and the heating rate to obtain *b*.

The evaluation of integral in eqn. (2.17) is not elementary solved in the case of linear heating rate. Therefore, Chen [28] has also assumed that the integral in this equation can be approximated after asymptotic series. In practical dosimetric applications, the glow peak is easily explained in terms of two parameters. They are namely the intensity of peak at the maximum I_{m} and the temperature at the maximum T_{m}. Then, by using successive integration by parts, in a second-order approximation (integral approximation) it becomes

$$\int_{T_0}^{T} \exp(-\frac{E}{kT'})dT' = \frac{kT^2}{E}(1-\frac{2kT}{E})\exp(-\frac{E}{kT}) \tag{2.20}$$

Hence, Eqn. (2.20) becomes

$$I(T) = sn_0 \exp\left(-\frac{E}{kT}\exp\left[-\frac{skT^2}{\beta E}(1-\frac{2kT}{E})\exp(-\frac{E}{kT})\right]\right) \tag{2.21}$$

From which the condition at the maximum is given as in Eqn.(2.18) or

$$s = \frac{\beta E}{kT_m^2}\exp\left\{-\frac{E}{kT_m}\right\} \tag{2.22}$$

inserting Eqn.(2.22) into Eqn.(2.21) one obtains

$$I_m = \frac{n_0 \beta E}{k T_m^2} \exp\left[-\left(1 - \frac{2kT_m}{E} \right) \right] \tag{2.23a}$$

or better

$$I_m = \frac{n_0 \beta E}{k T_m^2} \exp\left[-(1 - \Delta_m) \right] \tag{2.23b}$$

Equation (2.24b) can be rewritten as

$$\frac{n_0 \beta E}{k T_m^2} = I_m \exp\left[-(1 - \Delta_m) \right] \tag{2.24}$$

Inserting Eqn.(2.18) into Eqn.(2.17), Kitis et al. [29] have shown that eqn. (2.17) can be quite accurately approximated by

$$I(T) = I_m \exp\left[1 + \frac{E}{kT} \frac{T - T_m}{T_m} - \frac{T^2}{T_m^2} \exp\left\{ \frac{E}{kT} \frac{T - T_m}{T_m} \right\} (1 - \Delta) - \Delta_m \right] \tag{2.25}$$

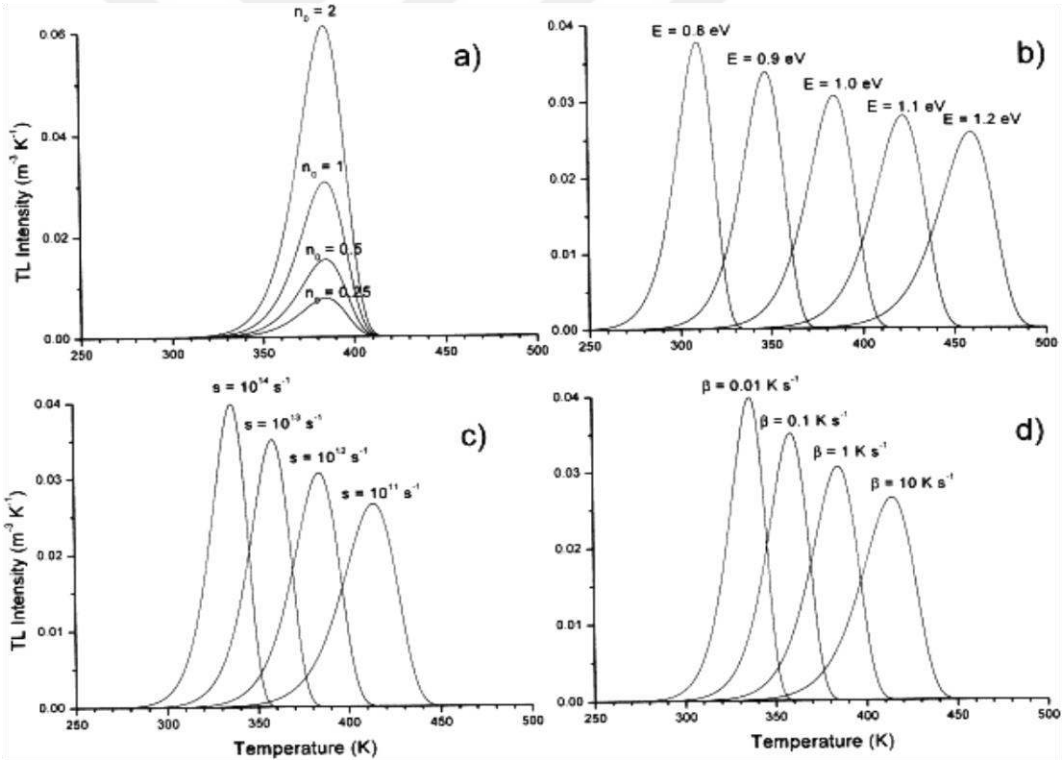

Figure 2.3: Some of the properties of the Randal–Wilkins first-order TL equation. It show glow curves after variation of (a) n_0, the concentration of trapped charge carriers after irradiation; (b) E, the activation energy, (c) s, frequency factor, (d) β, heating rate. Input parameter values are n_0=1 m^{-3}; E=1 eV; s=1×10^{12} s^{-1}, β=1 K/s of which one parameter is varied while the others are kept constant. [9]

with $\Delta=2kT/E$ and $\Delta_m=2kT_m/E$. On the other hand, by keeping a lot of terms in the above approximation, Bos et.al. [15] were approximated the following first-order TL glow curve expression,

$$I(T) = n_0 s \exp(-\frac{E}{kT}) \exp\left[(-\frac{s}{\beta}\frac{kT^2}{E}\exp(-\frac{E}{kT}) * (0.9920 - 1.620\frac{kT}{E_a}) \right] \quad (2.26)$$

2.3.2 Garlick-Gibson Model (Second-order kinetics)

In 1948, in their phosphorescence studies, Garlick and Gibson [27] have been considered that when a free charge carrier has probability of either being trapped or recombining within a recombination center. The second-order (b=2) TL kinetic models is used to depict a situation in which retrapping of electrons is present. According to this model, the escaping electron from the trap in the CB has equal probability of either being re-trapped by traps or recombining with hole in a recombination center.

They considered that if retrapping dominates, $mA << (N-n)\,Ar$. In addition, they assumed that the electron trap is far from saturation, i.e. $N>>n$ and $n=m$. The equation (2.11) becomes after these assumptions

$$I(t) = -\frac{dn}{dt} = s\frac{A}{NA_r}n^2 \exp\left\{-\frac{E}{kT}\right\} \quad (2.27)$$

Here, dn/dt is proportional to n^2, which means a second-order reaction. The equation (2.27) is solved with the additional assumption of equal probabilities of recombination and retrapping, $A_n=A_h$ which gives us

$$I(T) = \frac{n_0^2}{N}\frac{s}{\beta}\exp\left\{-\frac{E}{kT}\right\}\left[1 + \frac{n_0 s}{N\beta}\int_{T_0}^{T}\exp\left\{-\frac{E}{kT'}\right\}dT'\right]^{-2} \quad (2.28)$$

This equation is known as the Garlick–Gibson TL equation for second-order kinetics. The main property of this glow peak is that it is more symmetric than the first-order kinetics. In this case, the high temperature half side of the glow peak is slightly broader than the low temperature half-side. This can be understood from the consideration that electrons in the CB are retrapped before they recombine in the second-order (b=2) models. Meantime, it is giving rise to a delay in the luminescence emission and spreading out of the emission of light over a wider temperature range.

In the second-order model, the initial concentration of trapped electronsn_0 appears not merely as a multiplicative constant as in the first-order case. In this case, the shape of the glow curve changes after the variation of dose levels. It is represented in figure (2.4(a)). As seen, when n_0 increases T_m decreases. The shift in the peak temperature is easily derived by the following equation [30].

$$T_1 - T_2 \approx T_1 T_2 \frac{k}{E} \ln f \tag{2.29}$$

WhereT_1 is the peak temperature at a certain dose and $T_2$is the other peak temperature of same glow peak after *f*-times higher dose. Figure (2.4) show some of the glow curves after various kinetic parameters and dose levels. According to this model, if the absorbed dose is increased by a factor 1000, ≈77 K is expected in the peak temperature when we choose E=1 eV andT_1=400 K. From Eqn. (2.28) it can be understood that the shallower trap (the smaller E), the higher shift in the peak temperature. Figure (2.4(b)) demonstrates the variation in shape (peak temperature,

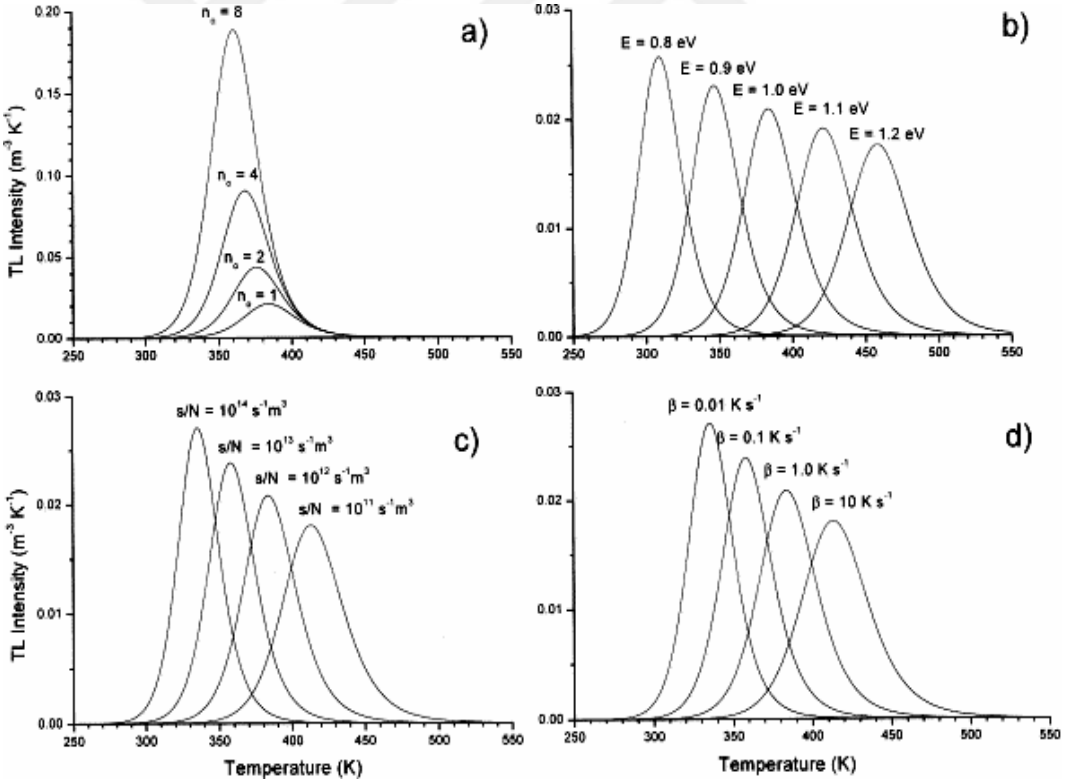

Figure 2.4: Properties of the Garlick–Gibson second-order (b=2) TL equation. It shows the variation of glow curves: (a)n_0, the concentration of trapped charge carriers after irradiation; (b) E, the activation energy; (c) s/N; (d) β, the heating rate. Input parameter values were chosen as: n_0=1 m^{-3}; E=1 eV; s/N=1×10^{12} s^{-1} m^3, β=1 K/s of which one parameter is varied while the others are kept constant [9].

position and size)of a second-order peak as function of *E*. Similarly, Figures (2.4(c)) and (2.4(d)) shows the variations in the shape of glow peaks as a function of *s*/*N* and heating rateβ, respectively. The area under the glow peak is proportional to the initial concentration $n_0$as in the case of first-order kinetics but the peak height is no longer directly proportional to the peak area, although the deviation is small.

As in the case of first-order kinetics, the exponential term (exp(-*E*/*kT*)) is dominating in the intensity of glow peak at the initial rise of glow curve. Therefore, the initial rise method can be applied for the determination of the trap depth *E*. The second-order kinetics is further simplified when inserting the integral given by Eqn. (2.20) into eqn. (2.28). So, one gets

$$I(T) = sn_0 \exp\left\{-\frac{E}{kT}\right\}\left[\frac{skT^2}{\beta E}(1-\Delta)\exp(-\frac{E}{kT})+1\right]^{-2} \tag{2.30}$$

from which the condition at the maximum, *s* is given by

$$s = \frac{\beta E}{kT_m^2}\frac{1}{1+\Delta_m}\exp\left(\frac{E}{kT_m}\right) \tag{2.31}$$

or rearranging it,

$$s\exp\left(-\frac{E}{kT_m}\right) = \frac{\beta E}{kT_m^2}\frac{1}{1+\Delta_m} \tag{2.32}$$

The eqn. (2.30) can be rewritten for the peak intensity at the maximum:

$$I_m = sn_0 \exp\left\{-\frac{E}{kT}\right\}\left[\frac{skT_m^2}{\beta E}(1-\Delta_m)\exp(-\frac{E}{kT})+1\right]^{-2} \tag{2.33}$$

The substution of eqn.(2.31) into eqn.(2.30) gives the following expression for *I(T)*

$$I(T) = \frac{n_0\beta E}{kT_m^2}\frac{1}{1+\Delta_m}\exp\left[\frac{E}{kT}\left(\frac{T-T_m}{T_m}\right)\right]\ x\left(\frac{T^2}{T_m^2}\frac{1-\Delta}{1+\Delta_m}\exp\left[\frac{E}{kT}\left(\frac{T-T_m}{T_m}\right)\right]+1\right)^{-2} \tag{2.34}$$

substituting Equation (2.32) into Equation (2.33) we get a more simplified expression for I_m:

$$I_m = \frac{n_0\beta E}{kT_m^2}\frac{1}{1+\Delta_m}(\frac{2}{1+\Delta_m})^2 \tag{2.35}$$

which can be rewritten as

$$\frac{n_0 \beta E}{k T_m^2} \frac{1}{1+\Delta_m} = I_m \left(\frac{2}{1+\Delta_m}\right)^2 \tag{2.36}$$

eqn. (2.35) is now put into eqn. (2.34) for getting the final expression for the TL intensity:

$$I(T) = 4 I_m \exp\left(\frac{E}{kT}\frac{T-T_m}{T_m}\right) \times \left[\frac{T^2}{T_m^2}(1-\Delta)\exp\left\{\frac{E}{kT}\frac{T-T_m}{T_m}\right\} + 1 + \Delta_m\right]^{-2} \tag{2.37}$$

with Δ and Δ_m the same meaning as in eqn. (2.25).

2.3.3 May- Partridge Model (General-order kinetics)

The Randal-Wilkins (b=1) and Garlick-Gibson (B=2) TL kinetic models have been derived after the using of some specific assumptions. However, some experimental studies have been represented that these models do not hold to explain some glow peaks that they will not fitted neither first- nor the second-order kinetics. To analyze these types glow peaks, May and Partridge [31] used an empirical expression which is namely called as general-order (b≠1 and 2) TL kinetics.

$$I(t) = -\frac{dn}{dt} = n^b s' \exp\left\{-\frac{E}{kT}\right\} \tag{2.38}$$

In here; s is called as pre-exponential factor and it has the dimension of $m^{3(b\text{-}1)}$ s^{-1} and b is kinetic order that is not necessarily 1 or 2. The integration of eqn. (2.38) for $b \neq 1$, which gives

$$I(T) = \frac{s''}{\beta} n_0 \exp\left\{-\frac{E}{kT}\right\}\left[1 + (b-1)\frac{s''}{\beta}\int_{T_0}^{T} \exp\left\{-\frac{E}{kT'}\right\} dT'\right]^{-b/(b-1)} \tag{2.39}$$

This equation includes the second-order kinetics (b=2) and reduces to first-order kinetics when $b \rightarrow 1$. It should be noted that the dimension of s' should be $m^{3(b\text{-}1)}$ s^{-1}in eqn. (2.38) to obtain a physical unit of s''. The general-order kinetics is useful since intermediate cases can be dealt with and it smoothly goes to first- and second-orders when $b \rightarrow 1$ and $b \rightarrow 2$, respectively (see Fig.2.5).

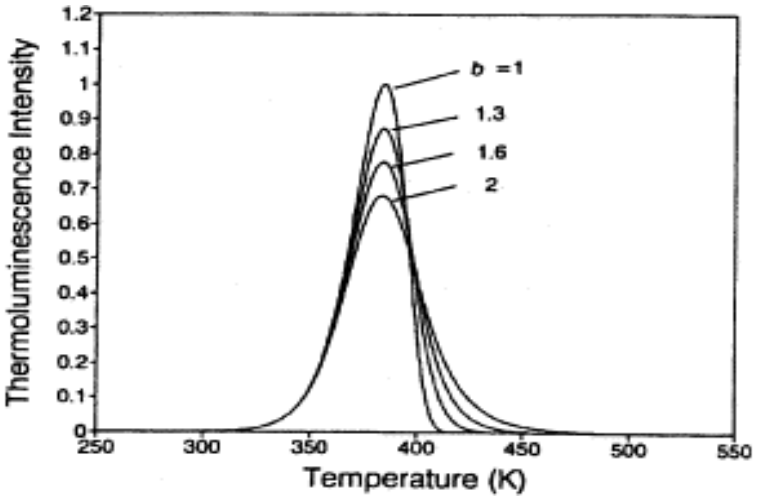

Figure 2.5: Comparison of first-order (b=1), second-order (b=2) and intermediate-order (b=1.3 and 1.6) TL glow peaks with E=1 eV, $s''=1\times10^{12}$ s^{-1}, $n_0=N=1$ m^{-3} and β=1 K/s (from [29]).

2.3.4 Advanced models

The TL phenomenon is generally and most simply explained by the one trap–one center (OTOR) model. This model is enough to explain the behavior of the area under the GC after various applied dose and heating rates. Unfortunately, there is no any TL material that accurately described by this simple model. This means that this model does not make sense. On the contrary, this model help us the interpretation of many features of TL phenomenon, which can be considered as variations of the OTOR model. On the other hand, there are many books and documents to discuss all the realistic advanced TL models in detail. For example; the reader is referred to the excellent text written by Chen and McKeever [12]. It has deeper and quantitative treatment about TL. In this thesis, we have only and very briefly mentioned by advanced model to get some idea about the complexity of the phenomenon in a real TL material.

It is well known that real TL materials have more than one single electron trap and recombination center. Moreover, some of them can be active and some of them can be inactive in the temperature range in which the material is heated. The inactive traps are called as thermally disconnected deep traps (TDDT). The TDDTs can be filled with electrons during irradiation process. But they have so trap depths which are much greater than the active traps such that when the TL material is heated only electrons trapped in the active trap (AT) are freed (see Fig.2.6(a)). The electrons trapped in the TDDTs are not affected by the heat energy. In the figure, this deep

traps is shown by deep electron trap (DET) (Fig.2.6 (a). Therefore, it is said to be thermally disconnected. On the other hand, its existence in the material affects trap filling processes which in turns it eventually affects the shape of the glow curve [32].

In the TL phenomena, it is generally assumed that the trapped electrons are released from the respective traps during heating process while the trapped holes are stable in the hole traps which is called as recombination center. On the other hand, a description of TL phenomena can be done in which the trapped holes are released from the hole traps and they recombine with an electron in an electron trap. In this case, the electrons are more stable than the holes during the heating of TL material. The mathematic of both approximations is identical to each other. There is another situation in which both trapped electrons and holes are released from their traps at the same time at the same temperature interval. In this case, the holes are being thermally released from the hole traps are acting as recombination center for the thermally released electrons at the same time and vice versa (see Fig.2.6 (b)). In this case, the eqn. (2.10) is no longer valid to explain the TL. New differential rate equations should be drafted to explain this model. On the other hand, the analysis of this complicated TL kinetic models reveal a TL glow curve which retains the simple

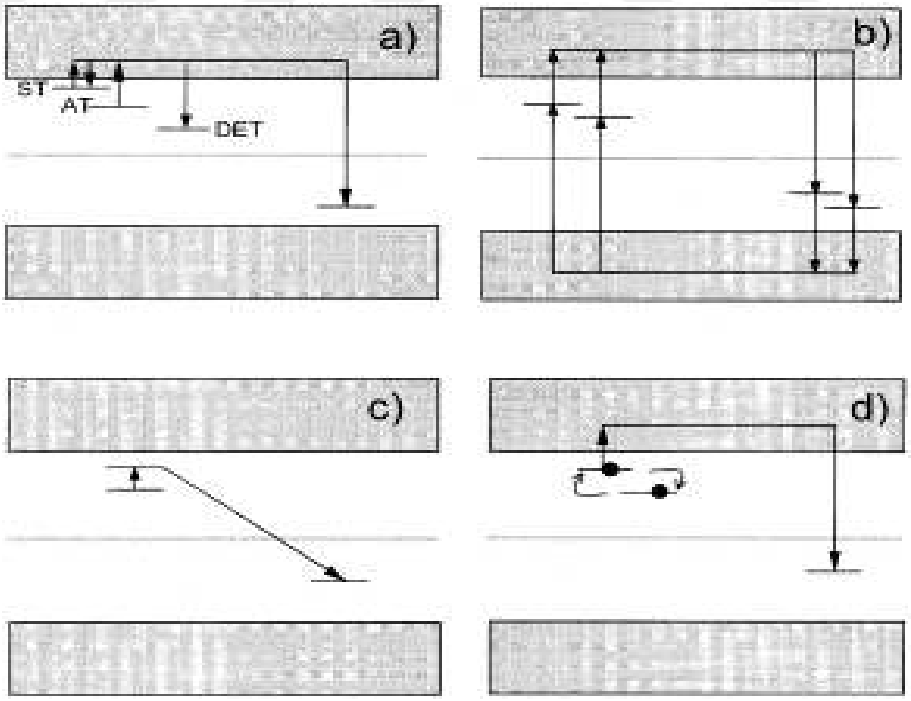

Figure 2.6: Advanced models to describe the thermally stimulation process of trapped charge carriers including: (a) a shallow trap (ST), a deep electron trap (DET), and an active trap (AT); (b) two active traps and two recombination centres; (c) localized transitions; (d) interaction of defects with another defect). [28]

first-order (Eq. (2.17)) or second-order (Eq.(2.29))glow peak shape, depending upon the chosen values of the trapping parameters. However, the *E* and *s* values used in the rate equations (2.17) and (2.29) in order to obtain a fit on this complicated kinetic model need further interpretation.

Another process, which can be, occurs in the TL phenomena. It is a recombination of electron with holes in the recombination center without a transition of the electron into the CB (Fig.2.6 (c)). In this case, the electron is firstly thermally stimulated into an excited state of electron trap from which a transition into the RC is allowed. This model can be done when the electron trap are very close to the recombination center. The transition probability may strongly depend upon the distance between the electron trap and recombination center. Under certain assumptions, a TL equation can be derived to explain the TL intensity [32], which has the same form as eqn. (2.16) but with *s* replaced by a quantity related to the probability for recombination. Therefore, these localized transitions are governed by first-order TL kinetics.

Another model which is shown in figure 2.6 (d) is that the defect which trapped by electron is not stable during the heating process. However, defect is involved in a reaction with another defect. The result may be that the trapped electron concentration by defects is stable while is changing of electrons at low temperature. At higher temperatures, electrons are involved in two processes. Firstly, the defects react with each other and the electrons escape to the conduction band from the shallow trap. In a study, Piters and Bos [33] used these defect reactions and they incorporated into the rate equations and then the TL glow curves simulated. It appears that the simulated glow curves can be very well fitted by first-order TL model. Moreover, it is clear that the fitting parameters do not the simple meaning of trap depth *E* and escape frequency factor *s*.

2.4 Interactive Multi Trap System(IMTS Model)

The IMTS model is shown in below figure 2.7 [34]. This model consists of a RC and two trapping states. The first trap is considered to be the one responsible for TL (denoted as the active trap (AT) below), and the second trap is denoted as the thermally disconnected deep trap (TDDT). The two trap symbolized by total

concentrations N and M, and by instantaneous occupancies n(t) and m(t), respectively.

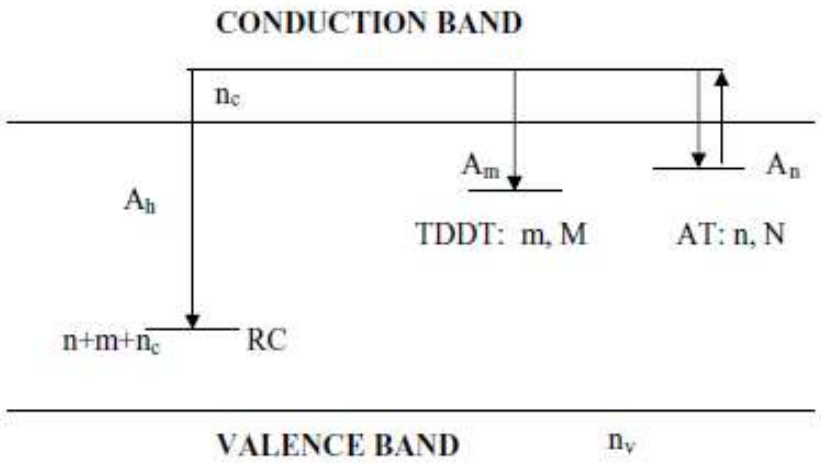

Figure 2.7: Energy level schematic diagram of interactive multi-trap system (IMTS).

Thermally connected traps (TDT): Traps which are considered thermally connected belong to overlapping trap states having a very close energy difference and producing overlapped glow peaks. Sweet and Urquhart have been introduced the thermally connected traps to explain their experimental results concerning ZnS single crystals [34].

Thermally disconnected deep traps (TDDT): In 1967, Dussel and Bube,a thermally disconnected deep trap is an extra energy level introduced for taking into account differences emerging in the results obtaining by simultaneous measurements of both thermoluminescence and thermally stimulated conductivity (TSC):

- the maxima of the two species of signals do not occur at the same temperature,
- important differences in the shape of the signals.

A thermally disconnected trap which can be filled by freed electrons produced by irradiation, but which has a trap depth which is much greater than the normal trapping levels. During heating the sample, only electrons in the shallower traps are freed, while the electrons trapped in the deeper levels (thermally disconnected) are not affected by heating. In other words, these trapping sites have a thermal stability of the trapped charges which is greater than that of the shallow traps related to the TL signal.

From an experimental point of view, it is quite difficult to prove the existence of the thermally disconnected traps because the limitation imposed by the black-body radiation background signal of the detection system, including TL sample, heating strip and surroundings.

Anyway, for a theoretical interpretation of the experimental data obtained by both thermoluminescence and thermally stimulated conductivity measurements, it is realistic to include the thermally disconnected traps into the energy band scheme and then to modify the rate equations describing trap filling and trap emptying processes [35]. From the conservation of charge, the concentration of holes in the RC at any moment must be equal to the total instantaneous concentration of electrons $n+m+n_c$, in the crystals. The rate equations for this model are [36];

$$\frac{dn}{dt} = -ns\ \exp(-E/kT) + A_n(N-n)n_c \tag{2.40}$$

$$\frac{dm}{dt} = A_m(M-m)n_c \tag{2.41}$$

$$\frac{dn_c}{dt} + \frac{dn}{dt} + \frac{dm}{dt} = -(n+m+n_c)n_c A_h \tag{2.42}$$

$$I = -\frac{d(n+m+n_c)}{dt} = (n+m+n_c)n_c A_h \tag{2.43}$$

The interpretation of the first equation is identical to the OTOR model. The second equation expresses the fact that electrons can be trapped into the TDDT with a probability coefficient A_m (term $A_m(M-m)n_c$).This trap is considered thermally disconnected, there is no thermal excitation of these electrons in the conduction band. The third equation represents the conservation of charge in the crystal, with the right-hand side equal to the rate of change of the concentration of holes in the crystal, and the left-hand side equal to the rate of change of the concentration of electrons. The last equation expresses the TL intensity that is equal to the rate of change of the concentration of holes in the RC (term $(n + m + n_c)n_cA_h$).

2.5 Trapping Parameter Determination Methods

The determination of trapping parameters from thermoluminescence glow curves has been a subject of interest for half a century. There are various methods for evaluating the trapping parameters from the glow curves [2,12, 37-40]. Some of them

are initial rise method, variable heating, two heating, isothermal decay, peak shape, partial thermal cleaning and peak area methods.

When one glow peak is highly isolated from the others, the experimental methods such as initial rise, variable heating rates, isothermally decay, and peak shape methods are suitable methods to determine these parameters. However in most materials, the glow curve consists of several peaks. In case of overlapping peaks, there are essentially two ways to obtain these parameters. The first one is the partial thermal cleaning method and the second one is the computer glow curve deconvolution program. In most cases, the partial thermal cleaning method cannot be used to completely isolate the peak of interest without any perturbation on it. Therefore, the computer glow curve deconvolution (CGCD) program has become very popular method to evaluate trapping parameters from TL glow curves in recent years [8,15].

2.6 CGCD method

Computer Glow Curve Deconvolution (CGCD) is one of the most important method to determine trapping parameters from TL glow curves. This method has the advantage over experimental methods in that they can be used in largely overlapping-peak glow curves without resorting to heat treatment

In this study, two CGCD programs were used to analyse the numerically generated TL glow curves. The first program was developed at the Reactor Institute at Delft, The Netherlands [15]. The second one is Microsoft Excel Spreadsheet CGCD program with the powerful solver utility [17]. The numerically obtained data with OTOR and IMTS models by Mathematica program were fitted with each of these programs, and both analysis results were compared with each other and input parameters and they are reviewed in detail.

The first program is capable of simultaneously deconvoluting as many as nine glow peaks from glow curve. Two different models were used in this program. In the first model, the glow curve is approximated from first order TL kinetic by the expression,

$$I(T) = n_0 s \ \exp(-\frac{E}{kT})\exp\left[(-\frac{s}{\beta}\frac{kT^2}{E}\exp(-\frac{E}{kT}) * (0.9920 - 1.620\frac{kT}{E_a})\right] \qquad (2.44)$$

In the second model the glow curve is approximated with general order TL kinetics by using the expression,

$$I(T) = n_0 s \quad \exp(-\frac{E}{kT})\left[1+(-\frac{(b-1)s}{\beta}\frac{kT^2}{E}\exp(-\frac{E}{kT})*(0.9920-1.620\frac{kT}{E_a})\right]^{\frac{b}{b-1}} \quad (2.45)$$

where n_0 (m^{-3}) is the concentration of trapped electrons at t=0, s (s^{-1}) is the frequency factor for first-order and the pre-exponential factor for the general-order, E (eV) the activation energy, T (K) the absolute temperature, k (eVK^{-1}) Boltzmann's constant, β($^0Cs^{-1}$) heating rate and b the kinetic order.

The summation of overall peaks and background contribution can lead to composite glow curve formula as shown below

$$I(T) = \sum_{i=1}^{n} I_i(T) + a + b\exp(T) \quad (2.46)$$

where $I(T)$ is the fitted total glow curve, a allows for the electronic noise contribution to the planchet and dosimeters infrared contribution to the background.

Starting from the above eqn. (2.31), the least square minimization procedure and also FOM (Figure of Merit) was used to judge the fitting results as to whether they are good or not. i.e.

$$FOM = \sum_{i=1}^{n}\frac{|N_i(T) - I(T)|}{A} = \sum_{i=1}^{n}\frac{|\Delta N_i|}{A} \quad (2.47)$$

where $N_i(T)$ is the i-th experimental points (total n=200 data points), $I(T)$ is the i-th fitted points, and A is the integrated area of the fitted glow curve.

From many experiences [41-42], it can be said that if the values of the FOM are between 0.0% and 2.5% the fit is good, 2.5 % and 3.5% the fit is fair, and > 3.5% it is bad fit. To have a graphic representation of the agreement between the experimental and fitted glow curves, the computer program also plots the function,

$$X(T) = \frac{N_i(T) - I_i(T)}{\sqrt{I_i(T)}} \quad (2.48)$$

which is a normal variable with an expected value 0 and σ=1 where $\sigma^2(T)=I_i(T)$.

2.7 Mathematica

Mathematica is a computational software program used in scientific, engineering, and mathematical fields and other areas of technical computing [36]. It was conceived by Stephen Wolfram and is developed by Wolfram Research of Champaign, Illionis [43]. *Mathematica* is split into two parts, the kernel and the front end. The kernel interprets expressions (*Mathematica* code) and returns result expressions. The *Mathematica* language was designed from the start to provide a clear and precise way of communicating ideas--from human to computer or from one human to another. Computer languages typically specify the operations in a rather low-level and literal way. But *Mathematica* is essentially unique among languages in common use because it operates at a much higher level, a level corresponding much more closely to normal human thinking.

Mathematica has emerged as an important tool in computer science and software development: its language component is widely used as a research, prototyping and interface environment. Therefore, *Mathematica* has become important in a remarkably wide range of fields over the years. *Mathematica* is used today throughout the sciences—physical, biological, social and other—and counts many of the world's foremost scientists among its enthusiastic supporters. It has played a crucial role in many important discoveries, and has been the basis for thousands of technical papers.

In engineering, *Mathematica* has become a standard tool for both development and production, and by now many of the world's important new products rely at one stage or another in their design on *Mathematica*.

Whether they have tasks that involve numbers, formulas, functions, graphics, data, documents, or interfaces, *Mathematica* gives automatic access to by far the largest collection of algorithms ever assembled. Mathematica perform the arithmetic calculations in seconds that would take humans months or years to do unaided.

Mathematica can perform all the usual calculus operations – such as integration, differentiation, series, limits, etc. However, the essence of *Mathematica* is its language for describing and manipulating expressions. The numerical and symbolic computations by *Mathematica* can be conducted and both two- and three-dimensional graphics, as well as counter and density plots can be produced. As a result, numeric of any precision, symbolic, or visualization- *Mathematica* is the

ultimate computational tool, with system-wide technology to ensure reliability, ease-of-use, and performance.

2.8 Numerical Solutions of Differential Equations by MATHEMATICA

The function NDSolve allows finding numerical solutions to differential equations by Mathematica [43]. NDSolve handles both single differential equations, and sets of simultaneous differential equations. You can use NDSolve to solve systems of coupled differential equations. This finds a numerical solution to a pair of coupled equations. It can handle a wide range of *ordinary differential equations* as well as some *partial differential equations*. In a system of ordinary differential equations there can be any number of unknown functions y_i, but all of these functions must depend on a single "independent variable" x, which is the same for each function. Partial differential equations involve two or more independent variables [43].

NDSolve[{*eqn*1, *eqn*2, … }, *y*, {*x*, *xmin*, *xmax*}] ⇨find a numerical solution for the function *y* with *x* in the range x_{min}tox_{max}

NDSolve[{*eqn*1, *eqn*2, … }, {y_1, y_1, …}, {*x*, *xmin*, *xmax*}] ⇨find numerical solutions for several functions y_i

NDSolve represents solutions for the functions y_i as InterpolatingFunction objects. The InterpolatingFunction objects provide approximations to the y_i over the range of values x_{min} to $x_{max}$for the independent variable x. NDSolve finds solutions iteratively. It starts at a particular value of x; then takes a sequence of steps, trying eventually to cover the whole range x_{min} to x_{max}. In order to get started, NDSolve has to be given appropriate initial or boundary conditions for the y_i and their derivatives. These conditions specify values for $y_i[x]$, and perhaps derivatives $y_i'[x]$, at particular points x. In general, at least for ordinary differential equations, the conditions you give can be at any x: NDSolve will automatically cover the range x_{min} to x_{max}.

When NDSolve was used, the initial or boundary conditions you give must be sufficient to determine the solutions for the y_i completely. When DSolve was used to find symbolic solutions to differential equations, you can get away with specifying fewer initial conditions. The reason is that DSolve automatically inserts arbitrary constants C[i] to represent degrees of freedom associated with initial conditions that you have not specified explicitly. Since NDSolve must give a numerical solution, it cannot represent these kinds of additional degrees of freedom. As a result, you must

explicitly give all the initial or boundary conditions that are needed to determine the solution. In a typical case, if differential equations were taken with up to n^{th} derivatives, then it is needed to give initial conditions for up to $(n-1)^{th}$ derivatives, or give boundary conditions at n points.

NDSolve has many methods for solving equations, but essentially all of them at some level work by taking a sequence of steps in the independent variable x, and using an adaptive procedure to determine the size of these steps. In general, if the solution appears to be varying rapidly in a particular region, then NDSolve will reduce the step size or change the method to be able to track the solution better. NDSolve follows the general procedure of reducing step size until it tracks solutions accurately. When NDSolve solves a particular set of differential equations, it always tries to choose a step size appropriate for those equations.

CHAPTER 3

GENERATION OF GLOW PEAKS USING MATHEMATICA

3.1 First, Second and General-Order

Firstly, a computer program was written in Mathematica [1] to numerically integrate the equations for first- (eqn. (3.1)), second-(eqn. (3.2)), and general-order (equation(3.3)) kinetics are listed as in below:

$$I(t) = -\frac{dn}{dt} = nse^{-\frac{E}{kT}} \tag{3.1}$$

$$I(t) = -\frac{dn}{dt} = \frac{n^2}{N} se^{-\frac{E}{kT}} \tag{3.2}$$

$$I(t) = -\frac{dn}{dt} = n^b \frac{s}{N} e^{-\frac{E}{kT}} \tag{3.3}$$

The relevant numerical values of n_0 (initial electron trap occupancies (cm^{-3})), N (Total concentration of the traps (cm^{-3})), β (Heating Rate), E_a (Thermal activation energy of the trap (eV)), k (Boltzmann constant (eVK^{-1}) were used as the inpıt parameters in the program, and the program modified so that it draw graphs for the solutions of different initial electron trap occupancies n_0 or kinetics parameters in the case of first-order (b=1), second-order (b=2) or general-order (2>b>1) kinetics. For example in case of first-order kinetics, changes in n_0 did not affect the position of the maximum intensity (T_m) of the first-order TL glow curve, but these changes affect the maximum height (I_m) of the glow curve.

```
s = 10^14;  E1 = 1;  k = 8.617*10^-5;  N1 = 1*10^8;  n1 = 1*N1;  β = 1;
TL1 = NDSolve[{n'[x] == -n[x]*s/β*E^(-E1/(k*(273+x))),
    n[0] == n1}, n, {x, 10, 100}];
TL2 = NDSolve[{n'[x] == -n[x]*s/β*E^(-E1/(k*(273+x))),
    n[0] == 0.6 n1}, n, {x, 10, 100}];
TL3 = NDSolve[{n'[x] == -n[x]*s/β*E^(-E1/(k*(273+x))),
    n[0] == 0.3 n1}, n, {x, 10, 100}];
TL4 = NDSolve[{n'[x] == -n[x]*s/β*E^(-E1/(k*(273+x))),
    n[0] == 0.1 n1}, n, {x, 10, 100}];
Plot[{Evaluate[-n'[x] /. TL1], Evaluate[-n'[x] /. TL2],
  Evaluate[-n'[x] /. TL3], Evaluate[-n'[x] /. TL4]},
 {x, 10, 100}, PlotRange → All, PlotLabel → "TL Glow Curves",
 ImageSize → 90×6, Frame → True, FrameLabel →
  {"Temperature (°C)", "TL Intensity (a.u.)"},
 LabelStyle → Directive[Bold, 12], PlotStyle →
  {{Black}, {Dashed, Black}, {Dashing[Large], Black}, {Blue}}]
```

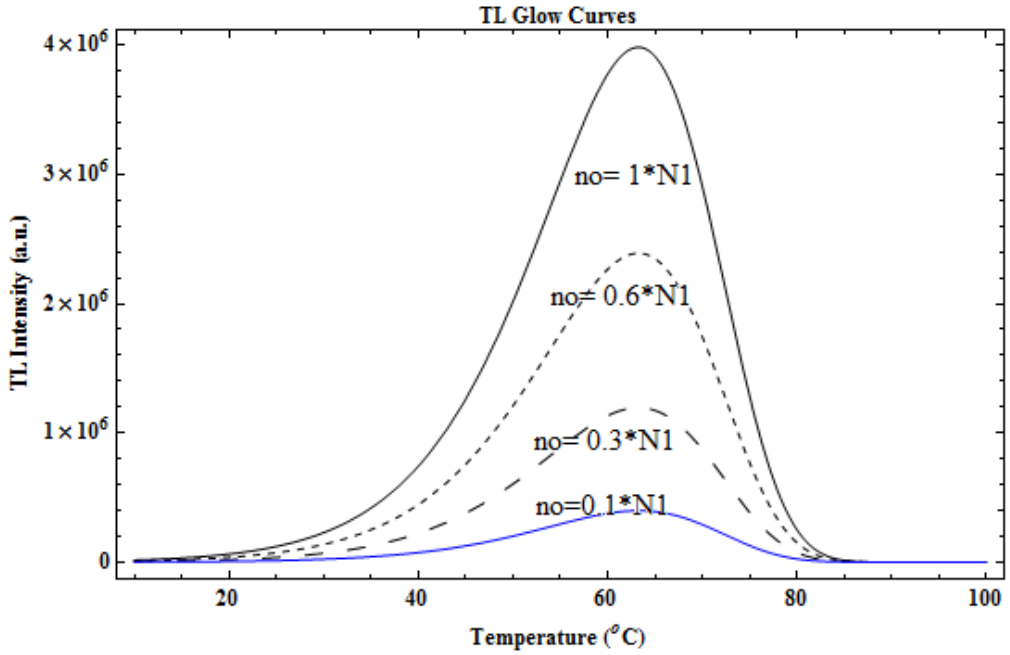

Figure 3.1: The Mathematica program solution of the differential equations for first-order kinetics for the variable initial value n_o (n_o/N= 1, 0.6, 0.3, 0.1). The command NDSolve is used to perform the numerical integration of the differential equation and the parameter x represents the temperature T (°C) and the function n[x] represents the electron concentration n(T).

```
s = 10^14;  E1 = 1;  k = 8.617*10^-5;  N1 = 1*10^8;  n1 = 1*N1;  β = 1;
TL1 = NDSolve[{n'[x] == -n[x]^2 / N1 * (s / β) *E^(-E1 / (k * (273 + x))),
    n[0] == n1}, n, {x, 10, 140}];
TL2 = NDSolve[{n'[x] == -n[x]^2 / N1 * (s / β) *E^(-E1 / (k * (273 + x))),
    n[0] == 0.6 n1}, n, {x, 10, 140}];
TL3 = NDSolve[{n'[x] == -n[x]^2 / N1 * (s / β) *E^(-E1 / (k * (273 + x))),
    n[0] == 0.3 n1}, n, {x, 10, 140}];
TL4 = NDSolve[{n'[x] == -n[x]^2 / N1 * (s / β) *E^(-E1 / (k * (273 + x))),
    n[0] == 0.1 n1}, n, {x, 10, 140}];
Plot[{Evaluate[-n'[x] /. TL1], Evaluate[-n'[x] /. TL2],
  Evaluate[-n'[x] /. TL3], Evaluate[-n'[x] /. TL4]},
 {x, 10, 140}, PlotRange → All, PlotLabel → "TL Glow Curves",
 ImageSize → 90 × 6, Frame → True, FrameLabel →
  {"Temperature (°C)", "TL Intensity (a.u.)"},
 LabelStyle → Directive[Bold, 12], PlotStyle →
  {{Black}, {Dashed, Black}, {Dashing[Large], Black}, {Blue}}]
```

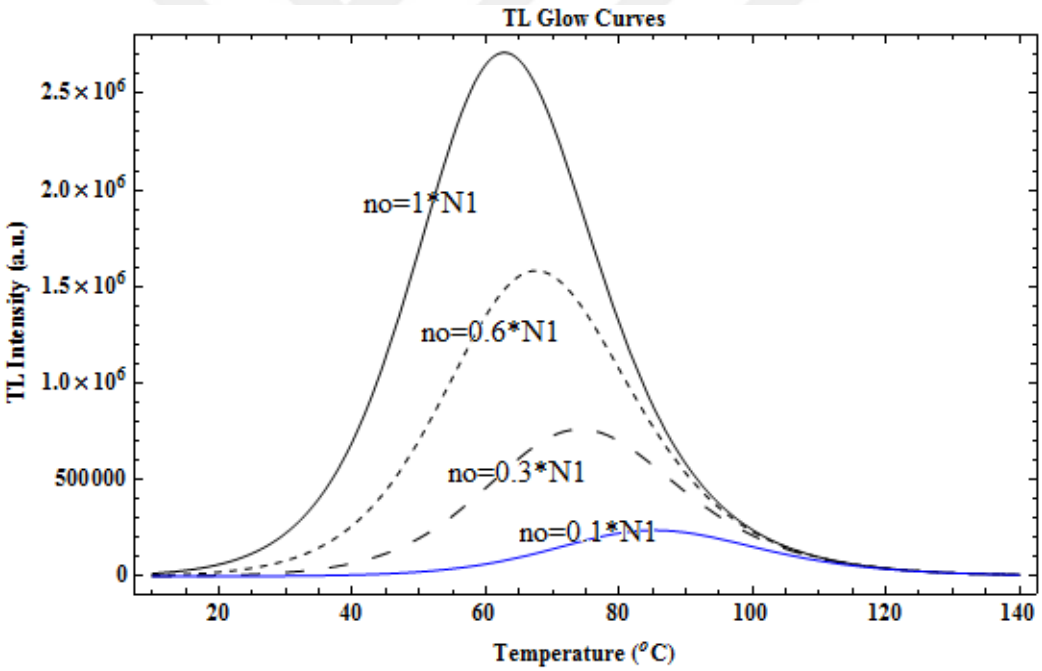

Figure 3.2: The Mathematica program solution of the differential equations for second-order kinetics for the variable initial value n_o (n_o/N= 1, 0.6, 0.3 ,0.1).

```
s = 10^14;  E1 = 1;  k = 8.617*10^-5;  N1 = 1*10^8;  n1 = 1*N1;  β = 1;
b1 = 1.2;  b2 = 1.4;  b3 = 1.6;  b4 = 1.8;
 TL1 = NDSolve[{n'[x] == -n[x]^b1 / N1 * (s / β) *E^(-E1 / (k * (273 + x))),
     n[0] == n1}, n, {x, 30, 400}];
TL2 = NDSolve[{n'[x] == -n[x]^b2 / N1 * (s / β) *E^(-E1 / (k * (273 + x))),
     n[0] == n1}, n, {x, 30, 400}];
TL3 = NDSolve[{n'[x] == -n[x]^b3 / N1 * (s / β) *E^(-E1 / (k * (273 + x))),
     n[0] == n1}, n, {x, 30, 400}];
TL4 = NDSolve[{n'[x] == -n[x]^b4 / N1 * (s / β) *E^(-E1 / (k * (273 + x))),
     n[0] == n1}, n, {x, 30, 400}];
Plot[{Evaluate[-n'[x] /. TL1], Evaluate[-n'[x] /. TL2],
   Evaluate[-n'[x] /. TL3], Evaluate[-n'[x] /. TL4]},
 {x, 30, 400}, PlotRange → All, PlotLabel → "TL Glow Curves",
 ImageSize → 90 × 6, Frame → True, FrameLabel →
  {"Temperature (°C)", "TL Intensity (a.u.)"},
 LabelStyle → Directive[Bold, 12], PlotStyle →
  {{Black}, {Dashed, Black}, {Dashing[Large], Black}, {Blue}}]
```

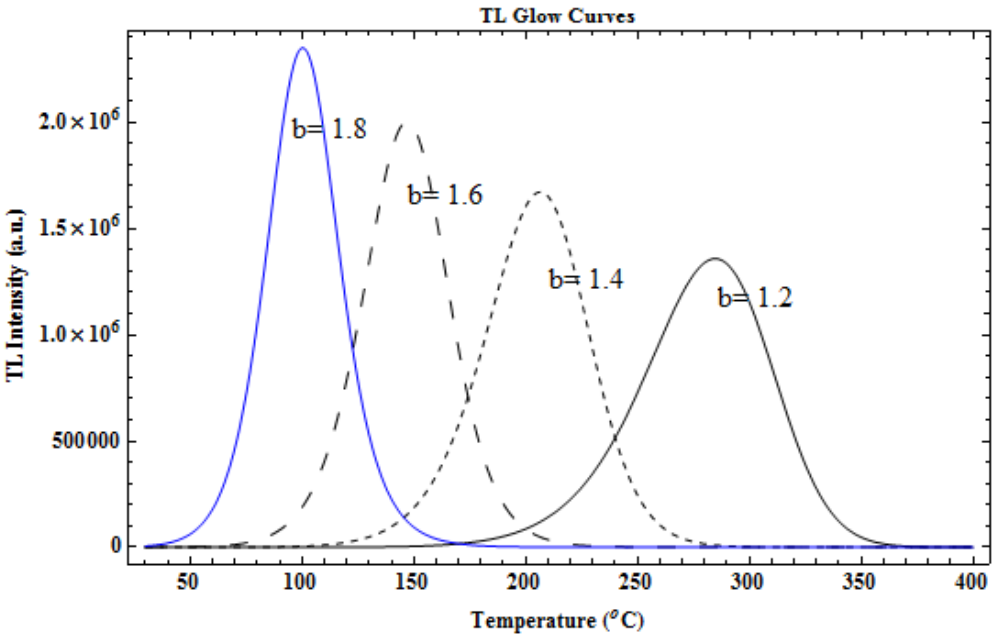

Figure 3.3: The Mathematica program solution of the differential equations for general-order kinetics for the variable kinetics degree.

```
E1 = 1;  k = 8.617*10^-5;  N1 = 1*10^8;  n1 = 1*N1;  β = 1;  b = 1.5
s1 = 10^11;  s2 = 10^12;  s3 = 10^13;  s4 = 10^14;
TL1 = NDSolve[{n'[x] == -n[x]*s1/β*E^(-E1/(k*(273+x))),
    n[0] == n1}, n, {x, 20, 200}];
TL2 = NDSolve[{n'[x] == -n[x]*s2/β*E^(-E1/(k*(273+x))),
    n[0] == n1}, n, {x, 20, 200}];
TL3 = NDSolve[{n'[x] == -n[x]*s3/β*E^(-E1/(k*(273+x))),
    n[0] == n1}, n, {x, 20, 200}];
TL4 = NDSolve[{n'[x] == -n[x]*s4/β*E^(-E1/(k*(273+x))),
    n[0] == n1}, n, {x, 20, 200}];
Plot[{Evaluate[-n'[x] /. TL1] + Evaluate[-n'[x] /. TL2] +
   Evaluate[-n'[x] /. TL3] + Evaluate[-n'[x] /. TL4],
  Evaluate[-n'[x] /. TL1], Evaluate[-n'[x] /. TL2],
  Evaluate[-n'[x] /. TL3], Evaluate[-n'[x] /. TL4]},
 {x, 20, 200}, PlotRange → All, PlotLabel → "TL Glow Curves",
 ImageSize → 90×6, Frame → True, FrameLabel →
  {"Temperature (°C)", "TL Intensity (a.u.)"},
 LabelStyle → Directive[Bold, 12], PlotStyle →
  {{Black}, {Dashed, Black}, {Dashing[Large], Black}, {Blue}, {Dashed, Blue}}]
```

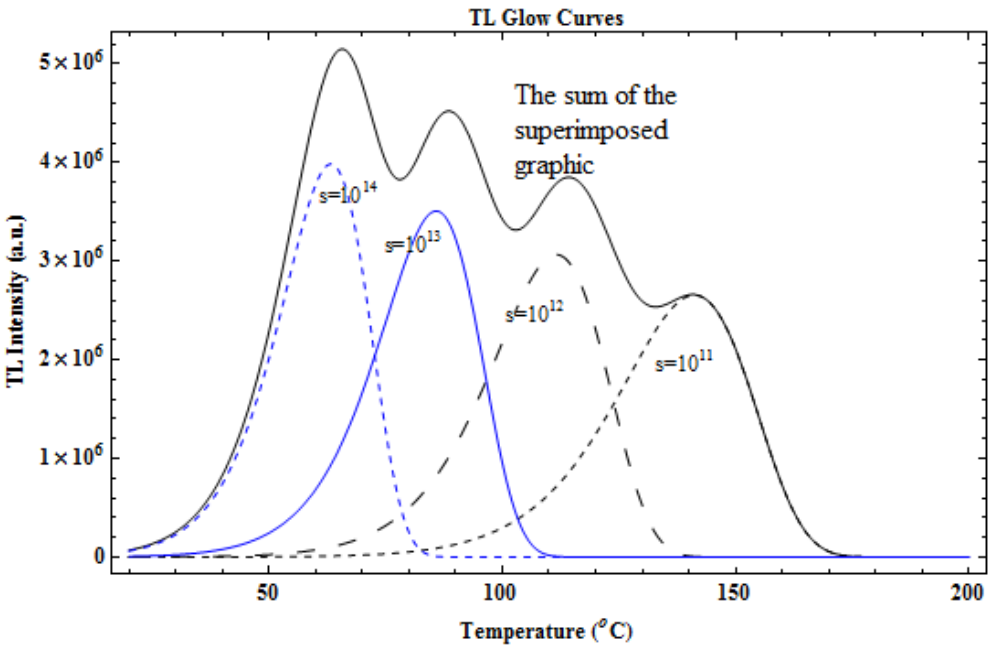

Figure 3.4: The Mathematica program solution of the differential equations for general-order kinetics for the variable frequency factor.

```
E1 = 1;  k = 8.617*10^-5;  N1 = 1*10^8;  n1 = 1*N1;   b = 1.5
s = 10^14;  β1 = 1; β2 = 10; β3 = 20; β4 = 30;
TL1 = NDSolve[{n'[x] == -n[x]*s/β1*E^(-E1/(k*(273+x))),
    n[0] == n1}, n, {x, 10, 130}];
TL2 = NDSolve[{n'[x] == -n[x]*s/β2*E^(-E1/(k*(273+x))),
    n[0] == n1}, n, {x, 10, 130}];
TL3 = NDSolve[{n'[x] == -n[x]*s/β3*E^(-E1/(k*(273+x))),
    n[0] == n1}, n, {x, 10, 130}];
TL4 = NDSolve[{n'[x] == -n[x]*s/β4*E^(-E1/(k*(273+x))),
    n[0] == n1}, n, {x, 10, 130}];
Plot[{Evaluate[-n'[x] /. TL1] + Evaluate[-n'[x] /. TL2] +
   Evaluate[-n'[x] /. TL3] + Evaluate[-n'[x] /. TL4],
  Evaluate[-n'[x] /. TL1], Evaluate[-n'[x] /. TL2],
  Evaluate[-n'[x] /. TL3], Evaluate[-n'[x] /. TL4]},
 {x, 10, 130}, PlotRange → All, PlotLabel → "TL Glow Curves",
 ImageSize → 90×6, Frame → True, FrameLabel →
  {"Temperature (°C)", "TL Intensity (a.u.)"},
 LabelStyle → Directive[Bold, 12], PlotStyle →
  {{Black}, {Dashed, Black}, {Dashing[Large], Black}, {Blue}, {Dashed, Blue}}]
```

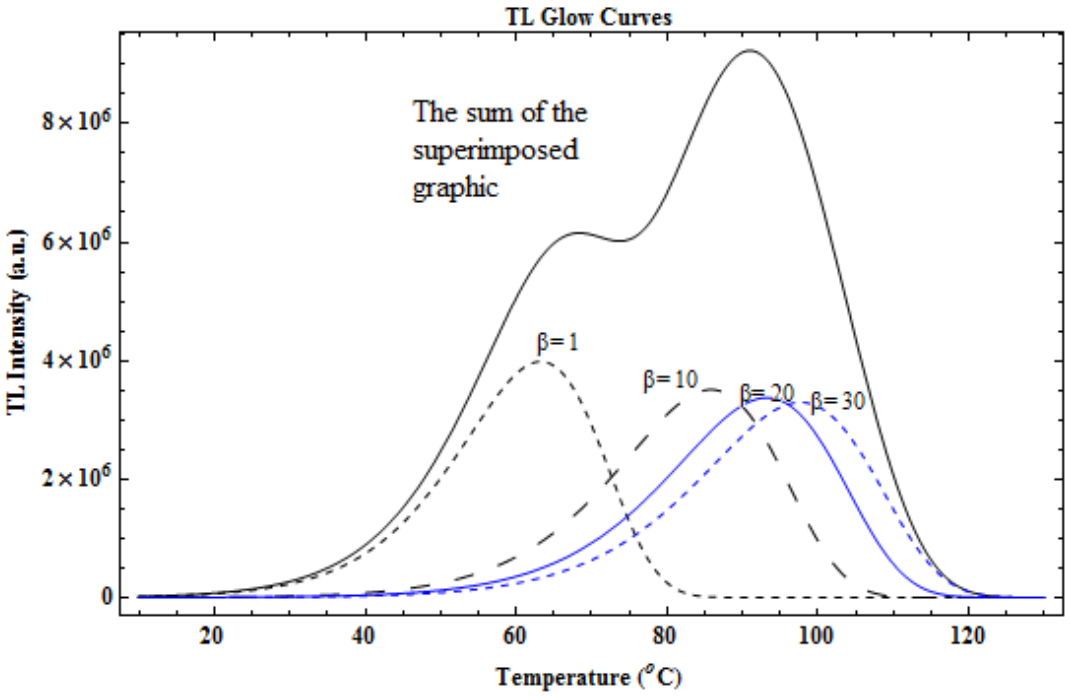

Figure 3.5: The Mathematica program solution of the differential equations for general-order kinetics for the variable heating rate factor.

```
k = 8.617*10^-5;  N1 = 1*10^8;  n1 = 1*N1;  β = 1;  b = 1.5
s = 10^14;  E1 = 0.94;  E2 = 0.96;  E3 = 1;  E4 = 1.04;
TL1 = NDSolve[{n'[x] == -n[x]*s/β*E^(-E1/(k*(273+x))),
    n[0] == n1}, n, {x, 0, 100}];
TL2 = NDSolve[{n'[x] == -n[x]*s/β*E^(-E2/(k*(273+x))),
    n[0] == n1}, n, {x, 0, 100}];
TL3 = NDSolve[{n'[x] == -n[x]*s/β*E^(-E3/(k*(273+x))),
    n[0] == n1}, n, {x, 0, 100}];
TL4 = NDSolve[{n'[x] == -n[x]*s/β*E^(-E4/(k*(273+x))),
    n[0] == n1}, n, {x, 0, 100}];
Plot[{Evaluate[-n'[x] /. TL1] + Evaluate[-n'[x] /. TL2] +
   Evaluate[-n'[x] /. TL3] + Evaluate[-n'[x] /. TL4],
  Evaluate[-n'[x] /. TL1], Evaluate[-n'[x] /. TL2],
  Evaluate[-n'[x] /. TL3], Evaluate[-n'[x] /. TL4]},
 {x, 0, 100}, PlotRange → All, PlotLabel → "TL Glow Curves",
 ImageSize → 90 × 6, Frame → True, FrameLabel →
  {"Temperature (°C)", "TL Intensity (a.u.)"},
 LabelStyle → Directive[Bold, 12], PlotStyle →
  {{Black}, {Dashed, Black}, {Dashing[Large], Black},
   {Blue}, {Dashed, Blue}}]
```

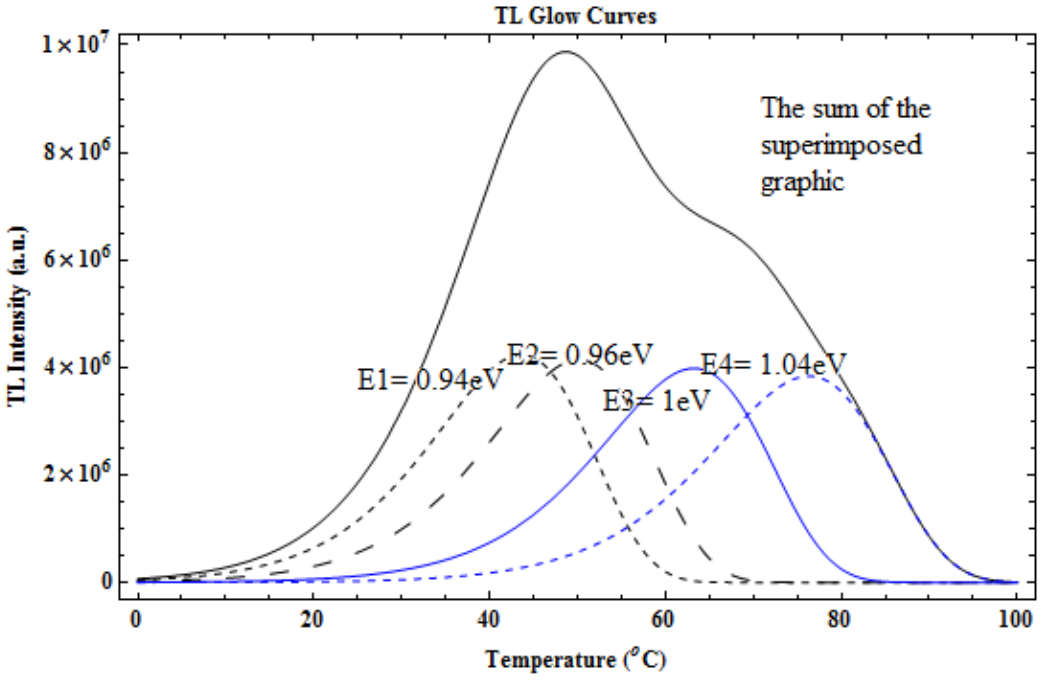

Figure 3.6: The Mathematica program solution of the differential equations for general-order kinetics for the variable heating rate factor.

3.2 The OTOR Model in Mathematica

A computer program was written in Mathematica to numerically integrate the equations for OTOR Model[1] and the relevant numerical values of kinetic parameters were used as input parameters in the program. The OTOR is described by the following equations:

$$\frac{\mathrm{dn}}{\mathrm{dt}} = -\mathrm{snexp}\left(-\frac{\mathrm{E}}{\mathrm{kT}}\right) + (\mathrm{N}-\mathrm{n})\mathrm{A_h}\,\mathrm{n_c} \tag{3.4}$$

$$\frac{dn_c}{dt} = -\frac{dn}{dt} - A_h n_c(n + n_c) \tag{3.5}$$

$$\frac{\mathrm{dn_h}}{\mathrm{dt}} = \frac{\mathrm{dn}}{\mathrm{dt}} + \frac{\mathrm{dn_c}}{\mathrm{dt}} \tag{3.6}$$

$$\mathrm{I_{TL}} = -\frac{\mathrm{dn_h}}{\mathrm{dt}} = A_h(n + n_c)n_c \tag{3.7}$$

In here, A_n is the probability coefficient of electron retrapping in the traps (cm^3s^{-1}), A_h is the probability coefficient of electron recombining with holes in the RC (cm^3s^{-1}). n_c (t) and n_h (t) represent the instantaneous concentrations of the electrons and holes in the CB and RC, respectively. The first equation expresses mathematically the fact that electrons in the trap can be either thermally excited to the conduction band (term $-sn\exp(-E/kT)$), or they can be retrapped in the trap with a probability coefficient A_n(term $(N-n)A_n n_c$). The second equation represents the change in the concentration of the electrons in the conduction band n_c. The concentration of these free electrons in the conduction band can be reduced by either trafficking into the trap (term $-dn/dt$), or by recombining in the RC with a probability coefficient A_h (term $-A_h n_c(n + n_c)$). The third equation describes the conservation of total charge in the crystal, with the left-hand side being equal to the rate of change of the concentration of holes trapped in the RC, and the right-hand side representing the rate of change of the total concentration of electrons in the crystal.

```
k = 8.617*10^-5; Tm = 300; s = 1*10^12; E1 = 1.0; β = 1;
Nt = 1*10^10; Ah = 1*10^-7; An = 100*Ah; no = 1*Nt
sol = NDSolve[{n1'[x] == -n1[x]*s/β*E^(-E1/(k*(273+x)))
      + An*(Nt-n1[x])*nc[x]/β,
    nc'[x] == -n1'[x] - Ah*nc[x]*(n1[x]+nc[x])/β,
    nh'[x] == n1'[x]+nc'[x], n1[0] == no, nc[0] == 0,
    nh[0] == n1[0]+nc[0]}, {n1, nc, nh}, {x, 0, Tm}];
Plot[Evaluate[-nh'[x] /. sol], {x, 0, Tm}, PlotRange →
  All, PlotLabel → "TL Glow Curve", ImageSize → 80×5,
 Frame → True, FrameLabel →
  {"Temperature (°C)", "TL Intensity (ar.un.)"},
 LabelStyle → Directive[Bold, 12], PlotStyle → {{Black}}]
```

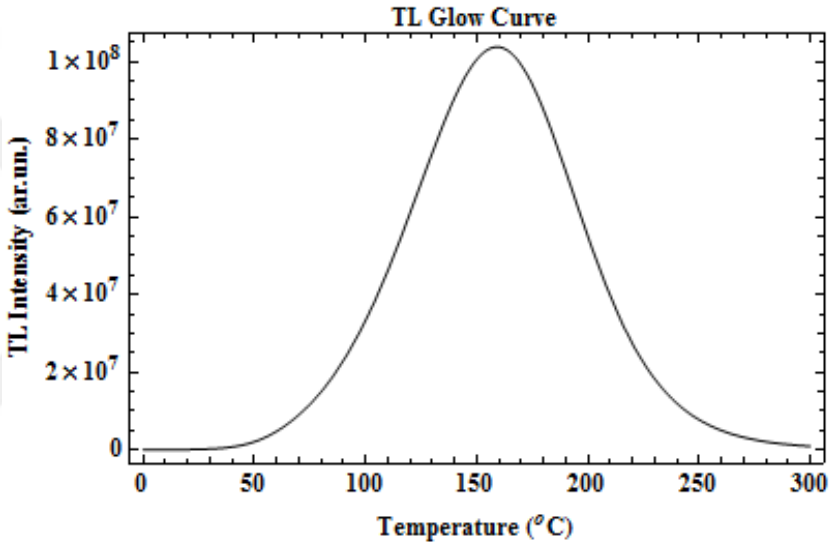

Figure 3.7: The Mathematica program solution of the differential equations for OTOR Model for A_n/A_h= 100.

In case of A_n/A_h= 100 (probability coefficient of retrapping is much larger than the recombination probability coefficient).

```
k = 8.617*10^-5; Tm = 200; s = 1*10^12; E1 = 1.0; β = 1;
Nt = 1*10^10; Ah = 1*10^-7; An = 1*Ah; no = 1*Nt
sol = NDSolve[{n1'[x] == -n1[x]*s/β*E^(-E1/(k*(273+x)))
      + An*(Nt - n1[x])*nc[x]/β,
    nc'[x] == -n1'[x] - Ah*nc[x]*(n1[x] + nc[x])/β,
    nh'[x] == n1'[x] + nc'[x], n1[0] == no, nc[0] == 0,
    nh[0] == n1[0] + nc[0]}, {n1, nc, nh}, {x, 0, Tm}];
Plot[Evaluate[-nh'[x] /. sol], {x, 0, Tm}, PlotRange →
  All, PlotLabel → "TL Glow Curve", ImageSize → 80×5,
 Frame → True, FrameLabel →
  {"Temperature (°C)", "TL Intensity (ar.un.)"},
 LabelStyle → Directive[Bold, 12], PlotStyle → {{Black}}]
```

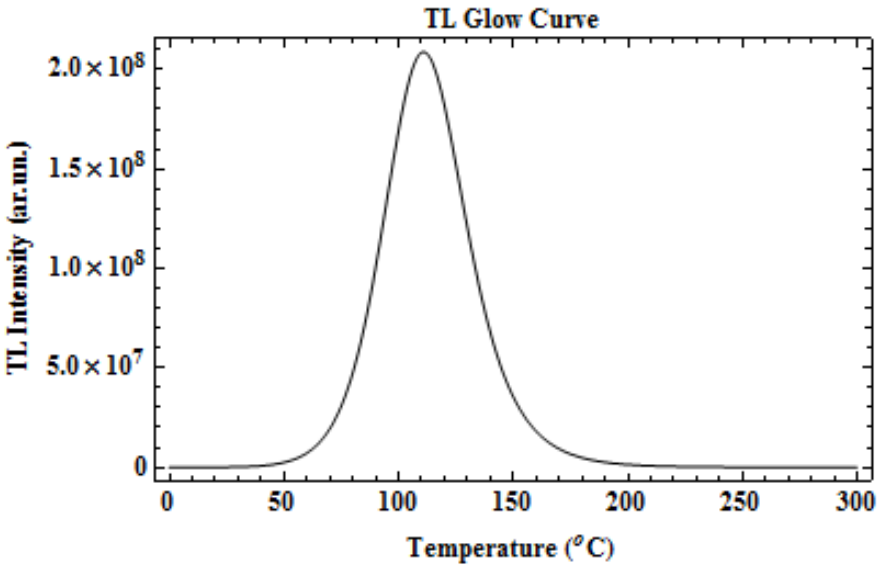

Figure 3.8: The Mathematica program solution of the differential equations for OTOR Model for A_n/A_h= 1.

In case of A_n/A_h= 1 and n_o= N (equal retrapping and recombination probabilities), the OTOR model produces a second-order TL peak.

```
k = 8.617*10^-5; Tm = 180; s = 1*10^12; E1 = 1.0; β = 1;
Nt = 1*10^10; Ah = 1*10^-7; An = 0.01*Ah; no = 1*Nt
sol = NDSolve[{n1'[x] == -n1[x]*s/β*E^(-E1/(k*(273+x)))
      + An*(Nt - n1[x])*nc[x]/β,
    nc'[x] == -n1'[x] - Ah*nc[x]*(n1[x] + nc[x])/β,
    nh'[x] == n1'[x] + nc'[x], n1[0] == no, nc[0] == 0,
    nh[0] == n1[0] + nc[0]}, {n1, nc, nh}, {x, 0, Tm}];
Plot[Evaluate[-nh'[x] /. sol], {x, 30, Tm}, PlotRange →
  All, PlotLabel → "TL Glow Curve", ImageSize → 90×5,
 Frame → True, FrameLabel →
  {"Temperature (°C)", "TL Intensity (ar.un.)"},
 LabelStyle → Directive[Bold, 12], PlotStyle → {{Black}}]
```

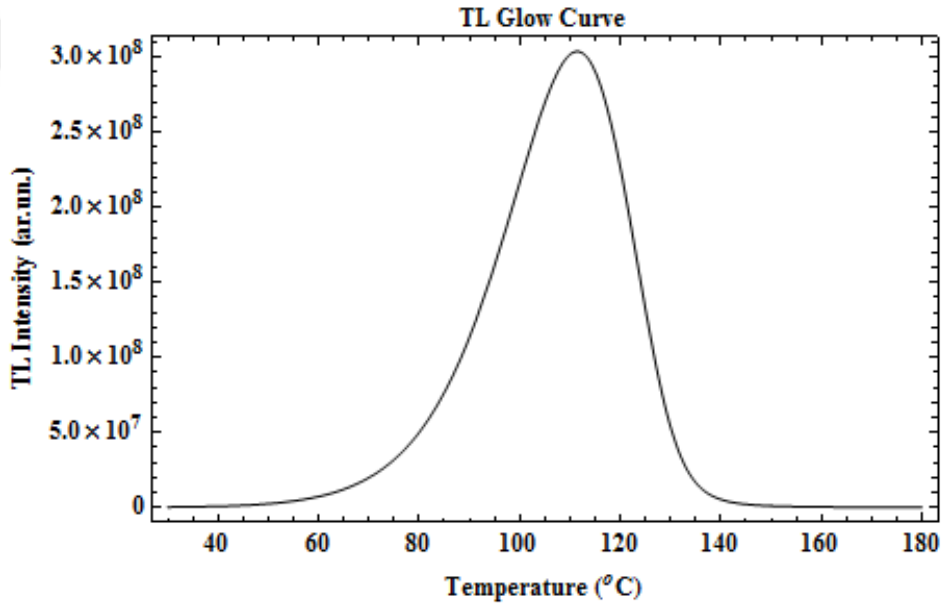

Figure 3.9: The Mathematica program solution of the differential equations for OTOR Model for A_n/A_h= 0.01.

In case of A_n/A_h= 0.01 and n_o= N, the OTOR model produces a first-order TL peak. This corresponds to the situation where the probability of retrapping of electrons in the trap is much smaller than the recombination probability of the electrons in the RC.

```
k = 8.617*10^-5; Ti = 50; Tf = 250; s1 = 1.2*10^12;
s2 = 1.3*10^12; E1 = 1.1; E2 = 1.2; β = 1;
Nt = 1*10^10; Ah1 = 1*10^-7; An1 = 0.01 Ah1;
Ah2 = 1*10^-7; An2 = 0.001*Ah2;
sol1 = NDSolve[{n1'[x] == -n1[x]*s1/β*E^(-E1/(k*(273+x)))
    + An1*(Nt - n1[x])*nc[x]/β,
  nc'[x] == -n1'[x] - Ah1*nc[x]*(n1[x] +
      nc[x])/β, nh'[x] == n1'[x] + nc'[x], n1[0] == 0.2 Nt,
  nc[0] == 0, nh[0] == n1[0] + nc[0]}, {n1, nc, nh}, {x, Ti, Tf}];
sol2 = NDSolve[{n1'[x] == -n1[x]*s2/β*E^(-E2/(k*(273+x)))
    + An2*(Nt - n1[x])*nc[x]/β,
  nc'[x] == -n1'[x] - Ah2*nc[x]*(n1[x] + nc[x])/β, nh'[x] == n1'[x]
    + nc'[x], n1[0] == 0.5 Nt,
  nc[0] == 0, nh[0] == n1[0] + nc[0]}, {n1, nc, nh},
 {x, Ti, Tf}];
Plot[{Evaluate[-nh'[x] /. sol1] + Evaluate[-nh'[x] /. sol2],
  Evaluate[-nh'[x] /. sol1],
  Evaluate[-nh'[x] /. sol2]}, {x, Ti, Tf}, PlotRange →
  All, PlotLabel → "TL Glow Curve",
 ImageSize → 80×5, Frame → True, FrameLabel →
  {"Temperature (°C)", "TL Intensity (ar.un.)"},
 LabelStyle → Directive[Bold, 12], PlotStyle →
  {{Black}, {Dashed, Black}, {Dashing[Large], Black}}]
```

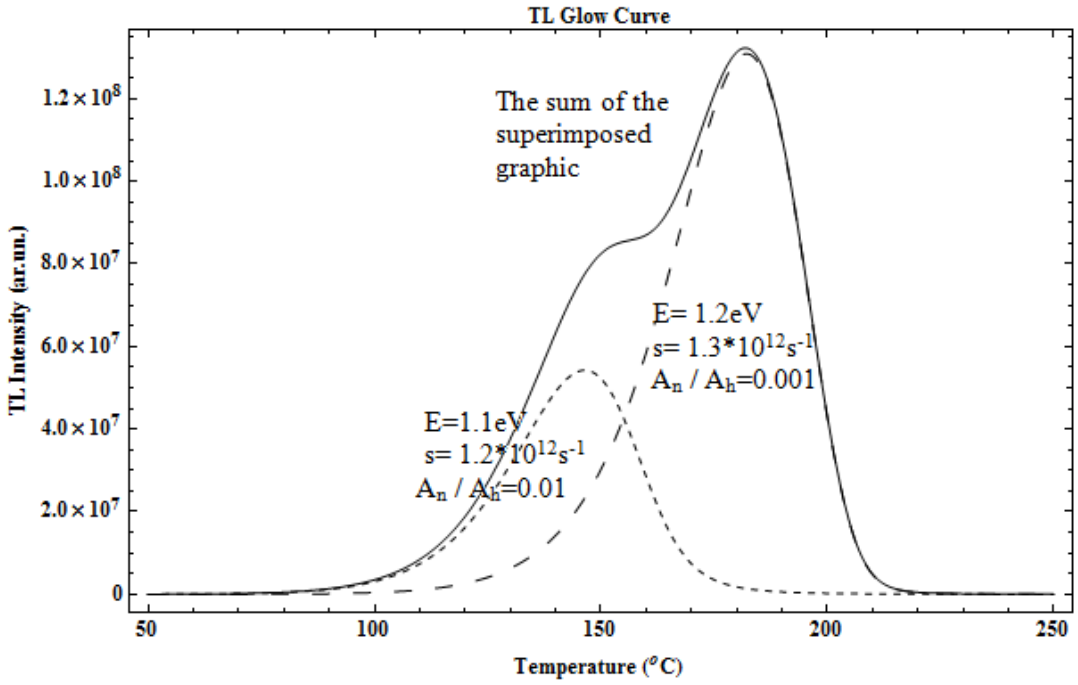

Figure 3.10: The Mathematica program solution of the differential equations for OTOR Model for variable E, s and A_n/ A_h for two peaks.

```
k = 8.617*10^-5; Ti = 50; Tf = 250; s1 = 1*10^12; s2 = 3*10^12; s3 = 5*10^12;
E1 = 1.1; E2 = 1.2; E3 = 1.3; β = 1; Nt = 1*10^10; Ah1 = 1*10^-7; An1 = 0.1 Ah1;
Ah2 = 1*10^-7; An2 = 0.01*Ah2;
Ah3 = 1*10^-7; An3 = 0.001*Ah3;
sol1 = NDSolve[{n1'[x] == -n1[x]*s1/β*E^(-E1/(k*(273+x))) + An1*(Nt-n1[x])*nc[x]/β,
    nc'[x] == -n1'[x] - Ah1*nc[x]*(n1[x]+nc[x])/β, nh'[x] == n1'[x]+nc'[x], n1[0] == Nt,
    nc[0] == 0, nh[0] == n1[0]+nc[0]}, {n1, nc, nh}, {x, Ti, Tf}];
sol2 = NDSolve[{n1'[x] == -n1[x]*s2/β*E^(-E2/(k*(273+x))) + An2*(Nt-n1[x])*nc[x]/β,
    nc'[x] == -n1'[x] - Ah2*nc[x]*(n1[x]+nc[x])/β, nh'[x] == n1'[x]+nc'[x], n1[0] == 0.3 Nt,
    nc[0] == 0, nh[0] == n1[0]+nc[0]}, {n1, nc, nh}, {x, Ti, Tf}];
sol3 = NDSolve[{n1'[x] == -n1[x]*s3/β*E^(-E3/(k*(273+x))) + An3*(Nt-n1[x])*nc[x]/β,
    nc'[x] == -n1'[x] - Ah3*nc[x]*(n1[x]+nc[x])/β, nh'[x] == n1'[x]+nc'[x], n1[0] == 0.5 Nt,
    nc[0] == 0, nh[0] == n1[0]+nc[0]}, {n1, nc, nh}, {x, Ti, Tf}];
Plot[{Evaluate[-nh'[x] /. sol1] + Evaluate[-nh'[x] /. sol2] + Evaluate[-nh'[x] /. sol3],
  Evaluate[-nh'[x] /. sol1],
  Evaluate[-nh'[x] /. sol2], Evaluate[-nh'[x] /. sol3]}, {x, Ti, Tf}, PlotRange →
  All, PlotLabel → "TL Glow Curve", ImageSize → 100×6, Frame → True, FrameLabel →
  {"Temperature (°C)", "TL Intensity (ar.un.)"}, LabelStyle → Directive[Bold, 12],
 PlotStyle → {{Black}, {Blue}, {Dashed, Black}, {Dashing[Large], Black}}]
```

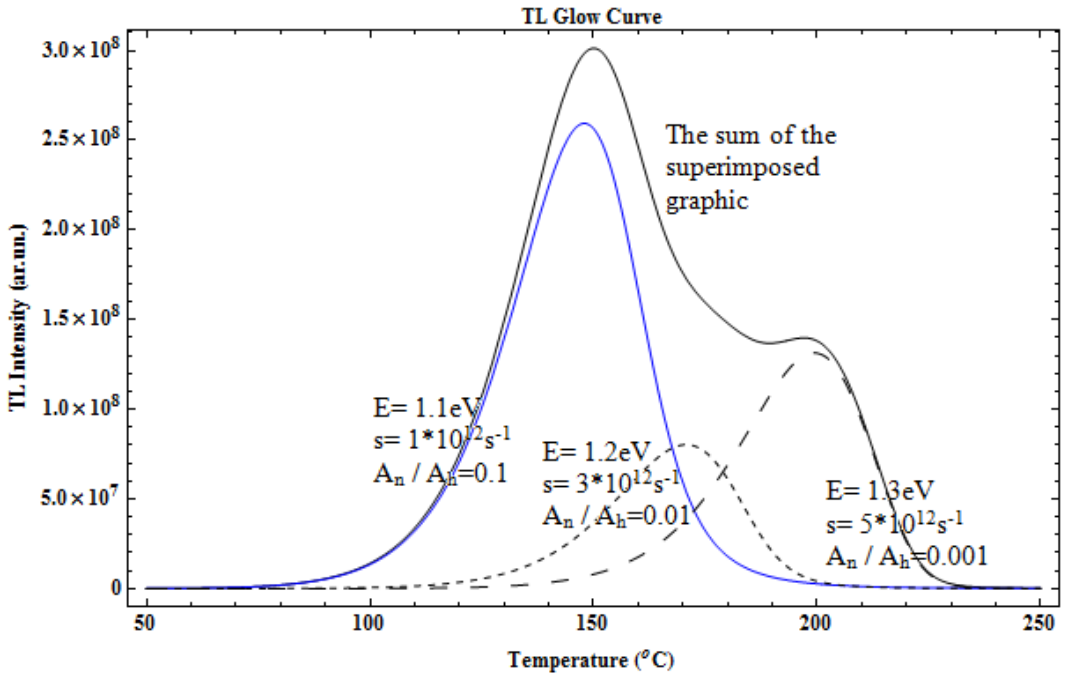

Figure 3.11: The Mathematica program solution of the differential equations for OTOR Model for variable E, s and A_n/ A_h for three peaks.

3.3 The IMTS Model in Mathematica

A computer program was then written in Mathematica to numerically solve the equations of IMTS Model (eqn. (2.40), (2.41), (2.42) and (2.43) [29]) which is shown in Figure 2.7, and the relevant numerical values were used for kinetics orders, A_n, A_h and A_m. Since the ratio A_n/A_h= 0.01, i.e. the recombination probability coefficient A_h is one hundred times larger than the retrapping probability coefficient A_h, one would expect that first-order kinetics will dominate the kinetic process. The calculated TL glow curve has indeed the characteristic shape for first-order peaks. The concentration of electrons in the AT decreases as the temperature increases, while the instantaneous concentration of electrons in the conduction band has a very similar shape to the measured TL glow curve.

The following Mathematica programs numerically solve the differential equations of the IMTS model. The solution of the system of differential equations (2.40)–(2.43) is stored in the parameter *sol* as in previous exercises, and the command *Plot* is used to graph the functions TL(T).

```
k = 8.617*10^-5; s1 = 10^12; E1 = 1; β1 = 1; Nt1 = 1*10^10; Mt = 1*10^10;
Ah1 = 1*10^-7; An1 = 10*Ah1; Am1 = 1*Ah1; Nps = 190;
sol = NDSolve[{n1'[x] == -n1[x]*s1/β1*E^(-E1/(k*(273+x))) +
       An1*(Nt1-n1[x])*nc1[x]/β1, nc1'[x] == -n1'[x] - Ah1*nc1[x]*(m1[x]+n1[x]+
          nc1[x])/β1 - nc1[x]*(Mt-m1[x])*Am1/β1,
     m1'[x] == nc1[x]*(Mt-m1[x])*Am1/β1, n1[0] == 1*Nt1, nc1[0] == 0, m1[0] == 0*Mt},
   {n1, nc1, m1}, {x, 30, Nps}, MaxSteps → 30000];
TL1 = Table[Evaluate[Ah1*nc1[x]*(m1[x]+n1[x]+nc1[x]) /. sol], {x, 30, Nps}];
nc1 = Table[Evaluate[nc1[x] /. sol], {x, 30, Nps}];
m1 = Table[Evaluate[m1[x] /. sol], {x, 30, Nps}];
n1 = Table[Evaluate[n1[x] /. sol], {x, 30, Nps}];
nh1 = Table[Evaluate[m1[x]+n1[x]+nc1[x] /. sol], {x, 30, Nps}];
Plot[Evaluate[{nc1[x]*(m1[x]+n1[x]+nc1[x])*Ah1} /. sol], {x, 30, Nps},
 PlotRange → All, PlotLabel → "TL Glow Curve", ImageSize → 72*5, Frame → True,
 FrameLabel → {"Temperature(⁰C)", "TL Intensity (ar.un.)"},
 LabelStyle → Directive[Bold, 12], PlotStyle → {{Black}}]
```

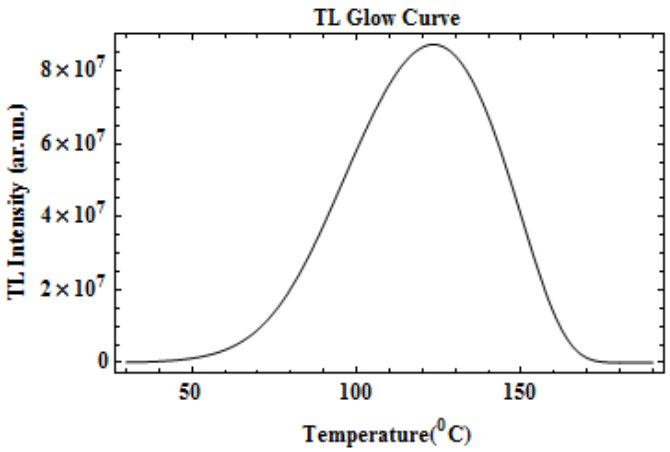

Figure 3.12: The Mathematica program solution of the differential equations for IMTS Model for A_n/A_h= 10 and A_m=A_h(one peak).

```
k = 8.617*10^-5; s1 = 10^12; E1 = 1; β1 = 1; Nt1 = 1*10^10; Mt = 1*10^10;
Ah1 = 1*10^-7; An1 = 0.001*Ah1; Am1 = 1*Ah1; Nps = 150;
sol = NDSolve[{n1'[x] == -n1[x]*s1/β1*E^(-E1/(k*(273+x))) +
        An1*(Nt1-n1[x])*nc1[x]/β1,
     nc1'[x] == -n1'[x] - Ah1*nc1[x]*(m1[x]+n1[x] +
           nc1[x])/β1 - nc1[x]*(Mt-m1[x])*Am1/β1,
     m1'[x] == nc1[x]*(Mt-m1[x])*Am1/β1,
     n1[0] == 1*Nt1, nc1[0] == 0, m1[0] == 0*Mt},
    {n1, nc1, m1}, {x, 50, Nps}, MaxSteps → 30000];
TL1 = Table[Evaluate[Ah1*nc1[x]*(m1[x]+n1[x] +
         nc1[x]) /. sol], {x, 50, Nps}];
nc1 = Table[Evaluate[nc1[x] /. sol], {x, 50, Nps}];
m1 = Table[Evaluate[m1[x] /. sol], {x, 50, Nps}];
n1 = Table[Evaluate[n1[x] /. sol], {x, 50, Nps}];
nh1 = Table[Evaluate[m1[x]+n1[x]+nc1[x] /. sol], {x, 50, Nps}];
Plot[Evaluate[{nc1[x]*(m1[x]+n1[x]+nc1[x])*Ah1} /. sol], {x, 50, Nps},
 PlotRange → All, PlotLabel → "TL Glow Curve", ImageSize →
  72*5, Frame → True, FrameLabel → {"Temperature(⁰C)", "TL Intensity (ar.un.)"},
 LabelStyle → Directive[Bold, 12], PlotStyle → {{Black}}]
```

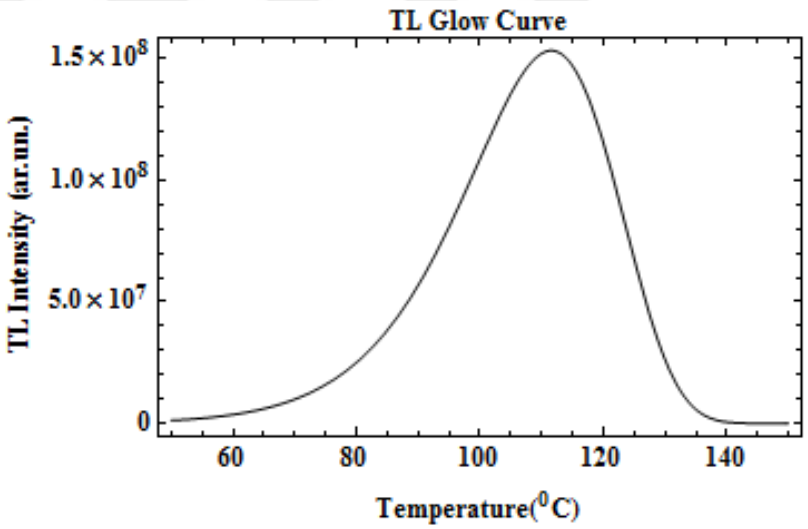

Figure 3.13: The Mathematica program solution of the differential equations for IMTS Model for A_n/A_h=0.001 and A_m=A_h(one peak).

```
k = 8.617*10^-5; s1 = 10^12; E1 = 1; β1 = 1; Nt1 = 1*10^10; Mt = 1*10^10;
Ah1 = 1*10^-7; An1 = 1*Ah1; Am1 = 10*Ah1; Nps = 200;
sol = NDSolve[{n1'[x] == -n1[x]*s1/β1*E^(-E1/(k*(273+x))) +
       An1*(Nt1-n1[x])*nc1[x]/β1,
     nc1'[x] == -n1'[x] - Ah1*nc1[x]*(m1[x]+n1[x] +
           nc1[x])/β1 - nc1[x]*(Mt-m1[x])*Am1/β1,
     m1'[x] == nc1[x]*(Mt-m1[x])*Am1/β1,
     n1[0] == 1*Nt1, nc1[0] == 0, m1[0] == 0*Mt},
   {n1, nc1, m1}, {x, 50, Nps}, MaxSteps → 3000];
TL1 = Table[Evaluate[Ah1*nc1[x]*(m1[x]+n1[x] +
        nc1[x]) /. sol], {x, 50, Nps}];
nc1 = Table[Evaluate[nc1[x] /. sol], {x, 50, Nps}];
m1 = Table[Evaluate[m1[x] /. sol], {x, 50, Nps}];
n1 = Table[Evaluate[n1[x] /. sol], {x, 50, Nps}];
nh1 = Table[Evaluate[m1[x]+n1[x]+nc1[x] /. sol], {x, 50, Nps}];
Plot[Evaluate[{nc1[x]*(m1[x]+n1[x]+nc1[x])*Ah1} /. sol], {x, 50, Nps},
 PlotRange → All, PlotLabel → "TL Glow Curve", ImageSize →
  72*5, Frame → True, FrameLabel → {"Temperature(⁰C)", "TL Intensity (ar.un.)"},
 LabelStyle → Directive[Bold, 12], PlotStyle → {{Black}}]
```

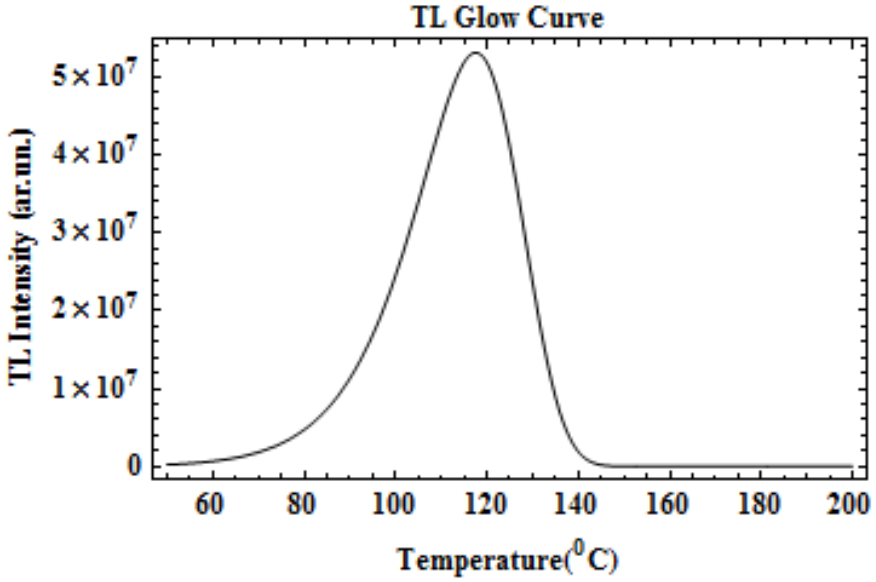

Figure 3.14: The Mathematica program solution of the differential equations for IMTS Model for $A_m/A_h=10$ and $A_n=A_h$ (one peak).

```
k = 8.617*10^-5; s1 = 10^12; E1 = 1; β1 = 1; Nt1 = 1*10^10; Mt = 1*10^10;
Ah1 = 1*10^-7; An1 = 1*Ah1; Am1 = 0.001*Ah1; Nps = 200;
sol = NDSolve[{n1'[x] == -n1[x]*s1/β1*E^(-E1/(k*(273+x))) +
       An1*(Nt1-n1[x])*nc1[x]/β1,
     nc1'[x] == -n1'[x] - Ah1*nc1[x]*(m1[x]+n1[x] +
           nc1[x])/β1 - nc1[x]*(Mt-m1[x])*Am1/β1,
     m1'[x] == nc1[x]*(Mt-m1[x])*Am1/β1,
     n1[0] == 1*Nt1, nc1[0] == 0, m1[0] == 0*Mt},
   {n1, nc1, m1}, {x, 50, Nps}, MaxSteps → 3000];
TL1 = Table[Evaluate[Ah1*nc1[x]*(m1[x]+n1[x] +
         nc1[x]) /. sol], {x, 50, Nps}];
nc1 = Table[Evaluate[nc1[x] /. sol], {x, 50, Nps}];
m1 = Table[Evaluate[m1[x] /. sol], {x, 50, Nps}];
n1 = Table[Evaluate[n1[x] /. sol], {x, 50, Nps}];
nh1 = Table[Evaluate[m1[x]+n1[x]+nc1[x] /. sol], {x, 50, Nps}];
Plot[Evaluate[{nc1[x]*(m1[x]+n1[x]+nc1[x])*Ah1} /. sol], {x, 50, Nps},
 PlotRange → All, PlotLabel → "TL Glow Curve",
 ImageSize → 72*5, Frame → True, FrameLabel →
  {"Temperature(⁰C)", "TL Intensity (ar.un.)"}, LabelStyle →
  Directive[Bold, 12], PlotStyle → {{Black}}]
```

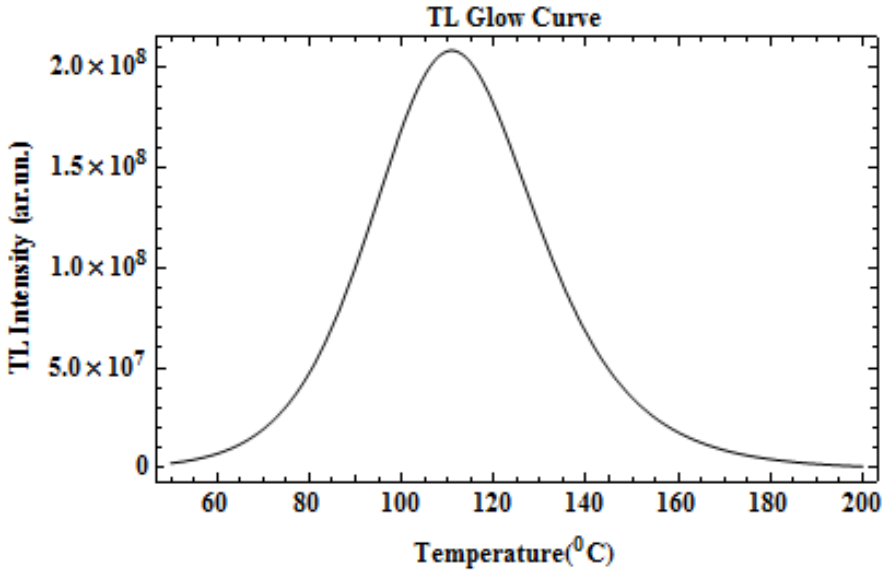

Figure 3.15: The Mathematica program solution of the differential equations for IMTS Model for A_m/A_h=0.001 and A_n=A_h(one peak).

```
k = 8.617*10^-5; s1 = 10^12; E1 = 1.1; β1 = 1; Nt1 = 1*10^10; Mt = 1*10^10;
Ah1 = 1*10^-7; An1 = 10*Ah1; Am1 = 10*Ah1; Nps = 250;
sol = NDSolve[{n1'[x] == -n1[x]*s1/β1*E^(-E1/(k*(273+x))) +
        An1*(Nt1-n1[x])*nc1[x]/β1,
     nc1'[x] == -n1'[x] - Ah1*nc1[x]*(m1[x]+n1[x]+
           nc1[x])/β1 - nc1[x]*(Mt-m1[x])*Am1/β1,
     m1'[x] == nc1[x]*(Mt-m1[x])*Am1/β1, n1[0] == 1*Nt1, nc1[0] == 0, m1[0] == 0*Mt},
    {n1, nc1, m1}, {x, 50, Nps}, MaxSteps → 10000];
TL1 = Table[Evaluate[Ah1*nc1[x]*(m1[x]+n1[x]+nc1[x]) /. sol], {x, 50, Nps}];
nc1 = Table[Evaluate[nc1[x] /. sol], {x, 50, Nps}]; m1 =
 Table[Evaluate[m1[x] /. sol], {x, 50, Nps}];
n1 = Table[Evaluate[n1[x] /. sol], {x, 50, Nps}]; nh1 =
 Table[Evaluate[m1[x]+n1[x]+nc1[x] /. sol], {x, 50, Nps}];
Plot[Evaluate[{nc1[x]*(m1[x]+n1[x]+nc1[x])*Ah1} /. sol], {x, 50, Nps},
 PlotRange → All, PlotLabel → "TL Glow Curve", ImageSize → 72*5,
 Frame → True, FrameLabel → {"Temperature(⁰C)", "TL Intensity (ar.un.)"},
 LabelStyle → Directive[Bold, 12], PlotStyle → {{Black}}]
```

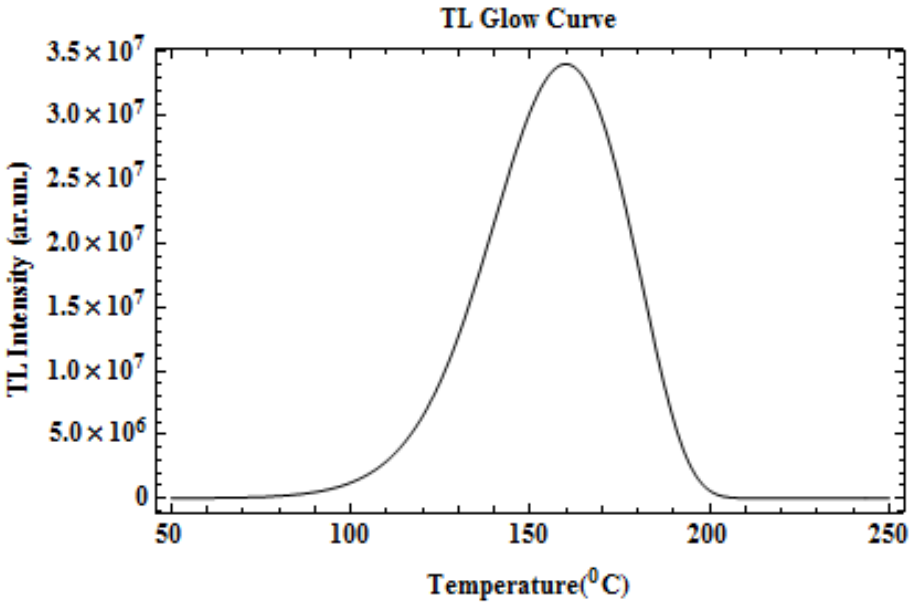

Figure 3.16: The Mathematica program solution of the differential equations for IMTS Model for $A_m/A_h=10$ and $A_n=A_m$ (one peak).

```
k = 8.617*10^-5; s1 = 10^12; E1 = 1.1; β1 = 1; Nt1 = 1*10^10; Mt = 1*10^10;
Ah1 = 1*10^-7; An1 = 0.001*Ah1; Am1 = 0.001*Ah1; Nps = 200;
sol = NDSolve[{n1'[x] == -n1[x]*s1/β1*E^(-E1/(k*(273+x))) +
        An1*(Nt1-n1[x])*nc1[x]/β1,
     nc1'[x] == -n1'[x] - Ah1*nc1[x]*(m1[x]+n1[x] +
           nc1[x])/β1 - nc1[x]*(Mt-m1[x])*Am1/β1,
     m1'[x] == nc1[x]*(Mt-m1[x])*Am1/β1, n1[0] ==
      1*Nt1, nc1[0] == 0, m1[0] == 0*Mt},
    {n1, nc1, m1}, {x, 50, Nps}, MaxSteps → 10000];
TL1 = Table[Evaluate[Ah1*nc1[x]*(m1[x]+n1[x]+nc1[x]) /. sol], {x, 50, Nps}];
nc1 = Table[Evaluate[nc1[x] /. sol], {x, 50, Nps}];
m1 = Table[Evaluate[m1[x] /. sol], {x, 50, Nps}];
n1 = Table[Evaluate[n1[x] /. sol], {x, 50, Nps}];
nh1 = Table[Evaluate[m1[x]+n1[x]+nc1[x] /. sol], {x, 50, Nps}];
Plot[Evaluate[{nc1[x]*(m1[x]+n1[x]+nc1[x])*Ah1} /. sol], {x, 50, Nps},
 PlotRange → All, PlotLabel → "TL Glow Curve", ImageSize →
  72*5, Frame → True, FrameLabel → {"Temperature(°C)", "TL Intensity (ar.un.)"},
 LabelStyle → Directive[Bold, 12], PlotStyle → {{Black}}]
```

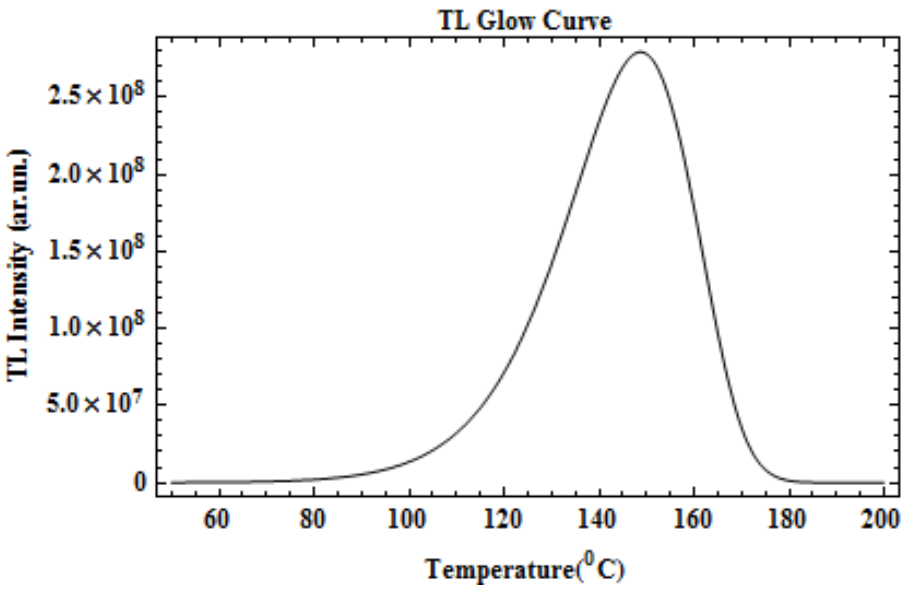

Figure 3.17: The Mathematica program solution of the differential equations for IMTS Model for A_m/A_h=0.001 and A_n=A_m (one peak).

```
k = 8.617*10^-5; s1 = 10^12; E1 = 1; E2 = 1.05; β1 = 1; Nt1 = 1*10^10; Mt = 1*10^10;
Ah1 = 1*10^-7; An1 = 10*Ah1; Am1 = 1*Ah1; Nps = 230;
sol1 = NDSolve[{n1'[x] == -n1[x]*s1/β1*E^(-E1/(k*(273+x))) + An1*(Nt1-n1[x])*nc1[x]/β1,
    nc1'[x] == -n1'[x] - Ah1*nc1[x]*(m1[x]+n1[x]+nc1[x])/β1 - nc1[x]*(Mt-m1[x])*Am1/β1,
    m1'[x] == nc1[x]*(Mt-m1[x])*Am1/β1, n1[0] == 1*Nt1, nc1[0] == 0, m1[0] == 0*Mt},
   {n1, nc1, m1}, {x, 50, Nps}, MaxSteps → 3000];
sol2 = NDSolve[{n1'[x] == -n1[x]*s1/β1*E^(-E2/(k*(273+x))) + An1*(Nt1-n1[x])*nc1[x]/β1,
    nc1'[x] == -n1'[x] - Ah1*nc1[x]*(m1[x]+n1[x]+nc1[x])/β1 - nc1[x]*(Mt-m1[x])*Am1/β1,
    m1'[x] == nc1[x]*(Mt-m1[x])*Am1/β1, n1[0] == 1*Nt1, nc1[0] == 0, m1[0] == 0*Mt},
   {n1, nc1, m1}, {x, 50, Nps}, MaxSteps → 3000];
TL1 = Table[Evaluate[Ah1*nc1[x]*(m1[x]+n1[x]+nc1[x]) /. sol1], {x, 50, Nps}];
nc1 = Table[Evaluate[nc1[x] /. sol1], {x, 50, Nps}]; m1 = Table[Evaluate[m1[x] /. sol1], {x, 50, Nps}];
n1 = Table[Evaluate[n1[x] /. sol1], {x, 50, Nps}]; nh1 = Table[Evaluate[m1[x] +
     n1[x] + nc1[x] /. sol1], {x, 50, Nps}];
TL2 = Table[Evaluate[Ah1*nc1[x]*(m1[x]+n1[x]+nc1[x]) /. sol2], {x, 50, Nps}];
nc1 = Table[Evaluate[nc1[x] /. sol2], {x, 50, Nps}]; m1 = Table[Evaluate[m1[x] /. sol2], {x, 50, Nps}];
n1 = Table[Evaluate[n1[x] /. sol2], {x, 50, Nps}]; nh1 = Table[Evaluate[m1[x] +
     n1[x] + nc1[x] /. sol2], {x, 50, Nps}];
Plot[{Evaluate[{nc1[x]*(m1[x]+n1[x]+nc1[x])*Ah1} /. sol1] + Evaluate[{nc1[x]*(m1[x]+n1[x]+
        nc1[x])*Ah1} /. sol2], Evaluate[{nc1[x]*(m1[x]+n1[x]+nc1[x])*Ah1} /. sol1],
  Evaluate[{nc1[x]*(m1[x]+n1[x]+nc1[x])*Ah1} /. sol2]}, {x, 50, Nps},
 PlotRange → All, PlotLabel → "TL Glow Curves", ImageSize → 72*5, Frame → True, FrameLabel →
  {"Temperature(⁰C)", "TL Intensity (ar.un.)"}, LabelStyle → Directive[Bold, 12], PlotStyle →
  {{Black}, {Dashed, Black}, {Dashing[Large], Black}}]
```

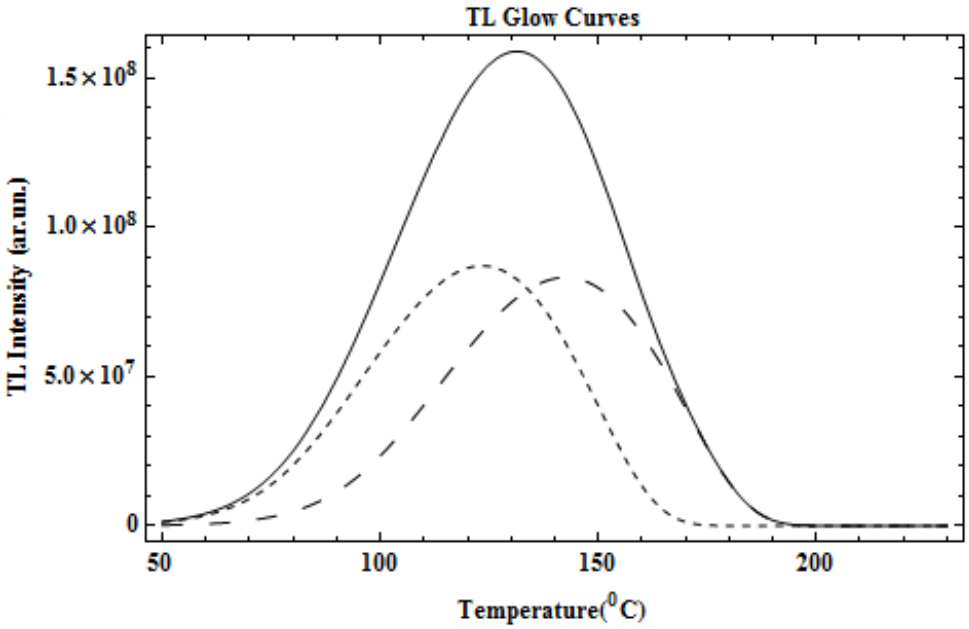

Figure 3.18: The Mathematica program solution of the differential equations for IMTS Model for A_n/A_h= 10 and A_m=A_h (β=1, two peaks).

```
k = 8.617*10^-5; s1 = 10^12; E1 = 1; E2 = 1.05; β1 = 1; Nt1 = 1*10^10; Mt = 1*10^10;
Ah1 = 1*10^-7; An1 = 0.001*Ah1; Am1 = 1*Ah1; Nps = 170;
sol1 = NDSolve[{n1'[x] == -n1[x]*s1/β1*E^(-E1/(k*(273+x))) + An1*(Nt1-n1[x])*nc1[x]/β1,
    nc1'[x] == -n1'[x] - Ah1*nc1[x]*(m1[x]+n1[x]+nc1[x])/β1 - nc1[x]*(Mt-m1[x])*Am1/β1,
    m1'[x] == nc1[x]*(Mt-m1[x])*Am1/β1, n1[0] == 1*Nt1, nc1[0] == 0, m1[0] == 0*Mt},
   {n1, nc1, m1}, {x, 50, Nps}, MaxSteps → 3000];
sol2 = NDSolve[{n1'[x] == -n1[x]*s1/β1*E^(-E2/(k*(273+x))) + An1*(Nt1-n1[x])*nc1[x]/β1,
    nc1'[x] == -n1'[x] - Ah1*nc1[x]*(m1[x]+n1[x]+nc1[x])/β1 - nc1[x]*(Mt-m1[x])*Am1/β1,
    m1'[x] == nc1[x]*(Mt-m1[x])*Am1/β1, n1[0] == 1*Nt1, nc1[0] == 0, m1[0] == 0*Mt},
   {n1, nc1, m1}, {x, 50, Nps}, MaxSteps → 3000];
TL1 = Table[Evaluate[Ah1*nc1[x]*(m1[x]+n1[x]+nc1[x]) /. sol1], {x, 50, Nps}];
nc1 = Table[Evaluate[nc1[x] /. sol1], {x, 50, Nps}];
m1 = Table[Evaluate[m1[x] /. sol1], {x, 50, Nps}];
n1 = Table[Evaluate[n1[x] /. sol1], {x, 50, Nps}];
nh1 = Table[Evaluate[m1[x]+n1[x]+nc1[x] /. sol1], {x, 50, Nps}];
TL2 = Table[Evaluate[Ah1*nc1[x]*(m1[x]+n1[x]+nc1[x]) /. sol2], {x, 50, Nps}];
nc1 = Table[Evaluate[nc1[x] /. sol2], {x, 50, Nps}]; m1 = Table[Evaluate[m1[x] /. sol2],
  {x, 50, Nps}]; n1 = Table[Evaluate[n1[x] /. sol2], {x, 50, Nps}]; nh1 = Table[Evaluate[m1[x] +
    n1[x]+nc1[x] /. sol2], {x, 50, Nps}];
Plot[{Evaluate[{nc1[x]*(m1[x]+n1[x]+nc1[x])*Ah1} /. sol1] + Evaluate[{nc1[x]*(m1[x] +
        n1[x]+nc1[x])*Ah1} /. sol2], Evaluate[{nc1[x]*(m1[x]+n1[x]+nc1[x])*Ah1} /. sol1],
  Evaluate[{nc1[x]*(m1[x]+n1[x]+nc1[x])*Ah1} /. sol2]}, {x, 50, Nps},
 PlotRange → All, PlotLabel → "TL Glow Curves", ImageSize → 72*5, Frame → True, FrameLabel →
  {"Temperature(⁰C)", "TL Intensity (ar.un.)"}, LabelStyle → Directive[Bold, 12], PlotStyle →
  {{Black}, {Dashed, Black}, {Dashing[Large], Black}}]
```

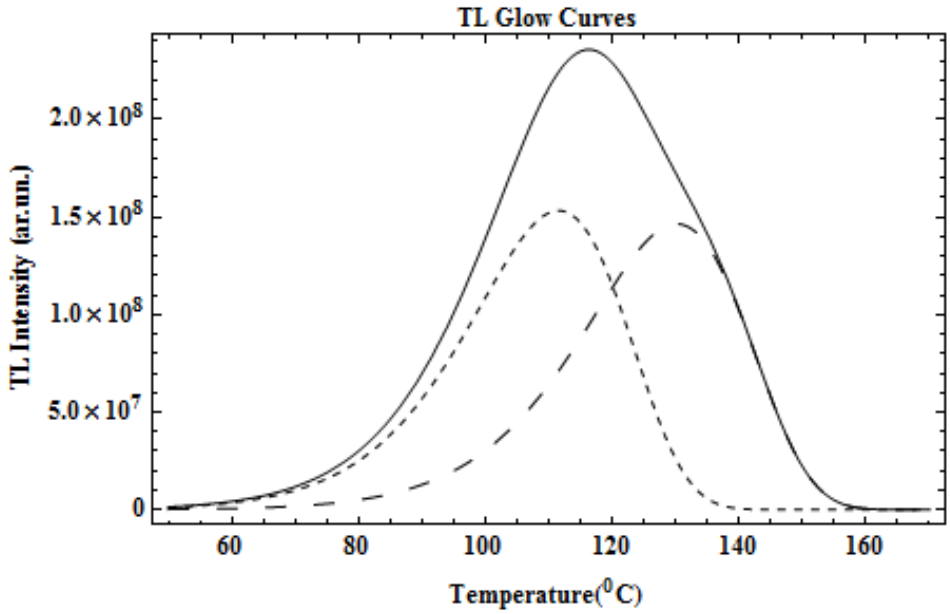

Figure 3.19: The Mathematica program solution of the differential equations for IMTS Model for A_n/A_h= 0.001 and A_m=A_h(β=1, two peaks).

```
k = 8.617*10^-5; s1 = 10^12; E1 = 1; E2 = 1.05; β1 = 10; Nt1 = 1*10^10; Mt = 1*10^10;
Ah1 = 1*10^-7; An1 = 10*Ah1; Am1 = 1*Ah1; Nps = 230;
sol1 = NDSolve[{n1'[x] == -n1[x]*s1/β1*E^(-E1/(k*(273+x))) + An1*(Nt1-n1[x])*nc1[x]/β1,
    nc1'[x] == -n1'[x] - Ah1*nc1[x]*(m1[x]+n1[x]+nc1[x])/β1 - nc1[x]*(Mt-m1[x])*Am1/β1,
    m1'[x] == nc1[x]*(Mt-m1[x])*Am1/β1, n1[0] == 1*Nt1, nc1[0] == 0, m1[0] == 0*Mt},
   {n1, nc1, m1}, {x, 50, Nps}, MaxSteps → 3000];
sol2 = NDSolve[{n1'[x] == -n1[x]*s1/β1*E^(-E2/(k*(273+x))) + An1*(Nt1-n1[x])*nc1[x]/β1,
    nc1'[x] == -n1'[x] - Ah1*nc1[x]*(m1[x]+n1[x]+nc1[x])/β1 - nc1[x]*(Mt-m1[x])*Am1/β1,
    m1'[x] == nc1[x]*(Mt-m1[x])*Am1/β1, n1[0] == 1*Nt1, nc1[0] == 0, m1[0] == 0*Mt},
   {n1, nc1, m1}, {x, 50, Nps}, MaxSteps → 3000];
TL1 = Table[Evaluate[Ah1*nc1[x]*(m1[x]+n1[x]+nc1[x])/.sol1], {x, 50, Nps}];
nc1 = Table[Evaluate[nc1[x]/.sol1], {x, 50, Nps}];
m1 = Table[Evaluate[m1[x]/.sol1], {x, 50, Nps}];
n1 = Table[Evaluate[n1[x]/.sol1], {x, 50, Nps}];
nh1 = Table[Evaluate[m1[x]+n1[x]+nc1[x]/.sol1], {x, 50, Nps}];
TL2 = Table[Evaluate[Ah1*nc1[x]*(m1[x]+n1[x]+nc1[x])/.sol2], {x, 50, Nps}];
nc1 = Table[Evaluate[nc1[x]/.sol2], {x, 50, Nps}];
m1 = Table[Evaluate[m1[x]/.sol2], {x, 50, Nps}];
n1 = Table[Evaluate[n1[x]/.sol2], {x, 50, Nps}];
nh1 = Table[Evaluate[m1[x]+n1[x]+nc1[x]/.sol2], {x, 50, Nps}];
Plot[{Evaluate[{nc1[x]*(m1[x]+n1[x]+nc1[x])*Ah1}/.sol1] +
   Evaluate[{nc1[x]*(m1[x]+n1[x]+nc1[x])*Ah1}/.sol2], Evaluate[{nc1[x]*(m1[x]+n1[x]
      +nc1[x])*Ah1}/.sol1], Evaluate[{nc1[x]*(m1[x]+n1[x]+nc1[x])*Ah1}/.sol2]}, {x, 50, Nps},
 PlotRange → All, PlotLabel → "TL Glow Curves", ImageSize → 72*5,
 Frame → True, FrameLabel → {"Temperature(⁰C)", "TL Intensity (ar.un.)"}, LabelStyle →
  Directive[Bold, 12], PlotStyle → {{Black}, {Dashed, Black}, {Dashing[Large], Black}}]
```

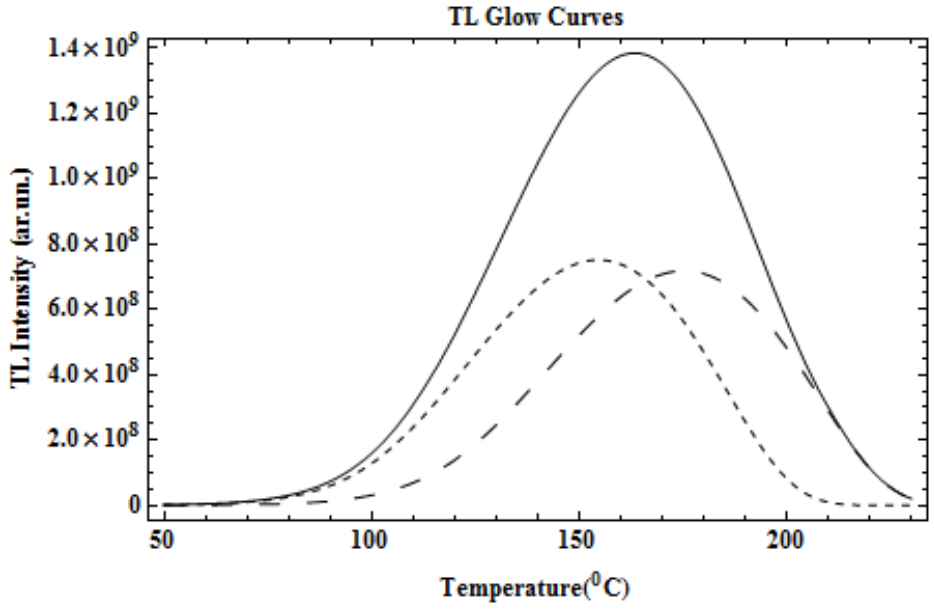

Figure 3.20: The Mathematica program solution of the differential equations for IMTS Model for A_n/A_h= 10 and $A_m=A_h$(β=10**,** two peaks).

```
k = 8.617*10^-5; s1 = 10^12; E1 = 1; E2 = 1.05; β1 = 10; Nt1 = 1*10^10; Mt = 1*10^10;
Ah1 = 1*10^-7; An1 = 0.001*Ah1; Am1 = 1*Ah1; Nps = 200;
sol1 = NDSolve[{n1'[x] == -n1[x]*s1/β1*E^(-E1/(k*(273+x))) + An1*(Nt1-n1[x])*nc1[x]/β1,
    nc1'[x] == -n1'[x] - Ah1*nc1[x]*(m1[x]+n1[x]+nc1[x])/β1 - nc1[x]*(Mt-m1[x])*Am1/β1,
    m1'[x] == nc1[x]*(Mt-m1[x])*Am1/β1, n1[0] == 1*Nt1, nc1[0] == 0, m1[0] == 0*Mt},
   {n1, nc1, m1}, {x, 20, Nps}, MaxSteps → 10000];
sol2 = NDSolve[{n1'[x] == -n1[x]*s1/β1*E^(-E2/(k*(273+x))) + An1*(Nt1-n1[x])*nc1[x]/β1,
    nc1'[x] == -n1'[x] - Ah1*nc1[x]*(m1[x]+n1[x]+nc1[x])/β1 - nc1[x]*(Mt-m1[x])*Am1/β1,
    m1'[x] == nc1[x]*(Mt-m1[x])*Am1/β1, n1[0] == 1*Nt1, nc1[0] == 0, m1[0] == 0*Mt},
   {n1, nc1, m1}, {x, 20, Nps}, MaxSteps → 10000];
TL1 = Table[Evaluate[Ah1*nc1[x]*(m1[x]+n1[x]+nc1[x]) /. sol1], {x, 20, Nps}];
nc1 = Table[Evaluate[nc1[x] /. sol1], {x, 20, Nps}];
m1 = Table[Evaluate[m1[x] /. sol1], {x, 20, Nps}];
n1 = Table[Evaluate[n1[x] /. sol1], {x, 20, Nps}]; nh1 = Table[Evaluate[m1[x] +
     n1[x] + nc1[x] /. sol1], {x, 20, Nps}];
TL2 = Table[Evaluate[Ah1*nc1[x]*(m1[x]+n1[x]+nc1[x]) /. sol2], {x, 20, Nps}];
nc1 = Table[Evaluate[nc1[x] /. sol2], {x, 20, Nps}];
m1 = Table[Evaluate[m1[x] /. sol2], {x, 20, Nps}];
n1 = Table[Evaluate[n1[x] /. sol2], {x, 20, Nps}];
nh1 = Table[Evaluate[m1[x] + n1[x] + nc1[x] /. sol2], {x, 20, Nps}];
Plot[{Evaluate[{nc1[x]*(m1[x]+n1[x]+nc1[x])*Ah1} /. sol1] + Evaluate[{nc1[x]*(m1[x]+n1[x]+
        nc1[x])*Ah1} /. sol2], Evaluate[{nc1[x]*(m1[x]+n1[x]+nc1[x])*Ah1} /. sol1],
  Evaluate[{nc1[x]*(m1[x]+n1[x]+nc1[x])*Ah1} /. sol2]}, {x, 20, Nps},
 PlotRange → All, PlotLabel → "TL Glow Curves", ImageSize → 72*5, Frame →
  True, FrameLabel → {"Temperature(⁰C)", "TL Intensity (ar.un.)"}, LabelStyle →
  Directive[Bold, 12], PlotStyle → {{Black}, {Dashed, Black}, {Dashing[Large], Black}}]
```

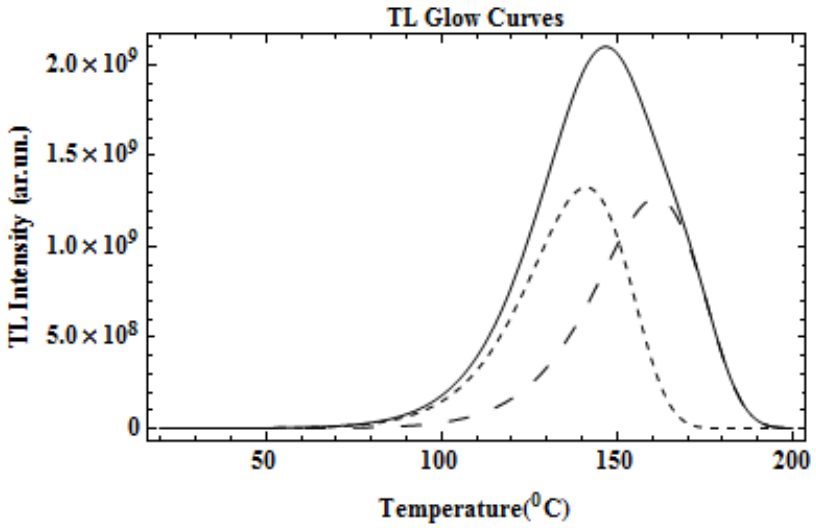

Figure 3.21: The Mathematica program solution of the differential equations for IMTS Model for A_n/A_h= 0.001 and A_m=A_h(β=10**,** two peaks).

```
k = 8.617*10^-5; s1 = 10^12; E1 = 1; E2 = 1.05; β1 = 30; Nt1 = 1*10^10; Mt = 1*10^10;
Ah1 = 1*10^-7; An1 = 10*Ah1; Am1 = 1*Ah1; Nps = 250;
sol1 = NDSolve[{n1'[x] == -n1[x]*s1/β1*E^(-E1/(k*(273+x))) + An1*(Nt1-n1[x])*nc1[x]/β1,
    nc1'[x] == -n1'[x] - Ah1*nc1[x]*(m1[x]+n1[x]+nc1[x])/β1 - nc1[x]*(Mt-m1[x])*Am1/β1,
    m1'[x] == nc1[x]*(Mt-m1[x])*Am1/β1, n1[0] == 1*Nt1, nc1[0] == 0, m1[0] == 0*Mt},
   {n1, nc1, m1}, {x, 50, Nps}, MaxSteps → 10000];
sol2 = NDSolve[{n1'[x] == -n1[x]*s1/β1*E^(-E2/(k*(273+x))) + An1*(Nt1-n1[x])*nc1[x]/β1,
    nc1'[x] == -n1'[x] - Ah1*nc1[x]*(m1[x]+n1[x]+nc1[x])/β1 - nc1[x]*(Mt-m1[x])*Am1/β1,
    m1'[x] == nc1[x]*(Mt-m1[x])*Am1/β1, n1[0] == 1*Nt1, nc1[0] == 0, m1[0] == 0*Mt},
   {n1, nc1, m1}, {x, 50, Nps}, MaxSteps → 10000];
TL1 = Table[Evaluate[Ah1*nc1[x]*(m1[x]+n1[x]+nc1[x]) /. sol1], {x, 50, Nps}];
nc1 = Table[Evaluate[nc1[x] /. sol1], {x, 50, Nps}]; m1 = Table[Evaluate[m1[x] /. sol1], {x, 50, Nps}];
n1 = Table[Evaluate[n1[x] /. sol1], {x, 50, Nps}];
nh1 = Table[Evaluate[m1[x]+n1[x]+nc1[x] /. sol1], {x, 50, Nps}];
TL2 = Table[Evaluate[Ah1*nc1[x]*(m1[x]+n1[x]+nc1[x]) /. sol2], {x, 50, Nps}];
nc1 = Table[Evaluate[nc1[x] /. sol2], {x, 50, Nps}]; m1 = Table[Evaluate[m1[x] /. sol2], {x, 50, Nps}];
n1 = Table[Evaluate[n1[x] /. sol2], {x, 50, Nps}];
nh1 = Table[Evaluate[m1[x]+n1[x]+nc1[x] /. sol2], {x, 50, Nps}];
Plot[{Evaluate[{nc1[x]*(m1[x]+n1[x]+nc1[x])*Ah1} /. sol1] + Evaluate[{nc1[x]*(m1[x]+
        n1[x]+nc1[x])*Ah1} /. sol2], Evaluate[{nc1[x]*(m1[x]+n1[x]+nc1[x])*Ah1} /. sol1],
  Evaluate[{nc1[x]*(m1[x]+n1[x]+nc1[x])*Ah1} /. sol2]}, {x, 50, Nps},
 PlotRange → All, PlotLabel → "TL Glow Curves", ImageSize → 72*5,
 Frame → True, FrameLabel → {"Temperature(⁰C)", "TL Intensity (ar.un.)"}, LabelStyle →
  Directive[Bold, 12], PlotStyle → {{Black}, {Dashed, Black}, {Dashing[Large], Black}}]
```

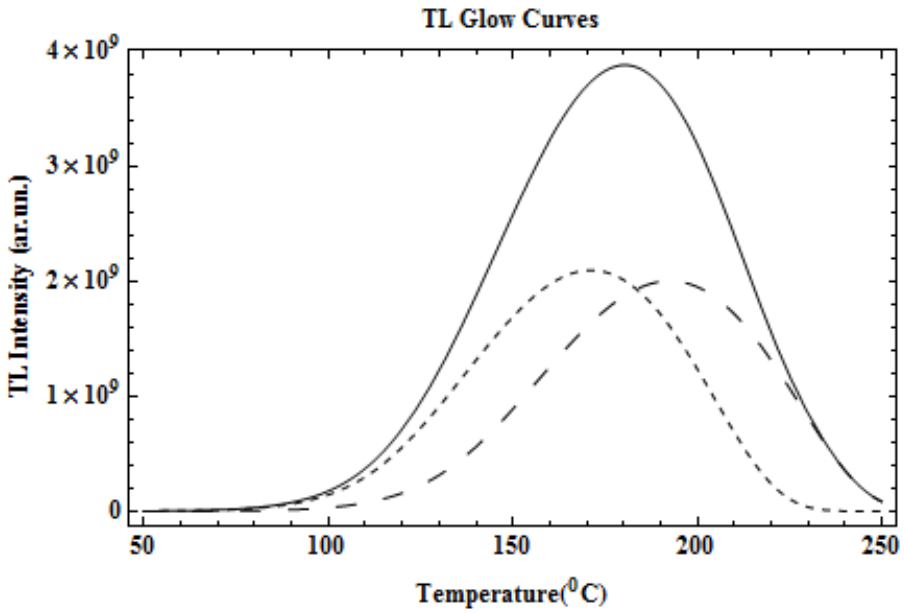

Figure 3.22: The Mathematica program solution of the differential equations for IMTS Model for A_n/A_h= 10 and A_m=A_h(β=30**,** two peaks).

```
k = 8.617*10^-5; s1 = 10^12; E1 = 1; E2 = 1.05; β1 = 30; Nt1 = 1*10^10; Mt = 1*10^10;
Ah1 = 1*10^-7; An1 = 0.001*Ah1; Am1 = 1*Ah1; Nps = 210;
sol1 = NDSolve[{n1'[x] == -n1[x]*s1/β1*E^(-E1/(k*(273+x))) + An1*(Nt1-n1[x])*nc1[x]/β1,
    nc1'[x] == -n1'[x] - Ah1*nc1[x]*(m1[x]+n1[x]+nc1[x])/β1 - nc1[x]*(Mt-m1[x])*Am1/β1,
    m1'[x] == nc1[x]*(Mt-m1[x])*Am1/β1, n1[0] == 1*Nt1, nc1[0] == 0, m1[0] == 0*Mt},
   {n1, nc1, m1}, {x, 50, Nps}, MaxSteps → 12000];
sol2 = NDSolve[{n1'[x] == -n1[x]*s1/β1*E^(-E2/(k*(273+x))) + An1*(Nt1-n1[x])*nc1[x]/β1,
    nc1'[x] == -n1'[x] - Ah1*nc1[x]*(m1[x]+n1[x]+nc1[x])/β1 - nc1[x]*(Mt-m1[x])*Am1/β1,
    m1'[x] == nc1[x]*(Mt-m1[x])*Am1/β1, n1[0] == 1*Nt1, nc1[0] == 0, m1[0] == 0*Mt},
   {n1, nc1, m1}, {x, 50, Nps}, MaxSteps → 12000];
TL1 = Table[Evaluate[Ah1*nc1[x]*(m1[x]+n1[x]+nc1[x]) /. sol1], {x, 50, Nps}];
nc1 = Table[Evaluate[nc1[x] /. sol1], {x, 50, Nps}];
m1 = Table[Evaluate[m1[x] /. sol1], {x, 50, Nps}];
n1 = Table[Evaluate[n1[x] /. sol1], {x, 50, Nps}];
nh1 = Table[Evaluate[m1[x]+n1[x]+nc1[x] /. sol1], {x, 50, Nps}];
TL2 = Table[Evaluate[Ah1*nc1[x]*(m1[x]+n1[x]+nc1[x]) /. sol2], {x, 50, Nps}];
nc1 = Table[Evaluate[nc1[x] /. sol2], {x, 50, Nps}];
m1 = Table[Evaluate[m1[x] /. sol2], {x, 50, Nps}];
n1 = Table[Evaluate[n1[x] /. sol2], {x, 50, Nps}];
nh1 = Table[Evaluate[m1[x]+n1[x]+nc1[x] /. sol2], {x, 50, Nps}];
Plot[{Evaluate[{nc1[x]*(m1[x]+n1[x]+nc1[x])*Ah1} /. sol1] + Evaluate[{nc1[x]*(m1[x]+
        n1[x]+nc1[x])*Ah1} /. sol2], Evaluate[{nc1[x]*(m1[x]+n1[x]+nc1[x])*Ah1} /. sol1],
  Evaluate[{nc1[x]*(m1[x]+n1[x]+nc1[x])*Ah1} /. sol2]}, {x, 50, Nps},
 PlotRange → All, PlotLabel → "TL Glow Curves", ImageSize → 72*5, Frame →
  True, FrameLabel → {"Temperature(⁰C)", "TL Intensity (ar.un.)"}, LabelStyle →
  Directive[Bold, 12], PlotStyle → {{Black}, {Dashed, Black}, {Dashing[Large], Black}}]
```

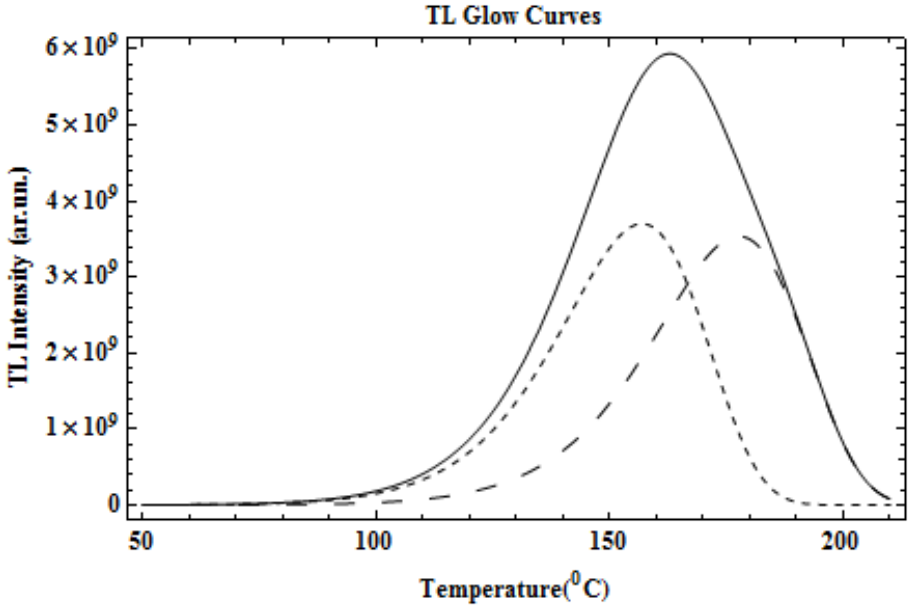

Figure 3.23**:** The Mathematica program solution of the differential equations for IMTS Model for A_n/A_h= 0.001 and A_m=A_h (β=30**,** two peaks).

```
k = 8.617*10^-5; s1 = 10^12; E1 = 1; E2 = 1.04; E3 = 1.08; β1 = 1; Nt1 = 1*10^10; Mt = 1*10^10;
Ah1 = 1*10^-7; An1 = 10*Ah1; Am1 = 1*Ah1; Nps = 230;
sol1 = NDSolve[{n1'[x] == -n1[x]*s1/β1*E^(-E1/(k*(273+x))) + An1*(Nt1-n1[x])*nc1[x]/β1,
    nc1'[x] == -n1'[x] - Ah1*nc1[x]*(m1[x]+n1[x]+nc1[x])/β1 - nc1[x]*(Mt-m1[x])*Am1/β1,
    m1'[x] == nc1[x]*(Mt-m1[x])*Am1/β1, n1[0] == 1*Nt1, nc1[0] == 0, m1[0] == 0*Mt},
   {n1, nc1, m1}, {x, 50, Nps}, MaxSteps → 3000];
sol2 = NDSolve[{n1'[x] == -n1[x]*s1/β1*E^(-E2/(k*(273+x))) + An1*(Nt1-n1[x])*nc1[x]/β1,
    nc1'[x] == -n1'[x] - Ah1*nc1[x]*(m1[x]+n1[x]+nc1[x])/β1 - nc1[x]*(Mt-m1[x])*Am1/β1,
    m1'[x] == nc1[x]*(Mt-m1[x])*Am1/β1, n1[0] == 1*Nt1, nc1[0] == 0, m1[0] == 0*Mt},
   {n1, nc1, m1}, {x, 50, Nps}, MaxSteps → 3000];
sol3 = NDSolve[{n1'[x] == -n1[x]*s1/β1*E^(-E3/(k*(273+x))) + An1*(Nt1-n1[x])*nc1[x]/β1,
    nc1'[x] == -n1'[x] - Ah1*nc1[x]*(m1[x]+n1[x]+nc1[x])/β1 - nc1[x]*(Mt-m1[x])*Am1/β1,
    m1'[x] == nc1[x]*(Mt-m1[x])*Am1/β1, n1[0] == 1*Nt1, nc1[0] == 0, m1[0] == 0*Mt},
   {n1, nc1, m1}, {x, 50, Nps}, MaxSteps → 3000];
TL1 = Table[Evaluate[Ah1*nc1[x]*(m1[x]+n1[x]+nc1[x]) /. sol1], {x, 50, Nps}];
nc1 = Table[Evaluate[nc1[x] /. sol1], {x, 50, Nps}]; m1 = Table[Evaluate[m1[x] /. sol1], {x, 50, Nps}];
n1 = Table[Evaluate[n1[x] /. sol1], {x, 50, Nps}]; nh1 = Table[Evaluate[m1[x]+n1[x]+nc1[x] /. sol1], {x, 50, Nps}];
TL2 = Table[Evaluate[Ah1*nc1[x]*(m1[x]+n1[x]+nc1[x]) /. sol2], {x, 50, Nps}];
nc1 = Table[Evaluate[nc1[x] /. sol2], {x, 50, Nps}]; m1 = Table[Evaluate[m1[x] /. sol2], {x, 50, Nps}];
n1 = Table[Evaluate[n1[x] /. sol2], {x, 50, Nps}]; nh1 = Table[Evaluate[m1[x]+n1[x]+nc1[x] /. sol2], {x, 50, Nps}];
TL3 = Table[Evaluate[Ah1*nc1[x]*(m1[x]+n1[x]+nc1[x]) /. sol3], {x, 50, Nps}];
nc1 = Table[Evaluate[nc1[x] /. sol3], {x, 50, Nps}]; m1 = Table[Evaluate[m1[x] /. sol3], {x, 50, Nps}];
n1 = Table[Evaluate[n1[x] /. sol3], {x, 50, Nps}]; nh1 = Table[Evaluate[m1[x]+n1[x]+nc1[x] /. sol3], {x, 50, Nps}];
Plot[{Evaluate[{nc1[x]*(m1[x]+n1[x]+nc1[x])*Ah1} /. sol1] + Evaluate[{nc1[x]*(m1[x]+n1[x]+
        nc1[x])*Ah1} /. sol2] + Evaluate[{nc1[x]*(m1[x]+n1[x]+nc1[x])*Ah1} /. sol3],
  Evaluate[{nc1[x]*(m1[x]+n1[x]+nc1[x])*Ah1} /. sol1], Evaluate[{nc1[x]*(m1[x]+n1[x]+
      nc1[x])*Ah1} /. sol2], Evaluate[{nc1[x]*(m1[x]+n1[x]+nc1[x])*Ah1} /. sol3]}, {x, 50, Nps},
 PlotRange → All, PlotLabel → "TL Glow Curves", ImageSize → 72*5, Frame →
  True, FrameLabel → {"Temperature(°C)", "TL Intensity (ar.un.)"}, LabelStyle → Directive[Bold, 12],
 PlotStyle → {{Black}, {Dashing[Large], Blue}, {Dashed, Black}, {Dashing[Large], Black}}]
```

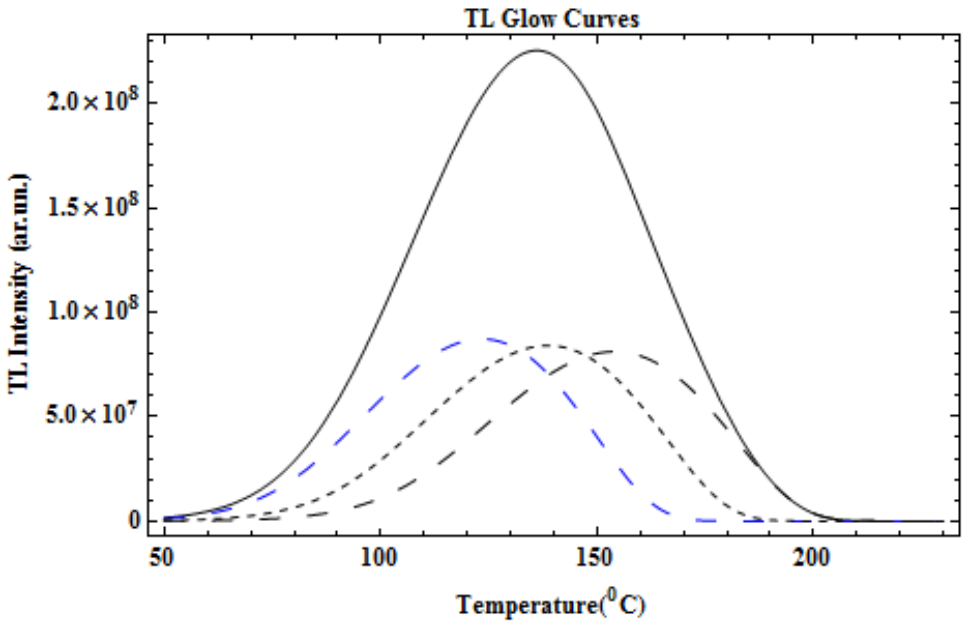

Figure 3.24**:** The Mathematica program solution of the differential equations for IMTS Model for A_n/A_h= 10 and A_m=A_h (three peaks).

```
Ah1 = 1 * 10^-7; An1 = 0.001 * Ah1; Am1 = 1 * Ah1; Nps = 230;
sol1 = NDSolve[{n1'[x] == -n1[x] * s1 / β1 * E^(-E1 / (k * (273 + x))) + An1 * (Nt1 - n1[x]) * nc1[x] / β1,
    nc1'[x] == -n1'[x] - Ah1 * nc1[x] * (m1[x] + n1[x] + nc1[x]) / β1 - nc1[x] * (Mt - m1[x]) * Am1 / β1,
    m1'[x] == nc1[x] * (Mt - m1[x]) * Am1 / β1, n1[0] == 1 * Nt1, nc1[0] == 0, m1[0] == 0 * Mt},
   {n1, nc1, m1}, {x, 50, Nps}, MaxSteps → 3000];
sol2 = NDSolve[{n1'[x] == -n1[x] * s1 / β1 * E^(-E2 / (k * (273 + x))) + An1 * (Nt1 - n1[x]) * nc1[x] / β1,
    nc1'[x] == -n1'[x] - Ah1 * nc1[x] * (m1[x] + n1[x] + nc1[x]) / β1 - nc1[x] * (Mt - m1[x]) * Am1 / β1,
    m1'[x] == nc1[x] * (Mt - m1[x]) * Am1 / β1, n1[0] == 1 * Nt1, nc1[0] == 0, m1[0] == 0 * Mt},
   {n1, nc1, m1}, {x, 50, Nps}, MaxSteps → 3000];
sol3 = NDSolve[{n1'[x] == -n1[x] * s1 / β1 * E^(-E3 / (k * (273 + x))) + An1 * (Nt1 - n1[x]) * nc1[x] / β1,
    nc1'[x] == -n1'[x] - Ah1 * nc1[x] * (m1[x] + n1[x] + nc1[x]) / β1 - nc1[x] * (Mt - m1[x]) * Am1 / β1,
    m1'[x] == nc1[x] * (Mt - m1[x]) * Am1 / β1, n1[0] == 1 * Nt1, nc1[0] == 0, m1[0] == 0 * Mt},
   {n1, nc1, m1}, {x, 50, Nps}, MaxSteps → 3000];
TL1 = Table[Evaluate[Ah1 * nc1[x] * (m1[x] + n1[x] + nc1[x]) /. sol1], {x, 50, Nps}];
nc1 = Table[Evaluate[nc1[x] /. sol1], {x, 50, Nps}]; m1 = Table[Evaluate[m1[x] /. sol1], {x, 50, Nps}];
n1 = Table[Evaluate[n1[x] /. sol1], {x, 50, Nps}]; nh1 = Table[Evaluate[m1[x] + n1[x] + nc1[x] /. sol1], {x, 50, Nps}];
TL2 = Table[Evaluate[Ah1 * nc1[x] * (m1[x] + n1[x] + nc1[x]) /. sol2], {x, 50, Nps}];
nc1 = Table[Evaluate[nc1[x] /. sol2], {x, 50, Nps}]; m1 = Table[Evaluate[m1[x] /. sol2], {x, 50, Nps}];
n1 = Table[Evaluate[n1[x] /. sol2], {x, 50, Nps}]; nh1 = Table[Evaluate[m1[x] + n1[x] + nc1[x] /. sol2], {x, 50, Nps}];
TL3 = Table[Evaluate[Ah1 * nc1[x] * (m1[x] + n1[x] + nc1[x]) /. sol3], {x, 50, Nps}];
nc1 = Table[Evaluate[nc1[x] /. sol3], {x, 50, Nps}]; m1 = Table[Evaluate[m1[x] /. sol3], {x, 50, Nps}];
n1 = Table[Evaluate[n1[x] /. sol3], {x, 50, Nps}]; nh1 = Table[Evaluate[m1[x] + n1[x] + nc1[x] /. sol3], {x, 50, Nps}];
Plot[{Evaluate[{nc1[x] * (m1[x] + n1[x] + nc1[x]) * Ah1} /. sol1] + Evaluate[{nc1[x] * (m1[x] + n1[x] +
        nc1[x]) * Ah1} /. sol2] + Evaluate[{nc1[x] * (m1[x] + n1[x] + nc1[x]) * Ah1} /. sol3],
  Evaluate[{nc1[x] * (m1[x] + n1[x] + nc1[x]) * Ah1} /. sol1], Evaluate[{nc1[x] * (m1[x] + n1[x] +
      nc1[x]) * Ah1} /. sol2], Evaluate[{nc1[x] * (m1[x] + n1[x] + nc1[x]) * Ah1} /. sol3]}, {x, 50, Nps},
 PlotRange → All, PlotLabel → "TL Glow Curves", ImageSize → 72 * 5, Frame → True, FrameLabel →
  {"Temperature(⁰C)", "TL Intensity (ar.un.)"}, LabelStyle → Directive[Bold, 12], PlotStyle →
  {{Black}, {Dashing[Large], Blue}, {Dashed, Black}, {Dashing[Large], Black}}]
```

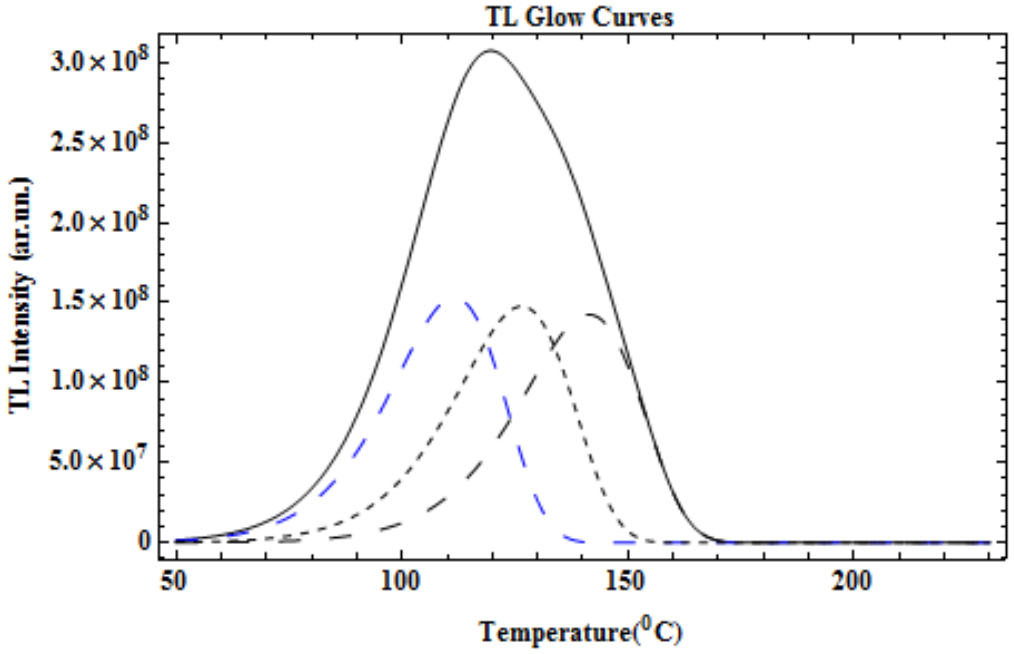

Figure 3.25: The Mathematica program solution of the differential equations for IMTS Model for A_n/A_h= 0.001 and A_m=A_h (three peaks).

CHAPTER 4

RESULTS AND DISCUSSIONS

4.1 First, Second and General-Order

First, second and general-order TL equations were numerically solved with a computer program in Mathematica and all numerically generated TL glow curves were then analyzed by computer curve fitting method with two different developed commercial computer programs; GLOCANIN [15] and Microsoft Excel Spreadsheet [17]. Some of the selected numerically generated glow curves and kinetic parameters obtained by fitting programs were presented in below figures and tables. All FOM values were also obtained by these programs and they are given in tables. It must be indicated that the fitting programs did not give directly values for the second-order and general-order kinetics. If we say $s^{*}=[((s)\times(n_0)^{b-1})/N_t]$, GLOCANIN fitting program gives us $\ln(s^{*})$ for all conditions. On the other hand, Excel Spreadsheet fitting program gives e^ln(s^{*}) values. So, we must be careful in looking into this case *s* results.

4.1. a First, Second and General-Order Glow Curves Generated with One Peak

In this study, the glow curves that includes only one glow peak were initially generated for first-, second- and general-orders by numerical method. To do, the eqn. (3.1), (3.2) and (3.3) were solved numerically with the help of the program prepared by using Mathematica after different kinetic parameters with assuming only one glow peak. Then, all numerically generated glow curves were analyzed (fitted) with the deconvolution programs, namely as GLOCANIN and Excel Spreadsheet, with the help of the data collected by numerical solutions. Finally, the numerical results of both deconvolution programs compared with each other and with the input kinetic parameters in Mathematica to check the success and failure of these programs. The results are given in the below figures and tables.

Figure 4.1 (a) and (c) show the first- and second-order glow curves obtained by using *Mathematica*. Figure 4.1 (b) and (d) show the fitted glow curves obtained by using Excel Spreadsheet program. The input values of kinetic parameters that used in the *Mathematica* programs to generate first- and second-order glow curves and the obtained kinetic parameters analyzing of these glow curves by mentioned CGCD programs are given in Table 4.1.

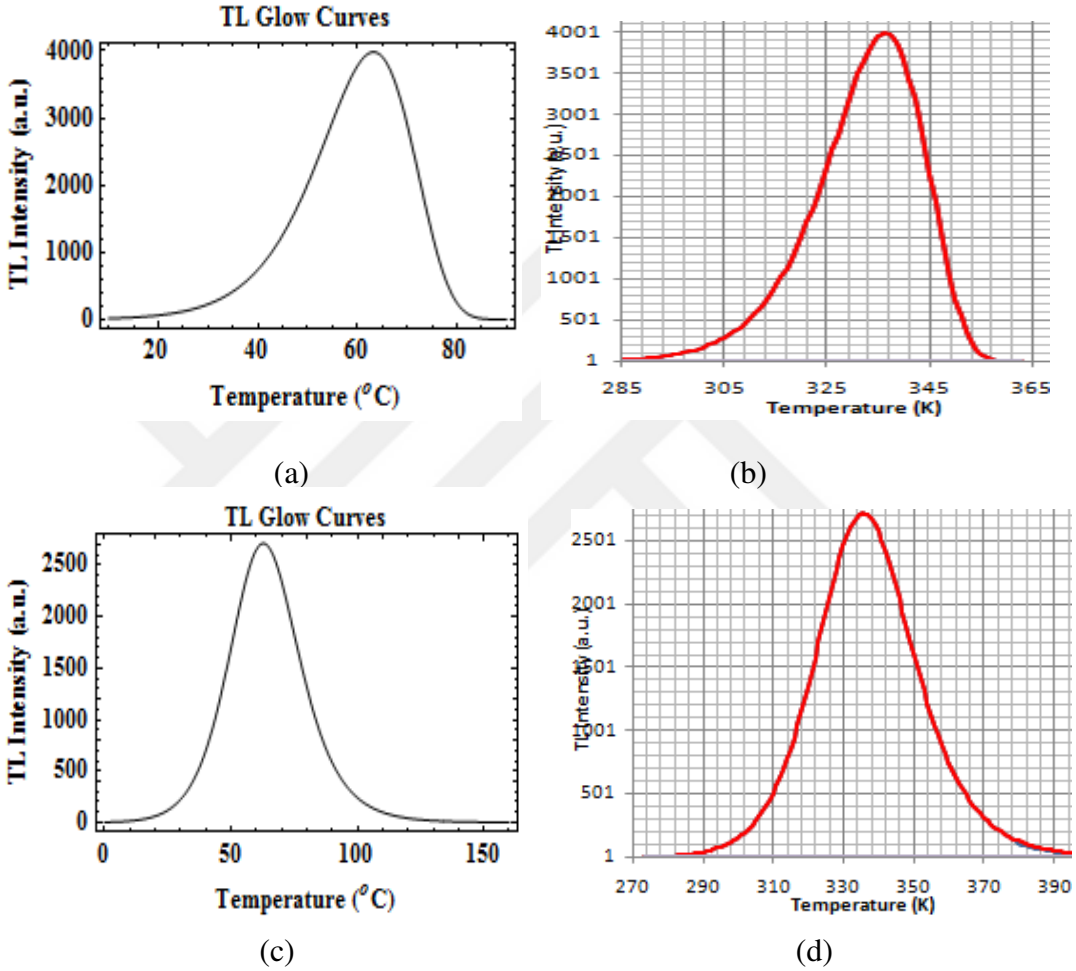

Figure 4.1: (a) and (c) the numerically generated first- and second-order TL glow peak by Mathematica (b) and (d) the fitting of these glow peak by Excel fitting program.

Table 4.1:The input parameters for first- and second-order kinetics which were used in numerical simulated TL glow curves and obtained kinetic parameters after their analysis with Excel (E) and GLOCANIN (G) curve fitting programs for one peak and their comparisons with each other. (For GLOCANIN*s* corresponds to $\ln(s^*)$).

Input Parameters: E=1eV, $s=1x10^{14}$, $((\ln(s^*)=32.2)$, $n_0=N_t=1x10^5$, $\beta=1$							
Kinetic order	E(eV)		b		$s(s^{-1})$		FOM
	E	G	E	G	E	G	
First order(b=1)	1.01	1.00	1.02	1.00	$1x10^{14}$	32.3	0.003
Second order(b=2)	0.99	1.00	1.98	2.00	$8x10^{13}$	32.3	0.020

Figure 4.2 shows the numerically generated TL general-order (b = 1.5) glow curves obtained by using *Mathematica*: It also shows the fitted glow curves by using GLOCANIN. The input values of kinetic parameters that used in the Mathematica to generate general-order glow curves and the obtained kinetic parameters analyzing of these glow curves by CGCD programs are given in Table 4.2.

Table 4.2: The input parameters for different (a) E, (b) b and (c) n_0 values for general-order kinetics which were used in numerical simulated TL glow curves and obtained kinetic parameters after analysis of numerically stimulated glow curves by Excel and GLOCANIN curve fitting programs for one peak. (For Excel fitting program *s* corresponds to e^{lns}, for GLOCANINlns^*).

Input Parameters: E_1=0,8eV, E_2=1,1eV, E_3=1.3, s=$1x10^{14}$ (($ln(s^*)$=26.47 ($e^{26.47}$=$3x10^{11}$)), n_0=N_t=$1x10^5$, b=1.5, β=1						
E(eV)		s (s^{-1})		b		FOM
E	G	E(e^{lns^*})	G(lns*)	E	G	
0.8	0.8	$3x10^{11}$	26.5	1.5	1.5	0.0015
1.1	1.1	$3x10^{11}$	26.49	1.5	1.5	0.0020
1.3	1.3	$2x10^{11}$	26.64	1.5	1.5	0.0017

(a)

Input Parameters:E=1eV, b_1=1.3, b_2=1.5,b_3=1.7,b_4=2, s=$1x10^{14}$ (($ln(s_1^*)$=24.17 ($e_1^{24.17}$=$3x10^{10}$) $ln(s_2^*)$=26.47 ($e_2^{26.47}$=$3x10^{11}$), $ln(s_3^*)$=28.80 ($e_3^{28.80}$=$3x10^{12}$ $ln(s_4^*)$=32.23 ($e_4^{32.23}$=$1x10^{14}$)), n_0=N_t=$1x10^5$, β=1						
E(eV)		s (s^{-1})		b		FOM
E	G	E(e^{lns^*})	G(lns*)	E	G	
1.00	1.00	$3x10^{10}$	24.19	1.3	1.3	0.0026
1.00	1.00	$3x10^{11}$	26.48	1.5	1.5	0.0020
1.00	1.00	$3x10^{12}$	28.80	1.7	1.7	0.0010
1.00	1.00	$1x10^{14}$	32.25	2	2	0.0014

(b)

Input Parameters: E=1eV, b=1.5, N_t=$1x10^5$, β=1, n_1=$1x10^5$,n_2=$0.5x10^5$, n_3=$1x10^4$, s=$1x10^{14}$ (($ln(s_1^*)$=26.47 ($e_1^{26.47}$=$3x10^{11}$), $ln(s_2^*)$=25.79 ($e_2^{25.79}$=$1.6x10^{11}$), $ln(s_3^*)$=25.30 ($e_3^{25.30}$=$1x10^{11}$)),						
E(eV)		s (s^{-1})		b		FOM
E	G	E(e^{lns^*})	G(lns*)	E	G	
1.00	1.00	$3x10^{11}$	26.49	1.5	1.5	0.0020
1.00	1.00	$2x10^{11}$	26.15	1.5	1.5	0.0020
1.00	1.00	$1x10^{11}$	25.34	1.5	1.5	0.0010

(c)

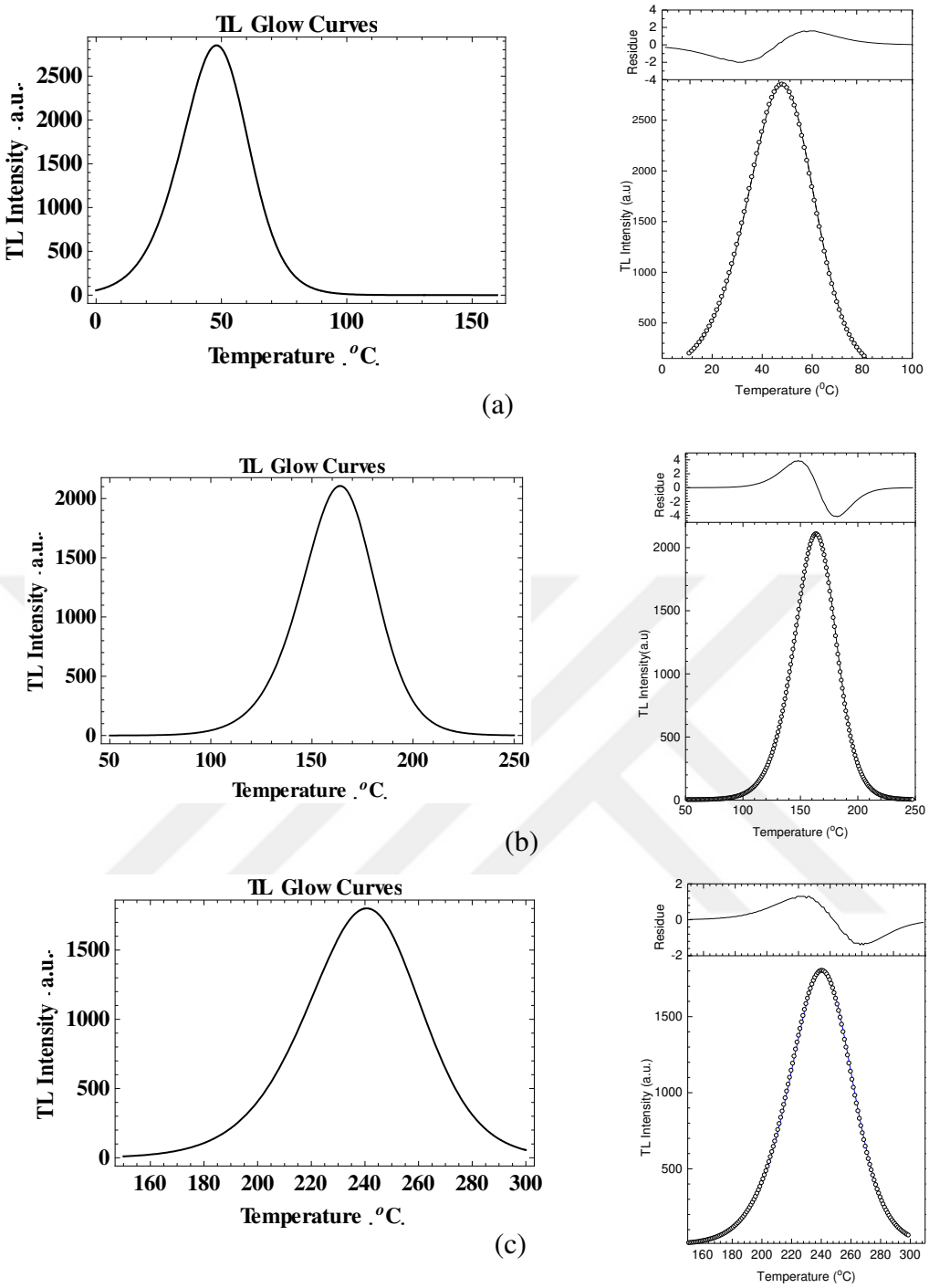

Figure 4.2: The solution of differential equations of general-order TL kinetic equation for b=1.5 by Mathematica. It shows the effect of changing activation energy (E) on the general-order thermoluminescence glow peaks. The fitting results of these glow curve with GLOCANIN are also shown in the figure. a) E= 0.8eV, b) E=1.1eV, c) E=1.3eV.

When the first-, second and general-order glow curves generated with a single glow peak, as seen from tables 4.1 and 4.2, the input values of kinetic parameters entered to Mathematica are very consistent with kinetic parameters obtained by using both GLOCANIN and Excel Spreadsheet programs. So that the obtained results by

fitting programs are very reliable when the glow curves include only one glow peak. The FOM (Figure of Merit) values that were founded by the analysis are also very good for these statements. The outcomes of this study shows that when the TL glow curves are very simple, i.e. they contain only one glow peak, it doesn't matter they are first-, second- and general-order glow peaks, both CGCD analysis programs can be reliable to determine the kinetic order values. However, the simple interface of Excel Spreadsheet program combined with the powerful Solver utility can be more advantageous as it is easier to handle and has more practical uses to perform the analysis in a shorter time.

4.1. b General-Order Glow Curves Generated with Two Peaks

In this study to obtain a little complex glow curves, the glow curves that consist of two general-order glow peaks were then generated by numerical solution of TL equations with Mathematica. Then, all numerically generated glow curves were again analyzed with both deconvolution programs. After the analyzing, the numerical results of deconvolution programs were again compared with the input kinetic parameters that enter in Mathematica to check the success and failure of these programs. The results are given in the below figures and tables.

Figure 4.3 (a-c) shows the general-order glow curves generated and fitted glow curves by using Mathematica, GLOCANIN and Excel Spreadsheet programs. Different kinetic parameters were chosen as input parameters in the *Mathematica* to observe their effects on the analyzing results by fitting programs. The input values of kinetic parameters that used in the *Mathematica* programs to generate general-order glow curves and the obtained kinetic parameters after analyzing these glow curves by CGCD programs are given in Table 4.2.

When the general-order glow curves generated with two glow peaks, as seen from figure 4.3, the input values of kinetic parameters entered to *Mathematica* are again very consistent with kinetic parameters obtained by using both deconvolution programs. Therefore, even if a little complex glow curves that include two general order glow peaks, the obtained results by fitting programs are very consistent with the input parameters. The FOM (Figure of Merit) values are also very good. The outcomes of this study shows that when the TL glow curves consist of one- and two glow peaks, it doesn't matter they are first-, second- and general-order glow peaks, CGCD analysis programs give exact result.

Table 4.3: The input parameters for different (a) E, (b) b and (c) n_0 values for general-order kinetics which were used in numerical simulated TL glow curves and obtained kinetic parameters after analysis of numerically stimulated glow curves by Excel and GLOCANIN curve fitting programs. (For Excel fitting program *s* corresponds to e^{lns}, for GLOCANINlns^*).

Input Parameters: E_1=1eV, E_2=1,1eV, $s=1x10^{14}$ (($ln(s^*)=26.47$ ($e^{26.47}=3x10^{11}$)), $n_0=N_t=1x10^5$, b=1.5, β=1						
E(eV)		$s(s^{-1})$		b		FOM
E	G	$E(e^{lnS^*})$	G(lns*)	E	G	
1.00	1.00	$3x10^{11}$	26.49	1.49	1.5	0.018
1.09	1.10	$3x10^{11}$	26.49	1.49	1.5	

(a)

Input Parameters: E=1eV, b_1=1.5, b_2=1.6, $s=1x10^{14}$ (($ln(s_1^*)=26.47$ ($e_1^{26.47}=3x10^{11}$) $ln(s_2^*)=27.637$ ($e_2^{27.63}=1x10^{12}$)), $n_0=N_t=1x10^5$, β=1						
E(eV)		$S(s^{-1})$		b		FOM
E	G	$E(e^{lnS^*})$	G(lnS*)	E	G	
1.00	1.00	$4x10^{11}$	26.48	1.50	1.50	0.003
1.00	1.00	$1x10^{12}$	27.65	1.59	1.60	

(b)

Input Parameters: E=1eV, b=1.5, $N_t=1x10^5$, β=1, $n_1=0.5x10^5$, $n_3=1x10^5$, $s=1x10^{14}$ (($ln(s_1^*)=25.79$ ($e_1^{25.79}=1.6x10^{11}$),$ln(s_2^*)=26.47$ ($e_2^{26.47}=3x10^{11}$)),						
E(eV)		$S(s^{-1})$		b		FOM
E	G	$E(e^{lnS^*})$	G(lns*)	E	G	
1.00	1.00	$2x10^{11}$	26.49	1.50	1.5	0.003
0.99	1.00	$3x10^{11}$	26.16	1.50	1.5	

(c)

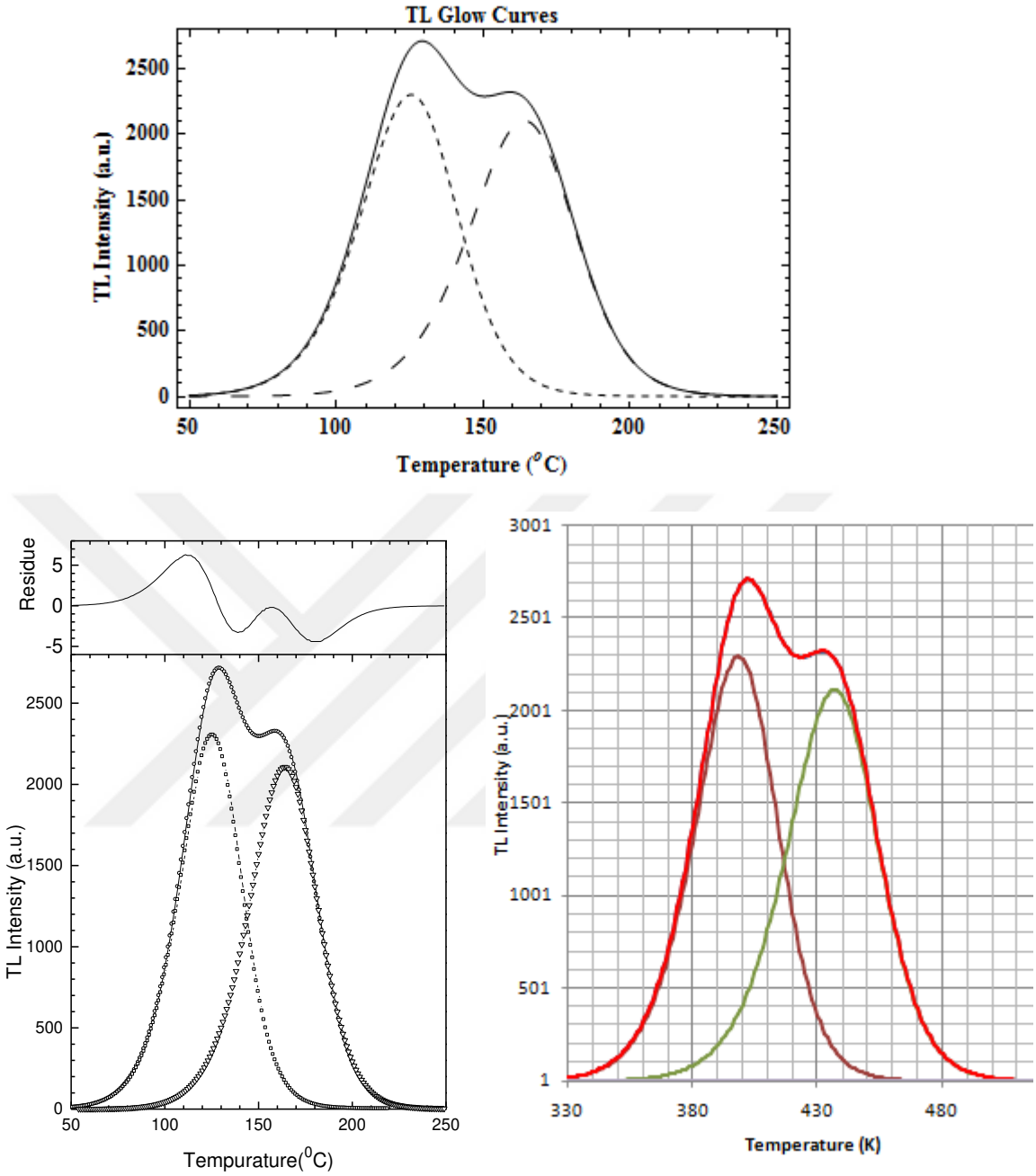
TL Glow Curves
TL Intensity (a.u.)
Temperature (^{o}C)
Residue
TL Intensity (a.u.)
Tempurature(^{0}C)
TL Intensity (a.u.)
Temperature (K)

Fig.4.3.(a)

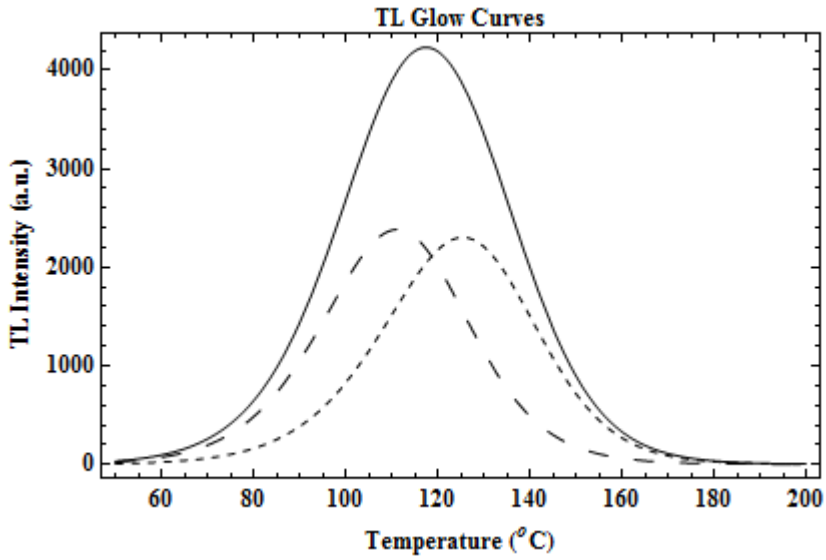
TL Glow Curves
TL Intensity (a.u.)
Temperature (°C)

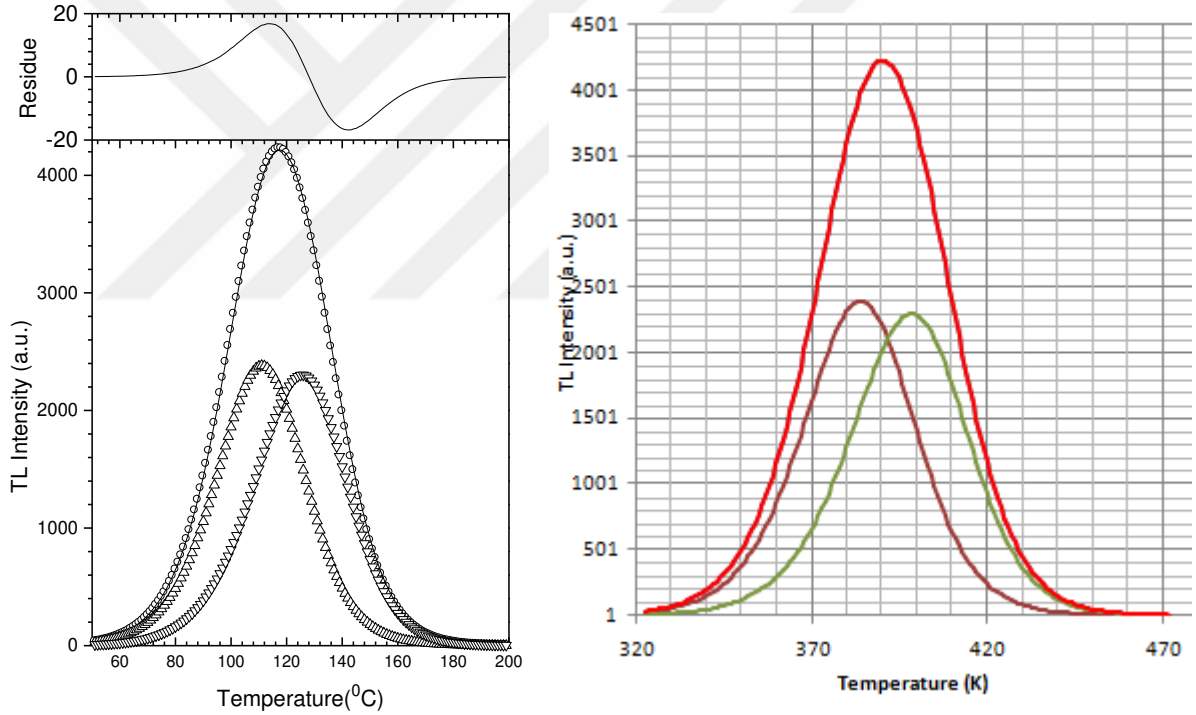
Residue
TL Intensity (a.u.)
Temperature(°C)
TL Intensity (a.u.)
Temperature (K)

Fig.4.3.(b)

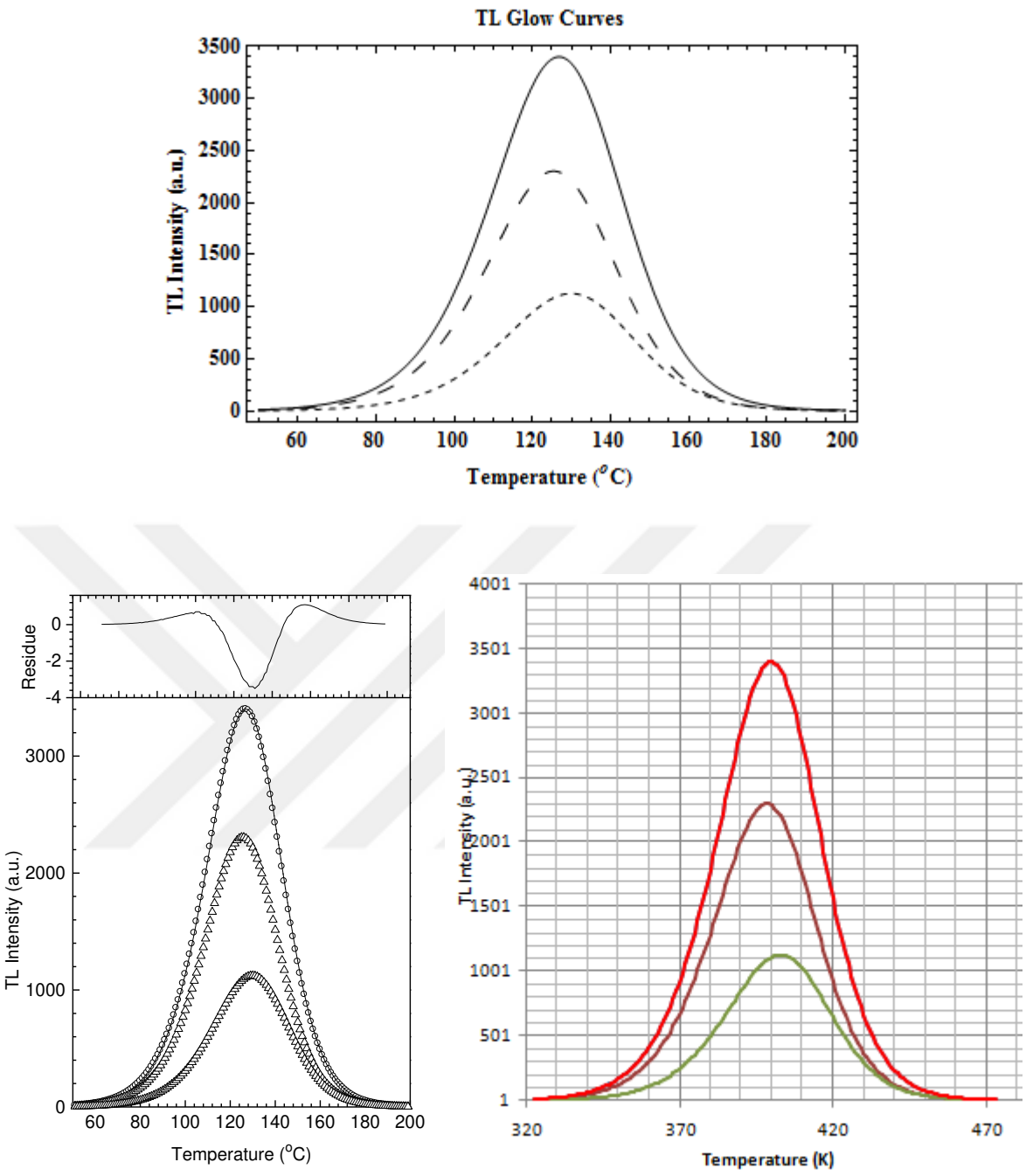

Fig.4.3.(c)

Figure 4.3: The TL glow curves consist of two general-order glow peaks. The glow curves were firstly obtained solution of differential equation of general-order TL kinetics by Mathematica after different values of kinetic parameters (a) activation energy, (b) kinetics order, (c) traps occupancy rate. These glow curves were also analyzed by GLOCANIN and Excel Spreadsheet programs and shown in the below of each glow curve.

4.1. c General-Order Glow Curves Generated with Three Peaks

Three general-order glow peaks included glow curves were also generated by the Mathematica program and tested with the deconvolution programs to check the success and failure of these programs. The results are given in the below figure and table. In the presented glow curve in figure 4.4, the glow peaks have same frequency factors, kinetic orders but different activation energies (E_1=1.0 eV, E_2=1.06 eV and E_3=1.12 eV) that were chosen very close to each other. Because, if the activation energies are very close to each other, the glow peaks are unseparated from each other and the success and failure of the glow curves by the CGCD programs are well understood from the well separated glow peaks.

As seen from the table 4.4, the kinetic parameters of first peak (E_1=1eV) obtained by both deconvolution programs came away different values from input values. On the other hand, the results of second peak (E_2= 1.06eV) were close to the input values in the Excel Spreadsheet program but they are far from the values in GLOCANIN program. Besides, the kinetic parameters of third peak (E_3=1.12eV) obtained by both deconvolution programs are very consistent with the input parameters that were entered in the Mathematica program for this peak. So, the obtained results are reliable for this peak. However, the input values entered to Mathematica which were no fully reliable for the first and second peak as third peak So; the obtained results by the deconvolution programs are not completely reliable when the number of glow peaks increase above two glow peaks. The outcomes of this study up to here shows that for general-order kinetic parameters, although Excel analysis program is more reliable than GLOCANIN program, they can't completely reliable to determine the kinetics parameters when the glow curves includes more than two glow peaks that are close and unseparated from each other.

Table 4.4: The input parameters for different E values for general-order kinetics, which were used in numerical simulated TL glow curves and obtained kinetic parameters after analysis of numerically stimulated glow curve by excel and GLOCANIN curve fitting programs. (For excel fitting program *s* corresponds to e^{lns}, for GLOCANIN lns^*).

Input Parameters: E_1=1eV, E_2=1,06eV, E_3=1.12, s=$1x10^{14}$ ((lns*)=26.47 ($e^{26.47}$=$3x10^{11}$)), n_0=N_t=$1x10^5$, b=1.5, β=1						
E(eV)		$s(s^{-1})$		b		FOM
E	G	$E(e^{lnS^*})$	G(lnS*)	E	G	
0.88	0.80	$2x10^9$	26.33	1.59	1.66	0.2793
1.06	1.23	$3x10^{12}$	31.33	1.37	1.67	
1.11	1.12	$3x10^{11}$	26.49	1.53	1.50	

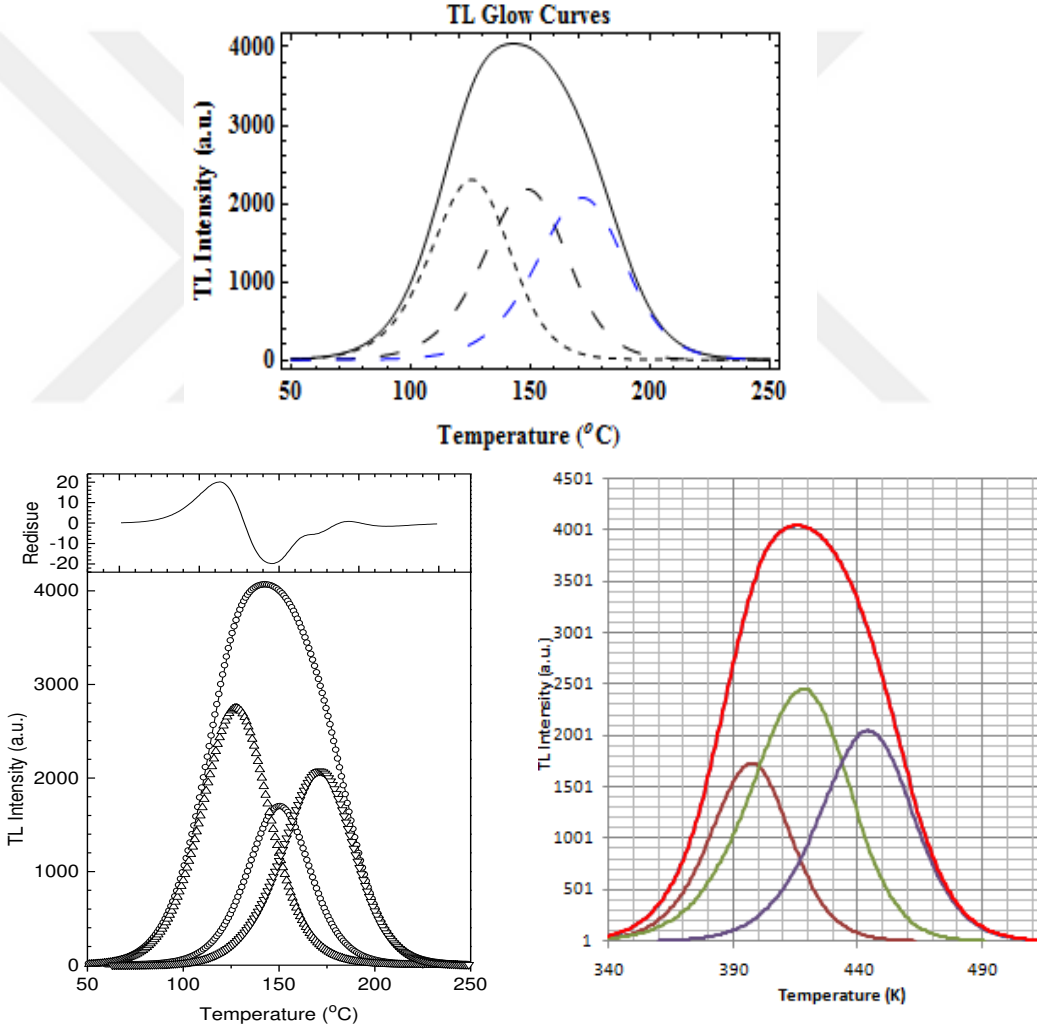

Figure 4.4: The TL glow curve consists of three general-order glow peaks. The glow curve was firstly obtained solution of differential equation of general-order TL kinetics by Mathematica after different E values. The glow curve was then also analyzed by GLOCANIN and Excel Spreadsheet programs to test the success and failure of deconvolution programs. The analyzed glow curves are shown in the below of glow curve.

4.2 OTOR Model

In the second part of this study, the OTOR equations (Eq.3.4-3.7) were numerically solved with a computer program in Mathematica and all obtained glow curves were analyzed by computer glow curve deconvolution methods [17] to check the success and failure of these programs in the investigations of kinetic parameters. Some of the analyzed glow curves and data obtained by fitting programs were presented in below figures and tables.

4.2. a Solutions of OTOR Model Rate Equations with Assuming One Glow Peak and Their Analysis by CGCD Programs

In this case, the eqns. (3.4-3.7) of OTOR model was solved numerically with the help of the program prepared by using Mathematica for different kinetic parameters. However, it was accepted that each numerically generated glow curve contains only one glow peak in this section of this study. Then, the numerically generated all glow curves were analyzed with the deconvolution programs with the help of the data collected. Finally, the results of analysis obtained by programs compared with the input parameters that were entered to the Mathematica to generate numerical glow curves. The input parameters are shown in the top row of each table (table 4.5, 4.6 and 4.7). The obtained kinetic parameters from the CGCD programs were also shown in the bottom rows of these tables. Some of the selected simulated and analyzed glow curves were shown in the figures 4.5 and 4.10.

In the OTOR model, when electron trap is completely filled with electron and if $A_n/A_h>1$, as seen from the table 4.5, the obtained results by CGCD programs and input data in the Mathematica did not match with each other. When $A_n=A_h$ and $A_n/A_h<1$, the analysis results and input data were in consistency with each other or at least small deviations between them were observed.

When the %50 electron traps are filled with electrons and if $A_n/A_h>1$, as seen from the table 4.6, it seems that the discrepancy between input parameters and obtained results have begun to decrease. This indicates that the decrease in the trap occupancy rate has made a positive contribution to the success of the deconvolution programs. In the case of $A_n/A_h\leq1$, the analysis results of CGCD programs are consistent with the input values and obtained kinetic parameters are reliable. On the other hand, a very interesting result is obtained when $A_n/A_h=0.1$. As seen from table 4.6, the discrepancy between input kinetic parameters and analyzed results are

increased and then when $A_n/A_h<0.1$, the discrepancy between them was quickly decreased and they are again start to begun consistent with each other.

When the 10 % electron traps are filled with electrons; and if $A_n/A_h>1$, as seen from the table 4.7, the discrepancy between input parameters and obtained results have been almost eliminated. In this case, it can be assumed that the analysis results are consistent with the input values and they are reliable. However, the discrepancy between them is again high at $A_n/A_h=0.1$ and $A_n/A_h=0.01$.

As a result, if the glow curve is generated by a single glow peak in the OTOR model, the obtained kinetic parameters are generally different from input parameters if $A_n/A_h>1$. So, the analysis results are generally not reliable when $A_n/A_h>1$. But filling percentage of electron traps is reduced, the consistency between input and analyzed kinetic parameters is greatly increased and the analysis results comes to reliable levels when $N_t/n_0<0.5$.

Table 4.5: The below table includes of the input parameters for OTOR model which were used in numerical simulated TL glow curves and obtained kinetic parameters after their analyzing by GLOCANIN and Excel Spreadsheet curve fitting programs if electron traps completely filled ($N_t= n_0$) (one peak).

Input Parameters: E=1eV, $s=1x10^{12}$, $N_t=1x10^{10}$, $\beta=1$, $A_h= 1x10^{-7}$							
A_n/A_h	E(eV)		$s(s^{-1})$		b		FOM
	E	G	E	G(exp(lns*))	E	G	
100	0.60	0.56	$6x10^5$	$3x10^5$	1.89	1.82	2.2466
10	0.65	0.66	$1.5x10^6$	$2x10^6$	1.7	1.75	3.3769
1	1.00	1.00	$1.1x10^{12}$	$2x10^{12}$	2.00	2.00	0.4126
0.1	1.04	1.02	$4x10^{12}$	$6x10^{12}$	1.24	1.29	1.904
0.01	1.01	0.99	$1x10^{12}$	$1x10^{12}$	1.03	1.03	0.967
0.001	1.00	0.99	$1x10^{12}$	$1x10^{12}$	1.00	1.00	0.1316

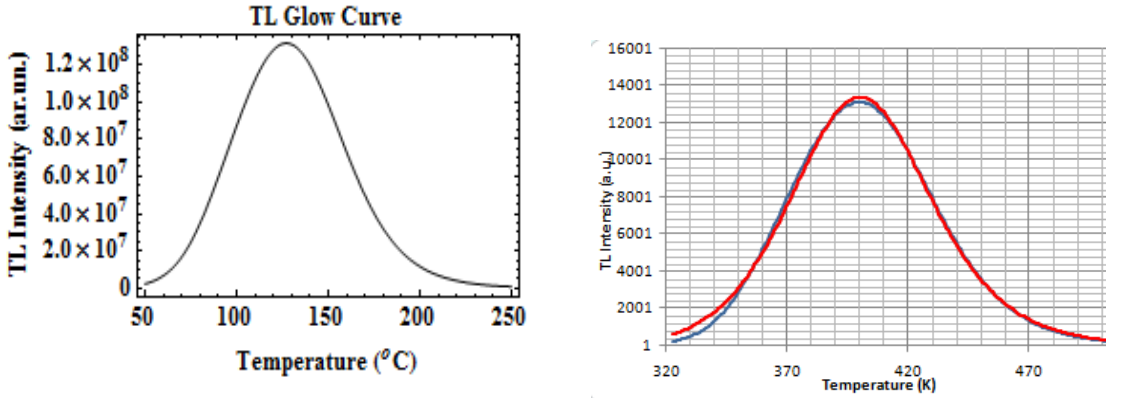

(a)

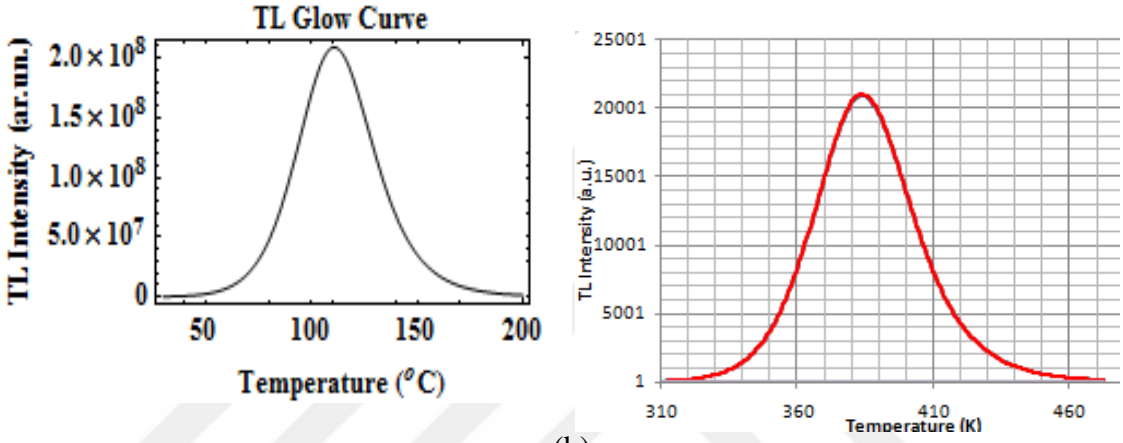

(b)

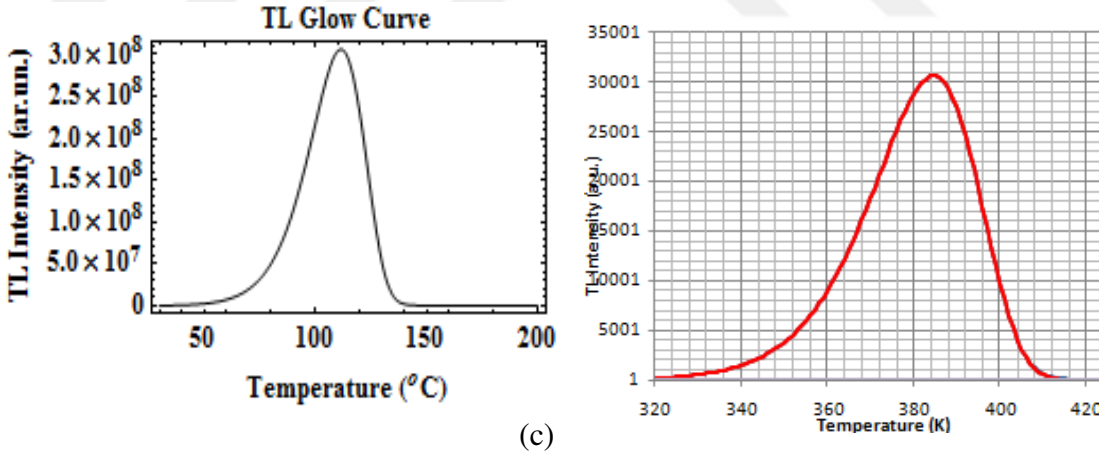

(c)

Figure 4.5: The numerically generated (left side) by the Mathematica and analyzed by Excel Spreadsheet program (right side) glow curves for the following input parameters: (One Peak), (N_t= n_0), (a) (An/Ah=10) (b) (An/Ah=1) (c) (An/Ah=0.001).

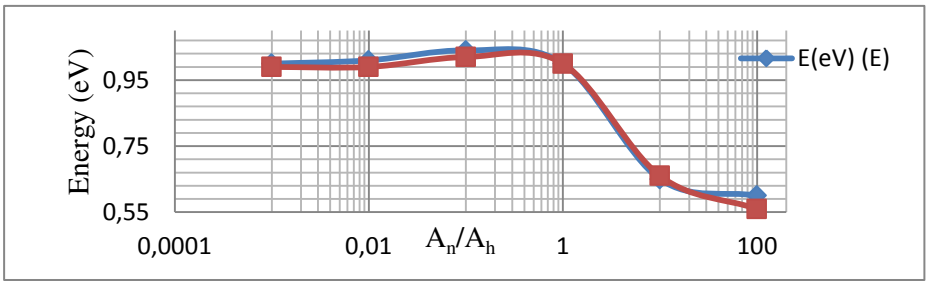

(a)

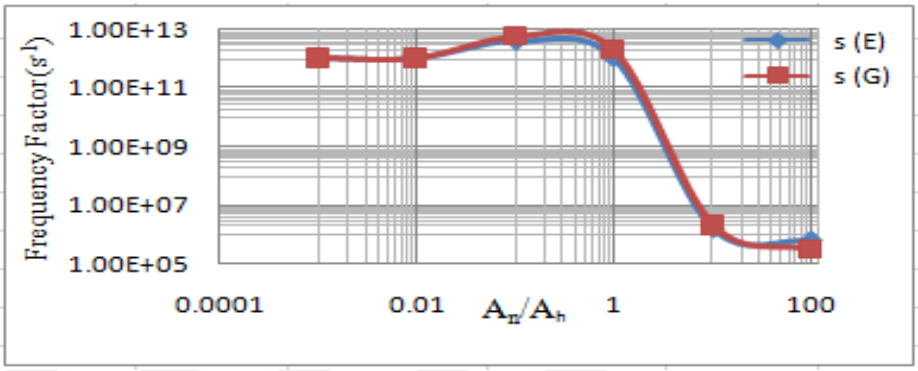

(b)

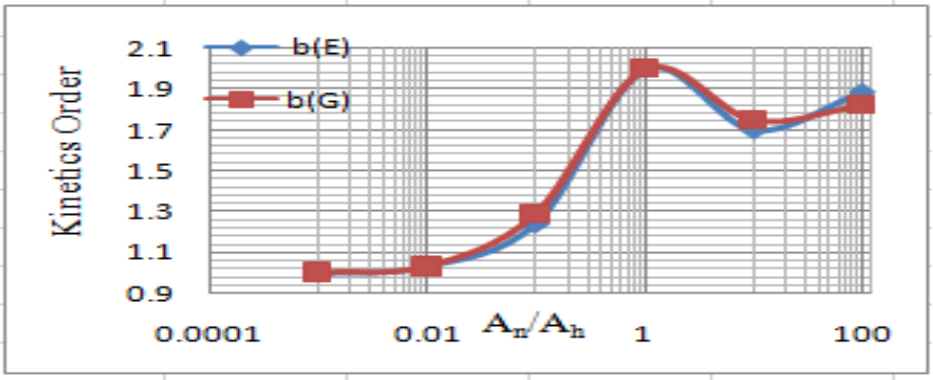

(c)

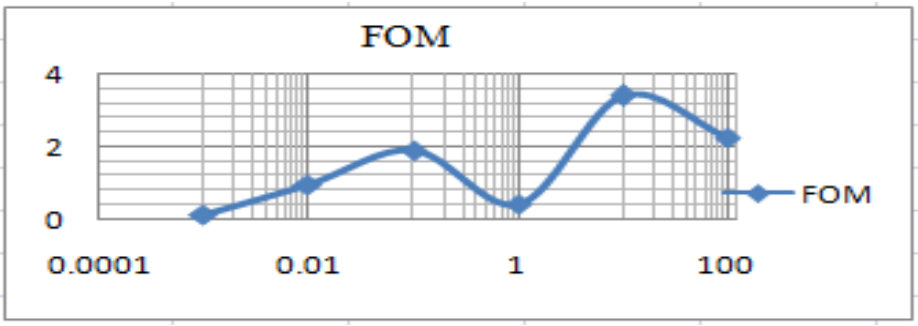

(d)

Figure 4.6: The comparisons of CGCD analysis(E:Excel Spreadsheet, G:GLOCANIN) results of the OTOR model for the following input parameters: ($N_t = n_0$), (One peak), (a) Activation Energy (b) Frequency factor (c) Kinetics order (d) FOM values (Excel).

Table 4.6: The below table includes of the input parameters for OTOR model which were used in numerical simulated TL glow curves and obtained kinetic parameters after their analyzing by GLOCANIN and Excel Spreadsheet curve fitting programs if 50% electron traps filled. ($N_t=0.5n_0$) (One peak).

Input Parameters: E=1eV, s=$1x10^{12}$,$N_t=1x10^{10}$, β=1, $A_h= 1*10^{-7}$							
A_n/A_h	E(eV)		s(s^{-1})		b		FOM
	E	G	E	G(exp(lns*))	E	G	
100	0.87	0.90	$2.3x10^{8}$	$5*10^{8}$	2.00	2.10	2.246
10	0.88	0.91	$2.7x10^{9}$	$6*10^{9}$	2.00	2.09	2.105
1	1.00	1.00	$5.0x10^{12}$	$4*10^{12}$	2.00	2.00	0.100
0.1	1.05	1.08	$6x10^{12}$	$6*10^{12}$	1.40	1.45	3.010
0.01	1.00	1.02	$1.3x10^{12}$	$1.4*10^{12}$	1.04	1.08	1.310
0.001	1.00	1.00	$1x10^{12}$	$1*10^{12}$	1.00	1.00	0.315

Table 4.7: The below table includes of the input parameters for OTOR model which were used in numerical simulated TL glow curves and obtained kinetic parameters after their analyzing by GLOCANIN and Excel Spreadsheet curve fitting programs if 10% electron traps filled. ($N_t=0.1n_0$) (One peak)

Input Parameters: E=1eV, s=$1x10^{10}$, $N_t=1x10^{10}$, β=1, $A_h= 1x10^{-7}$							
A_n/A_h	E(eV)		s(s^{-1})		b		FOM
	E	G	E	G(exp(lns*))	E	G	
100	0.98	0.99	$7x10^{6}$	$9x10^{6}$	2.00	2.05	0.3351
10	0.98	0.99	$7x10^{7}$	$8x10^{7}$	2.00	2.03	0.3120
1	1.00	1.00	$1x10^{9}$	$1x10^{9}$	2.00	2.00	0.2900
0.1	1.05	1.05	$2x10^{10}$	$3x10^{10}$	1.80	1.80	1.7470
0.01	1.04	1.06	$3x10^{10}$	$3x10^{10}$	1.22	1.28	2.6560
0.001	1.00	1.00	$1x10^{12}$	$1x10^{12}$	1.00	1.00	0.1350

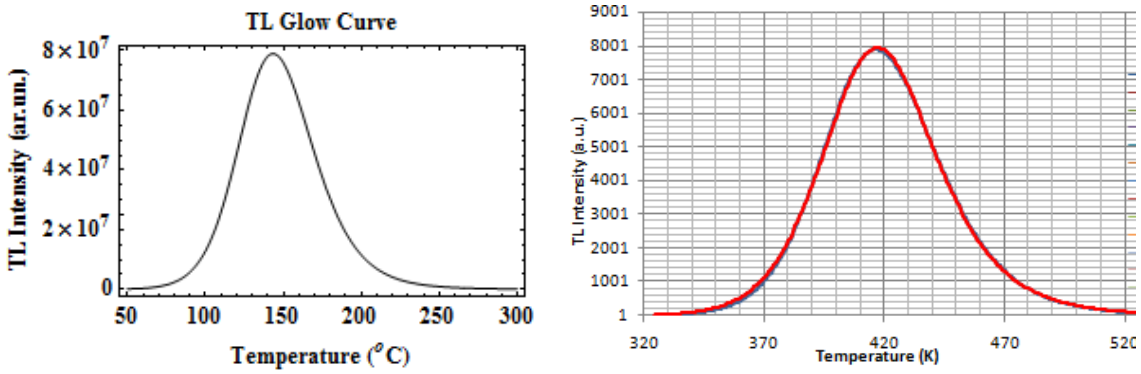

(a)

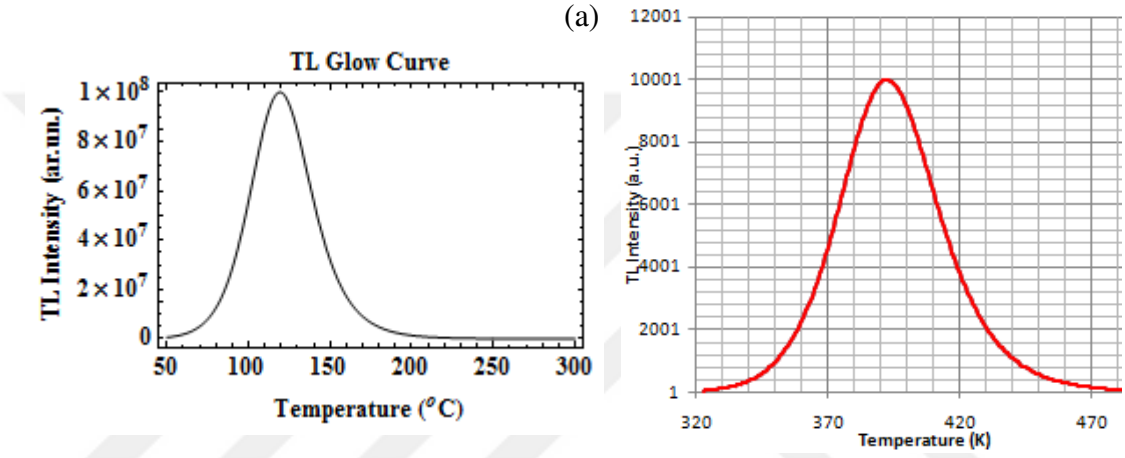

(b)

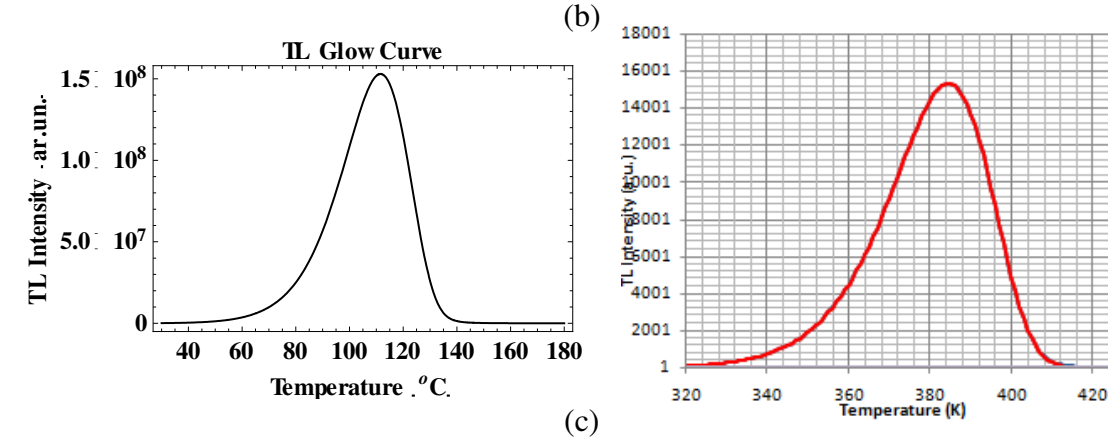

(c)

Figure 4.7: The numerically generated (left side) by the Mathematica and analyzed by Excel Spreadsheet program (right side) glow curves for the following input parameters: (One Peak), (N_t= $0.5n_0$), (a) (An/Ah=10) (b) (An/Ah=1) (c) (An/Ah=0.001).

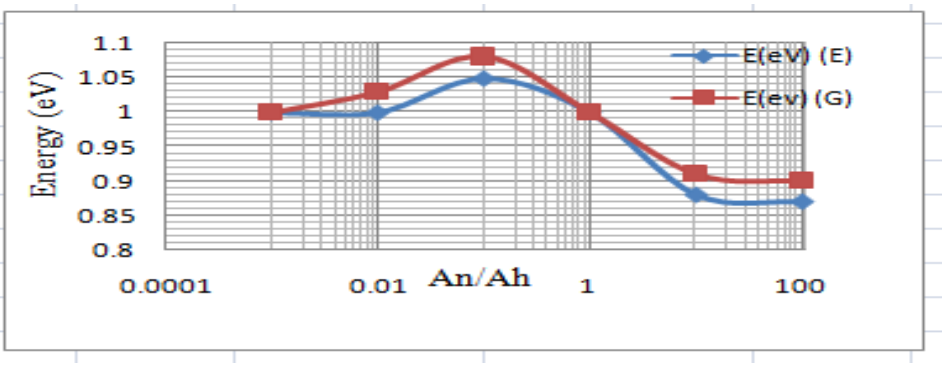

(a)

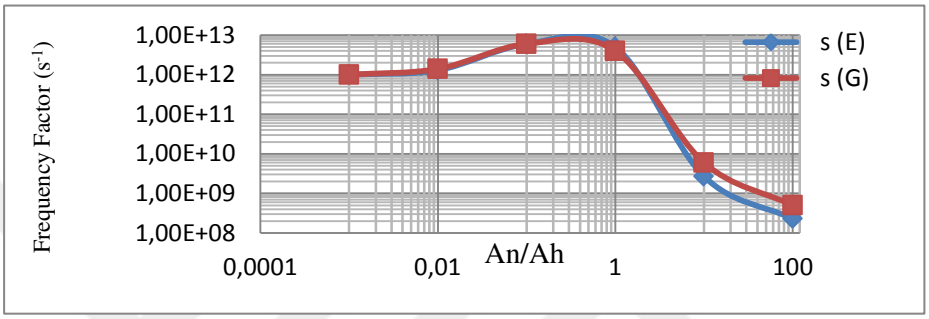

(b)

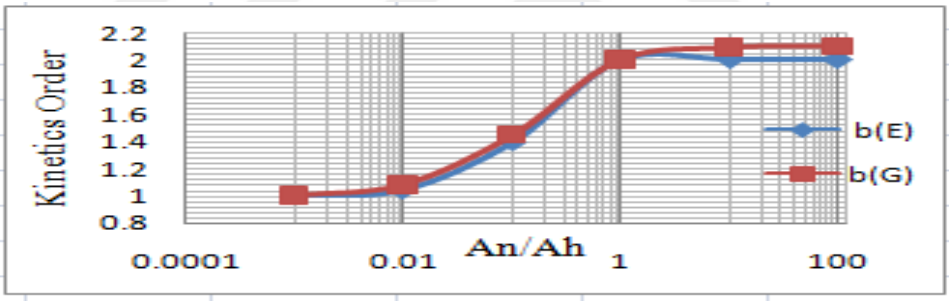

(c)

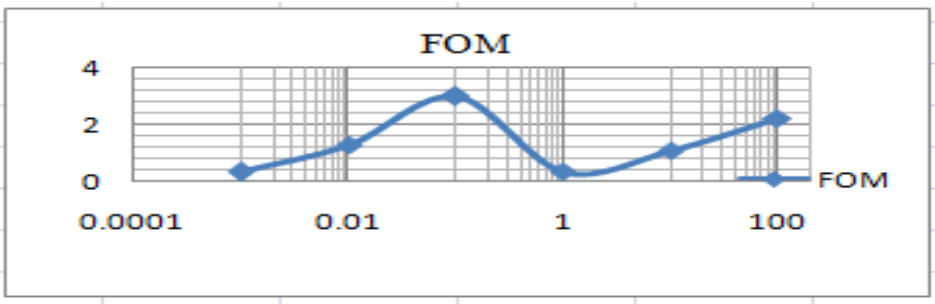

(d)

Figure 4.8: The comparisons of CGCD analysis(E:Excel Spreadsheet, G:GLOCANIN) results of the OTOR model for the following input parameters: (N_t=0.5n_0), (One peak), (a) Energy (b) Frequency factor (c) Kinetics order (d) FOM values (Excel).

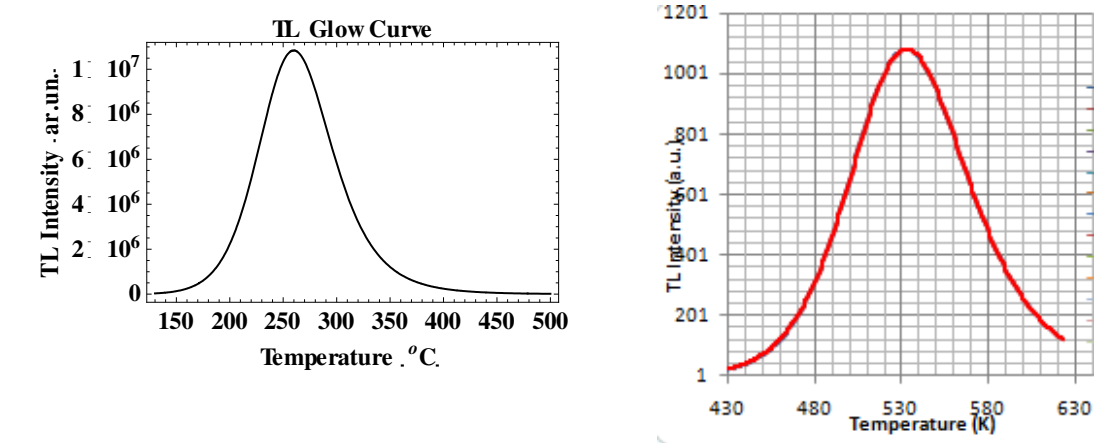

(a)

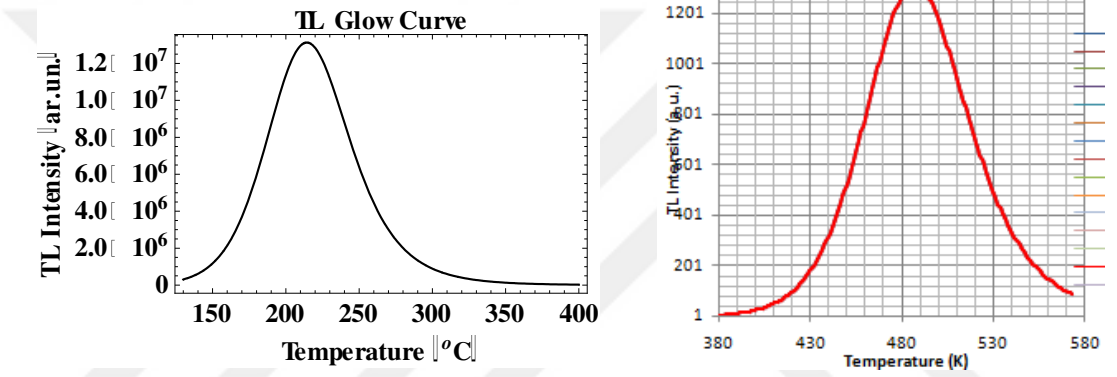

(b)

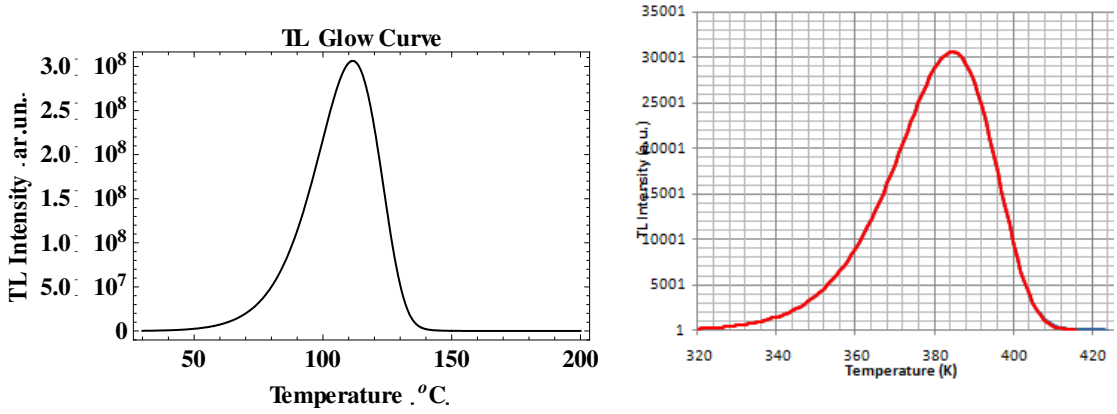

(c)

Figure 4.9: The numerically generated (left side) by the Mathematica and analyzed by Excel Spreadsheet program (right side) glow curves for the following input parameters: (One Peak), (N_t= $0.1n_0$), (a) (An/Ah=10) (b) (An/Ah=1) (c) (An/Ah=0.001).

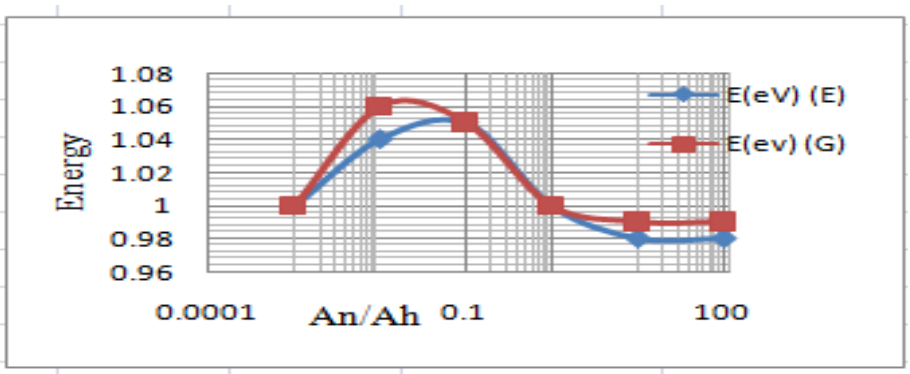

(a)

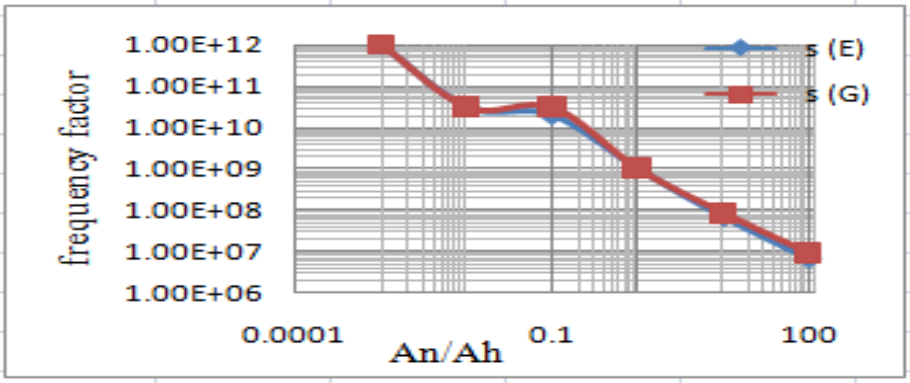

(b)

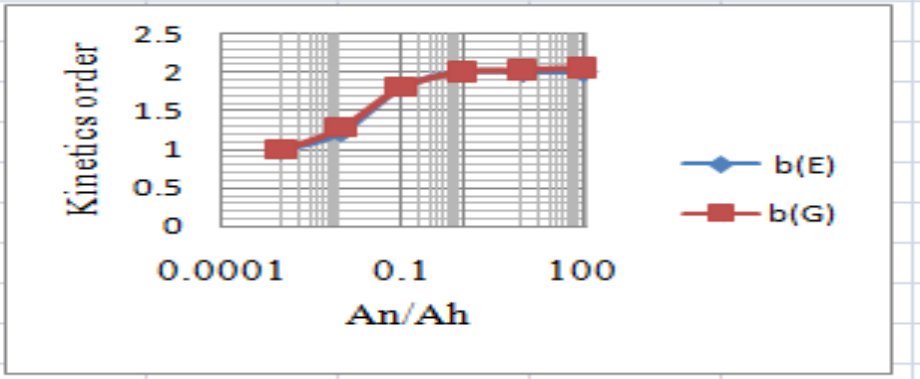

(c)

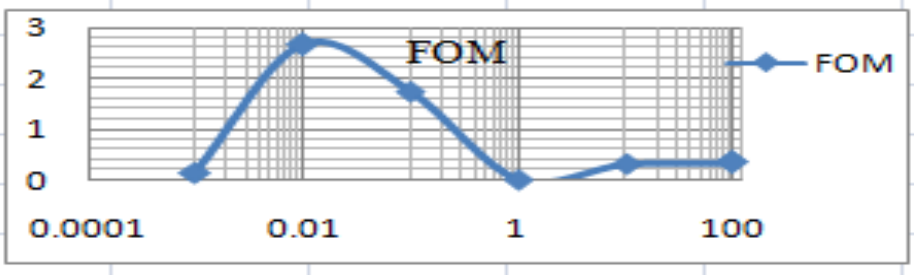

(d)

Figure 4.10: The comparisons of CGCD analysis (E: Excel Spreadsheet, G: GLOCANIN) results of the OTOR model for the following input parameters: (N_t=0.1n_0), (One peak), (a) Energy (b) Frequency factor (c) Kinetics order (d) FOM values (Excel).

4.2. b Solutions of OTOR Model Rate Equations with Assuming Two Glow Peaks and Their Analysis by CGCD Programs

In this case, the rate eqns. (3.4-3.7) of OTOR model was solved numerically with the help of the program prepared by using Mathematica for different kinetic parameters and accepting that each numerically generated glow curve contains two glow peaks. Then, the numerically generated glow curves were analyzed with the deconvolution programs. The results of analysis obtained by programs were again compared with the input parameters that were entered to the Mathematica during the generation of numerical glow curves. The input parameters are shown in the top row of each table (table 4.8, 4.9 and 4.10). The obtained kinetic parameters from the CGCD programs were also shown in the bottom rows of these tables. Some of the selected simulated and analyzed glow curves were shown in the figures 4.11 and 4.17.

When electron trap is completely filled($N_t = n_0$) and if $A_n/A_h > 1$, as seen from the table 4.8, the input data(E_1=1.0 eV, E_2=1.1 eV) in the Mathematica and obtained results by CGCD programs did not match with each other. There are very high discrepancies between these parameters. In this case, the differences between input parameters and obtained results are approximately equal to 50%. On the other hand, when $A_n=A_h$ and $A_n/A_h<1$, the obtained results and input data were in consistency with each other or at least small deviations between them were observed. Especially, the input parameters of second peak highly deviate from its input parameters. When the results of CGCD programs are compared with each other, it was seen that the results of Excel Spreadsheet is generally better than the results of GLOCANIN.

When the 50% electron traps are filled with electrons and if $A_n/A_h>1$, as seen from the table 4.9, it seems that the discrepancy between input parameters (E_1=1.0 eV, E_2=1.1 eV) and the results of CGCD programs for both peaks have begun to decrease. When $A_n/A_h \leq 1$, the analysis results of CGCD programs are consistent with the input values and obtained kinetic parameters are reliable. In the case of A_n/A_h=0.1 while the deviations between the input parameters and its obtained results of the first peak come out from both analysis programs are low, they are very high but for the second peak. As seen from table 4.6, the discrepancy between input kinetic parameters and analyzed results are decreased when $A_n/A_h<0.1$ and they are again start to begun approach to each other.

When the %10 electron traps are filled with electrons; and if $A_n/A_h>1$, as seen from the table 4.10, the discrepancy between input parameters and obtained results have been almost decreased when comparing with the high filling ratios. In the case of $A_n/A_h\leq1$, the analysis results are generally consistent with the input values, but for $A_n/A_h=0.1$ and $A_n/A_h = 0.01$, they are too far for the second peak in both deconvolution programs.

As a result, if the glow curve is generated by two glow peaks in the OTOR model, the obtained kinetic parameters are generally different from input parameters if $A_n/A_h>1$. So, the analysis results are certainly not reliable when $A_n/A_h>1$. But filling percentage of electron traps is reduced, the consistency between input and analyzed kinetic parameters is increased but no reliable results were obtained for both peaks at the same time.

Table 4.8: The below table includes of the input parameters for OTOR model which were used in numerical simulated TL glow curves and obtained kinetic parameters after their analyzing by GLOCANIN and Excel Spreadsheet curve fitting programs if electron traps are completely filled. ($N_t=n_0$) (Two peaks)

Input Parameters: E=1eV, E=1.1eV, $s=1x10^{12}$, $N_t=1x10^{10}$, $\beta=1$, $A_h= 1x10^{-7}$								
A_n/A_h		E(eV)		$s(s^{-1})$		b		FOM
		E	G	E	G(exp(lns*))	E	G	
E_1	10	0.60	0.58	$1x10^6$	$2x10^6$	1.59	1.51	1.2680
E_2		0.68	0.69	$3x10^6$	$4x10^6$	2	2.15	
E_1	1.0	0.99	1.00	$9x10^{11}$	$1x10^{12}$	1.81	2.00	0.1778
E_2		1.02	1.04	$2x10^{11}$	$4x10^{11}$	1.92	2.00	
E_1	0.1	1.00	1.03	$1x10^{12}$	$3x10^{12}$	1.06	1.21	1.440
E_2		1.05	1.33	$3x10^{11}$	$9.5x10^{14}$	1.21	1.47	
E_1	0.01	1.01	1.00	$1.4x10^{12}$	$1.2x10^{12}$	1.02	1.01	0.5220
E_2		1.10	1.11	$1.2x10^{12}$	$2x10^{12}$	1.03	1.05	
E_1	0.001	1.00	1.00	$1x10^{12}$	$1x10^{12}$	1.02	1.00	0.2741
E_2		1.13	1.10	$1.1x10^{12}$	$1x10^{12}$	1.03	1.00	

Table 4.9: The below table includes of the input parameters for OTOR model which were used in numerical simulated TL glow curves and obtained kinetic parameters after their analyzing by GLOCANIN and Excel Spreadsheet curve fitting programs if 50% electron traps are filled. ($N_t=0.5n_0$) (Two peaks).

Input Parameters: E=1eV, E=1.1eV, $s=1x10^{12}$, $N_t=1x10^{10}$, $\beta=1$, $A_h= 1x10^{-7}$								
A_n/A_h		E(eV)		$s(s^{-1})$		b		FOM
		E	G	E	G(exp(lns*))	E	G	
E_1	10	079	0.76	$7x10^{10}$	$2x10^{11}$	1.8	1.82	0.504
E_2		0.99	1.03	$3x10^{8}$	$1.2x10^{8}$	1.93	1.92	
E_1	1	1.01	1.00	$8x10^{11}$	$5x10^{11}$	1.99	2.00	0.4089
E_2		1.08	1.10	$3x10^{11}$	$5x10^{11}$	1.97	2.00	
E_1	0.1	1.03	1.04	$9x10^{11}$	$3x10^{12}$	1.32	1.33	1.052
E_2		1.42	1.41	$9x10^{15}$	$8x10^{15}$	1.72	1.7	
E_1	0.01	1.0	1.00	$1.4x10^{12}$	$1x10^{12}$	1.04	1.01	0.782
E_2		1.16	1.11	$3x10^{11}$	$5x10^{12}$	1.12	1.05	
E_1	0.001	1.00	1.00	$1.4x10^{12}$	$1x10^{12}$	1.02	1.00	0.3332
E_2		1.10	1.10	$1.3x10^{12}$	$1x10^{12}$	1.01	1.00	

Table 4.10: The below table includes of the input parameters for OTOR model which were used in numerical simulated TL glow curves and obtained kinetic parameters after their analyzing by GLOCANIN and Excel Spreadsheet curve fitting programs if 10% electron traps are filled. ($N_t=0.1n_0$) (Two peaks)

Input Parameters E=1eV, E=1.1eV, $s=1x10^{11}$ ($\ln(1x10^{11})=25.32$), $N_t=1x10^{10}$, $\beta=1$, $A_h= 1x10^{-7}$								
A_n/A_h		E(eV)		$s(s^{-1})$		b		FOM
		E	G	E	G(exp(lns*))	E	G	
E_1	10	0.99	0.99	$9x10^{9}$	$1x10^{10}$	1.98	2.06	0.098
E_2		1.06	1.06	$4x10^{9}$	$3x10^{9}$	1.99	1.96	
E_1	1	1.00	1.05	$1x10^{11}$	$1x10^{11}$	1.98	2.00	0.0064
E_2		1.08	1.10	$9x10^{10}$	$1x10^{11}$	2.00	2.00	
E_1	0.1	1.05	1.05	$3x10^{12}$	$1x10^{12}$	1.99	1.69	0.7311
E_2		1.36	1.36	$7x10^{14}$	$7x10^{14}$	2.00	2.07	
E_1	0.01	1.02	1.02	$2x10^{12}$	$3x10^{12}$	1.17	1.20	1.178
E_2		1.33	1.33	$7x10^{14}$	$7x10^{14}$	1.45	1.45	
E_1	0.001	1.00	1.00	$1.2x10^{12}$	$1.2x10^{12}$	1.01	1.01	0.5037
E_2		1.12	1.12	$2x10^{12}$	$2x10^{12}$	1.05	1.05	

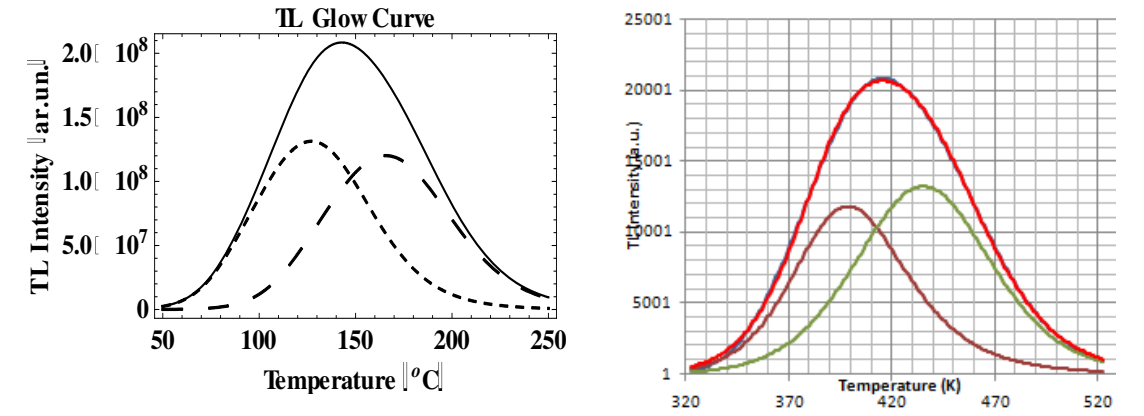

(a)

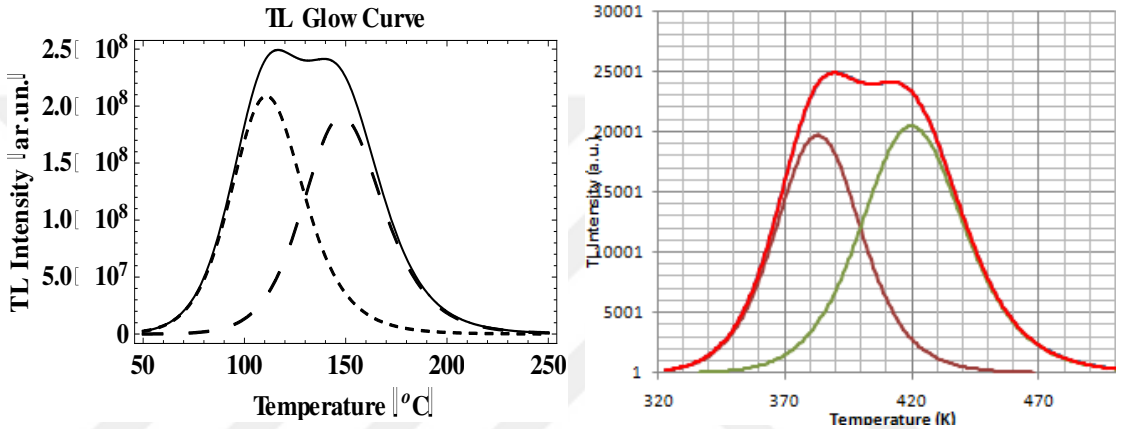

(b)

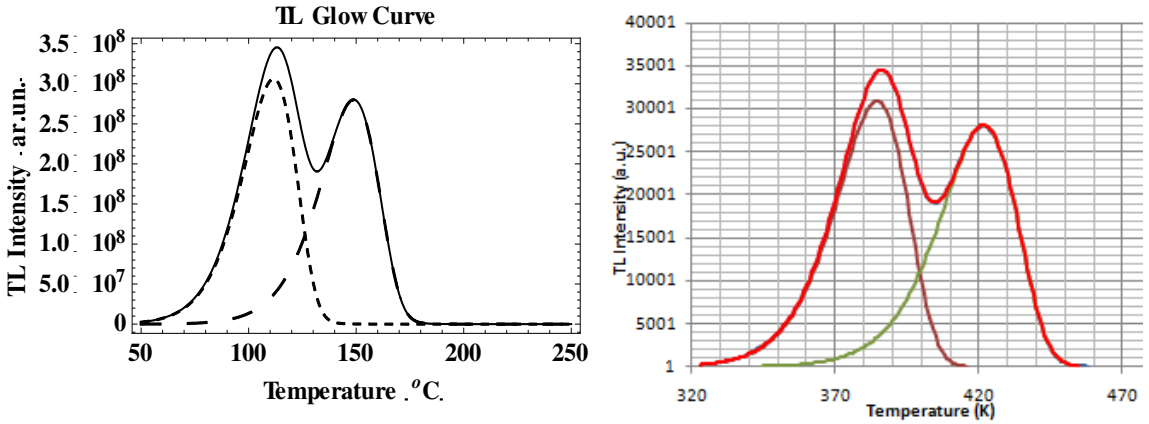

(c)

Figure 4.11: The numerically generated (left side) by Mathematica and then analyzed by Excel Spreadsheet program (right side) glow curves for the following input parameters: (N_t= n_0) (Two Peaks). (a) (A_n/A_h=10) (b) (A_n/A_h=1) (c) (A_n/A_h=0.001).

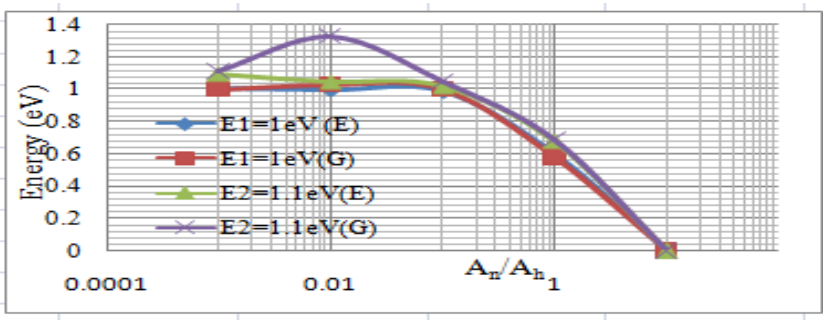

(a)

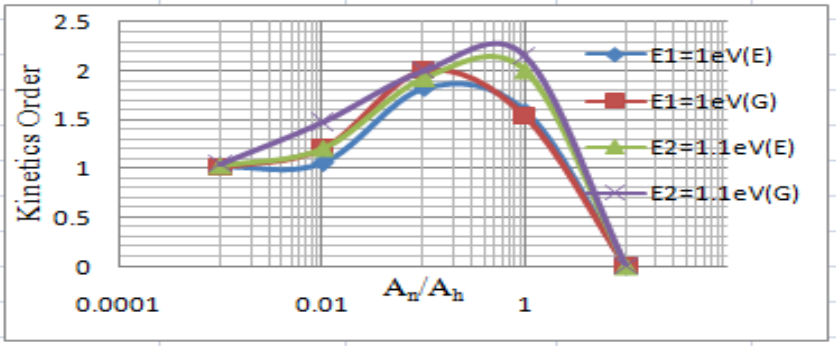

(b)

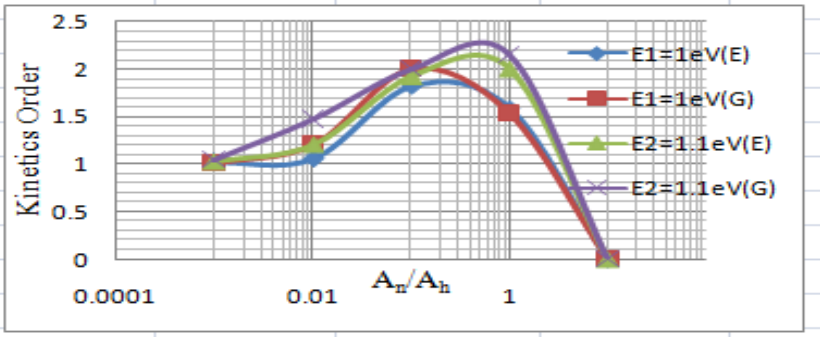

(c)

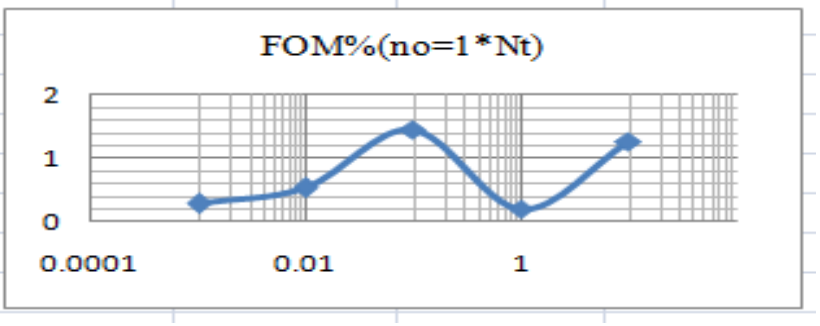

(d)

Figure 4.12: The comparisons of CGCD analysis (E: Excel Spreadsheet, G: GLOCANIN) results of the OTOR model for the following input parameters: (N_t=n_0), (Two peaks), (a) Activation Energy (b) Frequency factor (c) Kinetics order (d) FOM values (Excel).

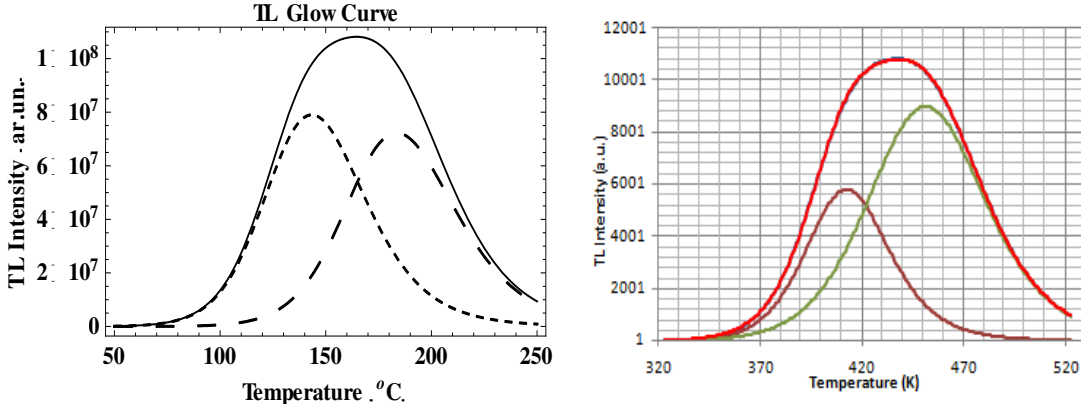

(a)

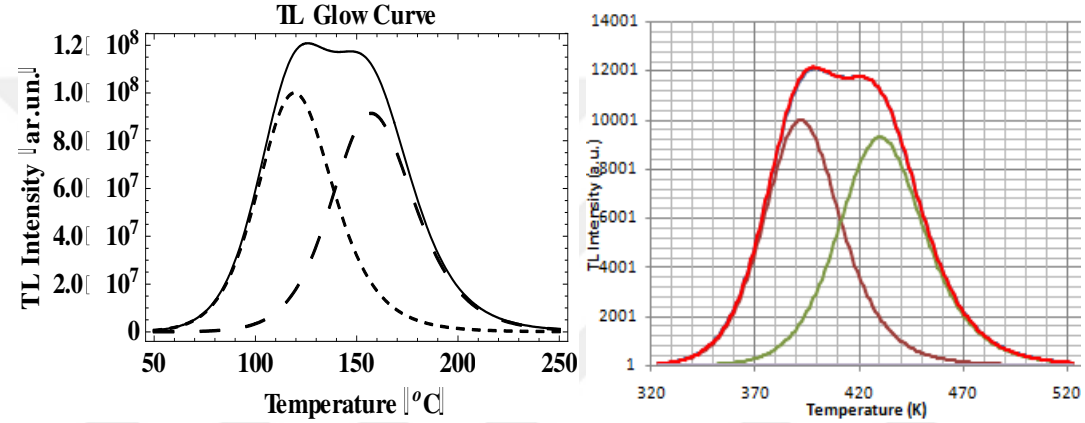

(b)

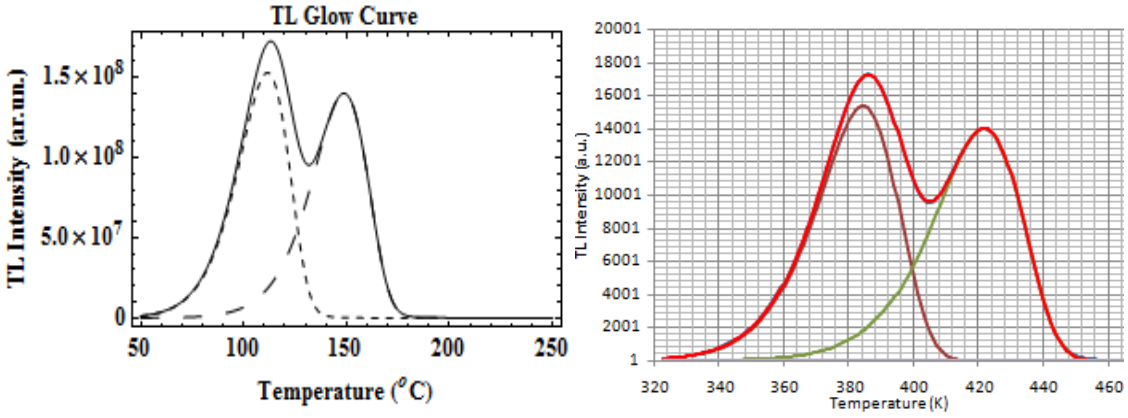

(c)

Figure 4.13: The numerically generated (left side) by Mathematica and then analyzed by Excel Spreadsheet program (right side) glow curves for the following input parameters: (N_t= $0.5n_0$) (Two Peaks). (a) (A_n/A_h=10) (b) (A_n/A_h=1) (c) (A_n/A_h=0.001).

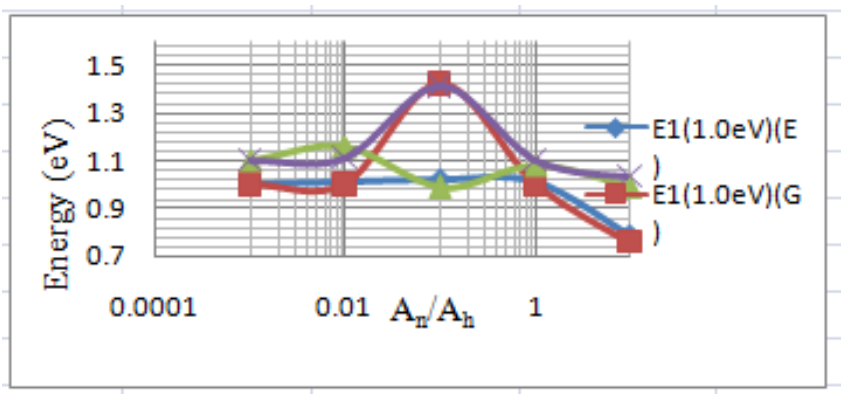

(a)

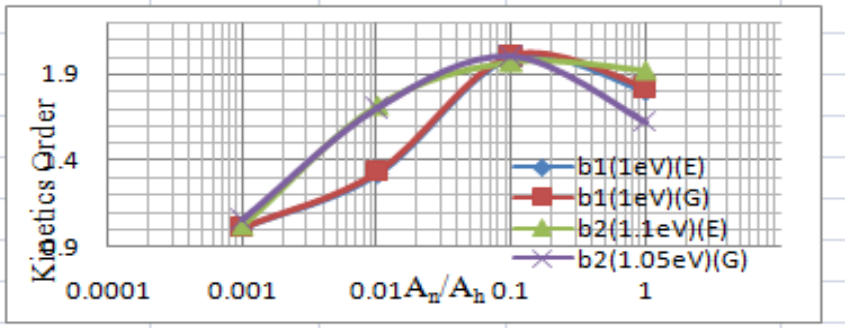

(b)

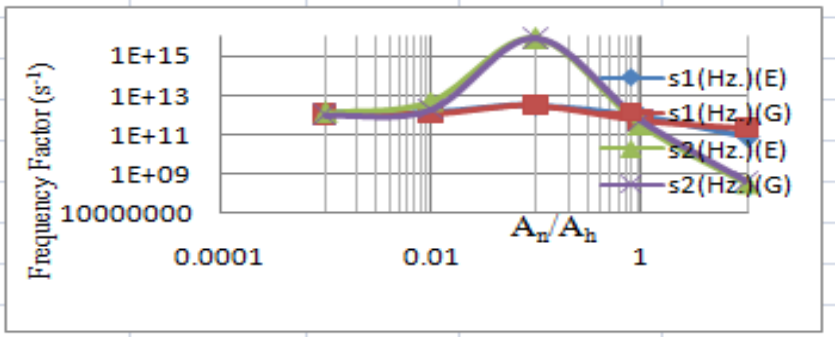

(c)

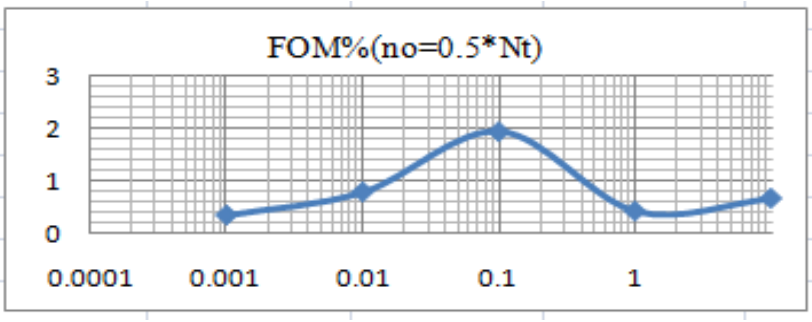

(d)

Figure 4.14: The comparisons of CGCD analysis (E: Excel Spreadsheet, G: GLOCANIN) results of the OTOR model for the following input parameters: (N_t=0.5n_0), (Two peaks), (a) Activation Energy (b) Frequency factor (c) Kinetics order (d) FOM values (Excel).

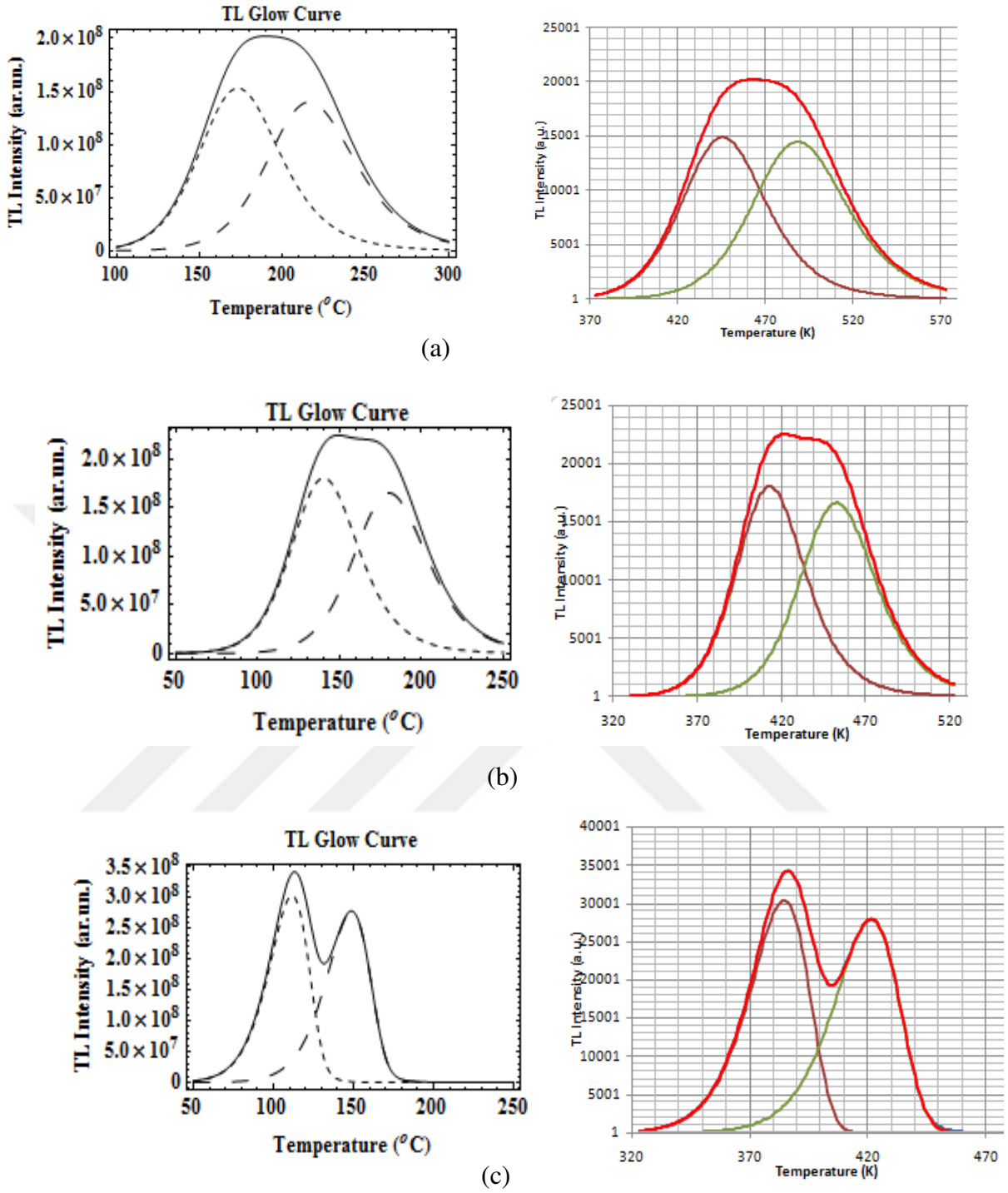

Figure 4.15: The numerically generated (left side) by Mathematica and then analyzed by Excel Spreadsheet program (right side) glow curves for the following input parameters: (N_t= $0.1n_0$) (Two Peaks). (a) (A_n/A_h=10) (b) (A_n/A_h=1) (c) (A_n/A_h=0.001).

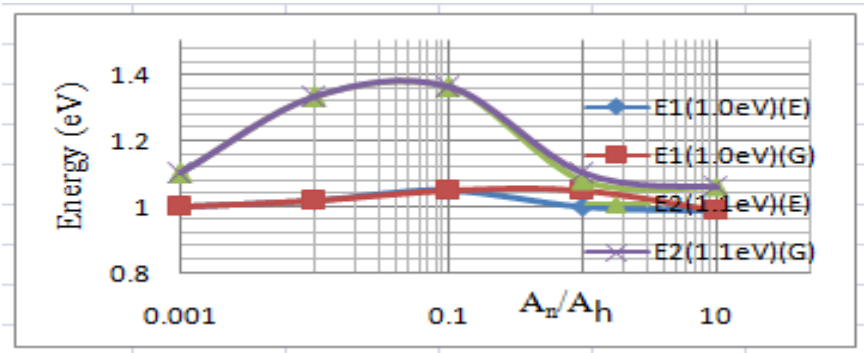

(a)

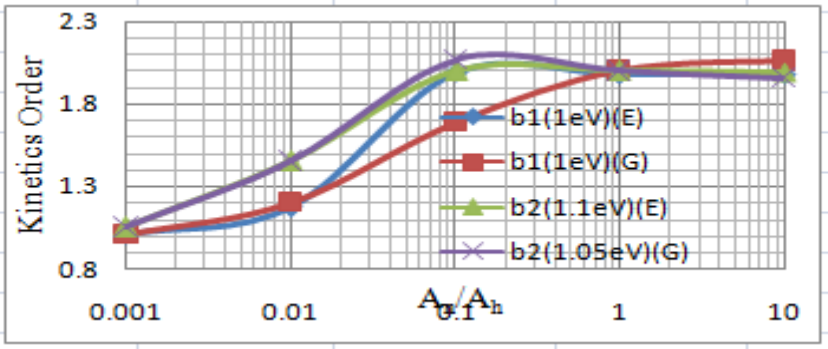

(b)

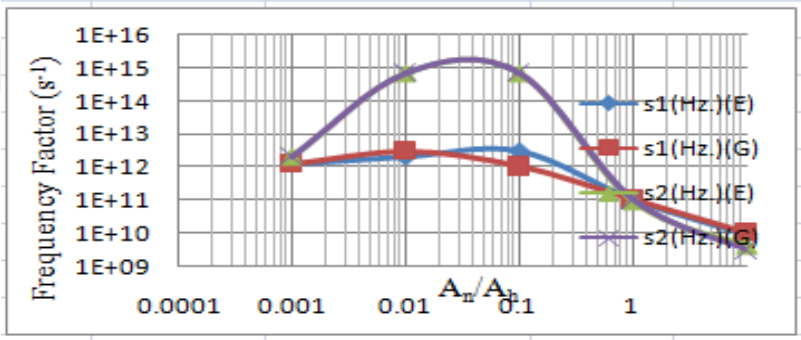

(c)

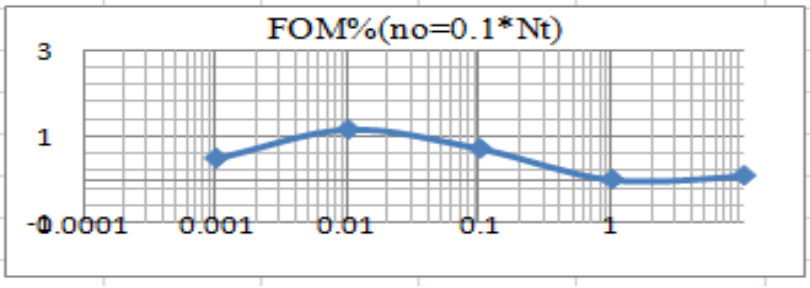

(d)

Figure 4.16: The comparisons of CGCD analysis (E: Excel Spreadsheet, G: GLOCANIN) results of the OTOR model for the following input parameters: (N_t=0.1n_0), (Two peaks), (a) Activation Energy (b) Frequency factor (c) Kinetics order (d) FOM values (Excel).

4.2. c Solutions of OTOR Model Rate Equations with Assuming Three Glow Peaks and Their Analysis by CGCD Programs

The rate equations (3.4-3.7) of OTOR model was solved numerically by using Mathematica for different kinetic parameters and accepting that each numerically generated glow curve contains three glow peaks. Then, they were analyzed with the deconvolution programs. The results of analysis obtained by programs were again compared with the input parameters that were entered to the Mathematica during the generation of numerical glow curves. The input parameters are shown in the top row of each table (table 4.11, 4.12 and 4.13). The obtained kinetic parameters from the CGCD programs were also shown in the bottom rows of these tables. Some of the selected simulated and analyzed glow curves were shown in the figures 4.19 and 4.23.

Table 4.11: The below table includes of the input parameters for OTOR model which were used in numerical simulated TL glow curves and obtained kinetic parameters after their analyzing by GLOCANIN and Excel Spreadsheet curve fitting programs if 10% electron traps are filled. ($N_t = n_0$) (Three peaks)

Input Parameters: E_1=1eV, E_2=1.1eV, E_3=1.2eV, $s=1x10^{12}$, $N_t=1x10^{10}$, β=1, $A_h= 1x10^{-7}$								
A_n/A_h		E(eV)		s(s^{-1})		b		FOM
		E	G	E	G(exp(lns*))	E	G	
E_1	10	0.6	0.57	$2x10^6$	$1x10^6$	1.36	1.52	1.73
E_2		0.78	0.69	$7x10^7$	$4x10^7$	1.78	1.66	
E_3		0.90	0.80	$1x10^9$	$2x10^8$	1.90	1.99	
E_1	1	0.84	0.80	$1.4x10^9$	$2x10^8$	1.99	1.39	1.65
E_2		1.03	0.88	$3x10^{12}$	$9x10^{14}$	2.00	3.54	
E_3		1.16	1.14	$4x10^{11}$	$2x10^{10}$	2.00	1.99	
E_1	0.1	0.95	3.32	$2x10^9$	$3x10^{30}$	1.03	2.95	1.84
E_2		0.98	1.25	$6x10^{11}$	$2x10^{15}$	1.01	2.72	
E_3		1.02	1.03	$1x10^{11}$	$7x10^{10}$	1.02	1.03	
E_1	0.01	1.00	0.82	$1x10^{12}$	$4x10^9$	1.01	1.00	0.37
E_2		1.10	0.85	$1x10^{12}$	$3x10^9$	1.02	0.68	
E_3		1.20	1.03	$1x10^{12}$	$7x10^{10}$	1.03	1.06	
E_1	0.001	1.00	1.00	$1x10^{12}$	$1x10^{12}$	1.01	1.07	0.20
E_2		1.11	1.11	$1x10^{12}$	$1x10^{12}$	1.02	1.06	
E_3		1.23	1.23	$3x10^{12}$	$1x10^{23}$	1.03	4.32	

As we have seen in the previous sections, when electron trap is completely filled ($N_t = n_0$) and if $A_n/A_h > 1$, as seen from the table 4.11, the input data(E_1=1.0 eV, E_2=1.1 eV, E_3=1.2 eV) in the Mathematica and obtained results by CGCD programs did not match with each other. Again, high discrepancies between input and obtained parameters were observed. Moreover, in contrast to one and two generated glow peaks by the Mathematica program, the results of Excel Spreadsheet are close to the input values for each of the three peaks than the results of GLOCANIN.

Table 4.12: The below table includes of the input parameters for OTOR model which were used in numerical simulated TL glow curves and obtained kinetic parameters after their analyzing by GLOCANIN and Excel Spreadsheet curve fitting programs if 10% electron traps are filled. ($N_t = 0.5n_0$) (Three peaks)

Input Parameters: E_1=1eV, E_2=1.1eV, E_3=1.2eV, s=1x10^{12}, N_t=1x10^{10} , β=1, A_h= 1x10^{-7}								
A_n/A_h		E(eV)		s(s^{-1})		b		FOM
		E	G	E	G (exp(lns^*))	E	G	
E_1	10	0.95	0.65	1.68x10^{10}	2x10^{10}	1.99	4.34	2.885
E_2		1.09	0.66	5x10^{10}	3x10^{7}	2.00	1.00	
E_3		1.15	0.86	2x10^{10}	1x10^{36}	2.01	1.99	
E_1	1	1.00	0.80	5x10^{11}	1x10^{8}	2.00	1.99	0.0045
E_2		1.10	1.07	4.9x10^{11}	8x10^{12}	1.99	1.00	
E_3		1.20	1.78	5x10^{11}	1x10^{36}	2.00	2.82	
E_1	0.1	0.82	0.62	5x10^{9}	9x10^{7}	1.03	6.47	2.347
E_2		0.97	0.97	3x10^{10}	4x10^{11}	1.02	1.00	
E_3		0.98	1.03	5x10^{7}	7x10^{10}	1.01	1.00	
E_1	0.01	1.00	0.56	1x10^{12}	1x10^{5}	1.01	4.23	0.6016
E_2		1.09	1.02	8x10^{11}	2x10^{12}	1.02	1.00	
E_3		1.17	1.03	5x10^{11}	7x10^{10}	1.03	1.00	
E_1	0.001	1.00	1.01	1x10^{12}	1x10^{12}	1.01	1.06	0,199
E_2		1.11	1.11	2x10^{12}	7x10^{10}	1.02	1.06	
E_3		1.23	1.45	1x10^{12}	1x10^{16}	1.03	37.54	

In fact, it should be in the presentation that the results of GLOCANIN are always far from the input values for all A_n/A_h values. Even, some of the obtained results from the GLOCANIN remain far away from the input values and they can be regarded as meaningless for physics. Even if the Excel Spreadsheet results are mostly consistent with the input values than the GLOCANIN results. However, we didn't obtain completely consistent results in all conditions if three glow peaks were assumed in the glow curves. So, the number of glow peaks within the glow curve are increased, the consistency of the CGCD results with input parameters are highly decreased and the reliability of CGCD results are completely vanished. So, if a glow curve consists of more than two glow peaks, it can be noted that the results of Excel Spreadsheet are better than the results of GLOCANIN for all conditions of trap occupancy rates.

Table 4.13: The below table includes of the input parameters for OTOR model which were used in numerical simulated TL glow curves and obtained kinetic parameters after their analyzing by GLOCANIN and Excel Spreadsheet curve fitting programs if 10% electron traps are filled. (N_t= $0.1n_0$) (Three peaks)

Input Parameters: E_1=1eV, E_2=1.1eV, E_3=1.2eV, s=$1x10^{12}$, N_t=$1x10^{10}$, β=1, A_h= $1x10^{-7}$								
A_n/A_h		E(eV)		$s(s^{-1})$		b		FOM
		E	G	E	G (exp(lns*))	E	G	
E_1	10	0.99	0.64	$1x10^{10}$	$3x10^{5}$	1.99	1.18	3.446
E_2		1.09	1.01	$1x10^{10}$	$7x10^{27}$	2.00	1.80	
E_3		1.18	1.02	$8x10^{10}$	$2x10^{8}$	2.01	1.99	
E_1	1	1.00	0.49	$1x10^{11}$	$5x10^{5}$	2.00	1.00	0.080
E_2		1.10	0.95	$1x10^{11}$	$2x10^{8}$	1.99	1.99	
E_3		1.20	1.15	$1x10^{11}$	$2x10^{17}$	2.00	1.96	
E_1	0.1	1.00	0.33	$8x10^{10}$	$4x10^{35}$	1.02	2.96	0.557
E_2		1.02	1.03	$1.4x10^{10}$	$7x10^{10}$	1.03	1.03	
E_3		1.27	1.25	$1.6x10^{9}$	$2x10^{15}$	1.04	2.72	
E_1	0.01	0.94	0.82	$1x10^{10}$	$4x10^{9}$	1.01	1.00	0.578
E_2		1.00	0.85	$3x10^{9}$	$2x10^{10}$	1.01	0.69	
E_3		1.04	1.03	$3x10^{7}$	$7x10^{10}$	1.02	1.06	
E_1	0.001	1.00	1.00	$1.2x10^{12}$	$1.1x10^{12}$	1.02	4.31	0.229
E_2		1.12	1.11	$1.7x10^{11}$	$7x10^{10}$	1.01	1.06	
E_3		1.17	2.01	$5x10^{11}$	$1x10^{23}$	1.01	4.31	

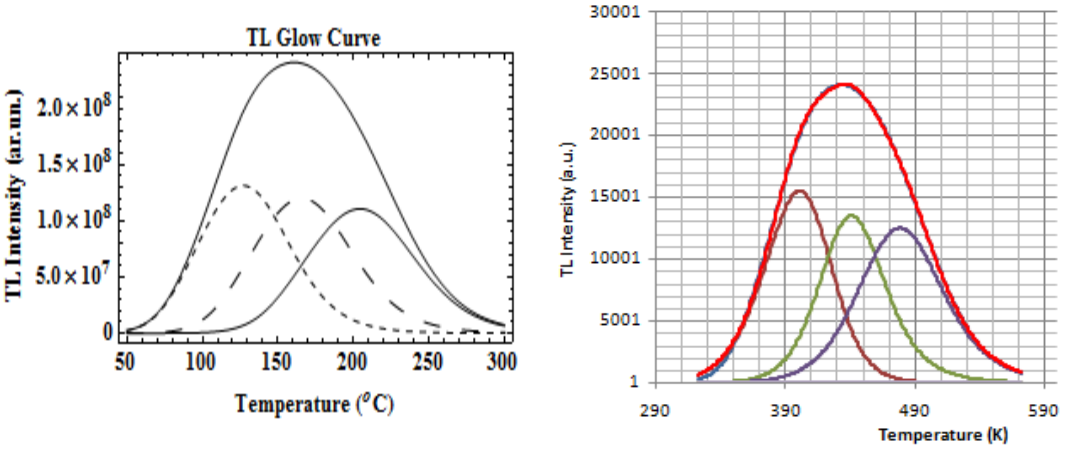

(a)

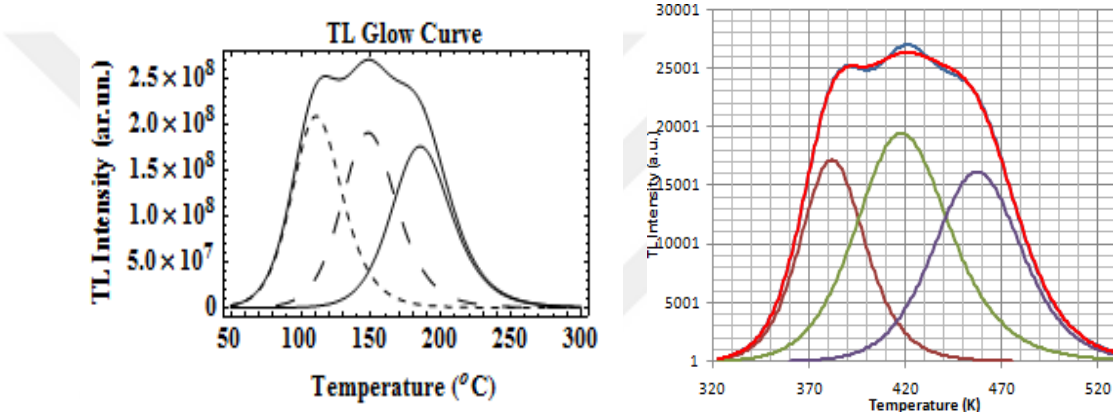

(b)

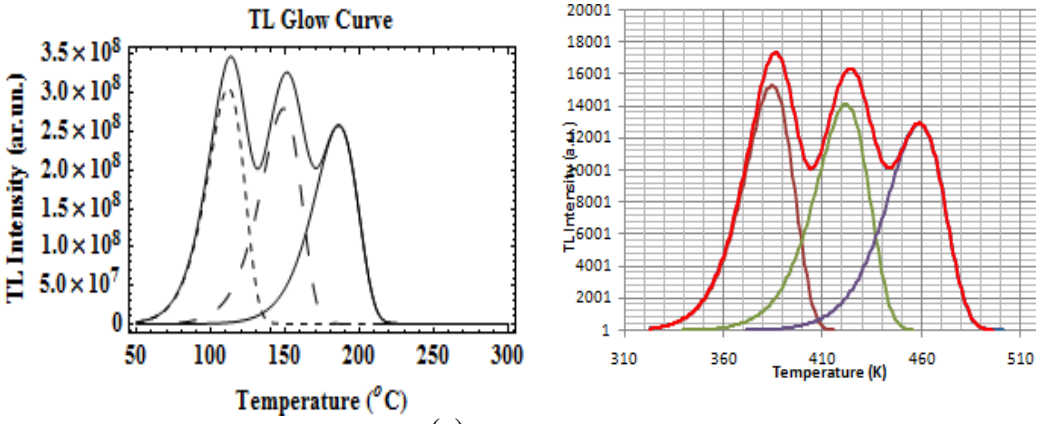

(c)

Figure 4.17: The numerically generated (left side) by Mathematica and then analyzed by Excel Spreadsheet program (right side) glow curves for the following input parameters: (N_t= n_0) (Three Peaks). (a) (A_n/A_h=10) (b) (A_n/A_h=1) (c) (A_n/A_h=0.001).

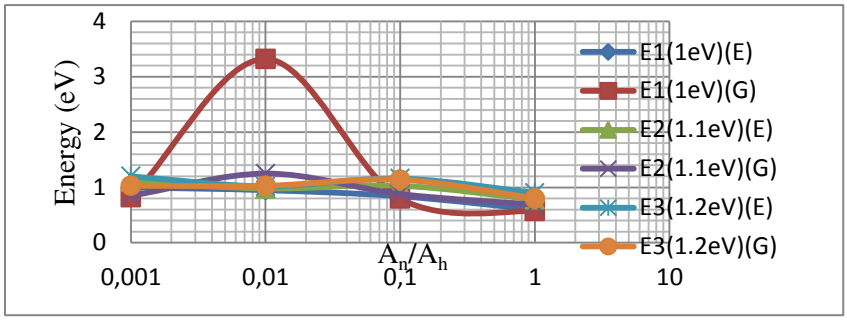

(a)

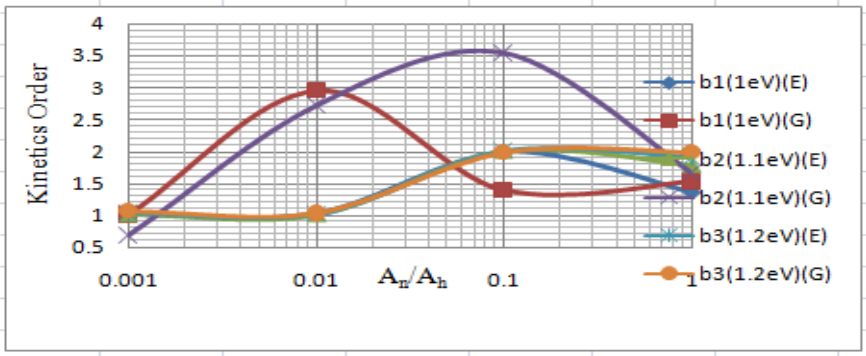

(b)

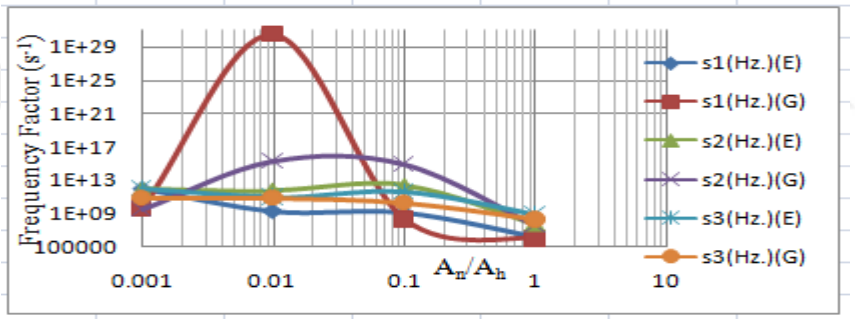

(c)

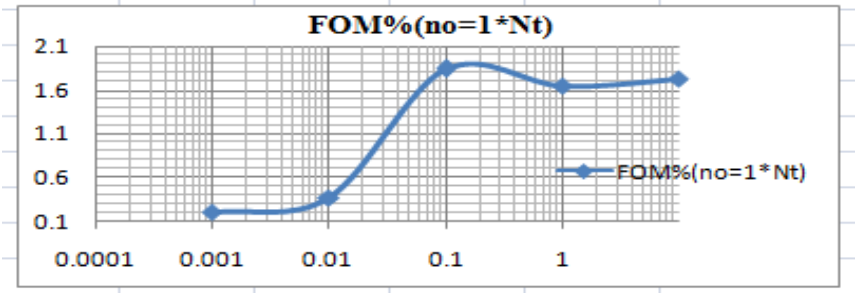

(d)

Figure 4.18: The comparisons of CGCD analysis (E: Excel Spreadsheet, G: GLOCANIN) results of the OTOR model for the following input parameters: (N_t=n_0), (Two peaks), (a) Activation Energy (b) Frequency factor (c) Kinetics order (d) FOM values (Excel).

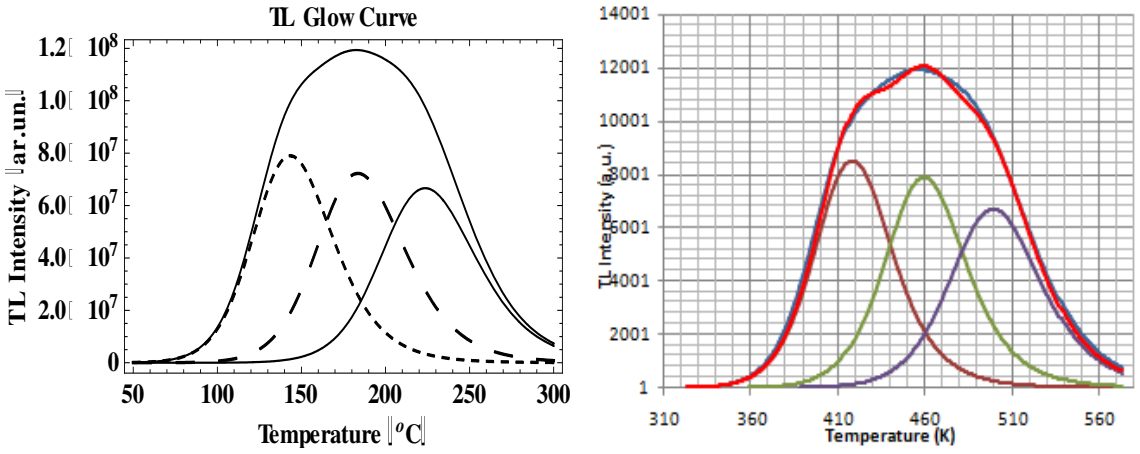

(a)

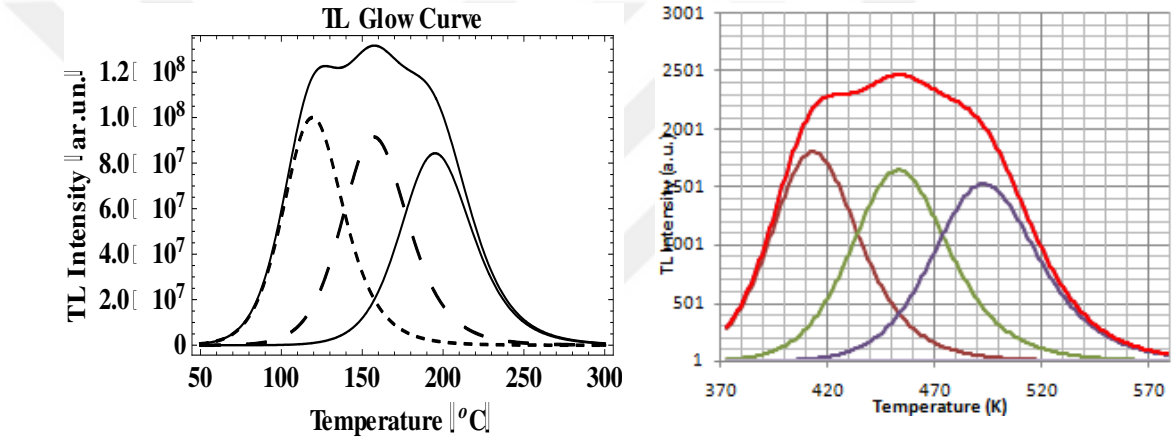

(b)

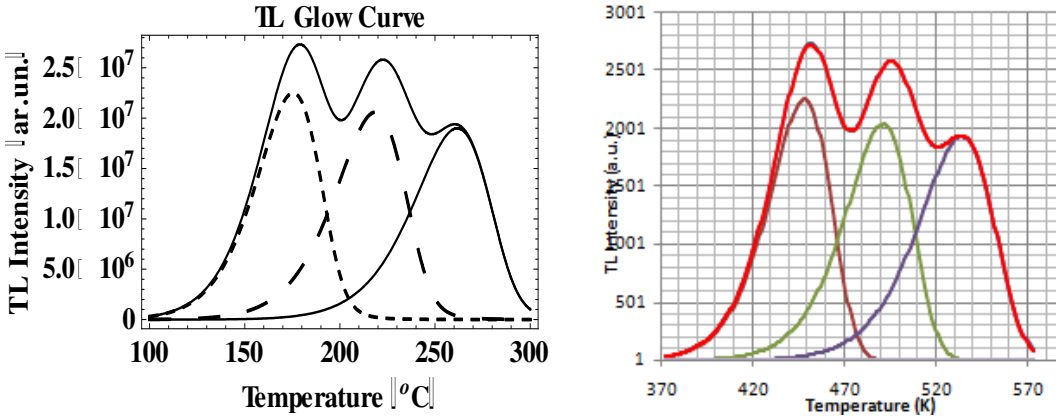

(c)

Figure 4.19: The numerically generated (left side) by Mathematica and then analyzed by Excel Spreadsheet program (right side) glow curves for the following input parameters: (N_t= $0.5n_0$) (Three Peaks). (a) (A_n/A_h=10) (b) (A_n/A_h=1) (c) (A_n/A_h=0.001).

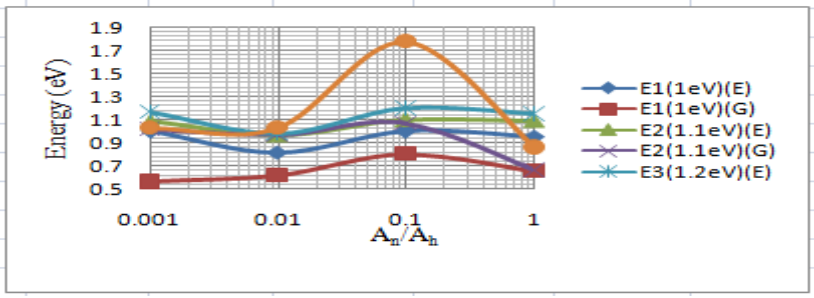

(a)

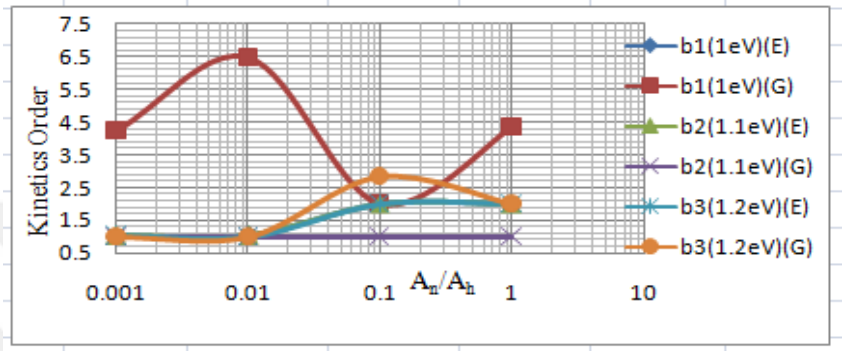

(b)

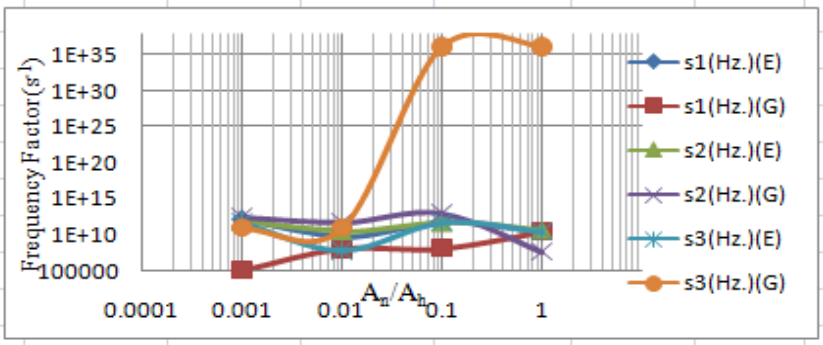

(c)

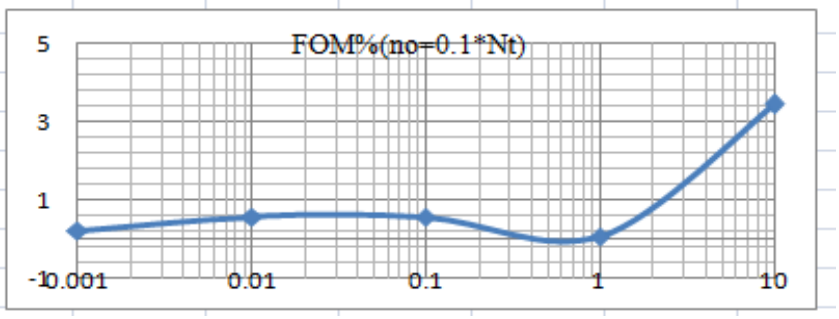

(d)

Figure 4.20: The comparisons of CGCD analysis (E: Excel Spreadsheet, G: GLOCANIN) results of the OTOR model for the following input parameters: (N_t= $0.5n_0$), (Three peaks), (a) Activation Energy (b) Frequency factor (c) Kinetics order (d) FOM values (Excel).

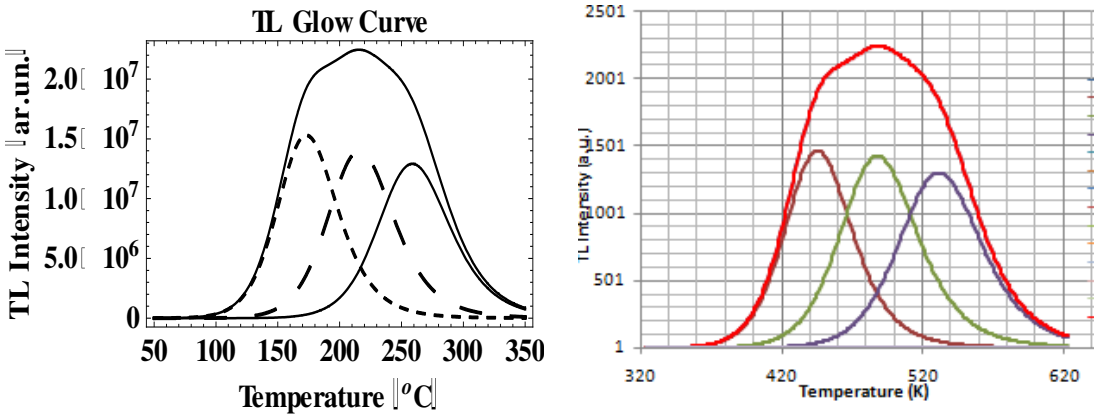

(a)

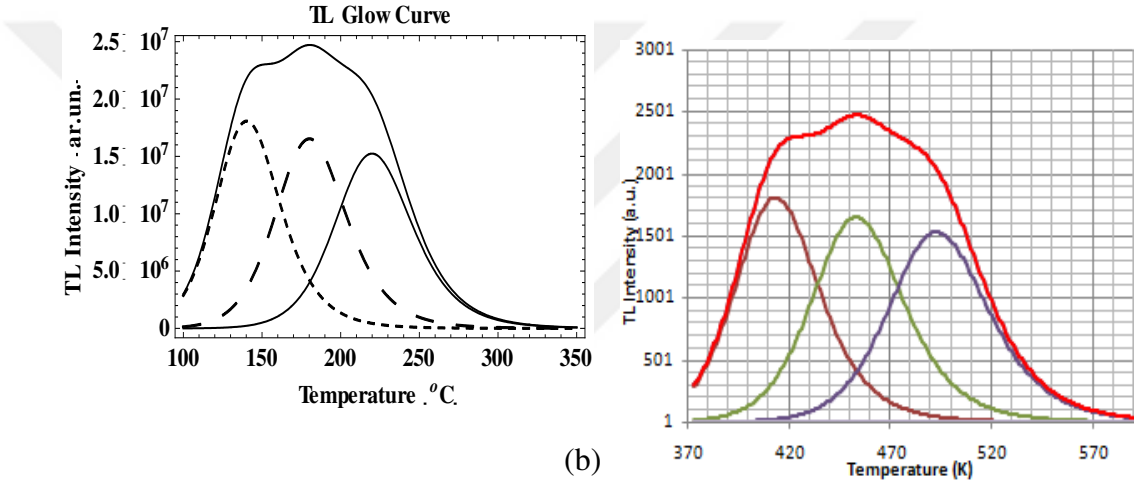

(b)

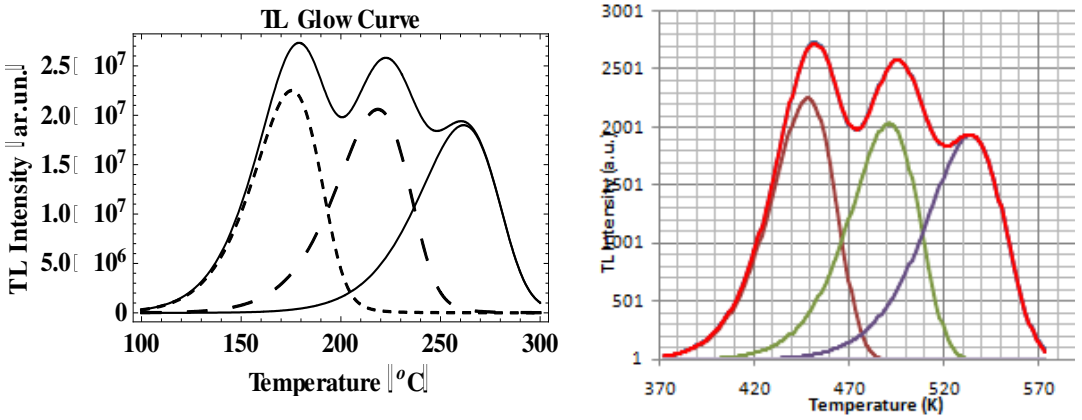

(c)

Figure 4.21: The numerically generated (left side) by Mathematica and then analyzed by Excel Spreadsheet program (right side) glow curves for the following input parameters: (N_t= $0.1n_0$) (Three Peaks). (a) (A_n/A_h=10) (b) (A_n/A_h=1) (c) (A_n/A_h=0.001).

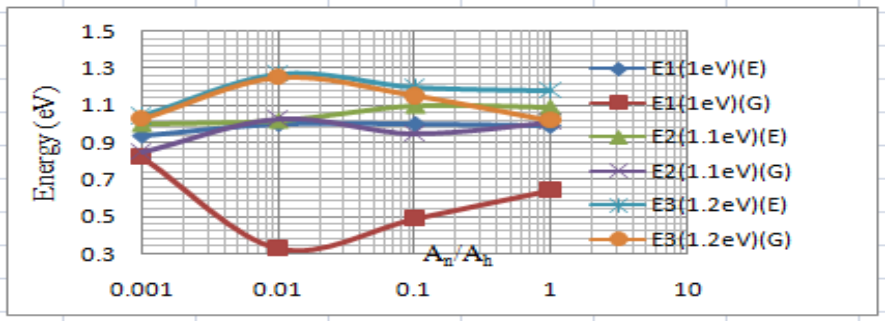

(a)

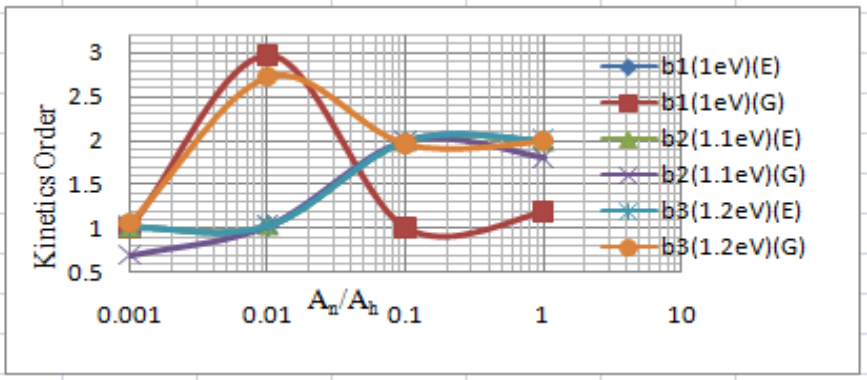

(b)

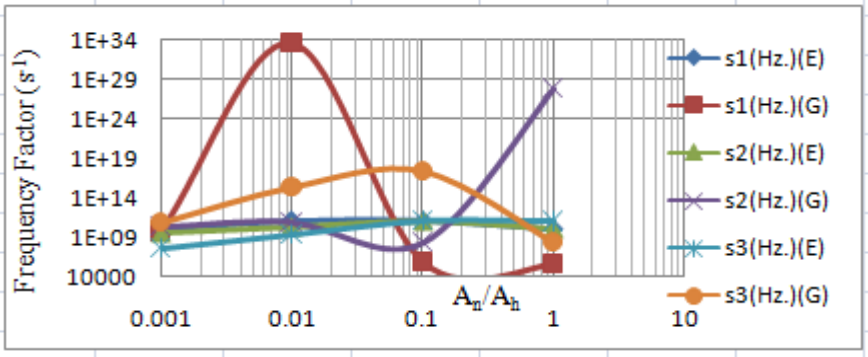

(c)

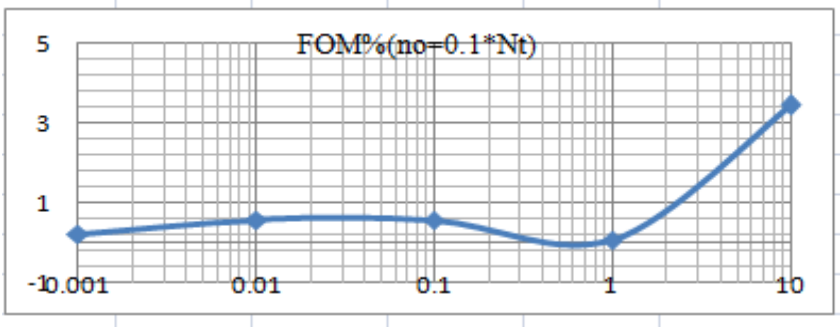

(d)

Figure 4.22: The comparisons of CGCD analysis (E: Excel Spreadsheet, G: GLOCANIN) results of the OTOR model for the following input parameters: (N_t= $0.1n_0$), (Three peaks), (a) Activation Energy (b) Frequency factor (c) Kinetics order (d) FOM values (Excel).

4.3 IMTS Model

In the last part of this study, the IMTS eqns. (Eq.2.41-2.44) were numerically solved with Mathematica and all obtained glow curves were analyzed by computer glow curve deconvolution methods [15, 17] to check the success and failure of CGCD programs in the investigations of kinetic parameters. Some of the analyzed glow curves and data obtained by fitting programs were presented in below figures and tables. The FOM values which were obtained by Excel Spreadsheet program is also shown in the last columns of the tables.

4.3.a Solutions of IMTS Model Rate Equations with Assuming One Glow Peak and Their Analysis by CGCD Programs

In this case, the equations (2.41-2.44) of IMTS Models were solved numerically by using Mathematica for different kinetic parameters. But, it was firstly accepted that each numerically generated glow curve contains only one glow peak. The numerically generated glow curves were then analyzed with the deconvolution programs to check their performance within the investigation of kinetic parameters by the curve fitting programs. To do, the results of analysis obtained by fitting programs were compared with the input parameters that were initially entered to the Mathematica during the generation of numerical glow curves. The input parameters that were entered to the Mathematica program are shown in the top row of each table (table 4.11, 4.12 and 4.13). The obtained kinetic parameters from the CGCD programs were also shown in the bottom rows of these tables together with the FOM values in the last columns. Some of the selected simulated and analyzed glow curves were shown in the figures 4.24 and 4.30.

In the IMTS model, when electron trap is completely filled with electron ($N = n_o$), the kinetic-order was obtained between b=1 and b=2 for different values of A_n/A_h and A_m/A_h ratios. For example; $A_m/A_h= 1$ and $A_n/A_h= 0.001$, the kinetic-order was obtained first-order while $A_m/A_h= 0.001$ and $A_n/A_h= 1$, the kinetic-order was obtained second-order.

In this model, as seen from table 4.14, if $A_m=A_h$, the results of GLOCANIN and Excel Spreadsheet are consistent with the input values for all values of $A_n/A_h<0.1$ while the reliability of analysis is reduced as the ratio of A_n/A_h increases above 0.5. On the other hand, if $A_n=A_h$, the results of GLOCANIN and Excel Spreadsheet are consistent with the input values for all values of $A_m/A_h<0.01$ while

the reliability of analysis is reduced as the ratio of A_m/A_h increases above 0.1. Moreover, if $A_n=A_m$, the results of GLOCANIN and Excel Spreadsheet are consistent with the input values for all values of $A_m/A_h<0.05$ while the reliability of analysis is reduced as the ratio of A_m/A_h increases above 0.1. In general, if A_n/A_h and A_m/A_h are greater than 1, the consistency between input values used in the Mathematica and results obtained from the deconvolution programs are very bad and they are largely deviated from each other.

In the OTOR model, we generally observed that the obtained results by CGCD programs and used input data in the Mathematica did not consistent with each other when $A_n/A_h>1$. On the other hand when $A_n=A_h$ and/or $A_n/A_h<1$, the analysis results and input data were in consistency with each other or at least small deviations between them. Similarly, in the IMTS model, the consistency between input data and obtained results are reduced when $A_n/A_h>0.1$ and $A_m/A_h>1$.

As a result, if the glow curve is generated by a single glow peak in the IMTS model, the obtained kinetic parameters are generally different from input parameters if $A_n/A_h>0.1$ and $A_m/A_h>1$. So, the analysis results are generally not reliable when $A_n/A_h>0.1$ and $A_m/A_h>1$. But when these ratios increased above mentioned values, the consistency between input and analyzed kinetic parameters is greatly increased and the analysis results comes to reliable levels.

Table 4.14: The below table includes of the input parameters for IMTS model which were used in numerical simulated TL glow curves and obtained kinetic parameters after their analyzing by curve fitting program with GLOCANIN (G) and Excel Spreadsheet (E) for different values of A_n/A_h if($A_m=A_h$).

INPUT KINETIC PARAMETERS							
$n_o = 1.10^{10}cm^{-3}$; E= 1eV; $\beta=1^oC/s$; $s=1x10^{12}Hz$; $n_o=1x\ N_t$; $A_h= 1x10^{-7}cm^3s^{-1}$; $A_m=1xA_h$							
A_n/A_h	E(eV)		b		$s(s^{-1})$		FOM
	G	E	G	E	G	E	
0.001	1.00	1.00	1.00	1.00	$1.0x10^{12}$	$1.0x10^{12}$	0.0084
0.005	1.00	0.99	1.00	1.00	$1.0x10^{12}$	$9.8x10^{11}$	0.0310
0.01	1.00	0.99	1.00	1.00	$1.0x10^{12}$	$9.8x10^{11}$	0.0340
0.05	0.99	0.99	1.01	1.02	$8.8x10^{11}$	$9.3x10^{11}$	0.1440
0.1	0.99	0.99	1.03	1.02	$7.6x10^{11}$	$7.2x10^{11}$	0.3990
0.5	0.96	0.97	1.10	1.12	$2.4x10^{11}$	$3.6x10^{11}$	1.3000
1	0.92	0.92	1.16	1.16	$6.7x10^{10}$	$6.7x10^{10}$	2.5000
3	0.80	0.80	1.22	1.19	$1.4x10^{09}$	$1.4x10^{09}$	4.9700
6	0.70	0.70	1.18	1.24	$4.6x10^{07}$	$5.0x10^{07}$	5.8500
10	0.63	0.63	1.12	1.47	$3.9x10^{06}$	$5.0x10^{06}$	5.7820

Table 4.15: The below table includes of the input parameters for IMTS model which were used in numerical simulated TL glow curves and obtained kinetic parameters after their analyzing by curve fitting program with GLOCANIN (G) and Excel Spreadsheet (E) for different values of A_m/A_h if ($A_n=A_h$).

INPUT KINETIC PARAMETERS							
$n_o = 1.10^{10}cm^{-3}$; E= 1eV; $\beta=1^0$ C/s; $s=1x10^{12}Hz$; $n_o=1x\ N_t$; $A_h= 1x10^{-7}cm^3s^{-1}$; $A_n=1xA_h$							
A_m/A_h	E(eV)		b		$s(s^{-1})$		FOM
	G	E	G	E	G	E	
0.001	1.00	0.99	1.99	2.00	$9.9*10^{11}$	$1.0*10^{12}$	0.917
0.005	1.00	0.99	1.97	1.95	$8.8*10^{11}$	$7.4*10^{11}$	0.902
0.01	0.99	0.99	1.93	1.96	$7.4*10^{11}$	$8.9*10^{11}$	0.328
0.05	0.95	0.98	1.67	1.79	$2.1*10^{11}$	$5.1*10^{11}$	1.746
0.1	0.93	0.94	1.53	1.61	$9.3*10^{10}$	$1.5*10^{11}$	2.960
0.5	0.90	0.92	1.24	1.29	$4.3*10^{10}$	$7.0*10^{10}$	3.080
1	0.92	0.92	1.16	1.17	$6.7*10^{10}$	$7.0*10^{10}$	2.588
3	0.98	0.98	1.07	1.07	$3.8*10^{11}$	$3.8*10^{11}$	0.87
6	1.03	1.03	1.02	1.02	$1.9*10^{12}$	$1.9*10^{12}$	0.45
10	1.09	1.08	1.00	1.00	$9.0*10^{12}$	$8.2*10^{12}$	1.39

Table 4.16: The below table includes of the input parameters for IMTS model which were used in numerical simulated TL glow curves and obtained kinetic parameters after their analyzing by curve fitting program with GLOCANIN (G) and Excel Spreadsheet (E) for different values of A_m/A_h if ($A_n=A_m$).

INPUT KINETIC PARAMETERS							
$n_o = 1.10^{10} cm^{-3}$; E= 1eV; β=1°C/s; $s=1*10^{12}$Hz ; $n_o = 1x\ N_t$; $A_h = 1x10^{-7} cm^3 s^{-1}$; $A_n = 1xA_m$							
A_m/A_h	E(eV)		b		$s(s^{-1})$		FOM
	G	E	G	E	G	E	
0.001	1.00	1.00	1.00	1.01	$1.0x10^{12}$	$1.1x10^{12}$	0.917
0.005	1.00	1.00	1.01	1.00	$1.3x10^{12}$	$1.0x10^{12}$	0.503
0.01	1.00	1.01	1.02	1.00	$1.6x10^{12}$	$1.4x10^{12}$	1.012
0.05	1.01	1.02	1.10	1.10	$2.1x10^{12}$	$2.0x10^{12}$	1.357
0.1	1.01	1.02	1.12	1.12	$1.6x10^{12}$	$2.0x10^{12}$	1.210
0.5	0.99	1.01	1.17	1.14	$1.9x10^{12}$	$2.0x10^{12}$	0.413
1	0.92	0.92	1.16	1.16	$6.7x10^{10}$	$6.7x10^{10}$	2.726
3	0.88	0.87	1.14	1.15	$6.0x10^{09}$	$7.0x10^{09}$	3.410
6	0.85	0.86	1.14	1.14	$5.3x10^{09}$	$6.0x10^{09}$	3.506
10	0.83	0.83	1.14	1.14	$2.2x10^{09}$	$2.2x10^{09}$	3.970

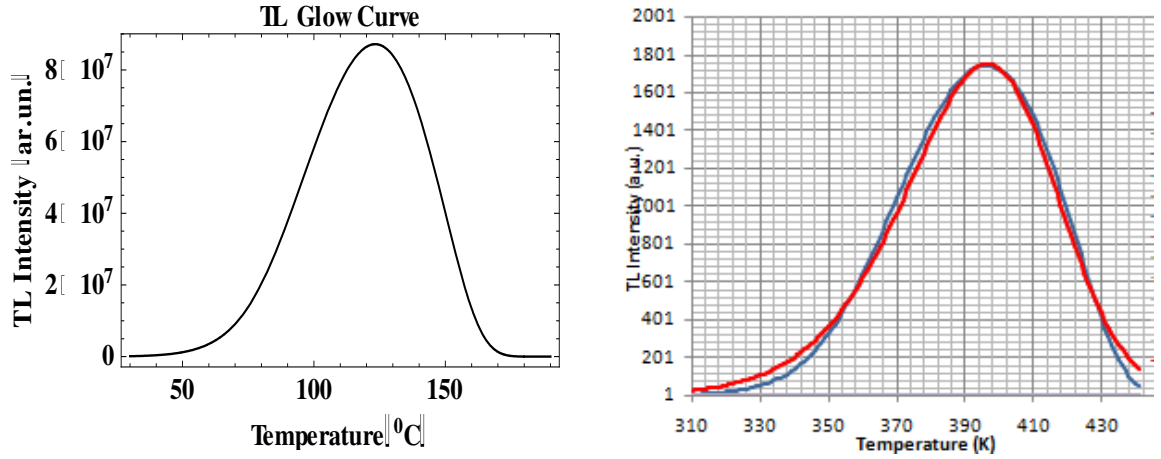

(a)

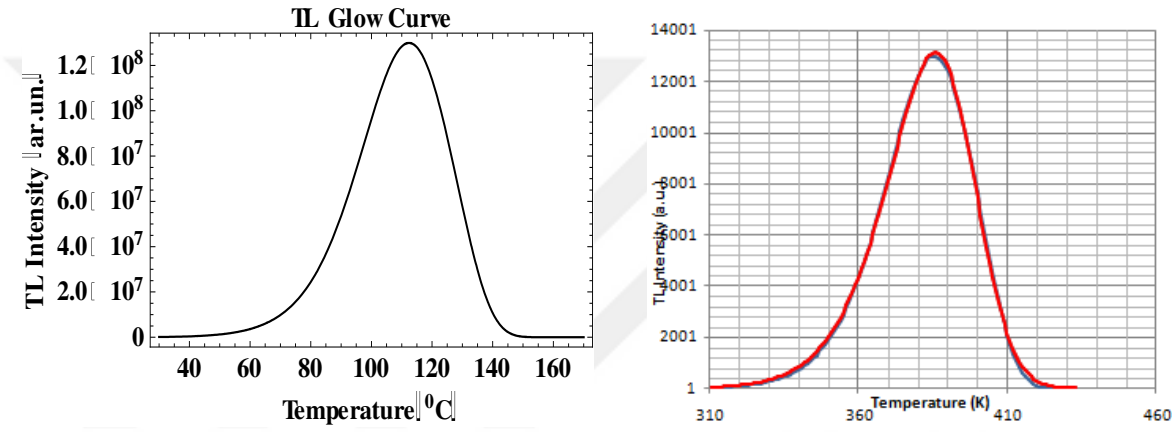

(b)

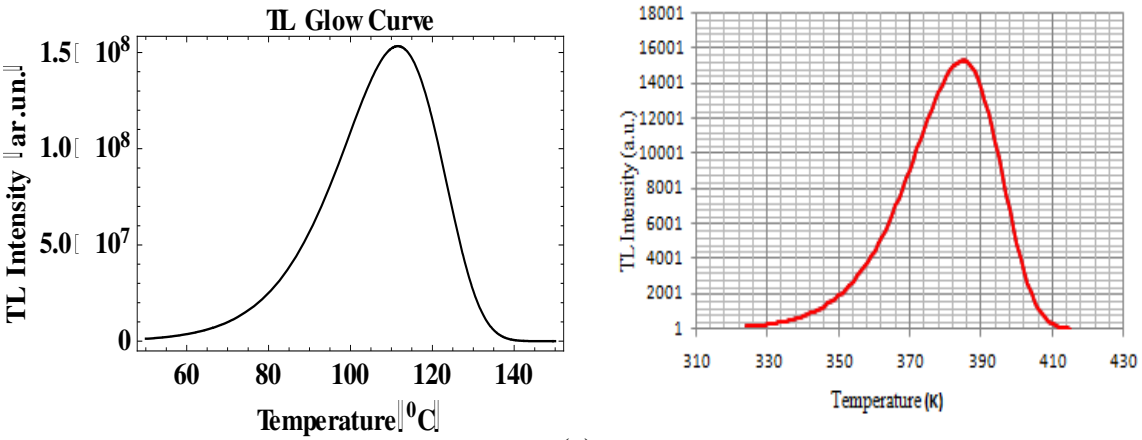

(c)

Figure 4.23: The numerically generated (left side) by Mathematica and then analyzed by Excel Spreadsheet program (right side) glow curves for the following input parameters: (One Peak). (a) (A_n/A_h=10) (b) (A_n/A_h=1) (c) (A_n/A_h=0.001).

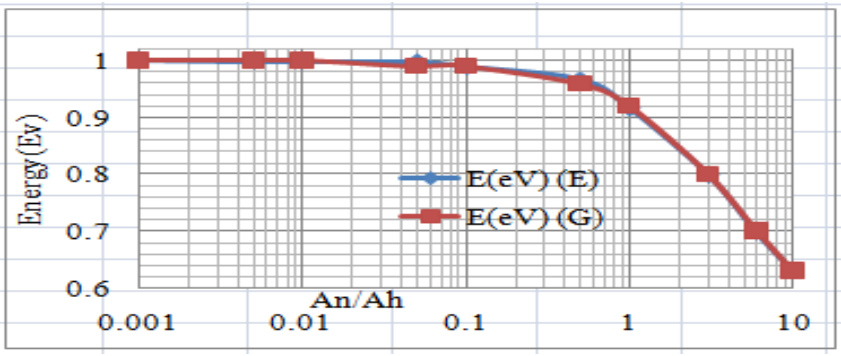

(a)

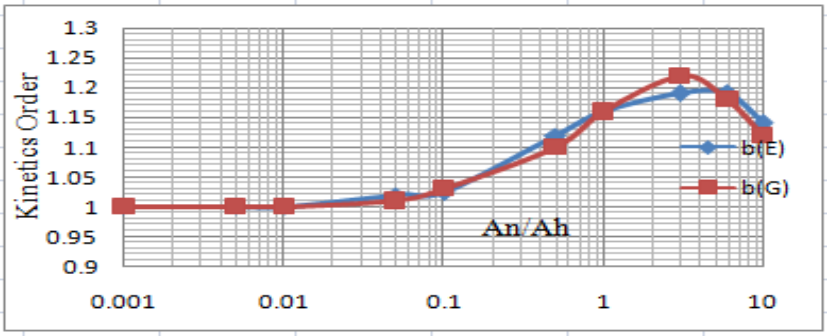

(b)

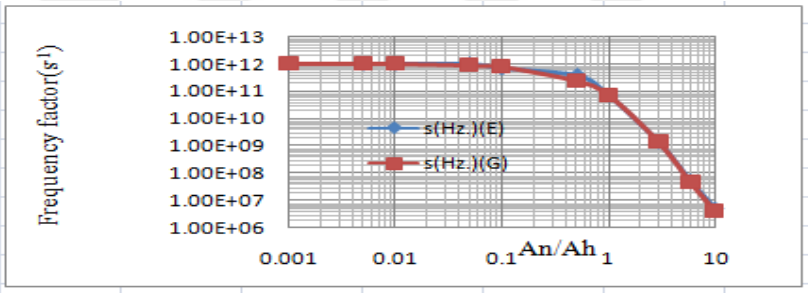

(c)

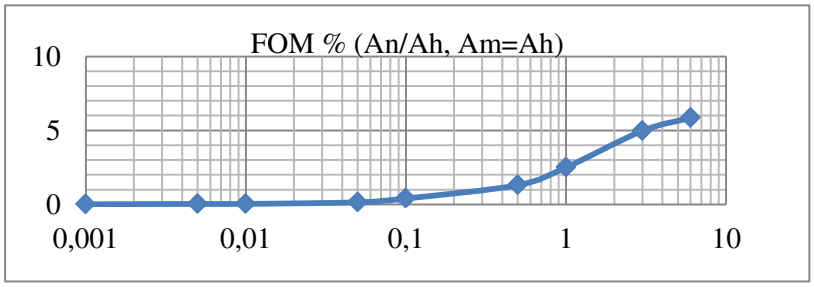

(d)

Figure 4.24: The comparisons of CGCD analysis (E: Excel Spreadsheet, G: GLOCANIN) results of the IMTS model as a function of A_n/A_h ($A_m = A_h$) for the following input parameters: (one Peak), (a) Activation Energy (b) Frequency factor (c) Kinetics order (d) FOM values (Excel).

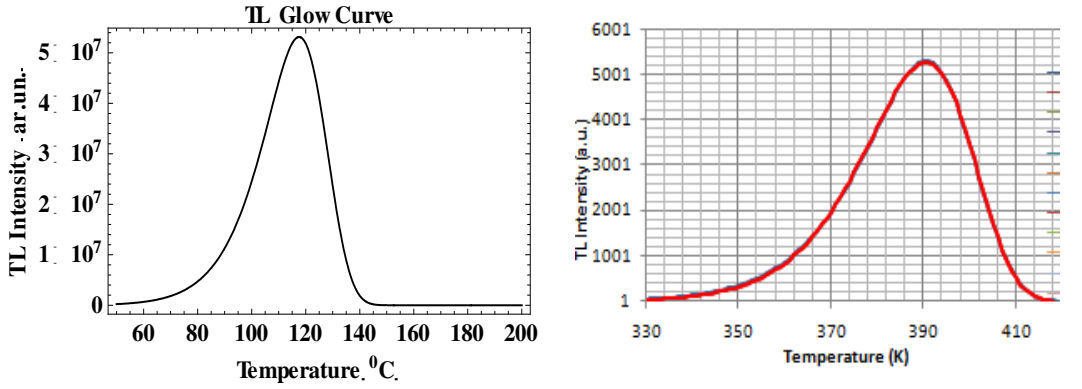

(a)

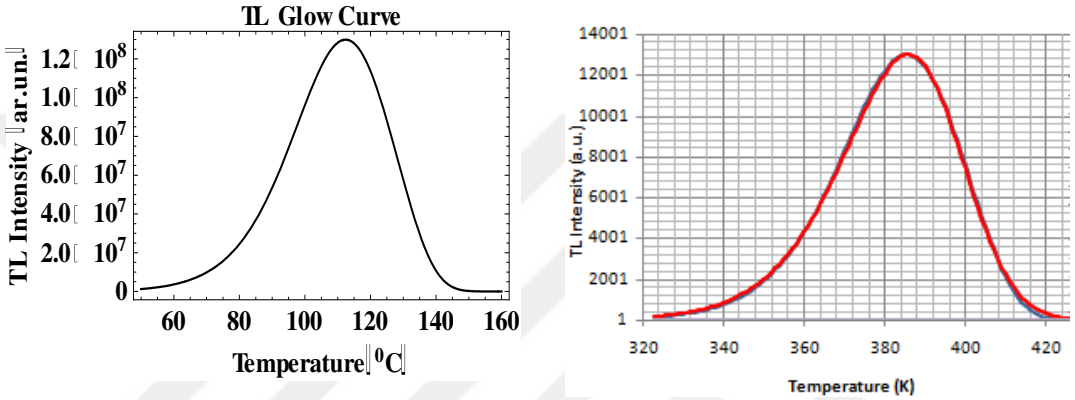

(b)

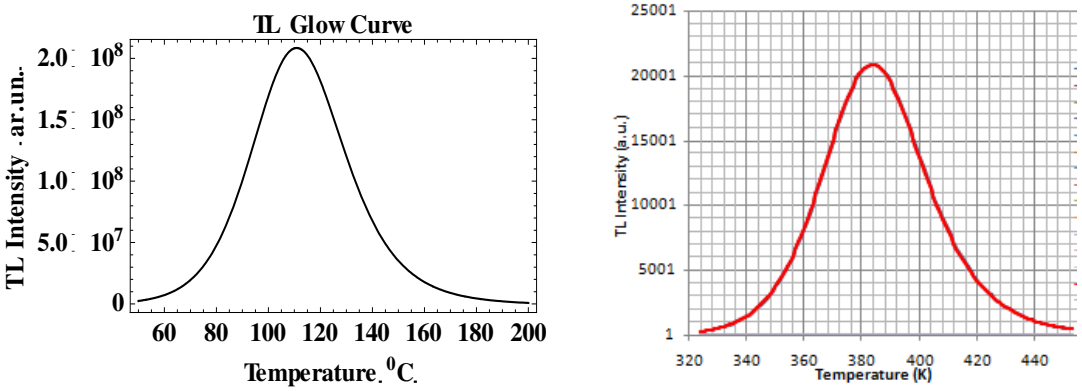

(c)

Figure 4.25: The numerically generated (left side) by Mathematica and then analyzed by Excel Spreadsheet program (right side) glow curves for the following input parameters: (One Peak). (a) (A_m/A_h=10) (b) (A_m/A_h=1) (c) (A_m/A_h=0.001).

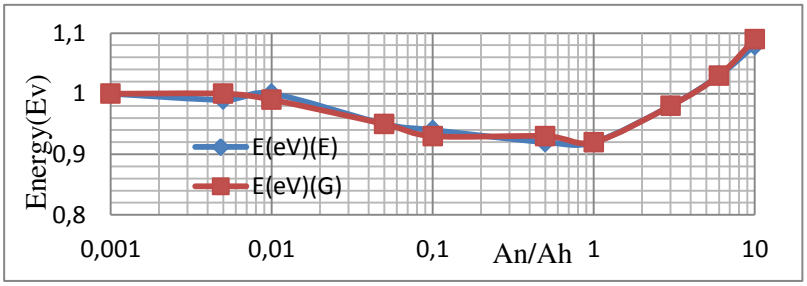

(a)

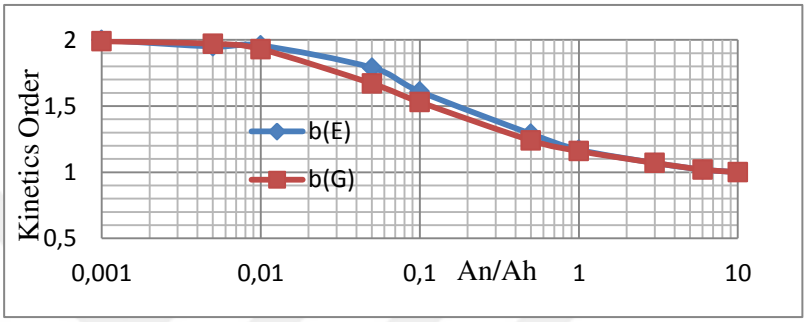

(b)

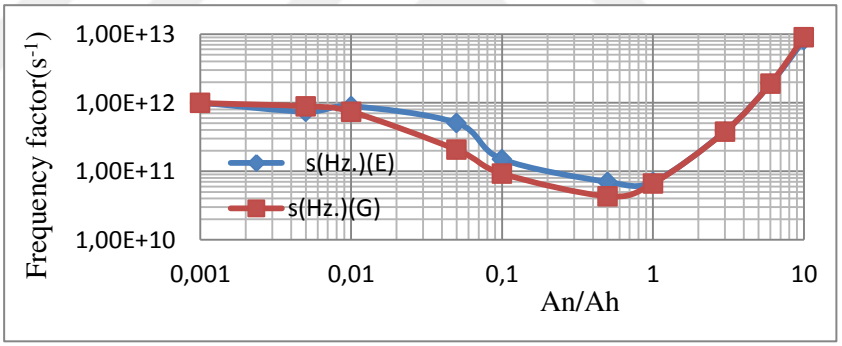

(c)

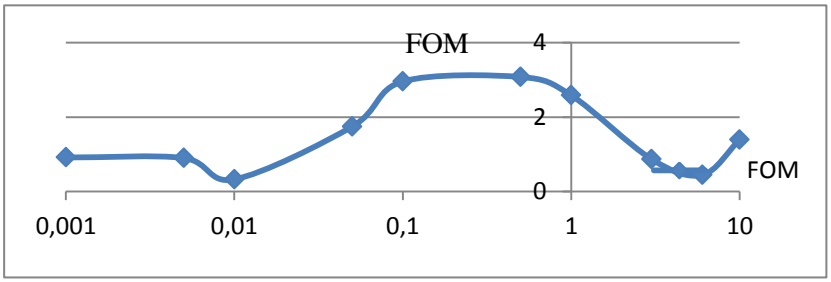

(d)

Figure 4.26: The comparisons of CGCD analysis (E: Excel Spreadsheet, G: GLOCANIN) results of the IMTS model as a function of A_m/A_h ($A_n = A_h$) for the following input parameters: (one Peak), (a) Activation Energy (b) Frequency factor (c) Kinetics order (d) FOM values (Excel).

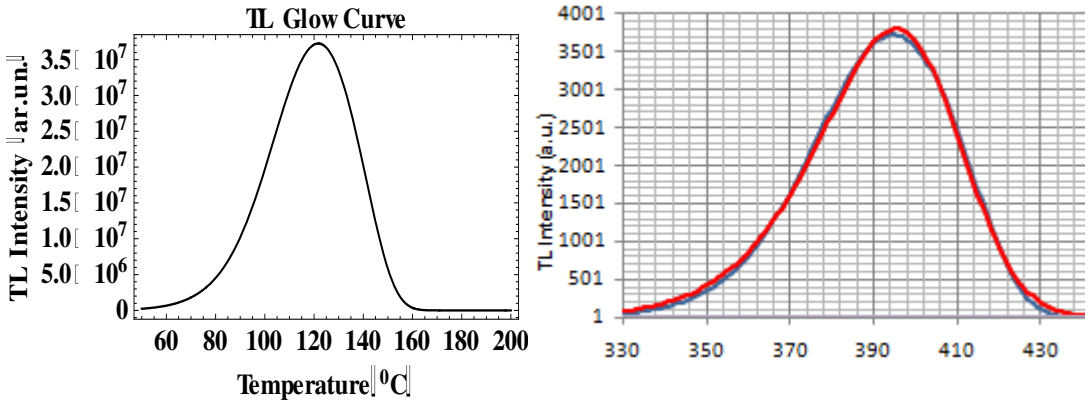

(a)

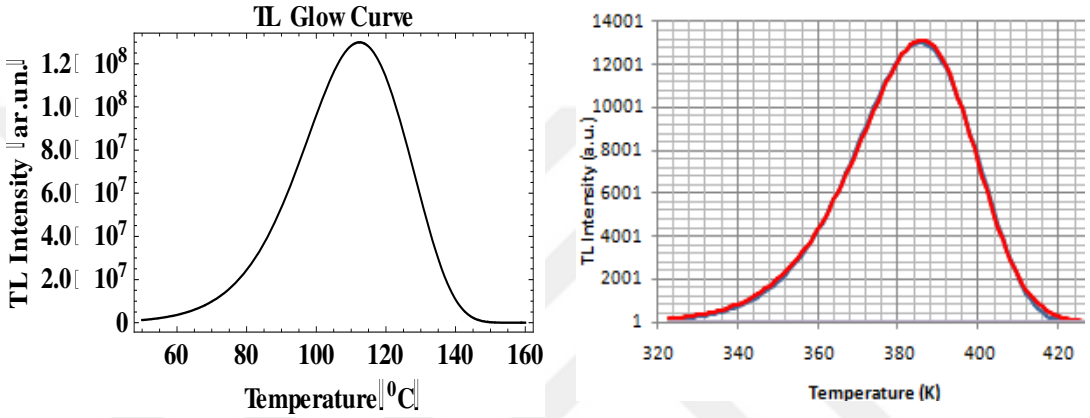

(b)

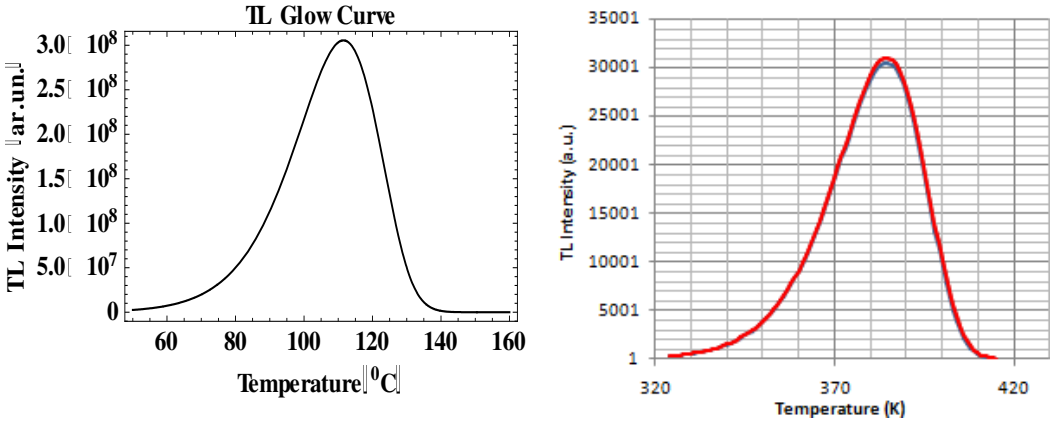

(c)

Figure 4.27: The numerically generated (left side) by Mathematica and then analyzed by Excel Spreadsheet program (right side) glow curves for the following input parameters: (One Peak).(a) (A_m/A_h=10) (b) (A_m/A_h=1) (c) (A_m/A_h=0.001).

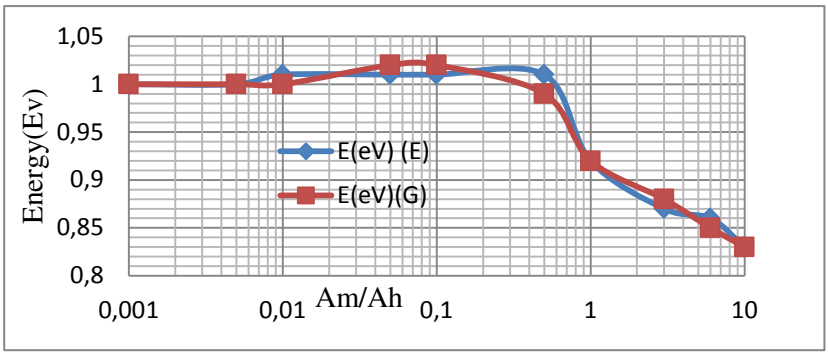

(a)

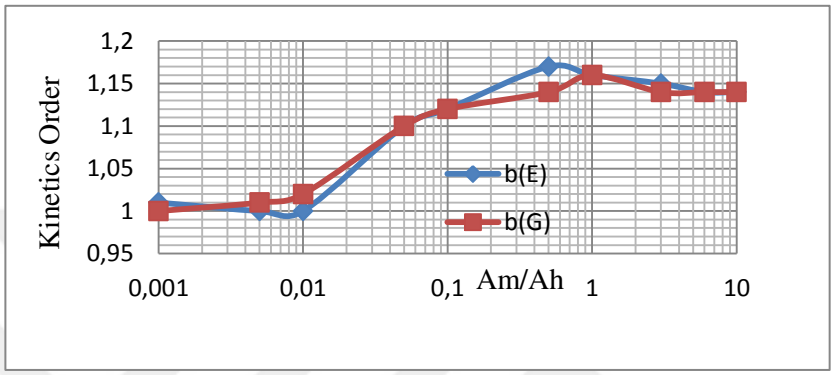

(b)

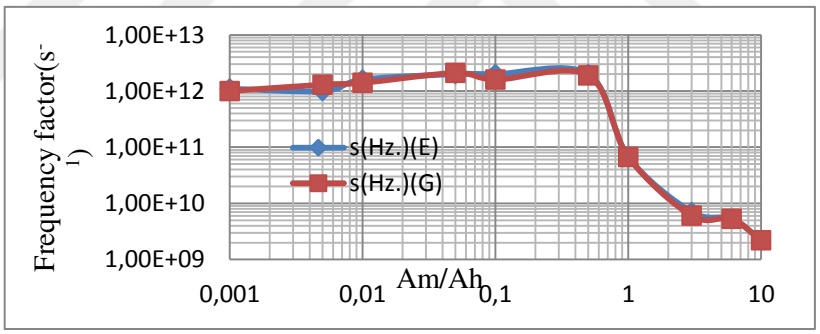

(c)

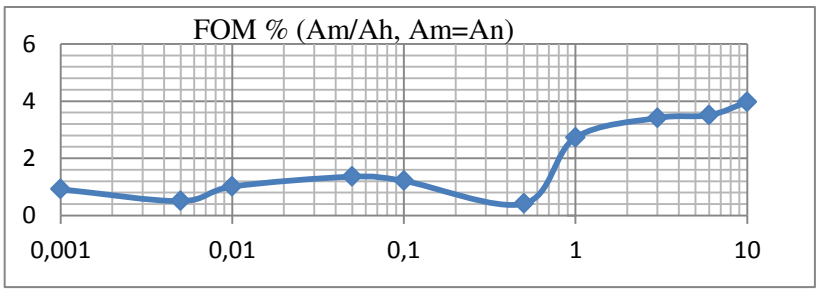

(d)

Figure 4.28: The comparisons of CGCD analysis (E: Excel Spreadsheet, G: GLOCANIN) results of the IMTS model as a function of A_m/A_h ($A_m = A_n$) for the following input parameters: (one Peak). (a) Activation Energy (b) Frequency factor (c) Kinetics order (d) FOM values (Excel).

When changing active occupancy rates of traps; the results are not consistent with the input values for $A_n/A_h>1$ if the traps are completely full. On the other hand, the analysis results become reliable as the occupancy of active traps decreases and the results of the analysis are getting better and better in all values of A_n/A_h ratios and the analysis results of the entire range provides exactly the same values of input parameters. From here it can be deduced that as the amount of active traps decreases, the reliability of the deconvolution program's results increases (see Table 17).

Table 4.17: The below table includes of the input parameters for IMTS model which were used in numerical simulated TL glow curves and obtained kinetic parameters after their analyzing by curve fitting program with GLOCANIN (G) and Excel Spreadsheet (E) programs after the changing active occupancy rates of traps.

INPUT PARAMETERS $N_t= M_t= 10^{10}$, $s=10^{12}s^{-1}$, E= 1eV, $A_m=A_h$, $\beta=1$, $m_0=0xM_t$								
A_n/A_h		E(eV)(E)	E(eV)(G)	b (E)	b (G)	s (s^{-1})(E)	s (s^{-1})(G)	FOM
100	$n_0=N_t$	0.49	0.48	1.01	1	$2x10^4$	$2x10^4$	3.930
	$n_0=0.5N_t$	0.82	0.82	1.15	1.14	$2x10^8$	$1x10^8$	4.320
	$n_0=0.1N_t$	0.92	0.92	1.05	1.03	$1x10^{10}$	$1x10^{10}$	1.433
	$n_0=0.01N_t$	1	1	1	1	$6x10^{10}$	$9x10^{10}$	1.076
	$n_0=0.001N_t$	1	1	1	1	$1x10^{10}$	$9x10^9$	0.005
10	$n_0=N_t$	0.6	0.63	1.1	1.12	$2x10^6$	$4x10^6$	6.402
	$n_0=0.5N_t$	0,85	0.85	1.15	1.16	$2x10^{10}$	$2x10^{10}$	3.251
	$n_0=0.1N_t$	0.96	0.97	1.04	1.03	$5x10^{10}$	$4x10^{10}$	0.066
	$n_0=0.01N_t$	1	0.99	1	1	$9x10^{10}$	$8x10^{10}$	0.738
	$n_0=0.001N_t$	1	0.99	1	1	$9x10^{10}$	$6x10^{10}$	0.004
1	$n_0=Nt$	0.9	0.92	1.15	1.16	$7x10^{10}$	$7x10^{10}$	2.390
	$n_0=0.5N_t$	0.95	0.94	1.1	1.08	$2x10^{11}$	$1x10^{11}$	1.495
	$n_0=0.1N_t$	0.98	0.98	1.01	1.01	$3x10^{11}$	$3x10^{11}$	0.391
	$n_0=0.01N_t$	1	1	1	1	$5x10^{11}$	$5x10^{11}$	0.039
	$n_0=0.001N_t$	1	1	1	1	$5x10^{11}$	$4x10^{11}$	0.025
0.1	$n_0=N_t$	1	0.99	1.02	1.03	$5x10^{11}$	$3x10^{11}$	0.317
	$n_0=0.5N_t$	1	0.99	1.01	1.01	$8x10^{11}$	$8x10^{11}$	0.228
	$n_0=0.1N_t$	1	1	1.01	1	$8x10^{11}$	$1x10^{12}$	0.228
	$n_0=0.01N_t$	1	1	1	1	$9x10^{11}$	$1x10^{12}$	0.005
	$n_0=0.001N_t$	1	1	1	1	$9x10^{11}$	$9x10^{11}$	0.003
0.01	$n_0=N_t$	1	1	1	1	$1x10^{12}$	$1x10^{12}$	0.043
	$n_0=0.5N_t$	1	1	1	1	$1x10^{12}$	$1x10^{12}$	0.024
	$n_0=0.1N_t$	1	1	1	1	$1x10^{12}$	$1x10^{12}$	0.006
	$n_0=0.01N_t$	1	1	1	1	$1x10^{12}$	$1x10^{12}$	0.001
	$n_0=0.001N_t$	1	1	1	1	$1x10^{12}$	$1x10^{12}$	0.004
0.001	$n_0=N_t$	1	1	1	1	$1x10^{12}$	$1x10^{12}$	0.003
	$n_0=0.5N_t$	1	1	1	1	$1x10^{12}$	$1x10^{12}$	0.002
	$n_0=0.1N_t$	1	1	1	1	$1x10^{12}$	$1x10^{12}$	0.001
	$n_0=0.01N_t$	1	1	1	1	$1x10^{12}$	$1x10^{12}$	0.002
	$n_0=0.001N_t$	1	1	1	1	$1x10^{12}$	$1x10^{12}$	0.004

4.3. b Solutions of IMTS Model Rate Equations with Assuming two Glow Peak and Their Analysis by CGCD Programs

In this case, the rate equations (2.41-2.44) of IMTS Model were solved numerically by using Mathematica for different values of input kinetic parameters by assuming that glow curve contains two glow peaks. Then, these glow curves were analyzed with the deconvolution programs. The results of analysis obtained by programs were again compared with the input parameters that were entered to the Mathematica during the generation of numerical glow curves. The input parameters are shown in the top row of table 4.16. The obtained kinetic parameters from the CGCD programs were also shown in the bottom rows of this table. Some of the selected simulated and analyzed glow curves and results were shown in the figures 4.30 and 4.31.

When electron trap is completely filled ($N_t = n_0$) and if $A_n/A_h > 0.5$, as seen from the table 4.16, the input data(E_1=1.0 eV, E_2=1.05 eV) in the Mathematica and obtained results by CGCD programs did not coincident with each other. There are very high discrepancies between these parameters. On the other hand, $A_n/A_h < 0.5$, the obtained results and input data were in consistency with each other or at least small deviations between them were existed. Especially, the obtained parameters of second peak highly deviate from its input parameters. When the results of CGCD programs are compared with the results of Excel Spreadsheet, it was seen that the results of Excel Spreadsheet is generally better than the results of GLOCANIN.

As a result, if the glow curve is generated by two glow peaks in the IMTS model, the obtained kinetic parameters are generally different from input parameters if $A_n/A_h > 0.5$. So, the analysis results are certainly not reliable when $A_n/A_h > 0.5$. But the value of this ratio is reduced, the consistency between input and analyzed kinetic parameters is increased and especially give very consistent results when $A_n/A_h < 0.05$

Table 4.18: The below table includes of the input parameters for IMTS model which were used in numerical simulated TL glow curves and obtained kinetic parameters after their analyzing by GLOCANIN and Excel Spreadsheet curve fitting programs if $A_m=A_h$. (Two peaks)

INPUT KINETIC PARAMETERS								
$n_0= 1.10^{10}cm^{-3}$; $\beta=1^0$ C/s; $s=1x10^{12}s^{-1}$; $n_0=1x\ N_t$; $n_0=1xM_t$; $A_m= 1xA_h$; $A_h= 1x10^{-7}cm^3s^{-1}$								
A_n/A_h		E(eV)		b		$s(s^{-1})$		FOM
		G	E	G	E	G	E	
E_1=1eV	0.001	1.01	1.00	1.00	1.00	$9.7x10^{11}$	$9.7x10^{11}$	0.032
E_2=1.05eV		1.05	1.06	1.00	1.00	$1.1x10^{12}$	$1.2x10^{12}$	
E_1=1eV	0.005	1.01	1.00	1.00	1.01	$1.1x10^{12}$	$1.0x10^{12}$	0.009
E_2=1.05eV		1.05	1.05	1.00	1.00	$9.7x10^{11}$	$9.6x10^{11}$	
E_1=1eV	0.01	1.00	1.00	1.00	1.00	$1.2x10^{12}$	$9.8x10^{11}$	0.006
E_2=1.05eV		1.06	1.06	1.00	1.00	$9.7x10^{11}$	$1.2x10^{12}$	
E_1=1eV	0.05	1.00	1.00	1.04	1.05	$9.7x10^{11}$	$1.0x10^{12}$	0.062
E_2=1.05eV		1.06	1.06	1.02	1.00	$2.6x10^{12}$	$1.6x10^{12}$	
E_1=1eV	0.1	1.00	0.99	1.10	1.12	$7.9x10^{12}$	$1.2x10^{11}$	0.156
E_2=1.05eV		1.04	1.05	1.02	1.02	$8.8x10^{11}$	$1.1x10^{12}$	
E_1=1eV	0.5	0.96	0.97	1.37	1.35	$4.4x10^{11}$	$6.8x10^{11}$	0.470
E_2=1.05eV		0.98	0.99	1.00	1.00	$1.2x10^{10}$	$6.8x10^{11}$	
E_1=1eV	1	0.96	0.97	1.41	1.46	$2.4x10^{11}$	$5.7x10^{11}$	1.000
E_2=1.05eV		0.87	0.87	1.02	1.02	$4.0x10^{11}$	$7.3x10^{11}$	
E_1=1eV	3	0.91	0.91	1.51	1.51	$5.4x10^{10}$	$5.4x10^{10}$	1.640
E_2=1.05eV		0.82	0.82	1.19	1.19	$8.9x10^{08}$	$8.9x10^{08}$	
E_1=1eV	6	0.88	0.88	1.60	1.59	$1.8x10^{10}$	$1.9x10^{10}$	1.740
E_2=1.05eV		0.76	0.76	1.22	1.22	$1.2x10^{08}$	$1.3x10^{08}$	
E_1=1eV	10	0.85	0.85	1.65	1.65	$5.9x10^{09}$	$6.1x10^{09}$	1.760
E_2=1.05eV		0.71	0.81	1.20	1.20	$2.2x10^{07}$	$2.3x10^{07}$	

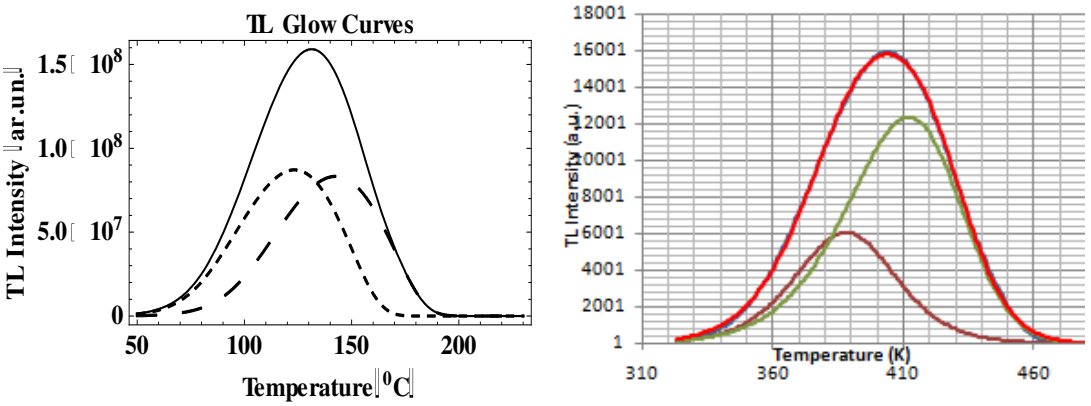

(a)

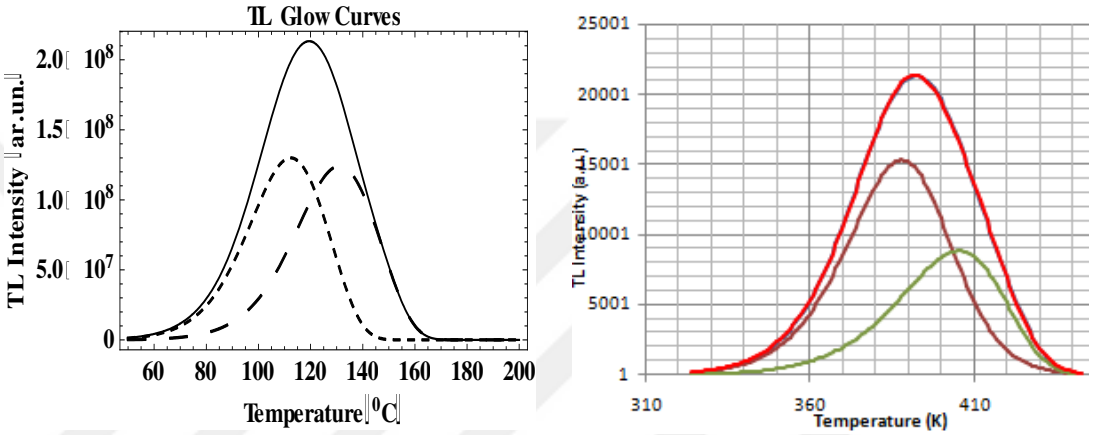

(b)

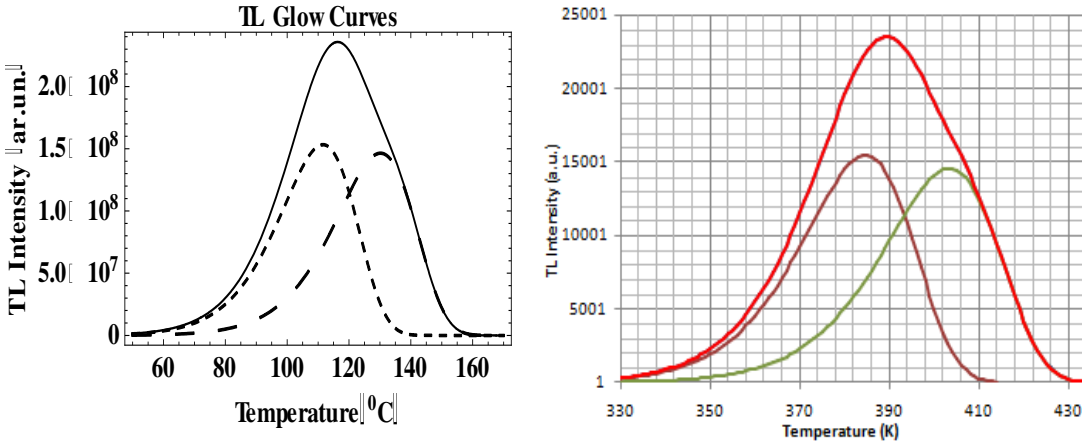

(c)

Figure 4.29: The numerically generated (left side) by Mathematica and then analyzed by Excel Spreadsheet program (right side) glow curves for the following input parameters: (Two Peaks) (A_n=A_m) (a) (A_m/A_h=10) (b) (A_m/A_h=1) (c) (A_m/A_h=0.001).

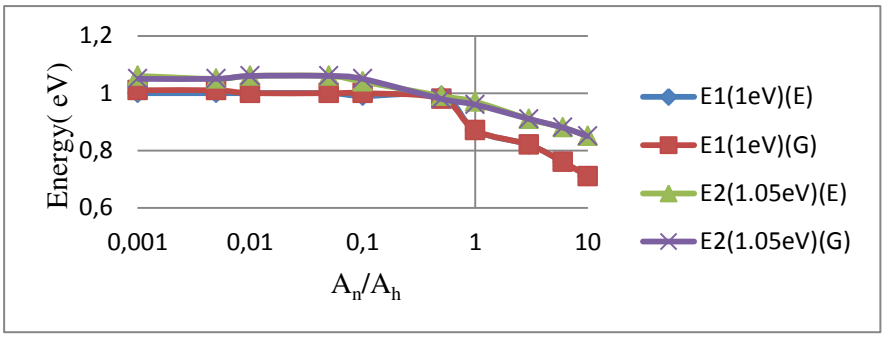

(a)

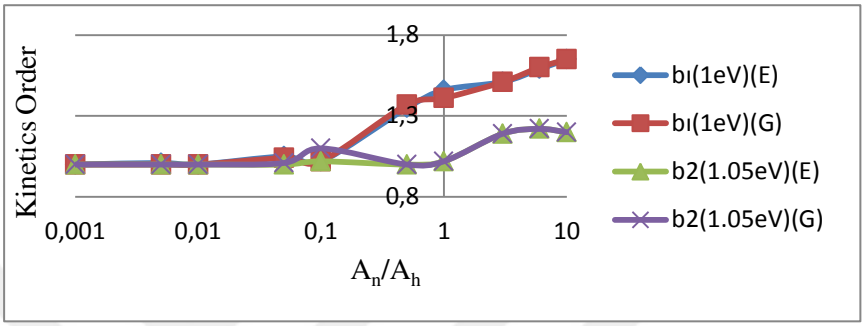

(b)

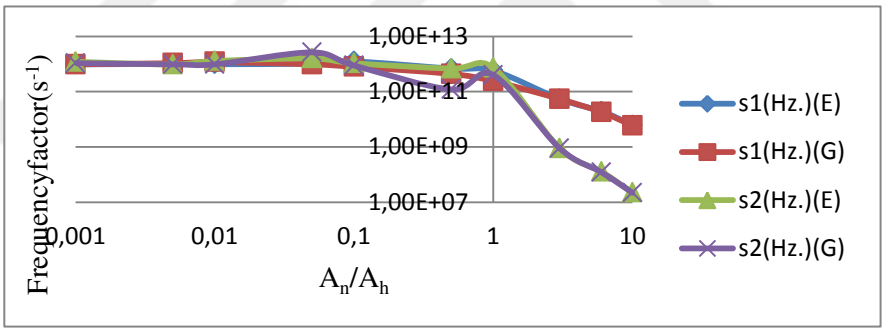

(c)

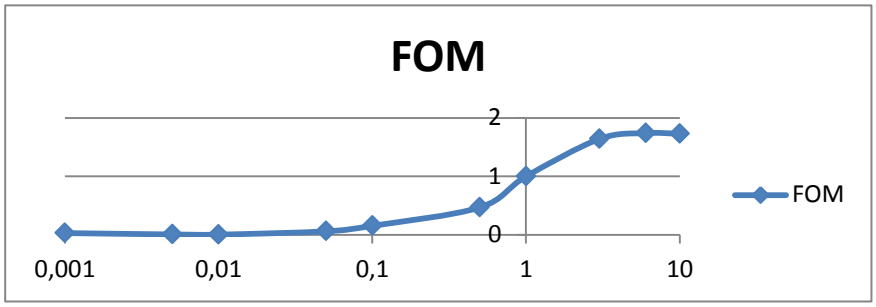

(d)

Figure 4.30: The comparisons of CGCD analysis (E: Excel Spreadsheet, G: GLOCANIN) results of the IMTS model as a function of A_n/A_h ($A_m = A_n$) for the following input parameters: (Two Peaks). (a) Activation Energy (b) Frequency factor (c) Kinetics order (d) FOM values (Excel).

When changing occupancy rates of active and deep traps; it is seen that the results of deconvolution programs are far from the input values especially if the traps are completely full for $A_n/A_h>1$. On the other hand, the analysis results approach the input values as the occupancy rates of active and deep traps decreases and the results of the analysis are getting better in higher values of A_n/A_h ratios. As seen in the previous part (if the glow curves include one peak), it can be concluded that as the occupancy rates of active and deep traps decreases, the results of the deconvolution programs close to the input data and become more reliable than the completely occupied active and deep traps (see below table 19).

Table 4.19: The below table includes of the input parameters for IMTS model which were used in numerical simulated TL glow curves and obtained kinetic parameters after their analyzing by curve fitting program by Excel Spreadsheet (E) and GLOCANIN (G) after changing occupancy rates of active and deep traps for two peaks (E_1=1eV, E_2=1.05eV).

INPUT KINETIC PARAMETERS: $n_0 = 1.10^{10} cm^{-3}$; $\beta = 1^0$ C/s; $s = 1x10^{12} s^{-1}$ Am= 1xAh; Ah= $1x10^{-7} cm^3 s^{-1}$												
$n_0 = N_t$, $m_0 = M_t$												
An/Ah	E_1(1eV)		E_2(1.05eV)		b_1		b_2		$s_1(s^{-1})$		$s_2(s^{-1})$	
FOM%	E	G	E	G	E	G	E	G	E	G	E	G
100/3.00	0.60	0.53	0.64	0.63	1.87	1.63	1.00	1.04	$8x10^5$	$5x10^4$	$8x10^5$	$3x10^6$
10/2.038	0.75	0.85	0.77	0.71	1.62	1.65	1.16	1.20	$2x10^8$	$6x10^9$	$1x10^8$	$2x10^7$
1/1.018	0.96	0.96	0.87	0.87	1.43	1.43	1.02	1.02	$2x10^{11}$	$2x10^{11}$	$4x10^9$	$4x10^9$
0.1/0.046	1.00	1.00	1.04	1.13	1.07	1.10	1.00	1.02	$1x10^{12}$	$9x10^{11}$	$7x10^{11}$	$8x10^{12}$
0.01/0.558	1.01	1.00	1.00	1.06	1.06	1.00	1.00	1.00	$2x10^{12}$	$1x10^{12}$	$2x10^{12}$	$3x10^{12}$
$n_0 = N_t$, $m_0 = 0.5M_t$												
An/Ah	E_1(1eV)		E_2(1.05eV)		b_1		b_2		$s_1(s^{-1})$		$s_2(s^{-1})$	
FOM%	E	G	E	G	E	G	E	G	E	G	E	G
100/1.315	0.60	0.63	0.60	0.53	1.75	1.64	1.07	1.05	$1x10^6$	$3x10^6$	$3x10^5$	$5x10^4$
10/1.660	0.85	0.85	0.71	0.71	1.67	1.67	1.20	1.20	$7x10^9$	$6x10^9$	$2x10^7$	$2x10^7$
1/1.070	0.96	0.96	0.87	0.87	1.41	1.41	1.02	1.02	$2x10^{11}$	$2x10^{11}$	$4x10^9$	$4x10^9$
0.1/0.028	1.00	1.00	1.06	1.12	1.08	1.10	1.00	1.02	$1x10^{12}$	$9x10^{11}$	$1x10^{12}$	$8x10^{12}$
0.01/0.071	1.00	1.00	1.06	1.06	1.02	1.00	1.00	1.00	$1x10^{12}$	$1x10^{12}$	$1x10^{12}$	$1x10^{12}$
$n_0 = 0.5N_t$, $m_0 = 0.5M_t$												
An/Ah	E_1(1eV)		E_2(1.05eV)		b_1		b_2		$s_1(s^{-1})$		$s_2(s^{-1})$	
FOM%	E	G	E	G	E	G	E	G	E	G	E	G
100/1.442	0.92	0.92	0.86	0.86	1.40	1.40	1.14	1.14	$2x10^9$	$2x10^9$	$2x10^8$	$2x10^8$
10/1.431	0.91	0.91	0.86	0.86	1.38	1.38	1.05	1.05	$1x10^{10}$	$6x10^9$	$7x10^8$	$7x10^8$
1/0.882	0.99	1.01	0.89	0.92	1.26	1.34	1.00	1.00	$5x10^{11}$	$8x10^{11}$	$6x10^9$	$2x10^{10}$
0.1/0.038	1.00	1.00	1.10	1.11	1.06	1.06	1.02	1.02	$8x10^{11}$	$8x10^{11}$	$3x10^{12}$	$1x10^{13}$
0.01/0.016	1.00	1.00	1.05	1.06	1.00	1.00	1.00	1.00	$1x10^{12}$	$1x10^{12}$	$1x10^{12}$	$1x10^{12}$

If the activation energy of second peak is increased from E_2 = 1.05 eV to E_2 = 1.08 eV or to E_2 = 1.1 eV while the activation energy of first peak (E_1 = 1eV) was kept constant during the generation of numerical glow curves, it appears that the results of deconvolution programs are again highly depend upon the occupancy rates of active and deep traps. In general, high deviations were observed between input parameters and obtained results by CGCD programs when the active and deep traps were completely filled by electrons ($n_0 = N_t$, $m_0 = M_t$). On the other hand, if the occupancy rates of active and deep traps decrease, the deviations between input and output results were also decreased. For example, if $n_o = 0.5N_t$, $m_o = 0.5M_t$, very close results were obtained between input parameters and obtained results from the CGCD programs. In addition, if two glow peaks within the same glow curve were separated from each other by increasing the activation energy of second peak, i.e. increasing its activation energy from 1.05 eV to 1.1 eV, the consistency between input parameters and obtained results becomes better than the two peaks closer to each other (see tables 20 and 21).

As a result, the analyzes in this study reveal that when the separation temperature between two peaks increased by occupancy rate variations or changing activation energies of glow peaks, the CGCD method gives more accurate results than the very composed glow peaks.

Table 4.20: The below table includes of the input parameters for IMTS model which were used in numerical simulated TL glow curves and obtained kinetic parameters after their analyzing by curve fitting program by Excel(E) and Glocanin(G) for changing occupancy rates (active and deep traps) of traps for two peaks (E_1=1eV, E_2=1.08eV).

INPUT KINETIC PARAMETERS: $n_0= 1.10^{10}cm^{-3}$; $\beta=1^0$ C/s; $s=1x10^{12}s^{-1}$ Am= 1xAh; Ah= $1x10^{-7}cm^3s^{-1}$												
$n_0= N_t$, $m_0= M_t$												
An/Ah	E_1(1eV)		E_2(1.08eV)		b_1		b_2		$s_1(s^{-1})$		$s_2(s^{-1})$	
FOM%	E	G	E	G	E	G	E	G	E	G	E	G
100/3.574	0.60	0.50	0.66	0.51	1.82	1.03	1.42	1.00	$1x10^6$	$3x10^4$	$1x10^6$	$1x10^4$
10/2.735	0.66	0.71	0.65	0.62	1.3	1.56	1.00	1.00	$1x10^7$	$4x10^7$	$2x10^6$	$8x10^5$
1/0.503	0.98	0.98	0.94	0.95	1.60	1.59	1.00	1.00	$4x10^{11}$	$4x10^{11}$	$1x10^{10}$	$2x10^{10}$
0.1/0.120	1.00	1.00	1.06	1.06	1.04	1.04	1.04	1.01	$9x10^{11}$	$9x10^{11}$	$6x10^{11}$	$6x10^{11}$
0.01/0.434	1.00	1.00	1.04	1.08	1.00	1.01	1.00	1.01	$1x10^{12}$	$1x10^{12}$	$3x10^{11}$	$1x10^{12}$
$n_0= N_t$, $m_0= 0.5M_t$												
An/Ah	E_1(1eV)		E_2(1.08eV)		b_1		b_2		$s_1(s^{-1})$		$s_2(s^{-1})$	
FOM%	E	G	E	G	E	G	E	G	E	G	E	G
100/2.927	0.60	0.50	0.65	0.51	1.80	1.05	1.41	1.00	$1x10^6$	$2x10^4$	$1x10^6$	$1x10^4$
10/2.488	0.68	0.69	0.71	0.64	1.47	1.52	1.00	1.00	$2x10^7$	$2x10^7$	$7x10^6$	$1x10^6$
1/0,511	0.97	0.97	0.94	0.96	1.60	1.59	1.00	1.00	$3x10^{11}$	$3x10^{11}$	$1x10^{10}$	$2x10^{10}$
0.1/0.120	1.00	1.00	1.08	1.07	1.06	1.04	1.02	1.01	$1x10^{12}$	$9x10^{11}$	$9x10^{11}$	$6x10^{11}$
0.01/0.014	1.00	1.00	1.08	1.08	1.00	1.00	1.00	1.00	$1x10^{12}$	$1x10^{12}$	$1x10^{12}$	$1x10^{12}$
$n_0= 0.5N_t$, $m_0= 0.5M_t$												
An/Ah	E_1(1eV)		E_2(1.08eV)		b_1		b_2		$s_1(s^{-1})$		$s_2(s^{-1})$	
FOM%	E	G	E	G	E	G	E	G	E	G	E	G
100/2.021	0.85	0.74	0.79	0.95	1.30	1.67	1.00	1.00	$3x10^8$	$5x10^9$	$1x10^7$	$3x10^6$
10/1.505	0.88	0.88	0.94	0.94	1.52	1.52	1.00	1.00	$4x10^9$	$4x10^9$	$3x10^9$	$3x10^9$
1/0.403	0.98	0.97	1.10	1.11	1.31	1.32	1.06	1.06	$3x10^{11}$	$4x10^{11}$	$9x10^{11}$	$1x10^{12}$
0.1/0.096	1.00	1.00	1.07	1.07	1.02	1.02	1.00	1.00	$8x10^{11}$	$8x10^{11}$	$6x10^{11}$	$7x10^{11}$
0.01/0.010	1.00	1.00	1.08	1.08	1.00	1.00	1.00	1.00	$1x10^{12}$	$1x10^{12}$	$1x10^{12}$	$1x10^{12}$

Table 4.21: The below table includes of the input parameters for IMTS model which were used in numerical simulated TL glow curves and obtained kinetic parameters after their analyzing by curve fitting program by Excel(E) and Glocanin(G) for changing occupancy rates (active and deep traps) of traps for two peaks (E_1=1eV, E_2=1.1eV).

INPUT KINETIC PARAMETERS: $n_0= 1.10^{10}cm^{-3}$; $\beta=1^0$ C/s; $s=1x10^{12}s^{-1}$ Am= 1xAh; Ah= $1x10^{-7}cm^3s^{-1}$												
$n_0= N_t$, $m_0= M_t$												
A_n/A_h	E_1(1eV)		E_2(1.1eV)		b_1		b_2		$s_1(s^{-1})$		$s_2(s^{-1})$	
FOM%	E	G	E	G	E	G	E	G	E	G	E	G
100/4.330	0.60	0.58	0.60	0.50	1.53	1.05	1.00	1.00	$5x10^5$	$5x10^4$	$9x10^4$	$3x10^4$
10/3,479	0.65	0.69	0.87	0.66	1.43	1.60	1.00	1.00	$5x10^6$	$2x10^7$	$3x10^8$	$1x10^6$
1/0.735	0.97	0.97	0.99	0.99	1.42	1.42	1.07	1.07	$3x10^{11}$	$3x10^{11}$	$4x10^{10}$	$4x10^{10}$
0.1/0.173	1.00	0.99	1.08	1.08	1.03	1.03	1.01	1.01	$9x10^{11}$	$8x10^{11}$	$6x10^{11}$	$6x10^{11}$
0.01/0.040	1.00	1.00	1.10	1.10	1.00	1.00	1.00	1.00	$1x10^{12}$	$1x10^{12}$	$9x10^{11}$	$1x10^{12}$
$n_0= N_t$, $m_0= 0.5M_t$												
A_n/A_h	E_1(1eV)		E_2(1.1eV)		b_1		b_2		$s_1(s^{-1})$		$s_2(s^{-1})$	
FOM%	E	G	E	G	E	G	E	G	E	G	E	G
100/4.349	0.60	0.51	0.60	0.68	1.53	1.41	1.00	1.00	$5x10^5$	$2x10^4$	$1x10^5$	$6x0^5$
10/2.430	0.62	0.69	0.89	0.66	1.35	1.54	1.00	1.00	$2x10^6$	$2x10^7$	$6x10^8$	$1x10^6$
1/0.723	0.97	0.97	0.99	0.97	1.44	1.42	1.06	1.07	$4x10^{11}$	$3x10^{11}$	$3x0^{10}$	$2x10^{10}$
0.1/0.182	1.00	1.00	1.09	1.08	1.03	1.02	1.03	1.01	$8x10^{11}$	$8x10^{11}$	$6x10^{11}$	$8x10^{11}$
0.01/0.024	1.00	1.00	1.10	1.10	1.00	1.00	1.00	1.00	$1x10^{12}$	$1x10^{12}$	$1x10^{12}$	$1x10^{12}$
$n_0= 0.5N_t$, $m_0= 0.5M_t$												
A_n/A_h	E_1(1eV)		E_2(1.1eV)		b_1		b_2		$s_1(s^{-1})$		$s_2(s^{-1})$	
FOM%	E	G	E	G	E	G	E	G	E	G	E	G
100/1.333	0.87	0.92	1.03	0.86	1.80	1.76	1.00	1.00	$5x10^8$	$2x10^9$	$3x10^9$	$2x10^7$
10/1.054	0.92	0.92	0.98	0.98	1.70	1.70	1.00	1.00	$1x10^{10}$	$1x10^{10}$	$5x10^9$	$5x10^9$
1/0.667	0.97	0.96	1.01	1.01	1.17	1.16	1.03	1.04	$3x10^{11}$	$2x10^{11}$	$6x10^{10}$	$6x10^{10}$
0.1/0.140	1.00	1.00	1.08	1.09	1.01	1.01	1.00	1.00	$8x10^{11}$	$8x10^{11}$	$5x10^{11}$	$6x10^{11}$
0.01/0.016	1.00	1.00	1.10	1.10	1.00	1.00	1.00	1.00	$1x10^{12}$	$1x10^{12}$	$1x10^{12}$	$1x10^{12}$

4.3.c Solutions of IMTS Model Rate Equations with Assuming Three Glow Peaks and Their Analysis by CGCD Programs

The rate equations (2.41-2.44) of IMTS Model were solved numerically by using Mathematica for different kinetic parameters and accepting that each numerically generated glow curve contains three glow peaks. And then, they were analyzed with the deconvolution programs. The results of analysis obtained by programs were again compared with the input parameters that were entered to the Mathematica during the generation of numerical glow curves. The input parameters are shown in the top row of table 4.17. The obtained kinetic parameters from the CGCD programs were also shown in the bottom rows of this table. Some of the selected simulated, analyzed glow curves and results were shown in the figures 4.32 and 4.33.

As seen from the table, the analysis results of GLOCANIN program are always highly deviated from the input parameters. GLOCANIN program gives good results only for the first peak (E_1 = 1 eV) at $A_n/A_h << 1$, but the results of other peaks are always deviating from real values, especially as the A_n/A_h ratio increases. This shows that the use of GLOCANIN analysis is not appropriate to use for multiple peaks in the IMTS model.

In the Excel Spreadsheet analysis, the deviations in the results of second and third peaks (E_2 = 1.04, E_3 = 1.08) are observed in A_n/A_h = 0.01, 0.05 and 0.1 values. Apart from these values, the reliable results of kinetic parameters of all peaks were obtained in all A_n/A_h ratios. Taking into account the fact that, it is difficult to obtain reliable results, especially for multi-peak analyzes, by the CGCD methods to obtained kinetic parameters. On the other hand, the preference of the Excel Spreadsheet analysis program provides serious advantages in favor of more reliable analysis than the GLOCANIN program in any situations.

Table 4.22 : The below table includes of the input parameters for IMTS model which were used in numerical simulated TL glow curves and obtained kinetic parameters after their analyzing by GLOCANIN and Excel Spreadsheet curve fitting programs if $A_m=A_h$. (Three peaks)

INPUT KINETIC PARAMETERS								
$n_0= 1.10^{10}cm^{-3}$; $\beta=1^0$ C/s; $s=1x10^{12}s^{-1}$; $n_0=1x\ N_t$; $m_0=1xM_t$; $A_m= 1xA_h$; $A_h= 1x10^{-7}cm^3s^{-1}$								
A_n/A_h		E(eV)		b		$s(s^{-1})$		FOM
		G	E	G	E	G	E	
E_1=1eV	0.001	1.01	1.00	1.50	1.00	$9.4x10^{11}$	$1.0x10^{12}$	0.033
E_2=1.04eV		0.96	1.04	1.12	1.03	$7.1x10^{10}$	$1.0x10^{12}$	
E_3=1.08eV		0.96	1.08	1.00	1.00	$3.1x10^{10}$	$1.0x10^{12}$	
E_1=1eV	0.005	1.01	1.00	1.50	1.00	$9.8x10^{11}$	$1.2x10^{12}$	0.023
E_2=1.04eV		0.96	1.04	1.00	1.02	$3.2x10^{10}$	$1.0x10^{12}$	
E_3=1.08eV		0.96	1.08	1.12	1.00	$6.7x10^{10}$	$1.0x10^{12}$	
E_1=1eV	0.01	1.02	1.00	1.44	1.00	$1.2x10^{12}$	$1.2x10^{12}$	0.185
E_2=1.04eV		1.00	0.98	1.00	1.05	$8.5x10^{10}$	$1.8x10^{11}$	
E_3=1.08eV		0.93	1.12	1.07	1.00	$2.6x10^{10}$	$3.0x10^{12}$	
E_1=1eV	0.05	1.01	1.01	1.50	1.04	$9.2x10^{11}$	$1.4x10^{12}$	0.104
E_2=1.04eV		0.96	0.99	1.12	1.08	$7.1x10^{10}$	$1.8x10^{11}$	
E_3=1.08eV		0.96	1.11	1.00	1.00	$3.1x10^{10}$	$2.3x10^{11}$	
E_1=1eV	0.1	1.07	1.00	1.37	1.06	$6.8x10^{12}$	$1.3x10^{12}$	0.069
E_2=1.04eV		0.96	0.99	1.12	1.07	$4.9x10^{10}$	$1.8x10^{11}$	
E_3=1.08eV		0.81	1.11	1.00	1.07	$6.6x10^{08}$	$2.3x10^{12}$	
E_1=1eV	0.5	1.01	0.98	1.50	1.25	$9.1x10^{11}$	$4.8x10^{11}$	0.383
E_2=1.04eV		0.96	1.04	1.14	1.32	$7.1x10^{10}$	$7.4x10^{11}$	
E_3=1.08eV		0.95	1.09	1.00	1.01	$1.7x10^{10}$	$8.2x10^{11}$	
E_1=1eV	1	1.04	0.98	1.52	1.36	$4.1x10^{12}$	$4.8x10^{11}$	0.543
E_2=1.04eV		1.01	1.04	1.36	1.27	$5.1x10^{11}$	$8.1x10^{11}$	
E_3=1.08eV		0.82	1.09	1.02	1.00	$5.4x10^{08}$	$5.4x10^{11}$	
E_1=1eV	3	1.00	0.98	1.71	1.73	$1.3x10^{12}$	$6.4x10^{11}$	0.616
E_2=1.04eV		0.93	1.04	1.36	1.45	$2.9x10^{09}$	$8.1x10^{11}$	
E_3=1.08eV		0.78	1.09	1.02	1.20	$1.3x10^{08}$	$5.4x10^{11}$	
E_1=1eV	6	0.95	0.98	1.81	1.97	$2.3x10^{11}$	$7.9x10^{11}$	1.216
E_2=1.04eV		0.86	1.04	1.36	1.57	$2.9x10^{09}$	$6.4x10^{11}$	
E_3=1.08eV		0.75	1.08	1.00	1.29	$3.1x10^{07}$	$3.8x10^{11}$	
E_1=1eV	10	0.90	0.99	1.80	2.00	$3.4x10^{10}$	$1.3x10^{12}$	0.620
E_2=1.04eV		0.91	1.04	1.33	2.00	$4.4x10^{08}$	$8.6x10^{11}$	
E_3=1.08eV		0.72	1.08	1.00	1.81	$1.1x10^{07}$	$5.3x10^{11}$	

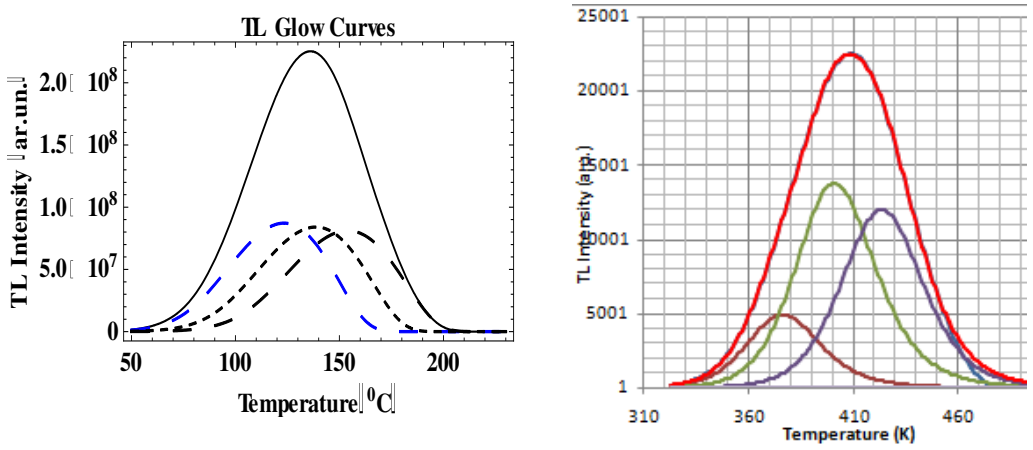

(a)

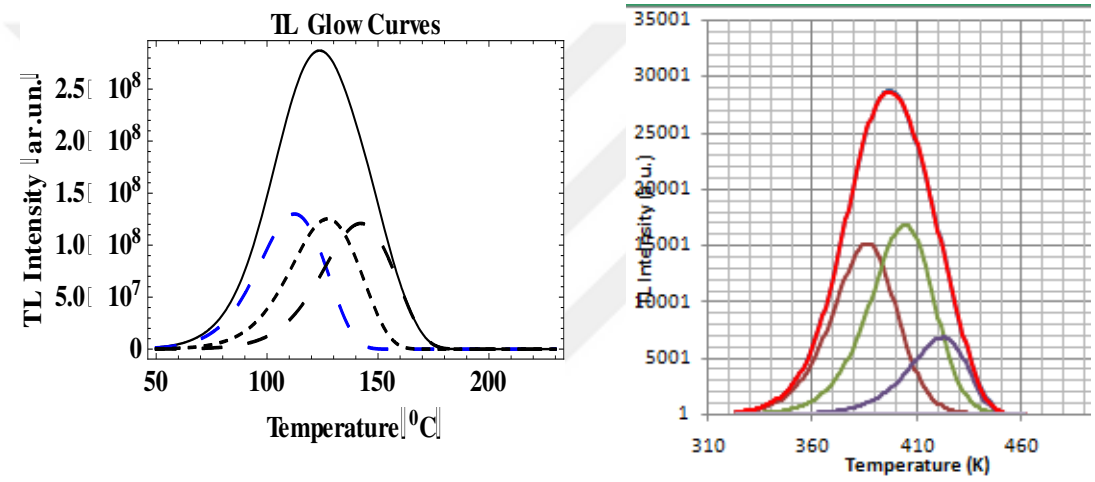

(b)

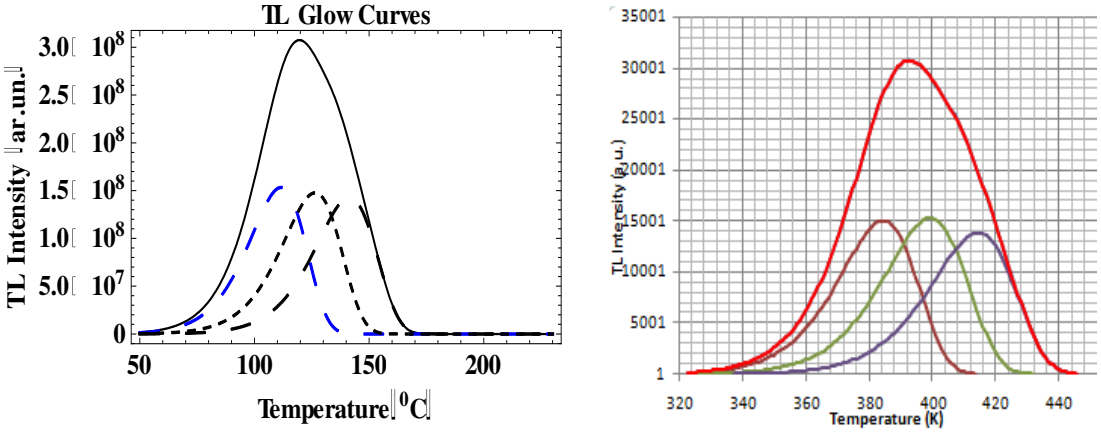

(c)

Figure 4.31: The numerically generated (left side) by Mathematica and then analyzed by Excel Spreadsheet program (right side) glow curves for the following input parameters: (Three Peaks) (A_n= A_m) (a) (A_n/A_h=10) (b) (A_n/A_h=1) (c) (A_n/A_h=0.001).

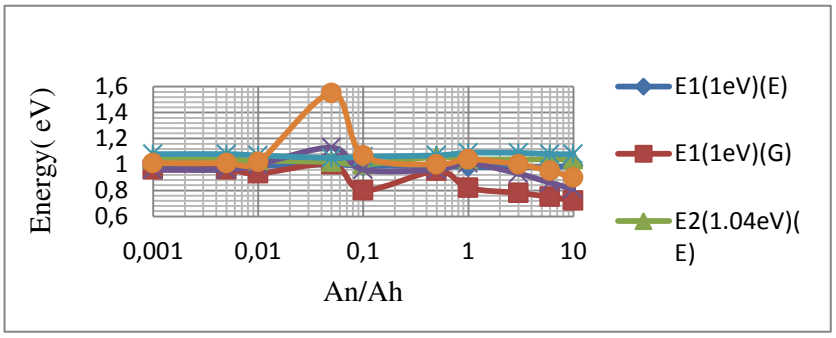

(a)

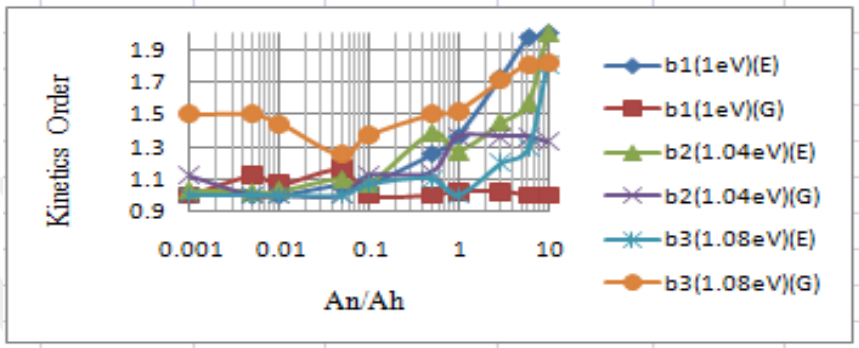

(b)

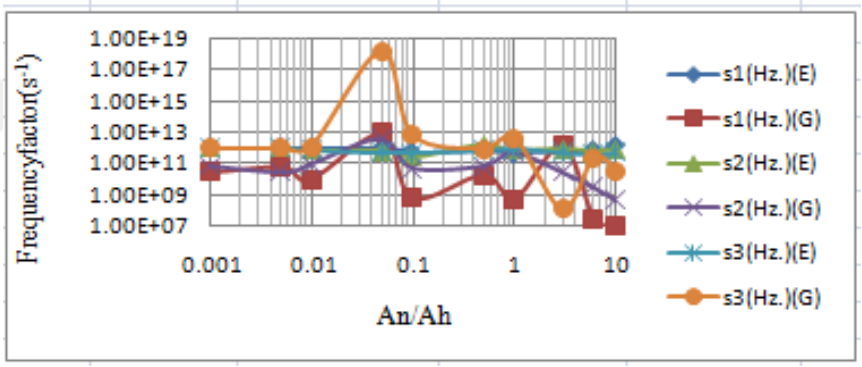

(c)

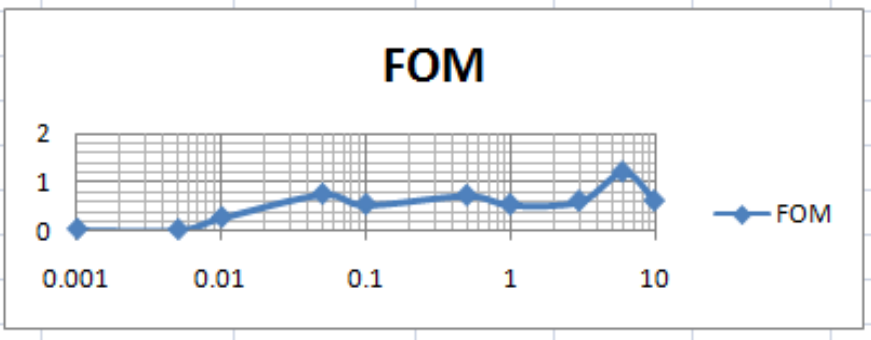

(d)

Figure 4.32: The comparisons of CGCD analysis (E: Excel Spreadsheet, G: GLOCANIN) results of the IMTS model as a function of A_n/A_h ($A_n = A_h$) for the following input parameters: (Three Peaks). (a) Activation Energy (b) Frequency factor (c) Kinetics order (d) FOM values (Excel)

CHAPTER 5

CONCLUSION

The computerized glow curve deconvolution (CGCD) analysis of thermoluminescence (TL) glow curves and optically stimulated luminescence (OSL) decay curves into their individual glow peaks and components respectively have been recognized over the last 30 years to be of major importance [8, 18-20]. The information by the CGCD concerning the trap energy depth (E), frequency factor (s), kinetic order (b), photoionization cross section (σ), etc, is very useful in order to understand the luminescence mechanism of materials [17]. The acquisition of kinetic parameters has emerged in this area of scientific work where this method has far greater advantages over other experimental methods (ie initial rise, peak shape, heating rate, etc.). The CGCD is easily performed by available software and it has established that it is not only a powerful technique in the analysis of glow curves but also for studying TL dosimetry (TLD) as well. In dosimetric investigations, it may be necessary to separate the glow curve into its individual glow peaks and finds the values for the glow peak parameters [8-12].

In this thesis, the TL glow curves were firstly generated numerically for the first, second and general-kinetics orders, and also for the OTOR and IMTS models with the aid of the Mathematica program. The obtained data from the Mathematica were analyzed using two different CGCD analysis programs, GLOCANIN and Excel Spreadsheet programs which were used different TL equations [15-17], to what extend the kinetics trap parameters obtained as a result of the analyzes were compatible with the input values entered in the Mathematica program, and which programs gave more successful results in this regard were investigated for different situations and under which conditions the results of analysis can be more efficient has been researched.

For the first-, second- and general-order kinetics; the numeric analyzes performed, the following methods were followed: 1) When the activation energy (E) taken as variables, the other parameters were kept constant. 2) Kinetic order (b) and

frequency factor (s) were kept variable and other kinetic parameters were kept fixed. 3) The initial electron traps values (n_0) and frequency factor (s) were variable and other kinetic parameter values were kept fixed. The kinetic parameters obtained from both analysis programs for one peak were collected in a table and when the generated glow curve was analyzed, if the input values entered to Mathematica are consistent with kinetic parameters determined by using both GLOCANIN and Excel Spreadsheet so that the produced results are reliable. The FOM (Figure of Merit) value that was founded by the analysis in Excel Spreadsheet is proof for this statement. The outcomes of this study shows that for first-, second- and general-order kinetic parameters, both CGCD analysis programs can be reliable to determine the kinetic parameter values for one peak. However, the simple interface of Excel Spreadsheet combined with the powerful Solver utility can be more advantageous as it is easier to handle and has more practical uses to perform the analysis in a shorter time. For generate glow peaks with two glow peaks; while entering input values to generation of numerical glow curves to be made, respectively; the activation energy was kept variable, the other kinetic parameter values fixed, or kinetic order and frequency factor variable, the other kinetic parameter values fixed, or trap occupancy at initial and frequency factor variable, the other kinetic parameter values fixed. When examining analysis results of glow curves for two peaks, the input values entered to Mathematica are very consistent with kinetic parameters determined by using both GLOCANIN and Excel Spreadsheet under some circumstances so that the produced results are reliable. The FOM (Figure of Merit) value that was founded by the analysis in Excel Spreadsheet is proof for this statement. The outcomes of this study show that for general-order kinetic parameters, both CGCD analysis programs can be reliable to determine the kinetics order values. For glow curves which contain three general-order glow peaks; while entering input values for the analysis to be made, the activation energy value was kept variable, other kinetic parameters were fixed. For general-order kinetics, when examining results of glow curves for three peaks, the first peak (E=1eV) came away from the output values of the input values for kinetic parameters in both programs, the second peak (E= 1.06eV) results were similar to the input values of kinetic parameters in the analysis carried out in Excel Spreadsheet but it is far from the values in GLOCANIN program, the third peak (1.12eV) input values entered to Mathematica are very consistent with kinetic

parameters determined by using both GLOCANIN and Excel Spreadsheet analysis programs so that the produced results are reliable for the third peak. The input values entered to Mathematica which were no fully reliable for all peaks with kinetic parameters determined by using both GLOCANIN and Excel Spreadsheet so that the produced results are not completely reliable for three or more glow peaks. The outcomes of this study shows that for general-order kinetic parameters, although Excel Spreadsheet analysis program reached more reliable, both CGCD analysis programs can't completely reliable to determine the kinetic parameter values for three or more glow peaks. In particular, the analysis of the second peak (E = 1.06eV), was much more consistent with the input values in the Excel Spreadsheet program, but GLOCANIN analysis was much more distant than the input values. This shows us that the use of the Excel Spreadsheet program in analyzes of glow curves with two or more glow peaks is a much better choice for analytical reliability and ease of use.

The OTOR (one-trap-one-recombination center) Model:

For one peak; the electron traps are respectively accepted that they are completely (100%) filled, or 50% filled, or 10% for different ratios of A_n/A_h (probability coefficient of electron re-trapping in the traps (cm^3s^{-1})/probability coefficient of electron recombining with holes in the RC (cm^3s^{-1})).The numerical solutions were made in the Mathematica program using OTOR equations and data were analyzed in both CGCD programs. Even if the results of the analysis for one peak in the OTOR model show that the analysis results for $A_n/A_h>1$ are not reliable, in the cases where the traps are less occupied, the inaccuracies are greatly reduced and the analysis to be done comes to levels that can be relied upon for all situations. The reliable analysis results cannot be also obtained at the values of $A_n/A_h = 0.1$ and 0.01. This situation is seen more in the results of GLOANIN. However, as the electron traps (N_t) become less filled, these discrepancies shifts from $A_n/A_h= 0.1$ to 0.01.

For two peaks; the analysis results by both deconvolution programs for $A_n/A_h>1$ would be unreliable. However, they show that in cases where the electron traps are less full, the errors are considerably reduced. The failure is seen to be higher in the analyzing results of GLOCANIN. Especially, these faults increase at the 2^{nd} peak ($E_2 = 1.1$ eV) while the 1^{st} peak ($E_1 = 1$ eV) is not much effected.

For three peaks; if the electron traps are completely filled; in contrast to one and two peaks, the Excel Spreadsheet analysis results are close to the input values for each of three peaks (E_1 = 1 eV, E_2 = 1.1 eV, E_3 = 1.2 eV) for $A_n/A_h > 1$, which in turn supports the fact that it leads towards credible assets for low trap fullness as a result. GLOCANIN analysis, on the other hand, remains far from the input values for all A_n/A_h values. Whereas some results of GLOCANIN are meaningful, there are some values that can be regarded as meaningless for physics and remain far away from the input values. On the other hand, the Excel Spreadsheet analysis results are mostly consistent with the input values and they are especially reliable in the case of $A_n/A_h \leq 1$. The previous situations continue in the same way and as the occupancy of electron traps decreases, the discrepancies between input data and obtained results are reduced.

Ultimately, the analysis of glow curves generated by OTOR model, it was seen that the results of GLOCANIN are far from reliable if the glow curves contains more than one-peaks. Nevertheless, the results of Excel Spreadsheet are more reliable than the GLOCANIN and the reliability of this program increases as the trap occupancy decreases even though the discrepancy decreases towards lower values of A_n/A_h. Therefore, the results of analysis presented in this work after different occupancy rates show that analyzes of glow curves by CGCD programs after low radiation doses applied to the TL materials will give more realistic trap parameters. In this case, the emptier electron traps are, the closer it will be to the correct results and the lesser the n_o/N ratio is, the more accurate analysis results will be obtained. However, as the number of glow peaks within the glow curve increases, good results can no longer be obtained in the CGCD methods, especially when the glow peaks overlaps with each other, the success of this method are quickly diminishing.

IMTS (interactive multiple-trap system) model consists of two trapping states and one recombination center (RC). The first trap is considered to be responsible with TL (active trap (AT)), and the second trap is denoted as the Thermally Disconnected Deep Trap (TDDT). The two traps are characterized by total concentrations N_t and M, and by instantaneous occupancies $n(t)$ and $m(t)$, respectively. For this model; A_n= probability coefficient of electron re-trapping in the AT traps (cm^3s^{-1}), A_h= probability coefficient of electron recombination with holes in the, RC (cm^3s^{-1}), A_m= probability coefficient of electron re-trapping in the

TDDT traps (cm^3s^{-1}), *m* = concentration of filled TDDT traps in the crystal (cm^{-3}), *M* = total concentration of available TDDT traps in the crystal (cm^{-3}), n_c= concentration of electrons in the conduction band (cm^{-3}), $n + m + n_c$= total instantaneous concentration of electrons and holes in the crystal (cm^{-3})

The IMTS Model:

For one peak; in case of A_n/A_h= 100 (A_m=1*A_h) and n_o= N_t, the IMTS model produces a second-order TL peak (b=2). On the other hand, in case of A_n/A_h= 0.01(A_m=1*A_h) and n_o= N, the IMTS model produces a first-order TL peak (b=1). In case of A_m/A_h= 100, the IMTS model produces a first-order TL peak (A_n=1*A_h), A_m/A_h= 0.01 (A_n=1*A_h) the IMTS model produces a second-order TL peak. IMTS model for A_n/A_h (A_m=1*A_h); in the case of A_n/A_h<<1, the results of the GLOCANIN and Excel analyzes are consistent with the input values, while the analysis reliability is reduced as the ratio increases in the case of $A_n/A_h\geq1$. On the other hand, IMTS model for A_m/A_h(A_n=1*A_h); in the case of A_m/A_h<<1, the results of the GLOCANIN and Excel analyzes are consistent with the input values, while the analysis reliability is reduced as the ratio increases in the case of $A_n/A_h\geq1$.IMTS model for A_m/A_h(A_n=A_m); both analytical results are reliable in the case of A_m/A_h<1. In the case of $A_m/A_h\geq1$, however, it is increasingly getting away from reliability.

In these analyzes for single peak, the analyzes made with both programs give similar results. IMTS Analysis, for two and three peaks; when the electron traps were taken as full, the analyzes were made for the different values of A_n/A_h (A_m = 1*A_h). As the values of A_n/A_h<1 for two peaks and when the ratio are smaller, both analysing results are much more reliable and values that match the input values are emerging. For $A_n/A_h\geq1$; both analysis programs give erroneous results, especially for the 2^{nd} peak (E = 1.05 eV) this error becomes too much. Even if GLOCANIN analysis gives good results only for the first peak (E = 1 eV) at A_n/A_h<<1 values for three peaks in the IMTS model, but all results are deviating from real values, especially as the A_n/A_h ratio increases which in turn shows that the use of GLOCANIN analysis is not appropriate for use for multiple peaks in the IMTS model. In Excel analysis, deviations for second and third peaks (E_2=1.04, E_3=1.08 eV) are observed in A_n/A_h=0.01 and 0.05 values, apart from this, reliable analytical results were obtained on all peaks in all A_n/A_h ratios. The results from these analyzes do not give a reliable result for glow curves GLOCANIN containing more than two

peaks, whereas Excel analyzes provide very advantageous reliable results in multiple peaks.

When changing active occupancy rates of traps; the results are not consistent with the input values for $A_n/A_h>1$ if the traps are completely full. On the other hand, the analysis results become reliable as the occupancy of active traps decreases and the results of the analysis are getting better and better in all values of A_n/A_h ratios and the analysis results of the entire range provides exactly the same values of input parameters. From here it can be deduced that as the amount of active traps decreases, the reliability increases.

The analysis of IMTS model was also performed for changing the active occupancy and deep traps for two peaks when electron traps were taken as full. The GLOCANIN and Excel analyzes done by keeping the first peak (E_1=1eV) constant and increasing the second peak (E_2=1.05eV, 1.08eV, 1.1eV) when the active and deep traps were full, ($n_0 = N_t$, $m_0 = M_t$). It appears that the analysis of the opening of the peak range has been positively reflected. The analysis results for $A_n/A_h\geq1$ are inconsistent with the input values, the incoherence increases as the ratio increases, and the input values agree with the analysis results for $A_n/A_h< 1$.

Similar results have been obtained from analyzes for $n_0 = N_t$, $m_0 = 0.5M_t$ with the same input values, from which the result that the fullness of deep traps does not affect the results of the analysis can be deduced. In the analysis with $n_0 = 0.5N_t$, $m_0 = 0.5M_t$ with the same input values, the empty half of the active traps ensures a much healthier result in the overall A_n/A_h ratios. Analyzes made reveal that separation of the peak intervals and low specificity of the active traps allow for very accurate results in the analysis, while the filling rate of the deep traps does not affect the results of the analysis.

In all analyzes, as the number of peaks in the glow curves increases, it is difficult to obtain accurate results from the analysis. However, the increase in the number of peaks in the IMTS method is negative in the analysis of GLOCANIN, while the analysis made by Excel allows us to obtain more reliable results. This offers great advantages of the analysis made by Excel in terms of both these aspects and providing opportunities for making analysis much easier by saving it from the chaos of difficulty. The use of irradiated dosimeters with low radiation for the calculation of trap parameters will positively affect the results of the analysis.

Increasing the n_0/N ratio causes the analysis results to be inconsistent with the actual values, therefore, materials subjected to low radiation will be a factor in obtaining more accurate kinetic parameters.

REFERENCES

[1] Pagonis, V., Kitis, G., Furetta, C.: Numerical and Practical Exercises in Thermoluminescence. Springer Science+Business Media, Inc., New York (2006).

[2] S.W.S. McKeever, "*Thermoluminescence of Solids*", Cambridge University Press, Cambridge, (1985).

[3] Daniels F. and Boyd C. A., "Thermoluminescence as a research tool", *Science*, **117**, 343-349, (1953).

[4] Aitken M. J., Tite M. S. and Reid J., "Thermoluminescencent dating of ancient ceramics"*, Nature*, **202**, 1032-1033, (1964).

[5] Aitken M. J., Zimerman D. W. and FlemingS. J., "Thermoluminescencent dating of ancient pottery", *Nature*, **219**, 442-444, (1964).

[6] Mejdahl V., "Thermoluminescence dating of ancient Danish ceramics", *Archaeometry*, **11**, 99-104

[7] Wintle A. G. and Huntley D. J., "Thermoluminescencent dating of ocean sediments", *Canadian journal of earth sciences,* (1985).

[8] Horowitz , Y.S. and D. Yossian, "Computerized Glow Curve Deconvolution: Application to Thermoluminescence Dosimetry", *Radiation Protection Dosimetry*, **60(1)**, 1-114, (1995).

[9] A. M. Sadek, H. M. Eissa, A. M. Basha, and G. Kitis *"*Properties of the thermoluminescence glow peaks simulated by the interactive multiple-trap system (IMTS) model*"*, *Phys. Status Solidi (b)*, **252(4)**, 721-729, 2015.

[10] R. Chen, G. Fogel, and C. K. Lee, *Radiat. Prot. Dosim*., **65**, 63–68 (1996).

[11] N. Suntharalingam and J. R. Cameron, *Phys. Med. Biol*., **14**, 397–410 (1969).

[12] Chen, R. and McKeever, S.W.S. "*Theory of Thermoluminescence and Related Phenomena*", World Scientific, Singapore, (1997).

[13] C. Furetta, Pao-Shan Weng, "*Operational Thermoluminescence Dosimetry*", World Scientific, Singapore, (1998).

[14] S. Basun, G. F. Imbusch, D. D. Jia and W. M. Yen, "The Analysis of Thermoluminescence Glow Curves", *Journal of Luminescence*, **104**, 283-294, (2003).

[15] Bos A. J. J., Piters J. M., Gomez Ros J. M. and Delgado A., GLOCANIN, and Intercomparision of Glow Curve Analysis Computer Programs IRI-CIEMAT Report, 131-93-005 IRI Delft, (1993).

[16] A.N. YAZICI and M.Y HACIİBRAHİMOĞLU, "Determination of the Trapping Parameters of Glow Peaks of CaF_2 :Dy (TLD-200) by Using Computer Glow Curve Deconvolution Method", *Turk J Phys.* **25(3),** 249-255, (2001).

[17] D. Afouxenidis, G. S. Polymeris, N.C. Tsirliganis and G. Kitis, "Computerised Curve Deconvolution of TL/OSL Curves using a popular spreadsheet program", *Radiation Protection Dosimetry*, **149**, 363-370, (2011).

[18] Horowitz, Y. S. and Moscovitch, M. "Computerized glow curve deconvolution applied to high dose (102–105 Gy) TL dosimetry", *Nucl. Instrum. Methods. Phys. Res. A* , **243(1)**, 207–214 (1986).

[19] Horowitz, Y. S, Moscovitch, M. and Wilt, M.Computerized glow curve deconvolution applied to ultralow dose LiF thermoluminescence dosimetry. *Nucl. Instrum. Methods. Phys. Res. A*, 244(3), 556–564 (1986).

[20] Horowitz, Y. S. and Yossian, D. "Computerized glow curve deconvolution: the case of LiF TLD-100", *J. Phys. D: Appl. Phys.*, **26(8)**, 1331–1332 (1993).

[21] A.N.Yazıcı, "*Thermal and optical Charateristics of Radiation Induced Defect Centers in Alkali Halide Crystal*", PhD Thesis, Gaziantep University, (1996).

[22] Braunlich, P. *Thermally stimulated relaxation in solids*, Springer-Verlag, (1983).

[23] Halpberian A. "Evaluation of thermal activation energies from glow curves", *Phys. Rev*., **117**, 40, (1985).

[24] Aitken MJ. An Introduction to Optical Dating. Oxford: Oxford University Press; (1998).

[25] Randall J.T. and Wilkins M.H.F., "Phosphorescence and Electron Traps. I. The Study of Trap Distributions", *Proc.R.Soc.London Ser. A***, 184,** 366, (1945).

[26] Furetta, C. and Kitis G., "Rewiev of Thermoluminescence", *Journal of Materials Science.* **39**, 2277-2294, (2004).

[27] Garlick G.F.J. and Gibson A.F., "The Electron Trap Mechanism of Luminescence in Sulphide and Silicate Phosphors", *Proc.Phys.Soc.* **60**, 574, (1948).

[28] Chen, R. in: Horowitz, Y.S. (Ed.), *Thermoluminescence and Thermoluminescence Dosimetry, Vol. 1,* CRC Press, Boca Raton, FL, (1984).

[29] Kitis, G., Gomez-Ros J.M. and Tuyn, J.W.N., "Thermoluminescence glow curve deconvolution functions for first, second and general orders of kinetics", *Journal of Physics D: Applied Physics*, **31**, 2636-2641, (1988).

[30] Bos, A.J.J. and Dielhof, J.B., "The Analysis of Thermoluminescent Glow Peaks in CaF_2:Tm (TLD-300)", *Radiat.Prot.Dosim.* **36**, 231, (1991).

[31] May C.E. and Partridge J.A. "Thermoluminescent kinetics of alpha;-rradiated alkali halides", *J.Chem.Phys.* **40**, 1401, (1964).

[32] Chen, R. and Winer, A.A., "Effects of various heating rates on glow curves", *Journal of Applied Physics*, **41**, 5227-5232, (1970).

[33] Piters T.M. and Bos A.J.J., "A model for the influence of defect interactions during heating on thermoluminescence in LiF:Mg,Ti (TLD-100)", *J.Phys.D:Appl.Phys.* **26**, 2255, (1993).

[34] Sweet M.A.S. and Urquhart D., *Phys. Stat. Sol. (a)*, **59**, 223, (1980).

[35] Dussel G.A. and Bube R.H., *Phys. Rev.*, **155**, 764, (1967).

[36] C. M. Sunta, W.E.F. Ayta, J.F.D. Chubaci, S. Watanabe, *Rad. Meas*., **35**, 47, (2002).

[37] R. Chen, "On the Calculation of the Activation Energies and Frequency Factors from Glow-Curves", *J.Appl.Physics*, **40**, 570, (1969).

[38] L. I. Grossweiner, "A note on the analysis of first-order glow curves", *J.Appl.Physics*, **24**, 1306, (1953).

[39] Halperin, A. and Braner. A., "Evaluation of thermal activation energies from glow curves", *Physical Review Letters*, **117**, 405-415, (1960).

[40] J. Azorin, "Determination of Thermoluminescence Parameters from Glow Curves: A review", *Nucl.Tracks*, **11**, 159, (1986).

[41] H.G. Balian and N.W. Eddy, "Figure-of-Merit (FOM), an Improved Criterion over the Normalized Chi-Squared Test for Assessing Goodness-of-Fit of Gamma-Ray Spectra Peaks", *Nucl. Instrum.Methods*, **145**, 389-395, (1977).

[42] S. K. Misra and N.W.Eddy, "IFOM, a Formula for Universal Assessment of Goodness-of-Fit of Gamma Ray Spectra", *Nucl.Instrum.Methods*, **166**, 537-540, (1979).

[43] http://www.wolfram.com/mathematica/

CURRICULUM VITAE

PERSONAL INFORMATION

Surname, Name: YILDIRIR Ünal
Nationality: Turkish (TC)
Date and Place of Birth: 15 December 1962 , Nizip
Marital Status: Married
Phone: +90 5337402410
Fax:
email: unalyildirir@mynet.com

EDUCATION

Degree	Institution	Year of Graduation
MS	GaziantepUniversity,health sciences-biophysics	2001
BS	Trakya University, Faculty of Science and Arts	1992
High School	Bolu Endüstri meslek lisesi	1982

WORK EXPERIENCE

Year	Place	Enrollment
1993-1997	Siirt Mehmet akif Ersoy Ortaokulu	Physics teacher
1997- 2001	Mevlana Mesleki ve Teknik Anadolu Lisesi	Physics teacher
2001-2010	Hasan Çapan Anadolu Lisesi	Physics teacher
2010-2014	Nizip Anadolu Öğretmen Lisesi	Physics teacher
2014-2017	Nizip Fen Lisesi	Physics teacher
2017-Present	Kemer Göynük Fen Lisesi	Physics teacher

FOREIGN LANGUAGES

English

PUBLICATIONS:

Yıldırır, Ü., Kafadar, V. E., Yıldırım, R.G. and Yazıcı, A.N. (2017). The Investigation of Success and Failure of CGCD Method in the Analyzing of TL Glow Curves Numerically Generated from IMTS Model, Ciencia e tecnica, 32, 120-136.

CONGRESS:

1. III. Ulusal Biyofizik Kongresi (5-7 eylül 2001, Eskişehir) Nöroimplantasyon Tekniklerine Yeni Yaklaşımlar: Biyo- Uyumlu Materyal Enkapsülasyonu ve Amaca dönük Fonksiyonlu Yeni Epidural Elektrotların Geliştirilmesi, poster sunumu.
Ü. YILDIRIR, B.R. ARSLAN, M. TULGAR.

2. 8. Uluslararası Lumidoz Kongresi (27-29 Ağustos 2014, Ankara) IMTS Modeli Kullanılarak çözümlenmiş TL ışıldama eğrilerinin CGCD yöntemi ile analizleri, sözlü sunum.
Ü. YILDIRIR, A. Necmeddin YAZICI, R. Güler YILDIRIM.

HOBBIES: Music, football, basketball